Tissue separation in *Hydra*:

Involvement of a Rho dependent pathway and the organization of actomyosin complexes during final bud detachment

Dissertation

„kumulativ“

zur Erlangung des Doktorgrades

der Naturwissenschaften

(Dr. rer. nat.)

dem Fachbereich Biologie

der Philipps-Universität Marburg

vorgelegt von

Oliver Holz

aus Friedrichroda (Thüringen)

Marburg, 2021

Die hier vorliegende Arbeit wurde in dem Zeitraum zwischen Oktober 2014 bis Oktober 2019 in der Arbeitsgruppe von Frau Prof. Dr. Monika Hassel, Abteilung Molekulare Zoologie, Morphologie und Evolution von Invertebraten an der Philipps-Universität Marburg angefertigt.

Vom Fachbereich Biologie der Philipps-Universität Marburg (Hochschulkennziffer 1180) als Dissertation angenommen am _____

Erstgutachter: Frau Prof. Dr. Monika Hassel

Zweitgutachter: Herr Prof. Dr. Christian Helker

Tag der Disputation _____

Für meine Mutter

Die Wissenschaft gibt mir eine teilweise Erklärung für das Leben.
Soweit es geht, basiert es auf Fakten, Erfahrungen und Experimenten.

Rosalind Franklin

Table of Contents

I. Danksagung

An dieser Stelle möchte ich mich bei all denjenigen bedanken, die mich während der letzten Jahre als Doktorand begleitet und unterstützt haben. Mein größter Dank gilt Frau. Prof. Dr. Monika Hassel für die Möglichkeit der Promotion in Ihrer Arbeitsgruppe. Danke für die Freiheiten die du mir gewährt hast, um mein Projekt eigenständig zu entwickeln. Dennoch hast du immer beherzt eingegriffen, wenn ich auf Abwege gekommen bin.

Herrn Prof. Dr. Christian Helker möchte ich für die freundliche Übernahme des Zweitgutachtens bedanken. Gleicher Dank gilt Frau Prof. Dr. Anette Borchers und Herrn Prof. Dr. Uwe Homberg, welche die weiteren Gutachterfunktionen übernommen haben.

Danke an die Deutsche Forschungsgesellschaft (DFG) für die Unterstützung des Forschungsvorhabens (HA1732-13).

Auch wenn erst kürzlich kennengelernt, möchte ich mich ganz besonders bei Frau Stefanie Schäfer bedanken, die mir spontan Tipps zur Formulierung des englischen Textes gegeben hat.

Kommen wir nun zum ,,Best of“, meinen Arbeitskollegen/innen der AG Hassel. Generell waren wir ein tolles Team mit großem Zusammenhalt und ihr wart für mich wie eine zweite Familie, dafür möchte ich mich bedanken. Danke an Heide Brandtner für die Unterstützung in allen Bereichen im Laboralltag, sowie einfach bei allem anderen. Du hattest immer ein offenes Ohr und hilfreiche Tipps in allen Lebenslagen. Danke an David Apel, Lisa Reichart, Annegret Rittershaus und Marcel Hemming. Ihr habt die Arbeitstage zudem gemacht, was sie waren und woran ich mich gerne erinnere. Danke für die vielen Diskussionen, wenn man mal nicht weiter wusste, aber auch für die vielen anderen Dinge die wir gemeinsam erlebt haben. Ganz besonders bedanken möchte ich mich bei Karolin Schäfer, die zu einer echten Freundin geworden ist. Danke für deine beherzigte Kritik aber auch für Zuspruch in den richtigen Situationen.

Auch bei den von mir betreuten Studenten/innen, Simon Hopfenmüller, Belinda Elisabeth Rotta, Salome Duch und Vera Auffenberg möchte ich mich bedanken. Zusammen haben wir wertvolles geleistet, um das Projekt positiv zu beeinflussen.

Das Beste kommt bekanntlich zum Schluss und dort möchte ich mich bei meiner Familie bedanken. Ihr habt mich während der gesamten Zeit unterstützt und alle Höhen und Tiefen mitgemacht. Dafür möchte ich mich bedanken.

II. Erklärung: Eigene Beiträge und veröffentlichte Teile der Arbeit

Laut §9, Absatz 3 der Promotionsordnung der Philipps-Universität Marburg (Fassung vom 15.07.2009) müssen bei den Teilen der Dissertation, die aus gemeinsamer Forschungsarbeit entstanden sind, ,,die individuellen Leistungen des Doktoranden deutlich abgrenzbar und bewertbar sein‘‘. Diese Leistungen sollen im Folgenden erläutert werden.

Allgemeine Vorarbeiten:

- Allgemeine Entwicklung und Planung des Forschungsvorhabens und Identifikation der Kandidatensignalwege.
- Auswahl der zu untersuchenden Komponenten innerhalb des Kandidatensignalwegs sowie den dazugehörigen Kofaktoren zur Ausbildung von komplexen kontraktilen Actomyosin Bündeln. Initiale Datenbankanalyse zur Identifikation der Faktoren im Genom von *Hydra*.
- Auswahl und Vorversuche der verwendeten pharmakologischen Inhibitoren zur Ermittlung der optimalen Konzentration sowie Inkubationszeit und Erstbeschreibung der resultierenden Phänotypen.
- Allgemeine Versuchsplanung und Etablierung der immunhistologischen Mehrfachfärbungen.

Von mir betreute Studenten, die an den Publikationen beteiligt sind:

- David Apel hat im Rahmen seiner Masterarbeit einen wichtigen Anteil zur Publikation beigetragen, der besonders im Bereich der Inhibitorexperimente sowie der phylogenetischen Analyse der identifizierten Rho Proteine in *Hydra* lag.
- Simon Hopfenmüller hat im Rahmen seiner Bachelorarbeit die Charakterisierung von *α-actinin* übernommen.

Die eigenen Anteile an den einzelnen Publikationen werden im Folgenden aufgezeigt:

II.1 Chapter 1:

Bud detachment in *Hydra* requires activation of FGFR and a Rho - ROCK - myosin II signaling pathway to ensure formation of a basal constriction

- Isolation der RNA, cDNA Synthese, Primer-Design, PCR, Klonierung, Sondensynthese und Durchführung aller *In situ* Hybridisierungen. Ausnahmen:
    - *nm-MyHC* und *st-MyHC*, Klone erhalten von Dr. Patrick Steinmetz
    - *α-actinin*: Isoliert und charakterisiert durch Simon Hopfenmüller
    - *In situ* Hybridisierung *FGFf* von Dr. Ellen Lange und *FGFc* von Kerstin Ohler, B.Sc.
- Anfertigen aller immunhistologischen Färbungen (pMLC20 und Phalloidin) mit Ausnahme der Phalloidinfärbung an Inhibitionsphänotypen (durchgeführt von Dr. David Apel)
- Anfertigen aller Aufnahmen am konfokalen Laserscan Mikroskop
- Durchführung der initialen Inhibitorexperimente für Rhosin, Rockout und Blebbistatin
- Durchführung der Inhibitorexperimente und Erstellen der Statistik mit dem ROCK Inhibitor Y-27632
- Erstellen von allen Abbildungen mit Ausnahme von: Figure 1 (Prof. Dr. Monika Hassel), Figure 4 (Dr. David Apel), Figure 7 (in Zusammenarbeit mit Dr. David Apel) und Figure 8 (Dr. David Apel)
- Finalisieren der Abbildungen für die Publikation
- Schreiben des Rohentwurfes der Publikation zusammen mit Prof. Dr. Monika Hassel; Korrektur in Kooperation mit Prof. Dr. Monika Hassel, Dr. David Apel und Dr. Patrick Steinmetz (Bergen, Norwegen)
- Das Kapitel wurde in der hier vorliegenden Form im Journal Developmental Dynamics veröffentlicht (**Holz, O**., Apel, D., Steinmetz, P., Lange, E., Hopfenmüller, S., Ohler, K., Sudhop, S., & Hassel, M. (2017). Bud detachment in *Hydra* requires activation of fibroblast growth factor receptor and a Rho-ROCK-myosin II signaling pathway to ensure formation of a basal constriction. *Developmental dynamics*, *246*(7), 502–516. https://doi.org/10.1002/dvdy.24508)

II.2 Chapter 2:

Alternative pathways control actomyosin contractility in epitheliomuscle cells during morphogenesis and body contraction

- Durchführung und Planung aller Experimente für die Publikation
- Durchführung aller immunhistologischen Färbungen
- Isolation der RNA, cDNA Synthese, Primer-Design, PCR, Klonierung, Sondensynthese und Durchführung aller *In situ* Hybridisierungen für *Hv_MRLC12b-like*
- Anfertigen aller Aufnahmen am konfokalen Laserscan Mikroskop
- Durchführung der Western-Blot Analyse (Quantitative Auswertung anschließend durchgeführt von Dr. David Apel)
- Erstellen von allen Abbildungen
- Entwurf des Konzeptes für das Manuskript und schreiben des Rohentwurfes; Korrektur in Zusammenarbeit mit Prof. Dr. Monika Hassel
- Das Kapitel wurde in der hier vorliegenden Form im Journal Developmental Biology veröffentlicht (**Holz, O**., Apel, D., & Hassel, M. (2020). Alternative pathways control actomyosin contractility in epitheliomuscle cells during morphogenesis and body contraction. *Developmental biology*, *463*(1), 88–98. https://doi.org/10.1016/j.ydbio.2020.04.001)

II.3 Weitere Publikationen

What lies beneath: *Hydra* provides cnidarian perspectives into the evolution of FGFR docking proteins

- Isolation der RNA, cDNA Synthese, Primer-Design, PCR, Klonierung, Sondensynthese für folgende Faktoren: *Grb2, SOS, Shp2/Csw*
- Unterstützung beim Schreiben und der Korrektur des Manuskriptes
- Das Manuskript wurde in der hier vorliegenden Form im Journal Development Genes and Evolution veröffentlicht (Suryawanshi, A., Schaefer, K., **Holz, O**., Apel, D., Lange, E., Hayward, D. C., Miller, D. J., & Hassel, M. **(2020).** What lies beneath: *Hydra* provides cnidarian perspectives into the evolution of FGFR docking proteins. *Development genes and evolution*, 230(3), 227–238. https://doi.org/10.1007/s00427-020-00659-4)

III. Zusammenfassung

Die Gewebetrennung ist ein wesentlicher Bestandteil während der Embryonalentwicklung. Der zugrundeliegende Mechanismus ist hoch konserviert und wird meistens durch apikale Konstriktion von Zellen kontrolliert. Dies erfordert eine Reorganisation des Aktin-Zytoskeletts und die asymmetrische Ansammlung kortikaler Aktomyosin-Komplexe. Diese Actomyosin-Komplexe sind für die Veränderungen der Zellform, Morphogenese, Grenzbildung und Gewebetrennung essentiell.

Bei intakten Hydren lässt sich Morphogenese besonders gut während des asexuellen Knospungsprozesses untersuchen. Dabei sind mehrere Rezeptor-Systeme beteiligt, wobei ein FGFR Signalweg die Knospenablösung von *Hydra* steuert, indem sich intakte Epithelien ohne Wunde voneinander trennen. Dieser morphogenetische Prozess wird dabei durch bifunktionale Epithelmuskelzellen reguliert, welche zum einen die Bewegung sowie morphogenetische Prozesse sicherstellen. Das Wissen über intrazelluläre Signalwege, welche diese Prozesse in *Hydra* regulieren, ist begrenzt und deren Aufklärung ist das Hauptthema meiner Arbeit.

Im Rahmen der hier vorliegenden Arbeit konnte ein Kandidatensignalweg durch Rho, ROCK und Myosin II identifiziert werden, welcher die Konstriktion an der Knospenbasis und letztendlich die Knospenablösung steuert. Die Genexpressionsanalyse bestätigt, dass Kandidatengene eines FGFR gekoppelten Signalwegs in überlappenden Regionen exprimiert werden, die morphogenetischen Veränderungen unterliegen. Darüber hinaus verhindert eine pharmakologische Inhibition aller Komponenten des Signalwegs jeweils die Knospenablösung und führt zu stabilen, nicht ablösenden Y-förmigen Phänotypen. Mit der Knospenablösung geht eine starke Akkumulation von F-Aktin in den sich verengenden Zellen an der Knospenbasis einher, die dynamisch ihre Zellform ändern. Parallel wird die regulatorische leichte Kette von Myosin (MLC) an der späten Knospenbasis phosphoryliert (pMLC20). Das MLC-Signal konnte durch Genexpressionsdaten und Antikörperfärbung in allen morphogenetisch aktiven Regionen nachgewiesen werden. Der pMLC20-Antikörper zeigte das phosphorylierte Protein in den basalen kontraktilen Fortsätzen von ektodermalen Epithelmuskelzellen, welche die Körperbewegung sowie die späte, für die Ablösung essentielle Konstriktion an der Knospenbasis steuern. Hier wurde pMLC20 in den apikalen und basolateralen Zellkompartimenten einer kleinen Zellpopulation nachgewiesen. Die pharmakologische Hemmung zeigte, dass die MLC-Phosphorylierung bei Bewegungsvorgängen und Morphogenese getrennt voneinander über mindestens zwei unabhängige Wege erfolgt. Während der Kontraktion der basalen Zellfortsätze (Bewegung) wird MLC primär durch Myosin Light Chain Kinase (MLCK) phosphoryliert. Im Gegensatz dazu wird die apikale und kortikale MLC-Phosphorylierung bei der Morphogenese in den sich verengenden Zellen an der Knospenbasis über einen Rho - ROCK - Myosin II Weg stimuliert. Die vorliegenden Daten ergeben ein neues, komplexes Bild der Funktion von Epithelmuskelzellen mit Rho-abhängiger Phosphorylierung von MLC bei der Knospenmorphogenese und Sicherung der normalen basalen Kontraktilität von ektodermalen Epithelmuskelzellen während der Körperbewegung über MLCK.

IV. Summary

Tissue separation is an essential process during embryonic development. The underlying mechanism is highly conserved and mostly controlled by apical constriction of cells. It requires a rearrangement of the actin cytoskeleton and the asymmetric establishment of cortical actomyosin complexes. These actomyosin complexes are essential for cell shape changes, morphogenesis, boundary formation and tissue separation.

In adult *Hydra*, morphogenesis is well observable during the asexual budding process. Various receptor systems are involved and FGFR signaling controls bud detachment in which intact epithelia separate from each other without a wound. This morphogenetic process is regulated by bifunctional epitheliomuscle cells which have to ensure movement and morphogenetic processes. The knowledge of intracellular signaling pathways targeting these processes in *Hydra* was limited and its elucidation is the main subject of my thesis.

A candidate signaling pathway through Rho, ROCK and myosin II was identified which controls bud base constriction and therewith also bud detachment. Gene expression analysis confirmed that candidate genes of an FGFR-coupled pathway are expressed in overlapping regions undergoing morphogenesis. In addition, pharmacological inhibition of any component of the pathway prevented bud detachment and led to stable non-detaching, Y-shaped phenotypes. Accompanying bud detachment, a strong accumulation of F-actin in the constricting cells at the bud base was detected which undergo dynamic cell shape changes. In parallel the myosin regulatory light chain (MLC) was phosphorylated (pMLC20) at the late bud base. The MLC signal was detected by gene expression data and antibody staining in all morphogenetic active regions. The pMLC20 antibody revealed the phosphorylated protein in the basal contractile processes of ectodermal epitheliomuscle cells which control body movement as well as the essential constriction of the bud base. Here, pMLC20 was detected in the apical and basolateral compartments of a small cell population. Pharmacological inhibition revealed that MLC phosphorylation occurs in distinct subcellular compartments during movement and morphogenesis and is controlled by at least two independent pathways. During contraction of the basal cell protrusions (movement) MLC is mainly phosphorylated by myosin light chain kinase (MLCK). In contrast, apical and cortical MLC phosphorylation is stimulated via a Rho-ROCK pathway during morphogenesis in constricting cells of the bud base. The present data provide a new, complex picture of the function of epitheliomuscle cells with Rho-dependent phosphorylation of MLC in bud morphogenesis and a housekeeping function fulfilled by MLCK in the normal basal contractility of ectodermal epitheliomuscle cells during body movement.

1 General Introduction

During embryonic development, morphogenetic processes ultimately shape the organism to allow the formation of complex structures (Lecuit and Le Goff, 2007). In these processes, cells show different behaviours, like migration or constriction which is coordinated by highly conserved mechanisms shared in all organisms (Pulido Companys et al., 2020; Lecuit and Le Goff, 2007). The cellular behaviour depends on the actin cytoskeleton, its contractility as well as junctional remodelling (Rauzi et al., 2010). Morphogenetic changes are driven by periodic actomyosin contractility, e.g. during apical as well as basal constriction (Lv and Großhans, 2016; Christodoulou and Skourides, 2015; He et al., 2010; Martin et al., 2009; Roh-Johnson et al., 2012). Decisive for this coordinated contractility is the cortical establishment of actomyosin complexes as cellular contractile elements (Sutherland and Lesko, 2020). The arrangement of these contractile elements and the intensity of contractility determine the cellular behavior and shape (Heer and Martin, 2017). Both of these parameters are regulated and modulated by different pathways and proteins (Fagotto, 2014).

Fibroblast growth factor receptor (FGFR) signaling is an important part during embryonic development and involved in cell migration, cell differentiation, patterning and morphogenesis (Babina and Turner et al., 2017). The freshwater polyp *Hydra* uses FGFR signaling at least during the detachment phase of the asexual reproduction process, called budding (Sudhop et al., 2004; Hasse et al., 2014). The separation within an intact epithelial tissue is a very rare process and therefore well suited to investigate and understand the formation of contractile elements within those cells and the underlying molecular mechanism regulating contractility of the peculiar epitheliomuscle cells of *Hydra*.

1.1 *Hydra* as a useful model organism

The freshwater polyp *Hydra* belongs to the phylum cnidarian. Its simple body plan is radial symmetric and the body is divided in three regions. These are, the head region with the hypostome and mouth opening which are surrounded by tentacles, the body column with the gastric region and the foot with the basal disc (Fig. 1.1 A) (Bode, 2009). The tissue of *Hydra* is diploblastic and consists of only two epithelial layers: the ectoderm which forms the outer body wall and the endoderm which lines the inner gastric region (Fig. 1.1 A, B). The epithelial layers are separated by a cell free matrix, called mesogloea which functions as an extracellular matrix (Sarras, 2012). Both cell layers are attached to the mesogloea (Shimizu et al., 2008) and small pores allow a communication between the cells sending finger-like protrusions into these pores (Sarras, 2012). Epithelial cells in *Hydra* are very peculiar, because they are bifunctional epitheliomuscle cells. The basal region takes over a muscle function, while the apical region functions as an epithelium (Leclére and Röttinger, 2017; Seybold et al., 2016). Contractility of the polyp is ensured by a local enrichment of actin bundles in the basal cellular possesses running along the mesogloea (called myonemes). Ectodermal myonemes run longitudinally to the body axis which ensures body contraction, while endodermal myonemes are aligned circularly which allows body elongation (Fig. 1.1 B) (Aufschnaiter et al., 2017).

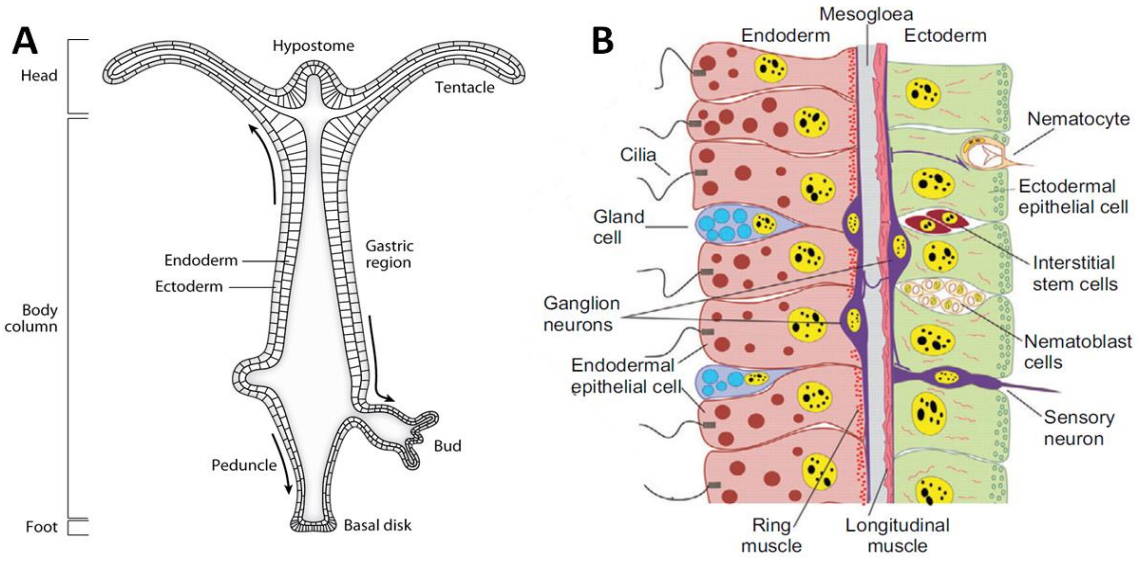

Figure 1.1: Schematic representation of the body plan and diploblastic tissue of *Hydra*. (A) The body is divided into three main regions, head, body column and foot. The head contains the hypostome and mouth opening which is surrounded by a ring of tentacles. The body column includes the budding region which shows an early bud (left) and a late detaching bud (right). The basal end consists of the peduncle which ends in the foot with the basal disc. The tissue consists of two epithelial layers, the outer ectoderm and the inner endoderm. Arrows indicate the direction of tissue movement in the polyp caused by constant proliferation of all cell types (Bode, 2009). (B) Representation of the diploblastic tissue and cell types in *Hydra*. Ectodermal epithelial cell (green), endodermal epithelial cell (red) form two stem cell lines in *Hydra*. The third stem cell line delivers interstitial cells (dark red) which include nematocytes and nematoblasts (orange), sensory and neuronal cells (violet), gland cells (blue) and germ cells (not shown) (Technau and Steele, 2011).

The double layered tissue is formed by three stem cell lines: ectodermal epithelial cells, endodermal epithelial cells and interstitial stem cells. Interstitial stem cells (I-cells) are multipotent stem cells and are located in the interstitium (extracellular space) between ectodermal cells (Fig. 1.1 B) (Technau and Steele, 2011; Hobmayer et al., 2012). A distinction is made between big I-cells which keep their stem cell character and are not migrating under normal circumstances and small I-cells which migrate actively to their final destinations in e.g. tentacles (Boehm and Bosch, 2012). Underways and within these structures, the I-cell subtypes differentiate into nematocytes, gland cells and sensory or ganglionic neuronal cells.

Ectodermal and endodermal cells of the midgastric region are subject to permanent cell proliferation and renew every four days (Martinez and Bridge, 2012). This leads to a continuous tissue movement in the polyp towards its terminally differentiates structures, the head and the foot (Fig. 1.1 A). Ectodermal cells are shifted permanently and likely passively, to the termini - like hypostome, tentacles and foot. At their final destination, epitheliomuscle cells terminally differentiate into, e.g. cnidarian specific battery cells of the tentacles (Hobmayer et al., 2012) or basal disc cells. Most of the proliferating cells (nearly 80 %) are exported in the mid body to form a bud in the budding region (Bode, 1996). This represents the typical asexual reproduction process in *Hydra*.

1.2 Reproduction in *Hydra*

Hydra propagates asexually as well as, rarely, sexually. During sexual reproduction the polyps generate a single egg (Fig. 1.2 A, A´) (female) or several testes (Fig. 1.2 B, B´) (male) (Martin et al., 1997), mostly in different polyps separated from each other or in hermaphrodites. The sexual reproduction is a stress reaction to starvation or adverse conditions. In the laboratory, this possibility of reproduction is necessary to generate transgenic polyps (Wittlieb et al., 2006; Klimovich et al., 2019).

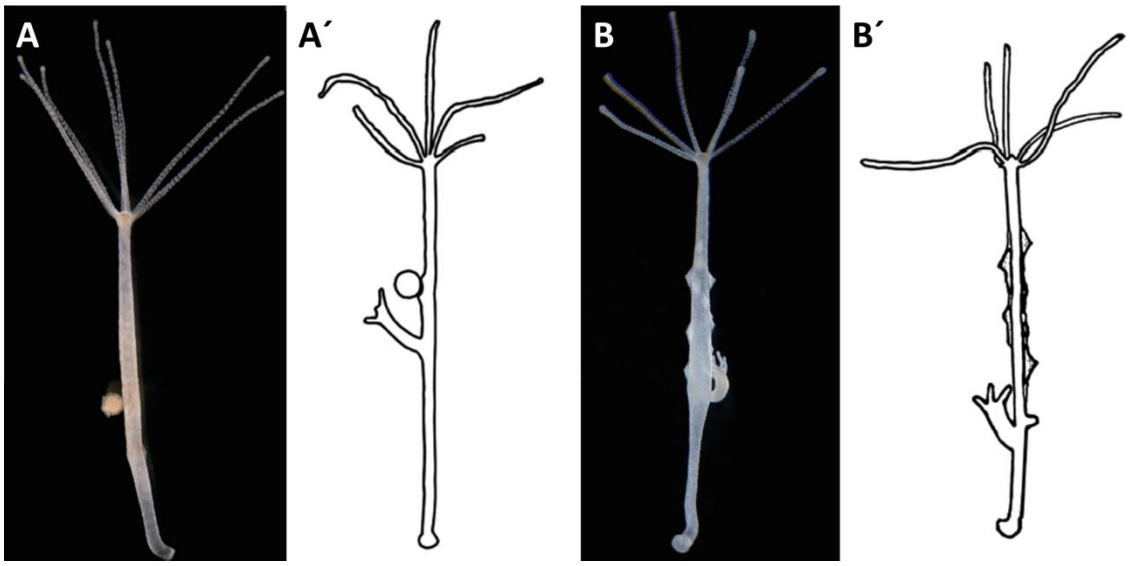

Figure 1.2: Sexual reproduction in *Hydra*. (A, A´) Female polyps develop a single egg. (B, B´) Male polyps develop multiple testes (Modified after Wang et al., 2012).

Under well suited conditions, *Hydra* usually propagates by budding. The bud evaginates from the body column and develops to a complete polyp which detaches after 4 days as an autonomous polyp (Otto and Campbell, 1977). The budding process is divided into three developmental phases and ten morphologically distinguishable stages (Fig. 1.3, Otto and Campbell, 1977). Morphogenetic changes and pattern formation occur during the budding process, in which various molecular signaling systems are involved (Böttger and Hassel, 2012). During the initiation phase (bud stage 1-3), the ectoderm starts to thicken by recruiting tissue (stage 1) which is controlled by canonical and non-canonical Wnt signaling (Philipp et al., 2009). In stage 2, the endoderm starts to push out and in stage 3 a clearly recognizable bud tip is visible (Fig. 1.3, green box). The ectodermal actin cytoskeleton is loosened, so that the endoderm can evaginate (Philipp et al., 2009; Aufschnaiter et al., 2017). The elongation phase is primarily characterized by the evagination of the newly formed bud which is mainly performed by tissue recruitment from the parental animal (Fabila et al., 2002). Tissue recruitment stops at bud stage 6 when the tentacles start to evaginate (bud stage 6-7, Fig. 1.3, orange box). Tentacle evagination occurs under control of Wnt signaling (Hobmayer et al., 2000; Philipp et al., 2009). The detachment phase starts with a tissue constriction at the bud base (stage 8, Fig. 1.3, red box). This constriction progresses continuously and finally the foot starts to differentiate (stage 9). In stage 10, foot differentiation is completed and the bud is connected by a tiny tissue bridge. Ultimately, a sphincter contraction leads to detachment (Takahashi et al., 1997).

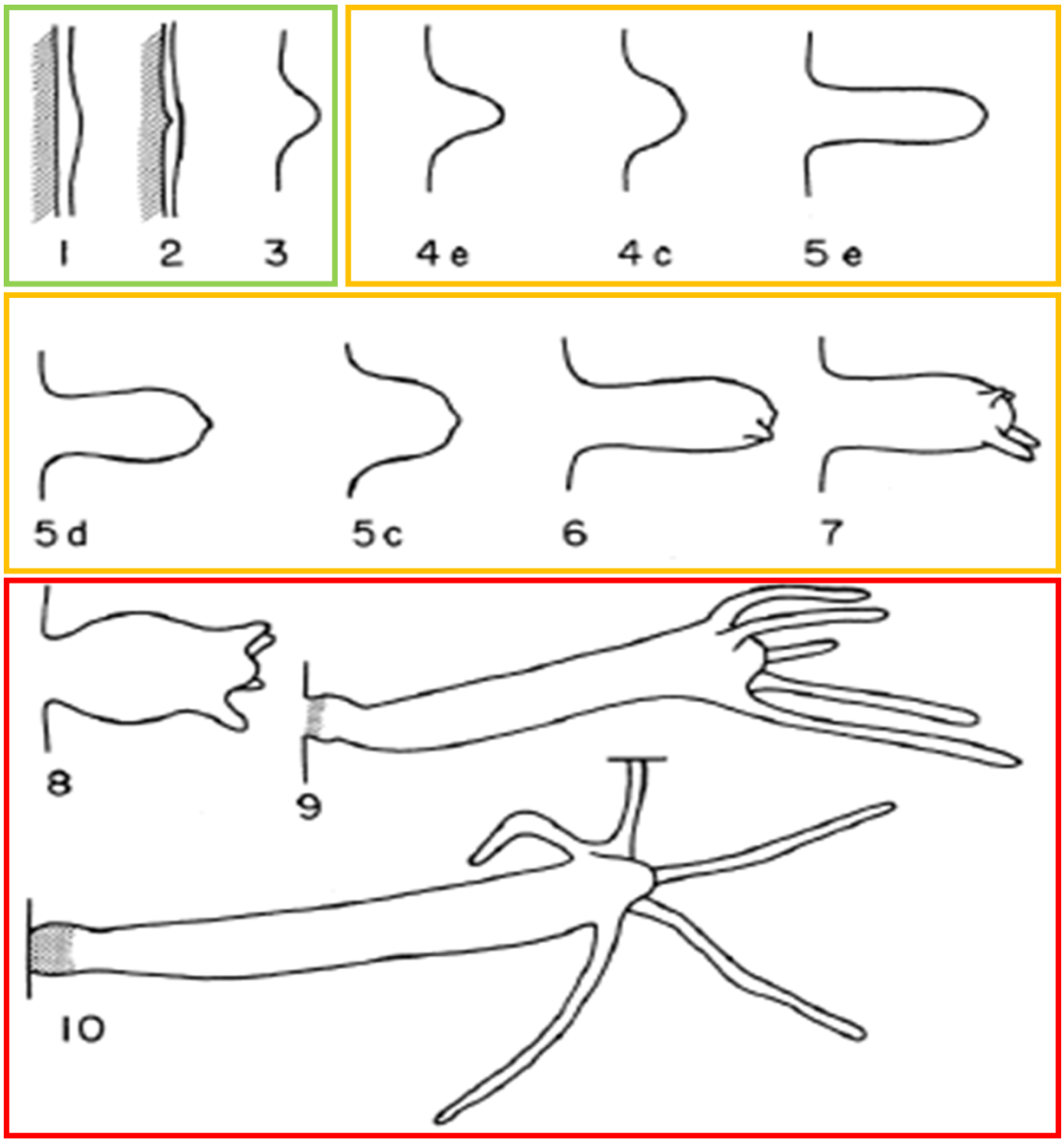

Figure 1.3: Budding process in *Hydra*. Initiation phase (green) includes bud stage 1-3. During this phase the ectoderm starts thickening, followed by the endoderm and a well recognizable bud tip is visible. Elongation phase ([orange] includes bud stage 4-7). This phase is mainly characterized by elongation of the bud and the start of tentacle development. Detachment phase ([red] includes bud stage 8-10). During this phase a strong constriction at the bud base is established and foot differentiation takes place. It ends up in tissue separation (Modified after Otto and Campbell 1977).

The tissue dynamics and its recruitment into the evaginating bud are interesting and not yet fully understood. It is assumed that the tissue is recruited via concentric rings into the new formed bud (Otto and Campbell, 1977; Fabila et al., 2002; Berking, 2003). Already in the early bud stages, two populations of cells were described which form the later head structure and the bud base. These areas are marked in grey (for head structures) and black (for the bud base) (Fig. 1.4, stage 1). In stage 5-6, the area marked black reaches the bud base which coincides with the static phase at the bud when no more tissue is recruited (Fig. 1.4, stage 5-6) (Otto and Campbell, 1977; Fabila

et al., 2002; Berking, 2003). During this phase the detachment process is initiated and the constriction starts at the bud base (Fig. 1.4 stage 7-8). Based on this, the fate of the cells is already determined in early stages. This partially coincides with the expression pattern of genes which are essential for bud development and detachment.

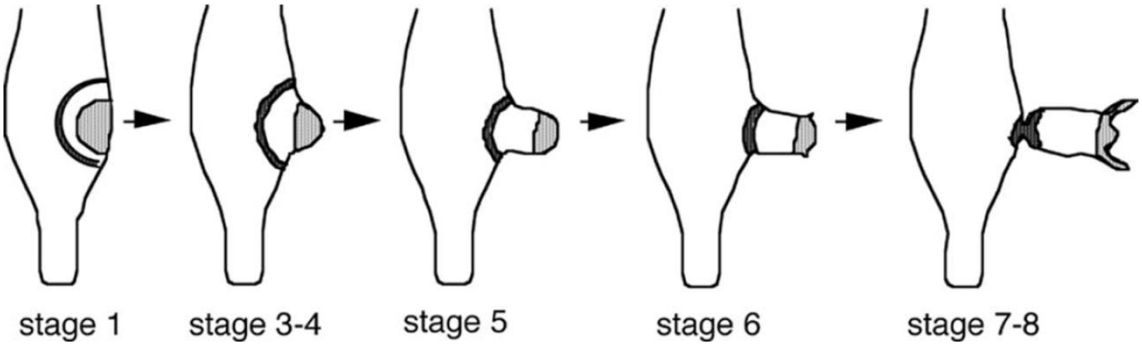

Figure 1.4: Schematic representation of tissue recruitment by concentric rings during budding process in *Hydra*. Grey areas indicate the region of the later differentiated head structure. Black areas show the tissue what later forms the base. (Fabila et al. 2002)

The detachment process is of particular interest, where a complete separation occurs within an intact double layered epithelium without apoptosis or a wound. *Hydra* contains a complex genetic toolkit which is comparable to vertebrates (Galliot, 2012; Steele, 2002). Especially during the detachment process multiple signaling pathways (FGFR, Notch, Ephrin and Wnt) are involved (Sudhop et al., 2004; Philipp et al., 2009; Münder et al., 2010; Prexl et al., 2011; Tischer et al., 2013; Böttger and Hassel, 2012). A sharp boundary at the bud base is generated by an interplay between FGFR and Notch signaling (Münder et al., 2010), while FGFR signaling taking a leading role for bud detachment (Sudhop et al., 2004; Hasse et al., 2014)

1.3 FGFR signaling is essential for bud detachment in *Hydra*

FGFR belong to the family of receptor tyrosine kinases and are highly conserved within the animal kingdom (Dai et al., 2019; Rebscher et al., 2009). They are essential during embryonic development and are involved in e.g. cell migration, cell differentiation, proliferation, pattern formation and morphogenesis (Thisse and Thisse, 2005). FGFRs are membrane bound receptors with three characteristic domains (Ornitz and Otoh, 2001). The extracellular domain consists in general of three Ig-loops that allow FGF ligand binding and an acidic box between Ig-loop I and II. The transmembrane domain anchors the receptor into the membrane and the typical intracellular tyrosine kinase domain (Fig. 1.5 A.). Ligand binding between Ig-loop II and III leads to dimerization of two receptors which results in transphosphorylation of the intracellular kinase domains

(Fig. 1.5 B). Phosphorylation generates binding sites for pTyr-specific downstream signaling elements and allows the activation of several intracellular signaling pathways (Xie et al., 2020). The specificity of intracellular signaling pathways that are activated in a certain cell type is ensured by different FGF receptors and a multitude of different FGF ligands (Ornitz and Itoh, 2015). In vertebrates, for example, four different FGFRs and 22 FGF ligands are described (Ornitz and Itoh, 2015). The diversity of the receptor is increased by alternative splicing which results in at least 48 FGFR isoforms (Duchesne et al., 2006).

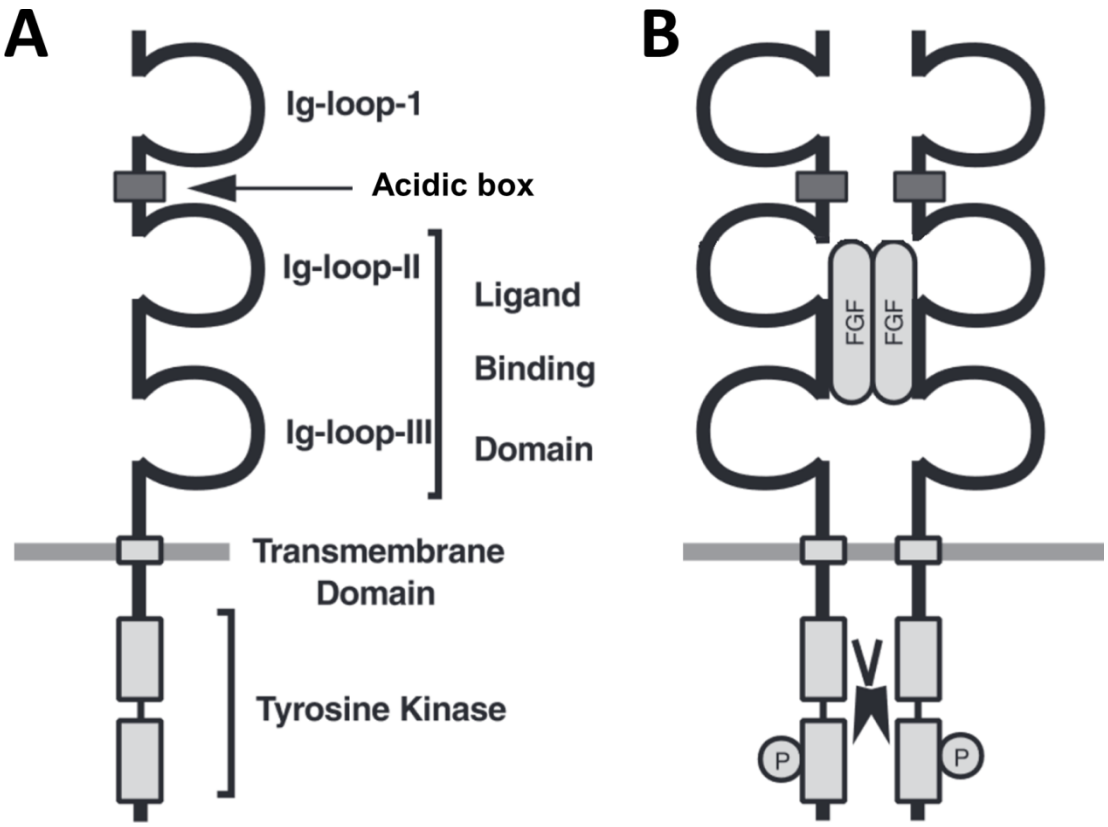

Figure 1.5: Schematic structure of FGFR and FGF mediated signaling. (A). FGFR consists of three domains: 1: extracellular domain consisting of Ig-loops and acidic box. 2: transmembrane domain. 3: intracellular tyrosine kinase domain. (B) Binding of FGF ligand between Ig-loop II and III leads to a dimerization and starts signal transduction (Dickson et al., 2000).

In *Hydra*, two FGFRs are known (Sudhop et al., 2004; Rebscher et al., 2009; Rudolf et al., 2013). The FGFRa (also called Kringelchen) is known to initiate and control the bud detachment process (Sudhop et al., 2004; Hasse et al., 2014), while the function of FGFRb still has to be investigated. Furthermore, four potential FGF ligands were identified in *Hydra*. Phylogenetic analysis showed that one of them is a member of the FGF8 group, while the others branch close to but not within known FGF groups (Lange et al., 2014). In addition to the ligands, a number of cDNAs encoding potential adapter /

docking proteins for FGFR signaling have been isolated from *Hydra* and show partial coexpression with FGFR (Suryawanshi et al., 2020).

The *FGFRa* (*kringelchen*) is expressed very weak throughout the entire body column which is shown by RT-PCR and is strongly up-regulated during the budding process (Sudhop et al., 2004). In early bud stages, it is expressed in the tip of the bud. From stage 4 onwards, a strong gene expression is observed at the bud base as a broad expression ring. This expression domain is sharpened in stage 6-7 when the detachment phase is initiated (Fig. 6 A). The expression persists on the parental side for a short time even after detachment (Sudhop et al., 2004; Münder et al., 2010). Pharmacological inhibition with the FGFR-specific inhibitor, SU5402, leads to non-detaching phenotypes (Y-shaped animals) and therewith a stable secondary axis (Fig. 1.6 E) (Sudhop et al., 2004). SU5402 interacts with the ATP binding site and prevents phosphorylation of the kinase domain and thus signaling (Mohammadi et al., 1997).

Further studies allowed direct insight into FGFRa function in *Hydra*. To achieve this, two FGFR transgenic lines are established which indicate a direct function during bud detachment and tissue separation. First, a truncated FGFR transgenic line in which the intracellular kinase domain is missing leads to animals that are not able to finalize bud detachment. This results in animals with multiple buds (Fig. 1.6 C). The animals are still able to develop a constriction at the bud base so that final detachment is prevented. The interpretation of the data is somewhat difficult, since the endogenous FGFR is still present. Therefore, the authors suggest a dominantly negative regulation of the FGFR signaling pathway in FGFR truncated transgenic animals missing the intracellular domain. Later on, the non-detaching buds shifted towards the basal disc following the normal tissue movement (Fig. 1.6 C) (Hasse et al., 2014). This is comparable to SU5402-treated animals when treatment took place after bud stage 3-4 (Sudhop et al., 2004). In contrast, overexpression of the full-length receptor leads to autotomy (tissue separation) within the tissue (Fig. 1.6 D) (Hasse et al., 2014). Based on these data, it is proposed that an FGFR dependent signaling pathway in *Hydra* plays a crucial role in tissue separation and proper bud detachment.

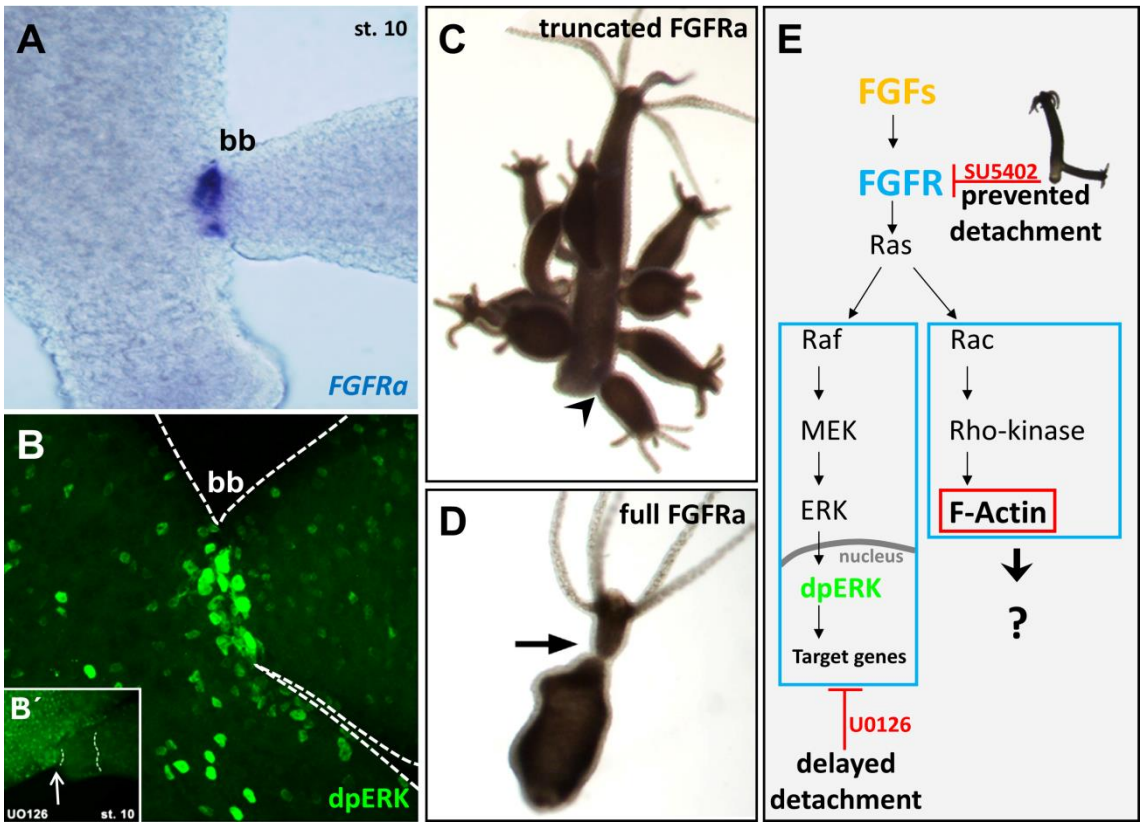

Figure 1.6: Summary of FGFR signaling and function in *Hydra*. (A) Expression of *FGFRa* (*kringelchen*) after *in situ* hybridization in an animal with a bud in stage 9-10. (B) Localization of dpERK by immunohistochemistry. A cluster of strongly dpERK-positive nuclei occurs at the bud base of a stage 9-10 bud. (B´) This phosphorylation is prevented by U0126 treatment. (C) Truncated FGFRa transgenic lines fail to finally detach buds. This leads to animals with multiple buds. (D) Ectopic overexpression of a full length FGFRa transgenic line leads to autotomy within the body column (arrow). (E) Model for FGFR dependent downstream pathways targeting tissue separation (According to, Sudhop et al., 2004; Hasse et al., 2014).

Furthermore, they elucidate an involvement of the extracellular signal-regulated kinase (ERK) during bud detachment in *Hydra*. A cluster of strong dpERK positive nuclei are detected from bud stage 8 onwards and coincides with the beginning of the constriction at the bud base (Fig. 1.6 B). This *de novo* phosphorylation of ERK is prevented by a specific inhibition of MEK with U0126 (Fig. 1.6 B´) (Favata et al., 1998; Duncia et al., 1998) but also by FGFR inhibition via SU5402. They propose an FGFR dependent activation of the Ras-MEK-ERK signaling pathway in *Hydra*. Compared to FGFR inhibition, ERK inhibition does not prevent detachment, it rather leads to a clearly delayed detachment (Fig. 1.6 E) (Hasse et al., 2014). Additionally, it is described that the actin cytoskeleton changes its organization level in regions of FGFR expression. Therefore, a Rho-dependent pathway targeting the cytoskeleton is proposed (Fig. 1.6 E). Rho signaling is well known to influence actin reorganization and leads to increased contractile forces for morphogenetic changes (Wheeler and Ridley, 2004; Menke and Giehl, 2012). The regulation of the actin cytoskeleton and Rho signaling during bud detachment is not investigated, but would be well suited to be involved in this morphogenetic process.

1.4 Cellular contractility ensured by actomyosin enables morphogenesis

During embryonic development, cellular contractility is a fundamental mechanism to regulate morphogenetic processes (Sutherland and Lesko, 2020). Essential is the establishment of actomyosin complexes at the cellular cortex which plays a major role for cell shape changes (Martin and Goldstein, 2014; Salbreux et al., 2012; Martin et al., 2009). Cortical actomyosin consists of actin filaments, non-muscle myosin II and different proteins which regulate the organization of the network stability and contractility (Martin, 2016). The subcellular localization and concentration therefore plays a crucial role for the tissue behavior during morphogenesis. For example, apical constriction is a highly conserved mechanism during developmental processes (Pearl et al., 2017). There, a periodic contraction of apically located actomyosin leads to tissue invagination, like during gastrulation (Fig. 1.7). During this process, the actomyosin is exclusively established in the apical compartment of the epithelium. The resulting locally limited contractile forces in this small population of cells lead to tissue invagination (Fig. 1.7 B) (Pearl et al., 2017). The level of network formation and contractility depends on different actin binding proteins which are involved to regulate network formation (Martin, 2016). Therefore, myosin motors exert the contractility in the network but also promotes network formation (Newell-Litwa et al., 2015). The following chapter describes the individual components of the contractile network in more detail.

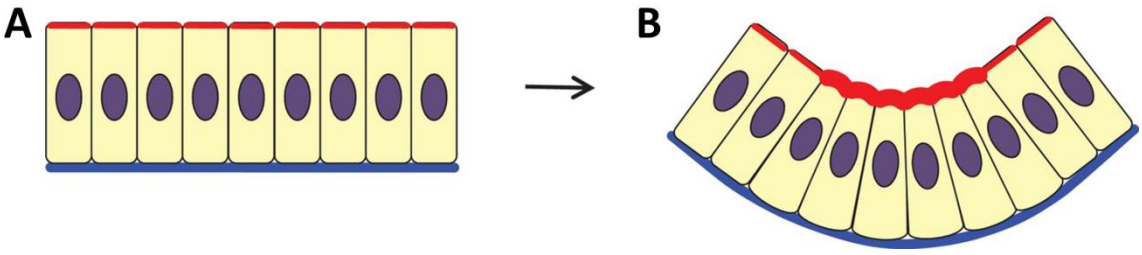

Figure 1.7: Schematic representation of apical constriction by actomyosin in an epithelial layer. Compartment-specific establishment of actomyosin complexes leads to morphogenetic changes in a tissue (Modified after Pearl et al., 2017).

1.5 Actomyosin: machinery for cellular contractility

Actin is a highly conserved structural protein which is found in all eukaryotic cells and gave the cell the ability to stabilize their shape, to change their shape and to form cellular protrusions for migration (Gunning et al., 2015; Dominguez and Holmes, 2011; Flechter and Mullins, 2010). A distinction is made between globular actin monomers (G-actin) and polymerized filamentous actin (F-actin) which forms the cellular actin cytoskeleton network (Pollard, 2016) (Fig 1.8). The actin cytoskeleton, a collection of F-

actin with regulatory proteins is the primary force generator in a cell and generates pushing forces (protrusion) by a continuous polymerisation or pulling forces (contraction) in conjunction with myosin II as a molecular motor (Svitkina et al., 2018). In order to modulate its properties, F-actin is organized in different architectures that generate versatile organization levels (Alberts et al., 2010). F-actin filaments are polar polymers consisting of G-actin with a barbed end (+ end) and pointed end (- end) which differ in their dynamics (Blanchion et al., 2014). Filament elongation mainly occurs at the fast-growing barbed end of the filament but also at the slow-growing pointed end and is controlled by nucleation factors (Pollard, 2016). For proper nucleation, cells use a set of actin nucleating proteins including the actin related protein 2/3 (Arp 2/3) complex, formin and tandem-monomer-binding nucleators (Fig. 1.8) (Firat-Karalar and Welch, 2010). Therefore, formins produce long, unbranched actin filament (Yang et al., 2007) while the Arp 2/3 complex generates branching daughter filaments from the side of the mother filament and is therefore also involved in network formation (Svitkina et al., 2018; Machesky et al., 1994; Welch et al., 1997).

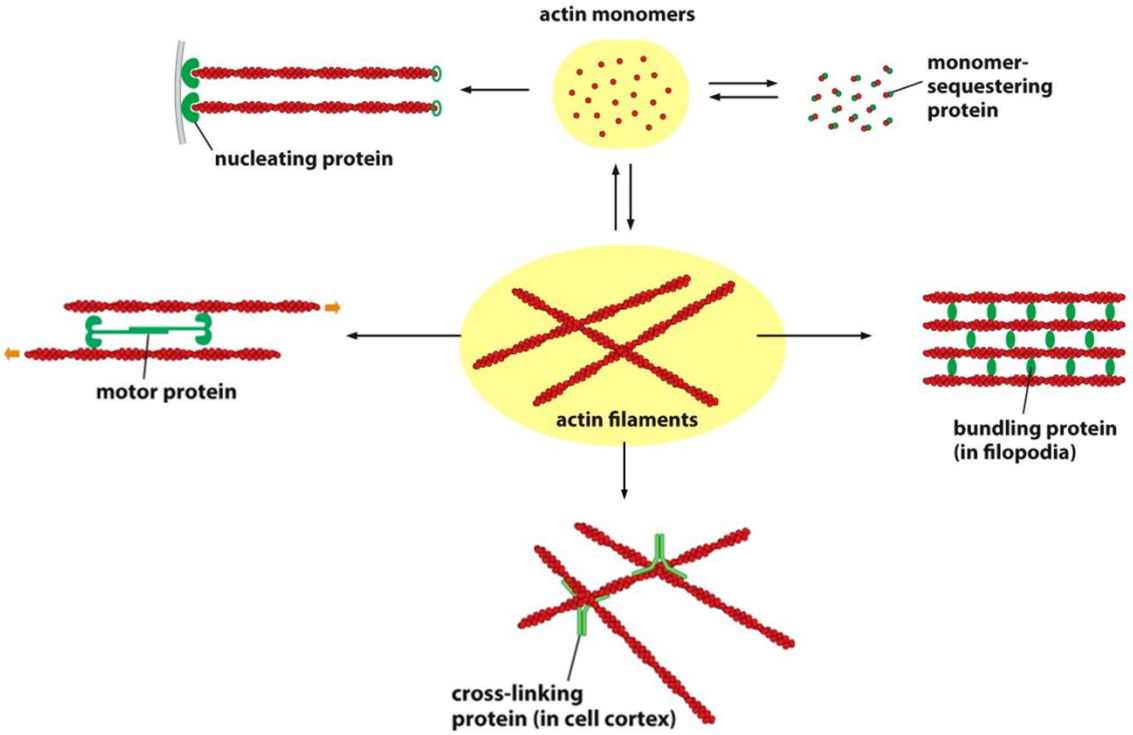

Figure 1.8: Schematic representation of F-actin nucleation and network formation. F-actin arises from actin monomers (G-actin) which is promoted by nucleation proteins. Network assembly is promoted by the motor protein myosin and, on the other hand, by special crosslinking and bundling proteins. A different composition of these actin related proteins decides over network architecture (Modified after Alberts et al., 2010).

Further network organization is modulated by actin binding proteins (Pollard, 2016). Cross-linking and bundling proteins such as filamin or α-actinin regulate either network or bundle formation depending on their concentration (Fig. 1.8) (Courson and Rock, 2010; Kasza et al., 2010; Meyer and Aebi, 1990; Schmoller et al., 2008; Wachsstock et al., 1993; Wachsstock et al., 1994). Furthermore, the nucleation kinetics influences the stability of crosslinked F-actin networks (Falzone et al., 2012). An increased rate of actin nucleation disturbes bundle and network formation and therefore represents an important factor for filament stability and network dynamics (Falzone et al., 2012).

To establish a contractile network that generates pulling forces, e.g. during morphogenetic changes, actin based myosin motor proteins are required (Svitkina et al., 2018). Myosins form a superfamily with at least 25 different classes (Conti and Adelstein, 2008). A distinction is made between conventional myosin (class II) which performs regular cellular contractility in muscle or non-muscle cells while all other identified myosins are called unconventional myosins. Besides the ordinary muscle contraction, especially nm-myosin II in involved in a large number of cellular processes and functions, such as transport of intracellular molecules, contractile network formation and complex pattern formation during developmental processes by contractile forces (Jena, 2020). Nm-myosin II is an actin binding motor protein that generates contractile forces with cross-linking properties. An nm-myosin II molecule is composed of two heavy chains, two essential light chains (ELC) and two regulatory light chains (RLC) (Fig. 1.9) (Vincente-Manzanares et al., 2009; Beach et al., 2014). The globular head domain of the heavy chains contains a binding site for actin and an ATPase domain to hydrolyse ATP. This hydrolysis is fundamental to generate contractile forces in which myosin molecules slide against actin filaments (Sekine and Yamaguchi, 1963). The head domain is followed by the neck region for light chain binding (which modulate activity and stability). The last domain is the tail which promotes dimerization of the heavy chains (Vincente-Manzanares et al., 2009).

The unphosphorylated / inactive state of myosin II is characterized by an intermolecular head-to-head interaction that inhibits the ATPase activity, accompanied by folding in a compact molecule which prevents actin binding and therefore filament assembly (Fig. 1.9) (Wendt et al., 2001; Vincente-Manzanares et al., 2009). By means of RLC phosphorylation, nm-myosin II changes into the active state which enables actin binding and leads to actomyosin bundles. Phosphorylation of RLC is essential for nm-myosin II activation, contractility as well as for filament assembly and is regulated by several signaling pathways (Kassianidou et al., 2017).

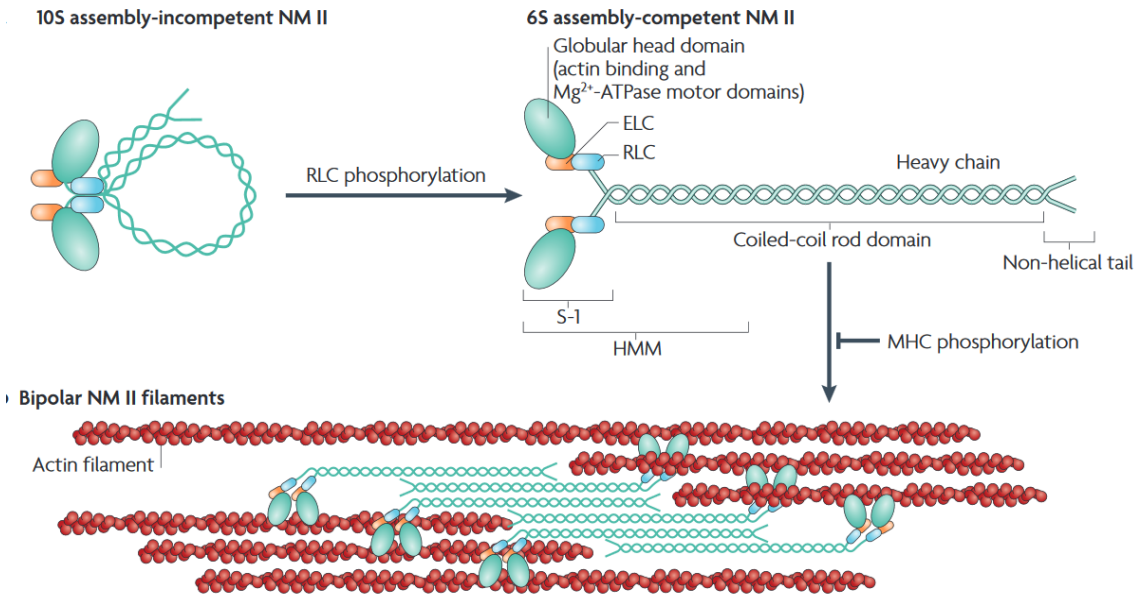

Figure 1.9: Schematic representation of nm-myosin II states and filament assembly. In the 10S conformation the myosin II molecule forms a hairpin structure that is not able to hydrolyze ATP or to bind actin. RLC phosphorylation leads to activation and changes the conformation into the 6S which is able to bind actin. This activation leads to actin and myosin interaction and results in actomyosin filaments (Vincente-Manzanares et al., 2009).

1.6 Phosphorylation of RLC regulates actomyosin networks

The N-terminal region of RLC (amino acids 1-20) includes a total number of five different phosphorylation sites which are required for proper myosin II activation and its regulation (Fig. 1.10 A). Phosphorylation at Ser1, Ser2 and Thr10 represents the inhibitory sites of RLC, leads to low contractility and allows network reorganization (Fig. 1.10 B). Phosphorylation at Thr19 and Ser20 (activation sites) is crucial for activation and formation of contractile actomyosin bundles (Nishikawa et al., 1984; Vincente-Manzanares et al., 2009; Komatsu and Ikebe, 2007). The monophosphorylation of RLC at Ser20 increases myosin II activity and actomyosin network stability, while diphosphorylation at Thr19 and Ser20 is synergistic for both (Fig. 1.10 C) (Ikebe and Hartshorne, 1985; Ikebe et al., 1987; Watanabe et al., 2007). The phosphorylation level thereby is responsible for the association / dissociation level during stress fiber assembly (Fig. 1.10 D). At a low phosphorylation level, the dissociation rate is higher than the association of new fibers. Mid-level phosphorylation results in an intermediate dissociation / association ratio, while high level phosphorylation significantly increases the association level, resulting in a strong contraction with stable actomyosin stress fibers (Watanabe et al., 2007; Newell-Litwa et al., 2015; Kassianidou et al., 2017).

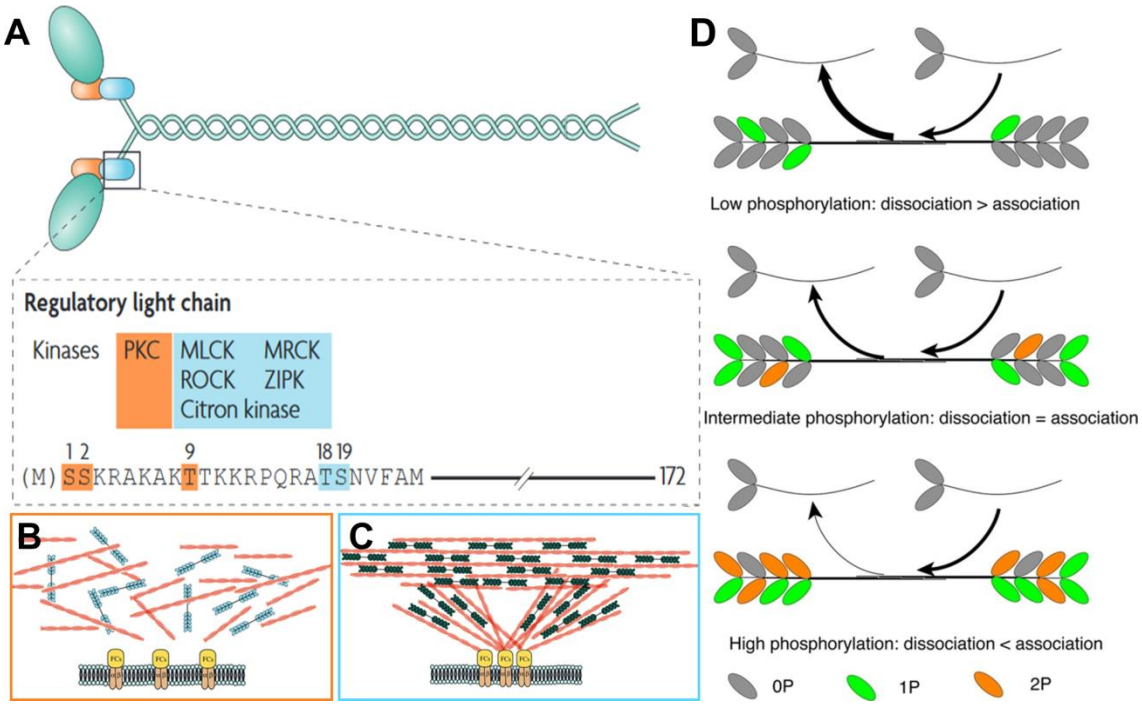

Figure 1.10: Phosphorylation level of the RLC is important for network formation. (A) The N-terminal region of RLC includes several phosphorylation sites. The phosphorylation therefore is performed by several pathways which are decisive for network assembly (B). Phosphorylation at Ser1, Ser2 and Thr9 leads to network reorganization and low contractility (B). Phosphorylation at Thr18 and Ser19 is essential for contractile networks (C). The level of phosphorylation and between mono- and double phosphorylation decides over the dissociation / association ratio (D) (According to Vincente-Manzanares et al., 2009; Komatsu and Ikebe, 2007; Watanabe et al., 2007).

A variety of signaling pathways affect RLC phosphorylation which leads to a different intensity of network formation and contractility (Vincente-Manzanares et al., 2009; Newell-Litwa et al., 2015). Two mainly considered ways for RLC phosphorylation are those by MLCK and Rho signaling (Lavayer and Lecuit, 2012; Betapudi, 2013). MLCK phosphorylates RLC in a calcium dependent manner at Thr19 and Ser20, while myosin-light-chain-phosphatase (MLCP) dephosphorylates RLC to decrease actomyosin network formation which leads to an intermediate level of network formation. This way of activation forms a balanced phosphorylation level with the MLCP (Watanabe et al., 2007).

However, Rho signaling modulates RLC phosphorylation in a positive way, either by inhibiting the MLCP to increase RLC phosphorylation or by phosphorylating RLC directly (Kimura et al., 1996; Hartshorne et al., 1998; Zhang et al., 2015). Therefore, the small GTPase RhoA activates the rho-associated-kinase (ROCK) which then fulfills dual functions. ROCK is able to phosphorylate RLC directly at the activation site (Thr19/Ser20) and additionally prevents RLC dephosphorylation by blocking the MLCP (Fig. 1.11) (Sellers, 1991; Bresnick, 1999). Furthermore, Rho signaling is essential for the cellular localization of phosphorylated RLC and leads to an apical enrichment of

actomyosin for apical constriction (Borges et al., 2011). Thus, Rho mediated influence on RLC phosphorylation results in a high level of network formation. This formation is typical for stress fibers during morphogenetic processes (Watanabe et al., 2007; Martin and Goldstein, 2014; Newell-Litwa et al., 2015).

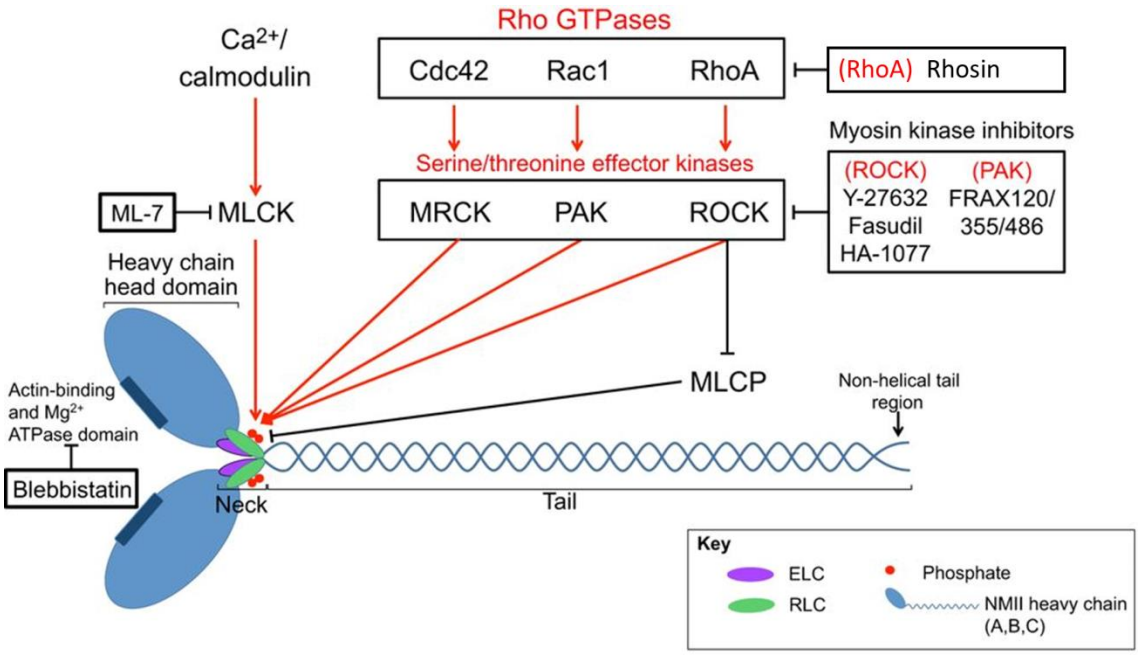

Figure 1.11: Model for several signaling pathways that converge on RLC phosphorylation. MLCK is a calcium/calmodulin dependent kinase that is able to phosphorylate RLC at Ser19 as well as Thr18. Different Rho GTPases phosphorylates RLC, while RhoA signaling is involved during morphogenetic changes. ROCK therefore takes over two functions: it directly phosphorylates RLC and, furthermore, it blocks RLC dephosphorylation by inhibiting MLCP. A toolkit of inhibitors is available to interfere within the pathways and influence filament assembly (Modified after Newell-Litwa et al., 2015).

1.7 Cortical actomyosin is an essential component of morphogenesis

Stress fibers are composed of F-actin, cross linkers like α-actinin and nm-myosin II motor proteins (Kassianidou et al., 2017). These stress fibers are relevant to generate contractile forces and transferring them to the extra cellular matrix due to direct attachment to focal adhesion complexes (Chang and Kumar, 2013; Kassianidou and Kumar, 2015; Kassianidou et al., 2017; Soiné et al., 2015; Lee and Kumar, 2016). The subcellular localization and concentration of actomyosin complexes are crucial for the cellular function within a tissue allowing boundary formation or tissue separation (Fagotto, 2014).

On single cell level, contractility is responsible to regulate, e.g. cell shape, motility, division and differentiation (Prager-Khoutorsky et al., 2011; Downing et al., 2013; Burnette et al., 2014). At multicellular level, contractile forces promote cell migration, tissue morphogenesis during development and wound healing (Tamada et al., 2007; Tambe et al., 2011; Heisenberg and Bellaiche, 2013; Schwayer et al., 2016). During tissue morphogenesis an asymmetric establishment of actomyosin complexes within the cells led to a unilateral increased contractility which results in boundary formation between cells (Fig 1.12. A). In addition to the increased contractility, cell-cell connections by e.g. cadherins are reinforced. Cadherins are the major adhesion molecules at intracellular junctions to connect cells together. They also function as mechanotransducers that detect tensional changes and trigger a reinforcement of intercellular connections (Leckband and Rooij, 2014). In a larger cell complex this cellular behavior leads to a sharp boundary (Fig. 1.12 B). This establishment of unilateral contractility and reinforced adhesion provides the basis for tissue separation. A distinction is made between different organization levels (Fig. 1.12 C). A normal cellular connection, as in dynamic tissues, is characterized by a dynamic cellular cortex and permanent active actin polymerization (Fig. 1.12 C/1). In case of morphogenesis, actomyosin complexes are established at the cellular cortex and the cadherin based cell adhesion is reinforced (Fig. 1.12 C/2). This constellation leads to high stiffness within the tissue which is necessary for morphogenetic changes in a tissue. In case of tissue separation, the cadherin adhesion is decreased and the actomyosin complexes contracts (Fig. 1.12 C/3). The separation between neighboring cells occurs by a rigid cellular cortex.

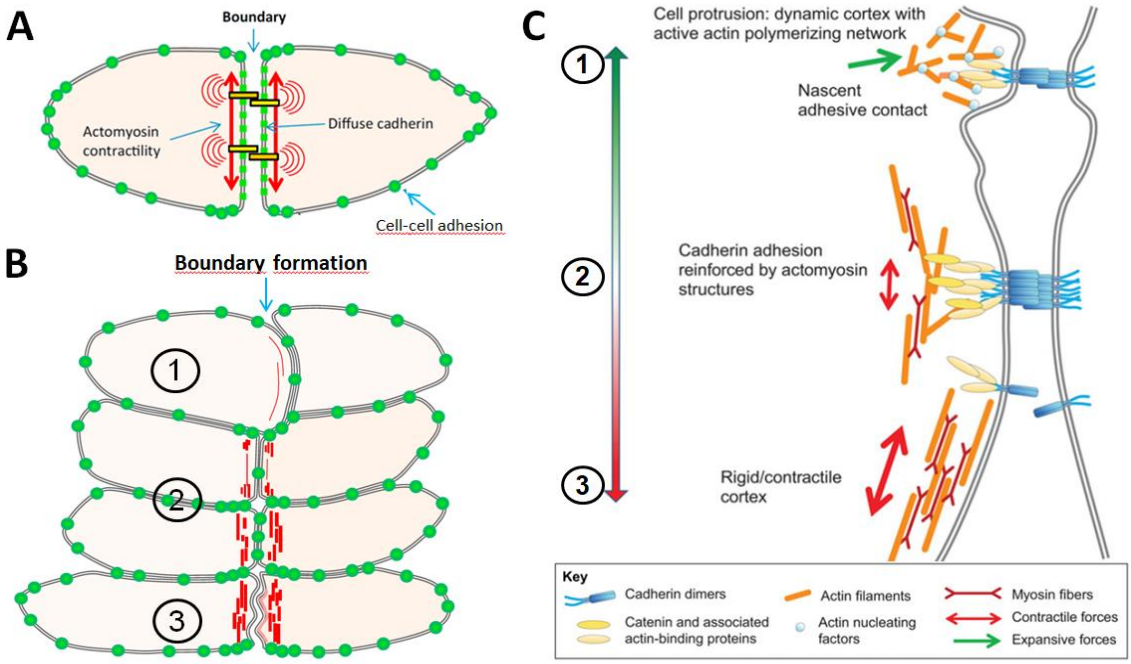

Figure 1.12: Schematic view on boundary formation by actomyosin and cell-cell adhesion. (A) Increased unilateral contractility at the boundary. Cell-cell adhesion by cadherin is shown in green. Decreased cell-cell adhesion is shown by the green dotted line. (B) Assembly of contractile fibers along the boundary (1-2). This accumulation of actomyosin leads to strong cortical contractility and alterations in cadherin localization (2). At last, contractile forces lead to disruption of the cell adhesion (3). (C) Detail of the establishment of contractile forces at the cellular cortex. (1) Dynamic cellular cortex. (2) Establishment of cortical actomyosin and reinforced cell adhesion (3) Contraction leads to separation in the cortex (Modified after Fagotto et al., 2013; Fagotto, 2014).

1.8 Pharmacological inhibition: A useful tool to modulate contractile filaments and disturb developmental processes

Inhibitors are used in research to block specific proteins in the cellular metabolism and are employed for different biological processes (Buker et al., 2012). As already mentioned, different signaling pathways phosphorylate RLC to activate filament assembly and contractile forces (Fig. 10 A, Fig. 11) (Vincente-Manzanares et al., 2009). To interfere with RLC phosphorylation several inhibitors are available to modulate RLC phosphorylation by different pathways. The most important inhibitors block consecutive steps in the signaling pathway and thereby influence developmental processes. ML-7 for example, represent a specific inhibitor for MLCK, prevents tissue invagination during gastrulation in the sea anemone *Nematostella* (Pukhlyakova et al., 2018).

Rhosin specifically inhibits RhoA activity as well as RhoA dependent cellular functions without affecting Cdc42 or Rac1 signaling (Shang et al., 2012). For the Rho associated kinase several inhibitors are available (Kroening et al., 2010). Rockout for example, which inhibits ROCK, prevents the FGFR dependent apical constriction during development of the posterior lateral line primordium (Harding and Nechiporuk, 2012).

Blebbistatin is a specific inhibitor for myosin II which binds at the globular head domain and blocks ATP hydrolysis as well as actin binding (Kovacs et al., 2004). Treatment of embryos with blebbistatin leads to a fusion of the notochord boundary and results in non-separating cells and a stable fused tissue (Fagotto et al., 2013).

The presented toolkit of inhibitors is well suited to investigate whether one of these signaling pathways is involved in morphogenesis during developmental processes.

1.9 Goals of the project

Bud detachment in *Hydra* is a well described process in which several signaling systems act in overlapping regions at the late bud base (Böttger and Hassel, 2012). In this process FGFR signaling plays a major role and initiates at least bud base constriction and tissue separation (Sudhop et al., 2004, Hasse et al., 2014). In addition, Hasse et al., 2014 demonstrated that FGFR signaling influences the organization level of the actin cytoskeleton at the constriction site. Neither rearrangement of the actin cytoskeleton nor the role of intracellular pathways targeting the actin cytoskeleton at the late bud base in *Hydra* has been investigated so far. Therefore, the main approaches in this project were to elucidate:

1. Whether the actin cytoskeleton is involved during the bud detachment process. For this purpose, phalloidin-TRITC staining was carried out in order to describe the behavior of the actin cytoskeleton during bud detachment. In comparison, the actin cytoskeleton is to be examined in other morphogenetic regions.

2. Which signaling pathways control bud detachment as well as a comparative analysis of identified pathways in other morphogenetic regions. Morphogenetic processes in vertebrate and fly are mostly under control of a Rho-ROCK dependent pathway. In order to answer the question whether *Hydra* uses this pathway for bud detachment, the following steps were carried out:
    a. Expression analysis of mRNA via whole mount *in situ* hybridization to localize the spatial distribution of candidate genes within a pathway as well as of cofactors for actomyosin bundle formation.
    b. Identification of suitable inhibitors for the signaling pathway with subsequent analysis of the effect on morphogenetic processes in *Hydra*.
    c. Specific examination on the protein level by using antibodies that detect highly conserved epitopes of certain proteins within a candidate pathway.

3. How the bifunctional epitheliomuscle cells in *Hydra* manage to generate a constriction at the late bud base. To ensure the constriction and detachment of the bud by epitheliomuscle cells, the following questions were addressed:
    a. Do epitheliomuscle cells use the basal myonemes or the cellular cortex to perform the constriction? To clarify this question, detailed analyses of cLSM stacks were carried out.
    b. Are different signaling pathways involved to control either basal contractility by the myonemes or morphogenesis in epithelia muscle cells?

Chapter 1

Holz et al., 2017

Bud Detachment in *Hydra* Requires Activation of Fibroblast Growth Factor Receptor and a Rho–ROCK–Myosin II Signaling Pathway to Ensure Formation of a Basal Constriction

Developmental Dynamics 246:502–516, 2017

DOI: 10.1002/DVDY.24508

2.1 Introduction to Chapter 1

In Chapter 1 (Holz et al., 2017), the main approach was to elucidate whether the actin cytoskeleton as well as a Rho-ROCK-dependent signaling pathway are involved during the detachment process in *Hydra*. Therefore Phalloidin-TRITC staining was performed to examine the actin cytoskeleton during bud detachment. Furthermore gene expression analysis was performed to describe the local expression of the candidate genes of the pathway. To check whether Rho-ROCK signaling is directly involved in the detachment process, inhibitor tests were carried out. In addition, an antibody against the phosphorylated, active form of RLC was used (pMLC20) to verify a direct involvement of actomyosin.

The obtained data show that the actin cytoskeleton accumulates strongly at the bud base during bud detachment. The gene expression data revealed that components of the Rho-ROCK dependent pathway are expressed in overlapping regions at the bud base. Last but not least, the inhibitor experiments indicate that the Rho-ROCK pathway is directly involved during the detachment process. Therefore inhibitor exposure leads to non-detaching phenotypes and prevents actin accumulation. The antibody data revealed, that pMLC20 is strongly localized at the late constricting bud base.

My part in this publication was the preparation of the phalloidin staining during bud detachment, the implementation of the expression analyzes including all necessary preliminary work, the immunohistological examinations with the pMLC20 antibody and the preliminary tests with the corresponding inhibitors.

David Apel was supervised by me in the laboratory work as part of his master thesis. He carried out the statistical analysis of the resulting phenotypes after inhibitor exposure (as well as the phalloidin staining) and the phylogenetic analysis of the Rho proteins identified in *Hydra*. In addition, Simon Hopfenmüller was supervised by me as part of his bachelor thesis, and carried out the characterization of *α-actinin*.

DEVELOPMENTAL DYNAMICS 246:502–516, 2017 THE AUTHORS DEVELOPMENTAL DYNAMICS PUBLISHED BY
DOI: 10.1002/DVDY.24508

RESEARCH ARTICLE

Bud Detachment in *Hydra* Requires Activation of Fibroblast Growth Factor Receptor and a Rho–ROCK–Myosin II Signaling Pathway to Ensure Formation of a Basal Constriction

Oliver Holz,[1] David Apel,[1] Patrick Steinmetz,[2] Ellen Lange,[1] Simon Hopfenmüller,[1] Kerstin Ohler,[1] Stefanie Sudhop,[3] and Monika Hassel [1]*

[1]Philipps-Universität Marburg, Faculty of Biology, Morphology and Evolution of Invertebrates, Marburg, Germany
[2]Sars International Centre for Marine Molecular Biology, University of Bergen, Bergen, Norway
[3]Center for Applied Tissue Engineering and Regenerative Medicine (CANTER), Munich University of Applied Sciences, Munich, Germany

Background: *Hydra* propagates asexually by exporting tissue into a bud, which detaches 4 days later as a fully differentiated young polyp. Prerequisite for detachment is activation of fibroblast growth factor receptor (FGFR) signaling. The mechanism which enables constriction and tissue separation within the monolayered ecto- and endodermal epithelia is unknown. **Results:** Histological sections and staining of F-actin by phalloidin revealed conspicuous cell shape changes at the bud detachment site indicating a localized generation of mechanical forces and the potential enhancement of secretory functions in ectodermal cells. By gene expression analysis and pharmacological inhibition, we identified a candidate signaling pathway through Rho, ROCK, and myosin II, which controls bud base constriction and rearrangement of the actin cytoskeleton. Specific regional myosin phosphorylation suggests a crucial role of ectodermal cells at the detachment site. Inhibition of FGFR, Rho, ROCK, or myosin II kinase activity is permissive for budding, but represses myosin phosphorylation, rearrangement of F-actin and constriction. The young polyp remains permanently connected to the parent by a broad tissue bridge. **Conclusions:** Our data suggest an essential role of FGFR and a Rho-ROCK-myosin II pathway in the control of cell shape changes required for bud detachment. *Developmental Dynamics 246:502–516, 2017*. © 2017 The Authors Developmental Dynamics published by Wiley Periodicals, Inc. on behalf of American Association of Anatomists

Key words: receptor tyrosine kinase; actin; Rhosin; myosin

Submitted 14 September 2016; First Decision 20 January 2017; Accepted 6 April 2017; Published online 15 April 2017

Introduction

Tissue morphogenesis depends on cell shape changes and requires rearrangement of the actin cytoskeleton (Burute and Thery, 2012; Levayer and Lecuit, 2012; Fagotto et al., 2013). When tissue layers or organs form from mesenchymal precursors, boundaries have to be established at which tissue separation can occur. To this end, the establishment of cortical actomyosin is required. Myosin II family members act together with F-actin to generate contractile forces which shape the new tissue, mostly by causing apical and/or apicobasal constriction of cells. Endogenous mechanical forces may even separate cells within an epithelium when cell–cell contacts (established by E-cadherin) are weakened due to increasing binding strength between cells and their extracellular matrix (ECM) (Burute and Thery, 2012).

Formation of a bud in the freshwater polyp *Hydra* (phylum Cnidaria), constitutes an extreme case of morphogenesis, with typical dynamic changes in the transcription of different signaling pathway elements (Bottger and Hassel, 2012). *Hydra* polyps are approximately 5 mm in size, attach to the substrate with a mucous-secreting basal disk and carry an apical mouth opening on top of a tissue cone, the hypostome. Below the hypostome, a ring of tentacles equipped with specialized stinging cells, the nematocytes, serves to catch and paralyze/kill prey. Between tentacle ring and basal disk, the body column extends, which is formed by two single-layered epithelial sheets with specialized functions, including organizer formation (Hobmayer et al., 2000). Bifunctional epitheliomuscular (EM) cells form the outer

Additional Supporting Information may be found in the online version of this article.
Grant sponsor: DFG; Grant number: Ha 1732/11-1, Grant number: 1732/13-1.
*Correspondence to: Monika Hassel, Philipps-Universität Marburg, FB 17, Morphology and Evolution of Invertebrates, Karl-von-Frisch-Str. 8, D-35032 Marburg, Germany. E-mail: hassel@biologie.uni-marburg.de

Article is online at: http://onlinelibrary.wiley.com/doi/10.1002/dvdy.24508/abstract

epithelium, ectoderm, and serve to shield the polyp from the surrounding medium (Buzgariu et al., 2015). They also ensure contractility in the longitudinal direction by actomyosin in basal cell processes extending along the mesogloea in the apicobasal direction (Anton-Erxleben et al., 2009). The endoderm lines the gastric cavity and its EM cells combine digestive function and circumferential contractility. Both secrete an intermitting extracellular matrix, called mesogloea in Cnidaria (Sarras, 2012).

This basal matrix has a stabilizing function by anchoring the EM cells and allows ecto–endodermal cell contacts through small pores (Shimizu et al., 2002, 2008; Seybold et al., 2016). The mesogloea is dynamically modified and degraded in morphogenetically active zones, such as the bud and tentacle region (Aufschnaiter et al., 2011). Tentacles consist of ecto- and endodermal EM cells, which reach the tentacle base zone by mass tissue movement. Here, cells undergo local rearrangement and form the regularly spaced small tentacles tubules (Hobmayer et al., 2012; Munder et al., 2013). The ectodermal EM cells transdifferentiate into battery cells and integrate stinging cells (nematocytes), which migrated actively as nematoblasts from the body column toward the tentacles (Beckmann and Ozbek, 2012).

A remarkable morphogenetically active zone is the budding zone of polyps in the mid body region. Buds evaginate in well-fed polyps by a lateral mass tissue movement, and they detach as a fully differentiated young polyp only 4 days later (Otto and Campbell, 1977). The budding process is easily observed under a dissection microscope in whole polyps due to the simple structure of the two single layered epithelia. Budding and evagination of tissue are initiated by canonical and noncanonical Wnt signaling (Hobmayer et al., 2000; Philipp et al., 2009; Nakamura et al., 2011). The evaginating tissue rearranges its actin cytoskeleton, forms a small cone and elongates by intercalation of cells to form a new body column. Complete pattern formation follows.

First, a head with a mouth opening and tentacles differentiates. Next, signaling by the fibroblast growth factor receptor, FGFRa, together with NOTCH ensures the formation of a sharp boundary between parent and bud, at which later separation occurs (Sudhop et al., 2004; Münder et al., 2010; Hasse et al., 2014). The precise mechanism by which adjacent epithelial cells are instructed to separate from each other is still unknown, but FGFR is essential: ectopic expression of HvFGFRa in a transverse row of cells causes ectopic tissue constriction and separation, even within the body column. A dominant-negative FGFRa, in contrast, is permissive for bud formation, but prohibits its detachment (Hasse et al., 2014).

A previous study indicated that FGFRa might target a pathway controlling *Hydra vulgaris* actin dynamics and/or actomyosin interactions by rearrangment of the actin cytoskeleton and formation of F-actin stress fibers at normal and ectopic separation sites (Hasse et al., 2014). It is known that during embryonic morphogenesis in Bilateria, RhoA-ROCK-myosin II–dependent pathways are often involved in regulating the actin cytoskeleton (Fagotto et al., 2013; Fagotto, 2014). Rho and ROCK are ancient signaling elements used in the prebilaterian phylum Porifera (sponges) to ensure proper morphogenesis of the aquiferous system. A connection to the actin cytoskeleton has, however, yet not been investigated (Schenkelaars et al., 2016). To elucidate whether members of the Rho, ROCK, and myosin II candidate pathway are involved in cell shape and actin dynamics during bud detachment in *Hydra*, we combined analyses of gene expression, F-actin and phosphomyosin localization with pharmacological inhibition studies to reveal potential functions of this putative FGFR downstream pathway for bud detachment.

Results

Characteristic Cell Shape Changes Occur at the Bud Base and in the Tissue Bridge

Hydra buds evaginate in well-fed animals one at a time and detach approximately 4 days later (Otto and Campbell, 1977). Because only little morphological data describing bud detachment is available (Graf and Gierer, 1980), we prepared serial thin sections from plastic embedded, budding *Hydra vulgaris* in the early to mid stages 3, 5, 7, and in late stages 8–10 (Fig. 1, graphical overview of late bud stages in Fig. 2A). The sections revealed that between early evagination (stage 3), formation of the constriction (stage 8) and final detachment (stage 10), cells in the bud and at the bud base change their shape concomitant with changes in thickness and shape of the basal matrix, the mesogloea. In the parent and in early buds (Fig. 1A–D), the mesogloea is a thick, smooth membrane-like structure, which becomes much thinner and irregular in the body of stage 7–9 buds (Fig. 1C,D).

A detailed analysis of the detachment zone of stage 9–10 buds (Fig. 1E–I) revealed well distinguishable changes in cell shapes of the ectodermal EM cells, while such changes were not conspicuous in endodermal cells. Ectodermal cells of the bud base are very compact, and form a phalanx of apicobasally shortened cells in the prospective basal disc region (Fig. 1E–G′). Their darker staining by methylene blue (Fig. 1E–H′), which highlights nuclei and negatively charged molecules, indicates the presence of acidic vesicles or granules. In contrast, large ectodermal cells with a vacuole almost filling the cell are typical in the tissue bridge as well as in the immediately adjacent parental tissue (Fig. 1E–H′).

Serial sections close to the surface of the tissue bridge revealed that these large ectodermal cells contain many vesicles in their apico-lateral parts strongly stained by methylene blue (Fig. 1G′,H′). Moreover, their apical cell membranes are irregularly folded and no longer in contact with neighboring cells, slit-like gaps are visible (Fig. 1H′). The compact shape of the conspicuously short ectodermal EM cells at the bud base and the folded apical membrane of ectodermal cells in the tissue bridge suggest cell shape changes and, thus, modification of the actin cytoskeleton.

Asymmetric Accumulation of F-Actin Along the Planar Cell Axis in Bud Base Cells

Systematic analysis of the distribution of F-actin in mid and late-stage buds (Fig. 2) revealed a local rearrangement of the actin cytoskeleton concomitant with cell shape changes. In late stage 7 (Fig. 2B), the initially broad bud base constricts toward the parent. From stage 8 onward, the constriction narrows and F-actin starts to accumulate in cells of the bud base circumference with an initially poorly defined boundary (Fig. 2D–F′). In stage 10, a clear boundary has been established between bud and parent ectodermal cells, indicated by cells strongly accumulating F-actin (Fig. 2G). The bud base closes concomitant with the formation of a narrow ring of ectodermal cells (Fig. 2F,G). The boundary also sharpens on the parent's side, where F-actin accumulates unilaterally toward the separation site (Fig. 2G,H).

A slightly tilted view of the developing bud's basal disc (Fig. 2F,F′) and a detailed analysis of the cLSM stack (Fig. 3) revealed several distinct cell populations in the parent and at the bud base. In parent

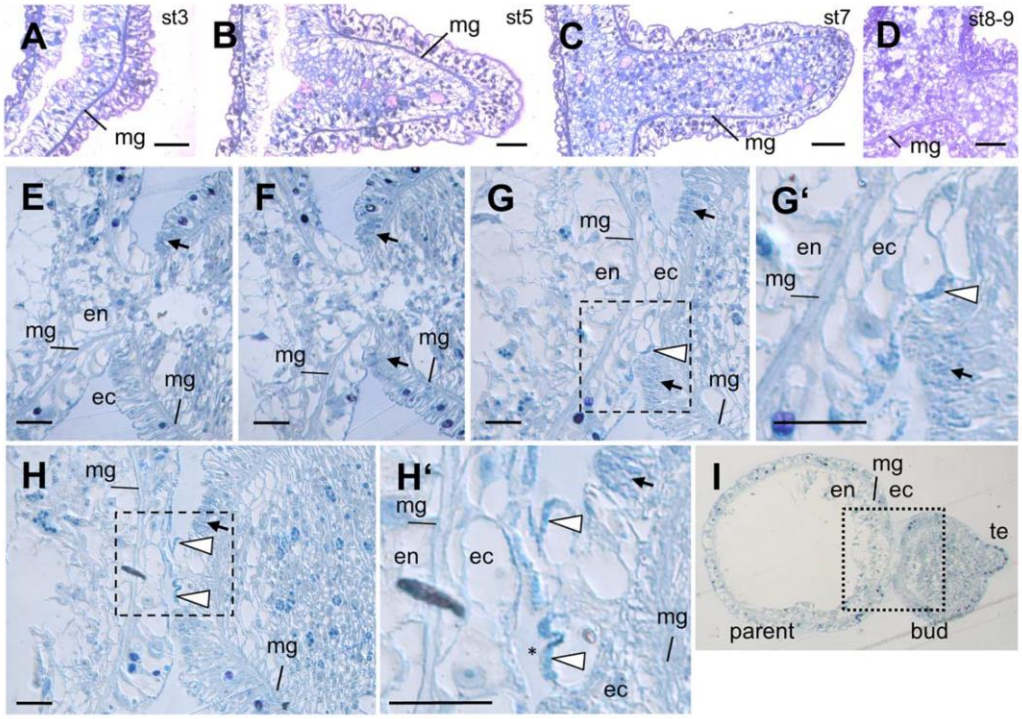

Fig. 1. Serial sections through plastic embedded Hydra vulgaris buds in stages 3–9. **A–D**: Longitudinal sections (2 μm), the parent's head is oriented upward, the bud to the right. A: Stage 3 (early evagination). B: Stage 5 (early elongation, combined from two pictures). C: Early stage 7 (fully elongated bud with a still broad base, combined from three pictures). D: Stage 8–9 (constriction of bud base). **E–I**: Transverse sections (2 μm) through the stage 8–9 tissue bridge connecting parent (left) and bud (oriented to the right). E,F: Sections through the tissue bridge close to the lumen. G,G′: Section through the large epitheliomuscular (EM) cells forming the tissue bridge ectoderm and the adjacent parental ectoderm. Compact ectodermal EM cells at the bud base (black arrow). Apical vesicles (white arrowhead). H,H′: Section at the level of the ectodermal surface of the tissue bridge. Apical vesicle accumulation (white arrow head) in the irregularly formed large EM cells, gaps develop between cells (asterisk). G′,H′: Digital close-up of (G) and (H), respectively. I: Section overview. Bud and parent axes are orthogonal. Therefore, the sections (E–I) through the parent are transversal, and through the bud are longitudinal. The bud body is compressed and endodermal cells are visible in all sections evoking the impression of a gastric cavity filled with cells. bt bud tip, ec ectoderm, en endoderm, mg mesogloea, te tentacle. Scale bars = 100 μm in A–D, 50 μm in E–H.

tissue, where the longitudinal muscle fibers of the ectodermal EM cells are well visible, cells form rosettes consisting of four to six cells in several locations. F-actin is concentrated unilaterally toward the rosette center (Fig. 3A,B) or unilaterally in cells arranging along an almost straight line instead of converging to a single center (Fig. 3A). These cells as well as those stretching out into the tissue bridge increase their diameter and often have an irregular shape, indicated by the irregular cell membranes (Fig. 3A,B).

On the bud's side, in contrast (Fig. 3C), a central cell population close to the tissue bridge has a small diameter and massively accumulates F-actin. Several of these cells, again, form rosettes of at least five cells (Fig. 3C). In the periphery of the newly forming basal disc, small cells show less cortical F-actin accumulation (Fig. 3C,D). Immediately adjacent to this central ring of cells, elongated cells stretch out along the bud body and contain a higher amount of cortical F-actin (Figs. 2G, 3D).

Shortly before detachment of the bud, the typical regular pattern of circularly and longitudinally oriented F-actin fibers in the basal processes of endodermal and ectodermal EM cells, respectively, reconstitutes along the mesogloea (Fig. 2H). At the detachment site, residual strongly F-actin-positive ectodermal cells persist for 1 to 2 hours in the parent as a wart-like protrusion with irregularly arranged F-actin fibers (Fig. 2I). Here, the circular and half-ring-like arrangement of F-actin stress fibers indicates that ectodermal cells undergo a truly exceptional rearrangement of their actin cytoskeleton. The basal processes, usually oriented longitudinally, were not traceable in these ectodermal EM cells.

Constriction also occurs at the tentacle bases, where EM cells move into the evenly spaced tentacle tubules by mass tissue movement from the body column. Here, ectodermal cells transdifferentiate into battery cells (Hobmayer et al., 2012). In contrast to the boundary between bud and body column (Fig. 2G), F-actin does not accumulate unilaterally in the tentacle base cells (Fig. 2J–K′). Instead, the existing longitudinally oriented F-actin fibers thicken and arrange in a triangle at the intersection of body and tentacle axes (Fig. 2K′).

In summary, detachment correlates with strong F-actin accumulation, formation of multicellular rosettes, and remarkable cell shape changes at the bud base, in the tissue bridge and in adjacent parental cells. These features are not observed at the tentacle bases, where EM cells just rearrange their basal processes and follow the tentacle axis.

Search for Genes Encoding Elements of a Candidate Signaling Pathway Controlling Actomyosin Dynamics and Phylogenetic Analysis of *Hydra* Rho Proteins

F-actin accumulation in cells changing their shape is a common feature and accompanies local actomyosin interactions. Very

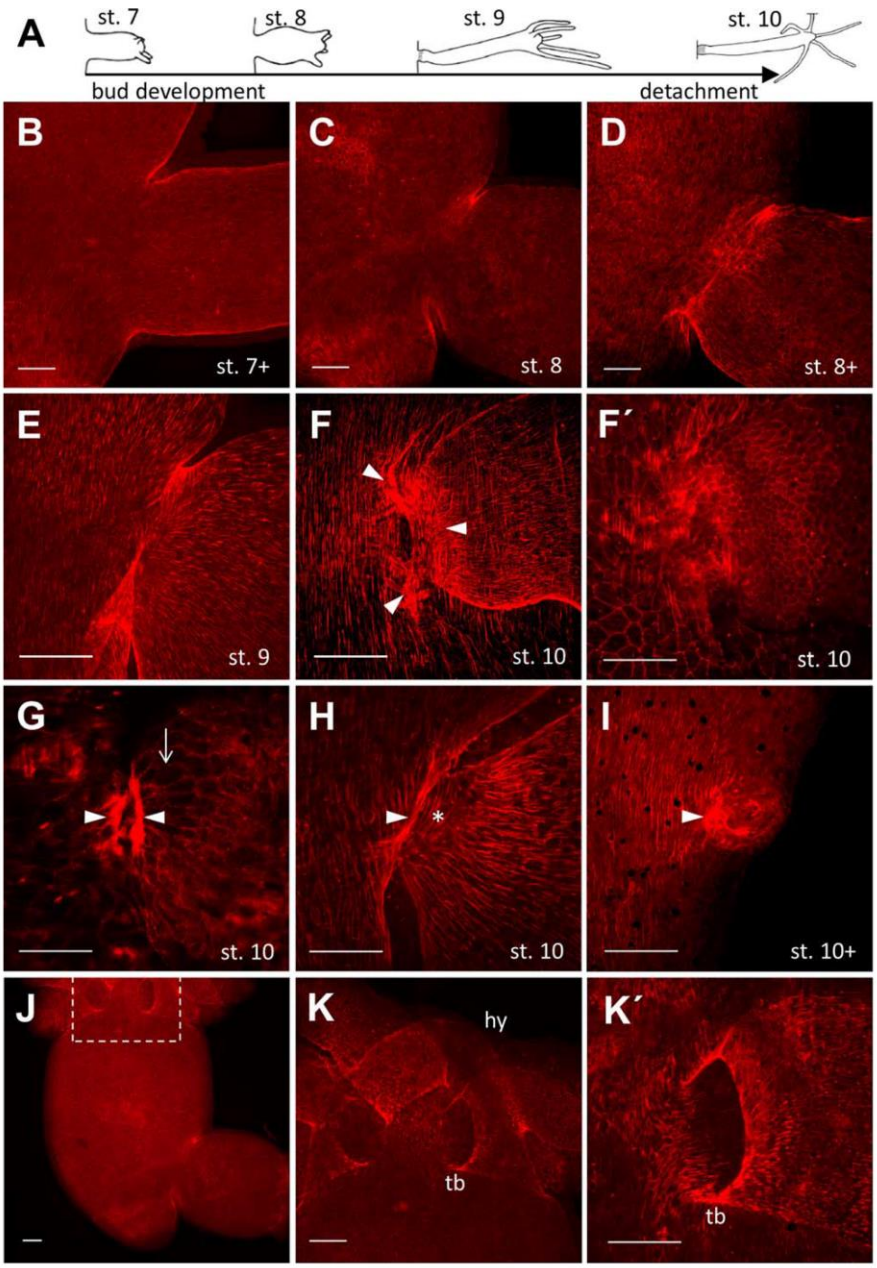

Fig. 2. F-actin accumulation at the bud base between stage 7 and detachment. **A**: Scheme of bud stages from 7 to 10 according to (Otto & Campbell, 1977). The detaching bud is not to scale. **B–K′**: TRITC phalloidin staining of F-actin in Hydra vulgaris AEP at bud bases and detachment site (B–I) as well as at tentacle bases (J–K′). B–D: Overview stage 7+ to stage 8+. E–I: Close-up view of stage 9–10 bud bases and detachment site (I). E,F,H,I: Optical sections on the mesogloea level visualizing the normal ectodermal, longitudinal F-actin fibers. Parental as well as bud stress fibers are indicated (F, arrowheads). F′,G: Optical sections closer to the ectodermal surface (lateral cell membranes visible). Actin stress fibers (arrowheads) and strongly elongated bud base cells (arrow). H: Late stage 10. Ectodermal stress fibers (arrowheads) and regular endodermal, circular F-actin fibers at the bud base (asterisk). J,K,K′: Overview and close-up of the parent's head region and tentacle bases, where F-actin fibers form a triangle (open arrowhead). hy hypostome, tb tentacle base. Bud is always oriented to the right. Scale bars = 100 μm.

often, a pathway involving RhoA, Rho-associated kinase (ROCK), and myosin II is involved (Levayer and Lecuit, 2012; Schwayer et al., 2016). If this pattern is the same in bud detachment, one might expect elements of this cascade to be transcriptionally up-regulated together with *Hydra* FGFRa (Kringelchen) at the bud base.

Previously identified were a *Hydra* ROCK homologue, *HvRok* and *HmRok* (Philipp et al., 2009; Schenkelaars et al., 2016); two *Hydra* myosin II subtypes, one nonmuscular myosin (*nm_MyHC*) and a striated-type myosin (*st_MyHC*) (Steinmetz et al., 2012); three *Hydra magnipapillata* Rho-encoding genes (*HmRho1-3*), of

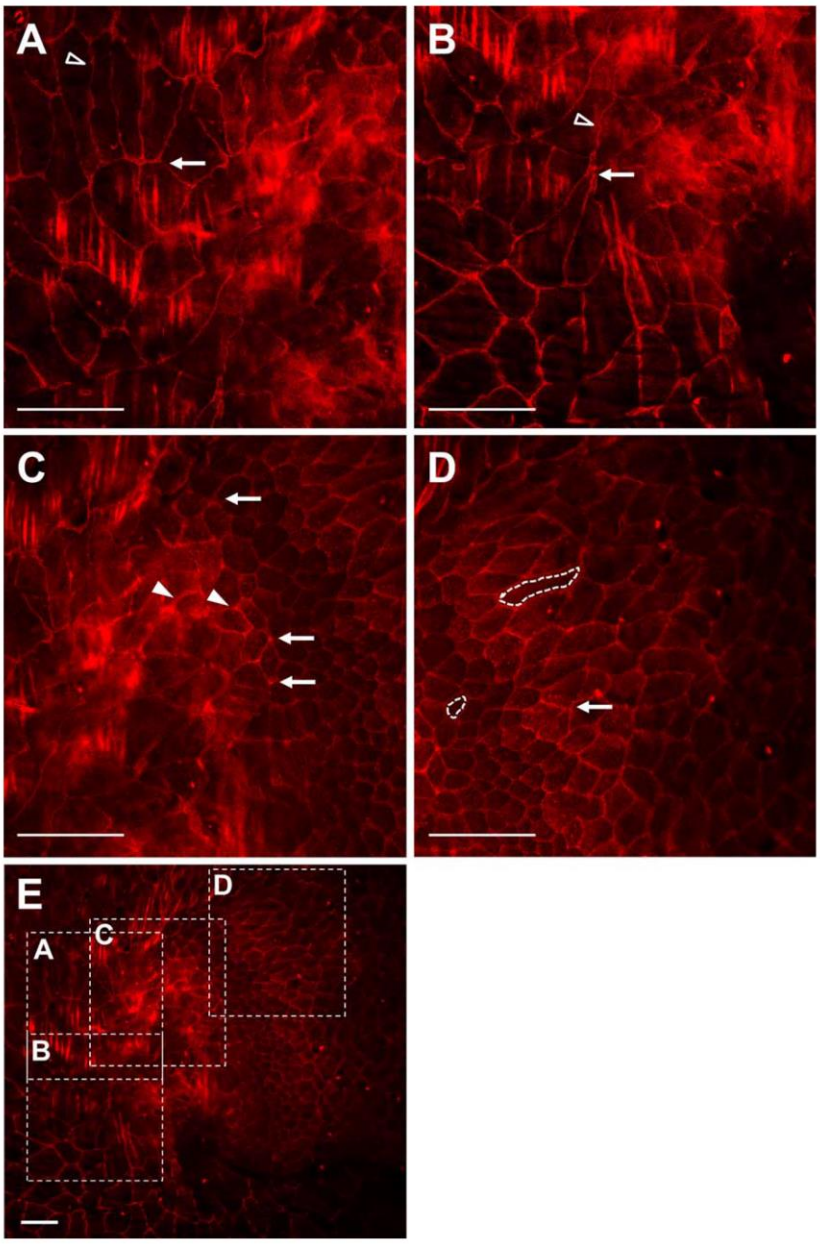

Fig. 3. Cell shape dynamics at the stage 10 bud base. Digital zoom of an optical section of the Figure 2F cLSM stack. **A,B**: Parent's side close to the bud base. A: Large, irregularly formed cells (empty arrowhead) arranged in a multicellular rosette (arrow). B: rosette (arrow) in an adjacent region, irregular cell shape (empty arrowhead). **C,D**: Bud base. C: Small central cells of the bud base immediately at the tissue bridge with strong cortical actin (arrowhead), peripheral small cells with less cortical actin forming a rosette (arrow). D: Adjacent elongated cells of the bud body with increased cortical F-actin. Dotted lines mark cell contours. **E**: Overview of the zoomed region in A–D. Scale bars = 50 μm.

which *HmRho1* and *-2* were assigned to the RhoABC group (Boureux et al., 2007). Reinvestigating the current database contents, we identified a fourth *Hydra* Rho gene (*HvRho4*, Supplementary Fig. S1, which is available online), and a single gene encoding α-actinin (Supplementary Fig. S2) in the *Hydra* genome project (Chapman et al., 2010). The α-actinin is of interest for the current study, because it is an essential actin crosslinker in stress fibers when cells change their shape and an important regulator of cell–cell and cell–matrix interactions (Foley and Young, 2014).

The HvRho4 sequence deviates in several residues within the highly conserved GTPase and interaction domains from other Rho sequences (Supplementary Fig. S1B,C′). Phylogenetic analysis clearly assigned *Hydra* Rho1, Rho2 and Rho3 proteins as

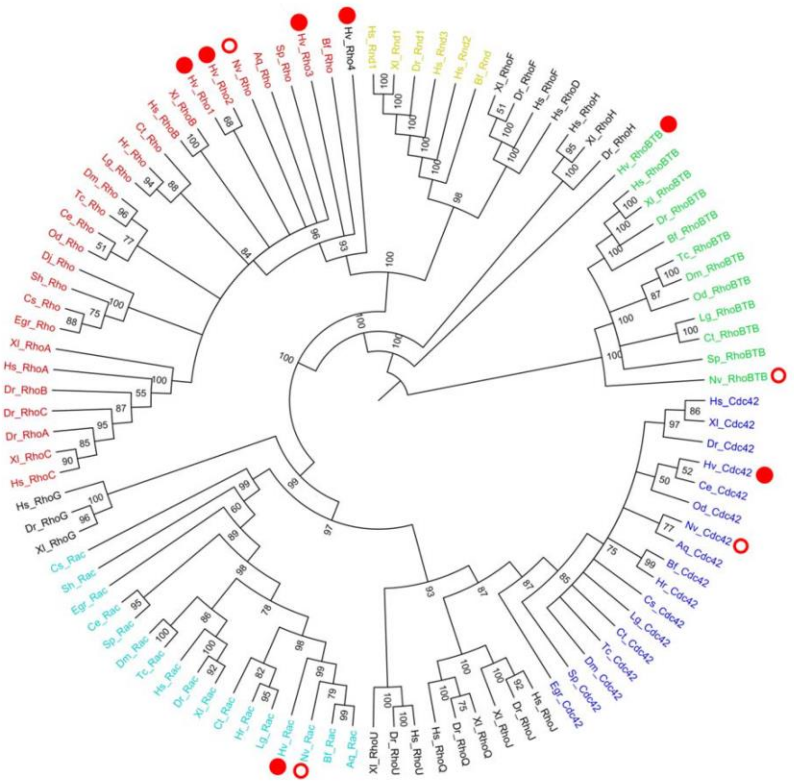

Fig. 4. Phylogenetic tree (MrBayes, MCMC) of Rho subfamilies. A, *Amphimedon queenslandica*; Bf, *Branchiostoma floridae*; Ce, *Caenorhabditis elegans*; Cs, *Clonorchis sinensis*; Ct, *Capitella teleta*; Dm, *Drosophila melanogaster*; Dj, *Dugesia japonica*; Dr, *Danio rerio*; Egr, *Echinococcus granulosus*; Hr, *Helobdella robusta*; Hs, *Homo sapiens*; Hv, *Hydra vulgaris* (red dots); Lg, *Lottia gigantea*; Nv, *Nematostella vectensis* (red circles); Od, *Oikopleura dioica*; Sh, *Schistosoma haematobium*; Sp, *Strongylocentrotus purpuratus*; Tc, *Tribolium castaneum*; Xl, *Xenopus laevis*. Accession numbers are given in Supplement Figure S1A.

orthologues to the RhoABC group, while HvRho4 was placed on an isolated branch, basal to the RhoABC family (Fig. 4). ROCK interaction sites were predicted for HvRho1 and HvRho2, but not for HvRho3 or HvRho4 (Supplementary Fig. S1B).

Taken together, a Rho-Rok-myosin II toolkit exists in *Hydra* with three RhoABC orthologues. RhoA is known to be essential in vertebrates for cell shape changes and actin regulation. For two of the *Hydra* Rhos, a ROCK binding site is predicted.

Gene Expression of *Hydra* FGFR, FGFf, FGFe, and Components of a Rho–ROCK–Myosin II Candidate Pathway

Synexpression of genes often correlates with connected signaling pathways and their function (Niehrs and Pollet, 1999; Bottger and Hassel, 2012). Because the *Hydra* body consists of only two monolayered epithelia (Fig. 1), gene expression domains are easily identified by whole-mount in situ hybridization (WMISH).

The expression patterns of *HvRho1, 2, and 3*, Rok, the two myosin II genes and of *Hydra α-actinin* were analyzed in late bud stages and compared with *Hydra FGFRa* (*Kringelchen*), *FGFRb*, and two recently identified *Hydra* FGF-encoding genes (Fig. 5). None of the sense probes yielded a signal (not shown). All genes showed distinct zones of stronger expression in addition to weaker ecto- and/or endodermal expression along the body column (Fig. 5). As described previously (Sudhop et al., 2004), *Hydra FGFRa* (*Kringelchen)* gene expression was up-regulated ectodermally at the late bud base and detachment site, where also *FGFRb* is strongly expressed (Fig. 5A,B).

In addition to a low endodermal expression in the body column, *HvRho1* mRNA was found up-regulated differentially in the ectoderm of the late bud base and in the adjacent parental tissue from stage 8 onward (Fig. 5C,C′). Neither *HvRho2* nor *HvRho3* were up-regulated at the bud base: *HvRho2* was expressed mainly ectodermally in the body column between budding region and tentacle zone (Fig. 5D), while high levels of *HvRho3* were detected in a few endodermal cells surrounding the mouth opening (Fig. 5E,E′). The *Hydra* ROCK homologue, *HvRok*, was slightly up-regulated in the parent's ectoderm cells close to the bud base extending a short distance up and down the body column (Fig. 5F,F′). For *HvRho1, HvRho2*, and *Rok*, an additional, very weak upregulation at the tentacle bases was observed, which is not just due to an overlay of tissues (Fig. 5C,D,F).

The two *MyHC* mRNAs (Fig. 5G–H′) differed in their respective tissue localization. The nonmuscle, *nm_MyHC*, was expressed mostly endodermally, the striated-type *st_MyHC* predominantly ectodermally. Both were strongly up-regulated at the tentacle bases and the bud detachment site. *nm_MyHC* was detected in the peduncle region of parent and bud and in an additional patch of parental cells right at the detachment site, while *st_MyHC* was

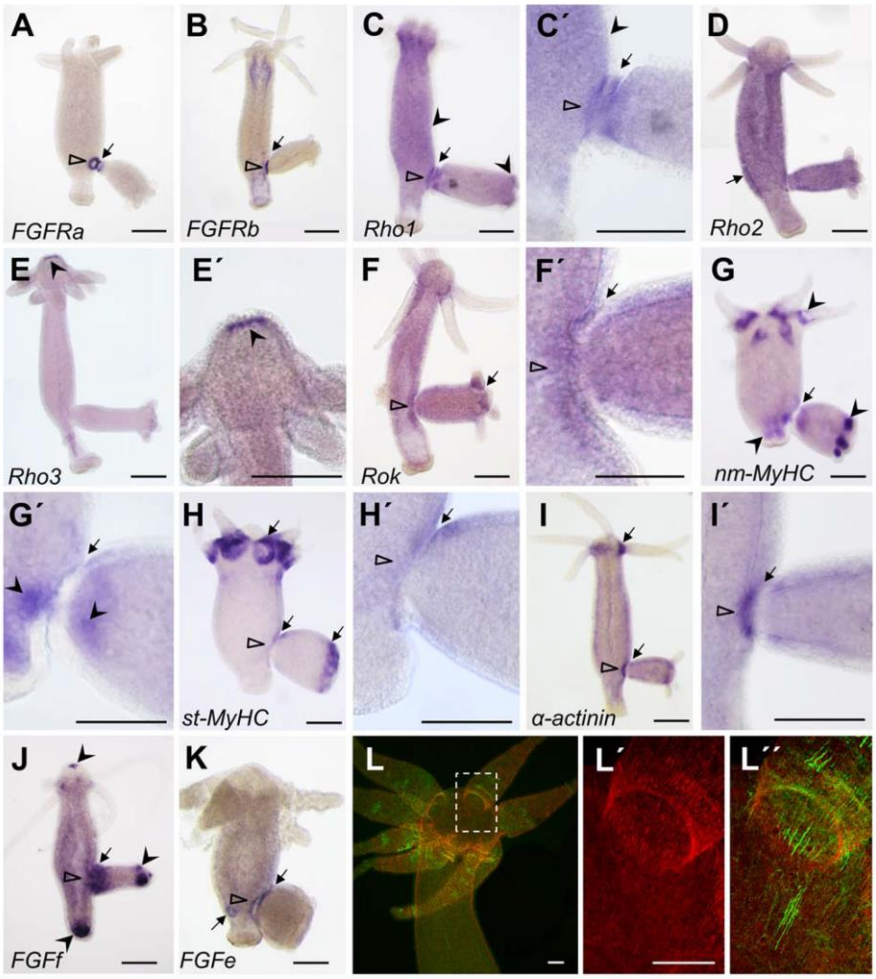

Fig. 5. **A–L′**: Gene expression patterns of Hydra FGFRa and b, Rho1-3, ROCK, nm_MyHC, st_MyHC, α-actinin, FGFf and FGFe and localization of phospho-myosin in the Hydra tentacle zone. A–G: Black arrows indicate ectodermal transcription, arrow heads endodermal gene expression and open triangles ectodermal expression in the parent close to the detachment site. A: FGFRa in a polyp carrying a stage 9–10 bud. B: FGFRb, stage 9. C,C′: HvRho1, stage 9. D: HvRho2, stage 10. E,E′: HvRho3, stage 10. F,F′: Rok, stage 9–10. G,G′: nm_MyHC, stage 10. H,H′: st_MyHC, stage 9–10. The mRNA is localized asymmetrically in bud ectoderm directed toward the parent head. I,I′: α-actinin, stage 9. J: HvFGFf, stage 6–7. K: HvFGFe, stage 9. L–L′: Immunodetection of phospho-myosin light chain (MLC20, and F-actin (TRITC phalloidin) at the tentacle bases. L: Overview, merged MLC20 and phalloidin. L′: Phalloidin. L′: merged. Scale bars = 250 μm in A–K, 100 μm in L–L′.

localized in a ring of parental ectoderm and surrounding the bud base/peduncle region. Both myosins overlap ectodermally in a small domain at the detachment site. This domain is oriented apically, toward the parent's head (Fig. 5G′,H′). Analysis of *Hv_α-actinin* revealed transcriptional upregulation in parental ectodermal cells close to the bud base as well as in the tentacles bases (Fig. 5I,I′).

Two potential FGFR ligands, the *Hydra* FGF8-homologue, *HvFGFf* (Lange et al., 2014) and *HvFGFe*, were detected ectodermally at the bud base with *FGFf*, as described previously, being expressed endodermally also at all boundaries and termini of the polyps (Fig. 5J,K). *FGFe* expression at the detachment site parallels *FGFRa* (Sudhop et al., 2004).

In summary, both FGFRs, two FGFs, *HvRho1, HvRok, st-MHC*, and *α-actinin* colocalise in the parental ectoderm close to the detachment site. With the exception of *Rok* (weakly expressed) and *α-actinin* (down-regulated), these genes are additionally upregulated in the bud base ectoderm. The two myosins colocalise with each other in a small domain of the bud base oriented toward the parent's head.

Actomyosin interactions require the presence of actin as well as of phosphorylated (activated) myosin light chain (MLC). Analysis of phospho-myosin localization using the MLC20 antibody revealed presence of phosphorylated MLC at the tentacle bases (Fig. 5L,M) and at the bud base (Fig. 6). Moreover, isolated fibers are visible in a scattered pattern along the body column and at the tentacle bases (Fig. 5L′, below the tentacle). Controls without first antibody showed no staining (not shown). At the late bud base, actin and MLC are colocalized ectodermally (Fig. 6C–C′′,F–F′′). In bud stage 8–9 phospho-myosin was found strongly enriched in the central-most ectodermal bud cells, surrounding the lumen of the tissue bridge, as well as in cells of the tissue

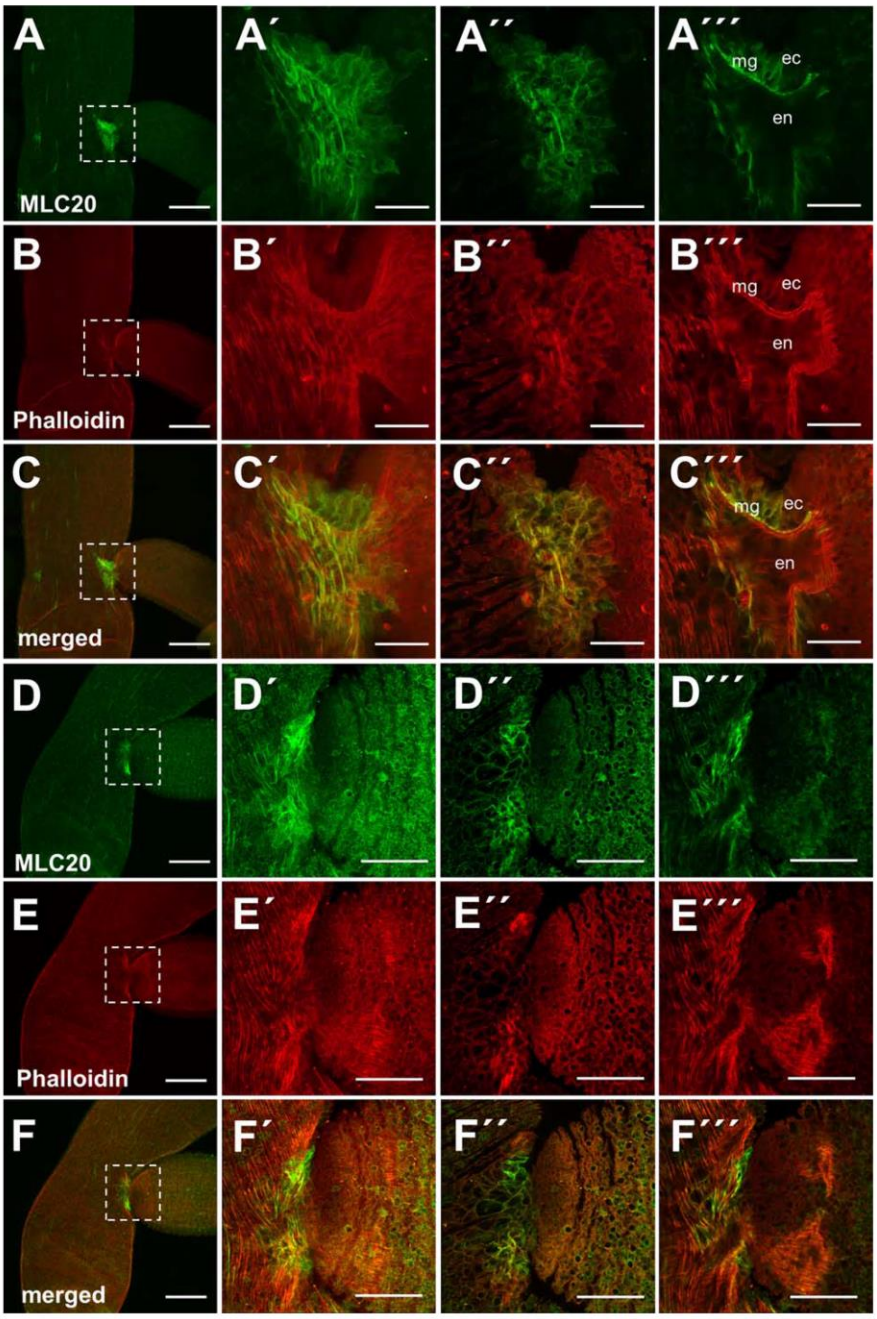

Fig. 6. **A–F″**: Colocalization of F-actin and phospho-myosin at the late bud base. A–E: Overview of the bud base in stage 8–9 (A–C) and stage 9–10 (D,E). The second column (A′–F′) represents a maximum projection, the third column (A′–F′) shows a surface view of the tissue bridge between bud and parent, and the fourth column (A″–F″) shows a deep view close to the lumen of the tissue bridge. A–A″,D–D″: Phospho-myosin antibody MLC20. B–B″,E–E″: TRITC-phalloidin. C–C″ and F–F″: merged. Scale bars = 250 μm in A–F first column; 100 μm in A′–F″.

bridge proper and in parental cells adjacent to the tissue bridge (Fig. 6A–A″,C–C″). In stage 9–10, phospho-myosin was detectable on the parent's side only (Fig. 6D–D″, F–F″).

In summary, all elements necessary for signal transduction through an FGF/FGFR–RhoABC–ROCK–myosin II pathway are transcribed in overlapping domains at the late bud base. Moreover, Hv_α-actinin, a protein known from other organisms to cross-link F-actin stress fibers (Sjoblom et al., 2008), joins this synexpression group. The strong and localized dynamic phospho-myosin signal at the late bud base, in the tissue bridge and in adjacent parental tissue indicates dynamic actomyosin interactions at this site.

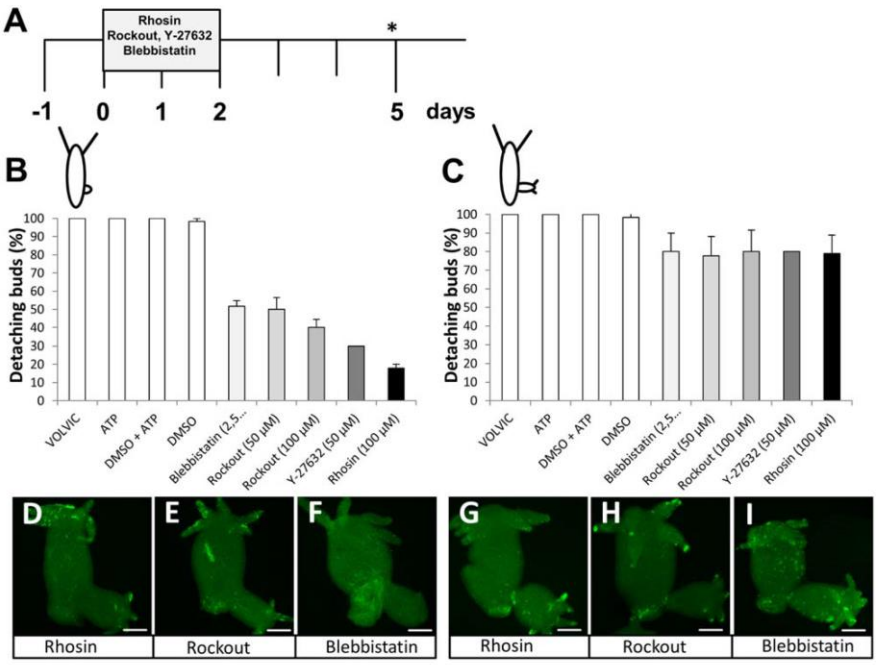

Fig. 7. Inhibition of RhoA, ROCK, and myosin II leads to failure to detach and loss of phospho-myosin. **A**: Treatment scheme. The last feeding was 24 hrs before the start of the experiment (-1). Polyps were incubated for 2 days and phenotypes evaluated and animals fixed for phalloidin and/or MLC20 staining another three days later (asterisk). **B,C**: Results of treatment of early buds (stage 3–5) (B) or late buds (stage 5–7) (C) with the inhibitors Rhosin, Rockout, Y-27632, or Blebbistatin. With the exception of the ROCK inhibitor Y-27632, all experiments were repeated at least six times with a sample size of 10 animals per inhibitor and experiment. The percentage of detaching buds and the standard error of the mean (SEM) are given. Rhosin (100 µM) (early and late buds n = 90 each); Rockout (100 µM) (early and late buds n=60 each); Rockout (50 µM) (early and late buds n = 60 each); Y-27632 (50 µM, early and late buds n = 10 each); Blebbistatin (2.5 µM) (early and late buds n = 60 each). **D–I**: Phospho-myosin (MLC20) in buds inhibited in early (D–F) or late (G–I) stages. Scale bars = 250 µm.

Pharmacological Inhibition of FGFR, Rho, ROCK, and Myosin II Prohibits Constriction at the Bud Base

A straightforward approach, by which multiple potential functions of signaling pathways can be studied in living *Hydra*, is the pharmacological inhibition of enzymes. We previously reported that SU5402, a specific FGFR inhibitor, inhibits bud detachment in *Hydra* in a similar way as *FGFRa* antisense oligonucleotides or a dominant-negative FGFRa (Sudhop et al., 2004; Hasse et al., 2014).

Because highly conserved protein sequences were found for the signaling elements of interest, we used well-established inhibitors against RhoA, ROCK and myosin II. In *Hydra* Rho1 and Rho2, the binding site for the RhoA inhibitor Rhosin (Shang et al., 2012) is 100% identical to the vertebrate binding site (Supplementary Fig. S1B). This site is neither predicted in HvRho3 nor in HvRho4. Two potent ROCK inhibitors, Rockout (Harding and Nechiporuk, 2012) and Y-27632 op. cit. (Kroening et al., 2010), both with unknown binding sites, were compared. Blebbistatin is a widely used inhibitor of the highly conserved myosin ATPase activity (Kovacs et al., 2004).

All four inhibitors showed effects on bud detachment comparable to SU5402. The Rho inhibitor, Rhosin, had the strongest impact (Fig. 7B). Treatment of early bud stages prohibited formation of a constriction and detachment, and 82% of buds failed to detach (Fig. 7B), while treatment of stage 5–7 buds allowed detachment of approximately 80% young polyps. Sixty percent of the polyps treated with the high Rockout concentration (100 µM) and 50% of the ones treated with 50 µM Rockout failed to detach. Treatment with the ROCK inhibitor Y-27632 prohibited detachment in 7 of 10 polyps. Blebbistatin (2.5 µM) prevented detachment in 48% of the cases. In control incubations with DMSO less than 2% failed to detach, no effects were found with DMSO + ATP, ATP alone or using incubations with VOLVIC medium. Treatment of late buds with each of the inhibitors caused failure to detach in approximately 20% of the polyps. Toxicity of the used compounds was low or not detectable (Supplementary Fig. S3).

The phenotype generated by treating polyps carrying either early or late buds was similar to SU5402 treatment (Sudhop et al., 2004; Hasse et al., 2014). Young buds later formed a broad tissue bridge, while further developed buds formed a narrow one (Fig. 8). No phospho-myosin was detected at the base of nondetaching, early-treated buds (drug exposure as in Fig. 7A), even 3 days after the end of treatment (n = 10 each; Fig. 7D–F). A variable pattern of scattered single phospho-myosin–positive fibers was found in the body column (particularly following Blebbistatin treatment) and in tentacles. The phospho-myosin–positive fibers colocalized with actin fibers (similar to Fig. 5L′). A weak phospho-myosin signal appeared at the bud base of polyps treated in late bud stages (n = 10 each, Fig. 7G–I).

Detection of F-actin in the branched polyps resulting from treatment of early buds (Fig. 8) revealed a triangular alignment of actin fibers at the intersection of parent tissue and the broad tissue bridge to the bud (Fig. 8A–C′). This F-actin triangle resembles the one detected at the tentacle bases (Fig. 2K′) and indicates that

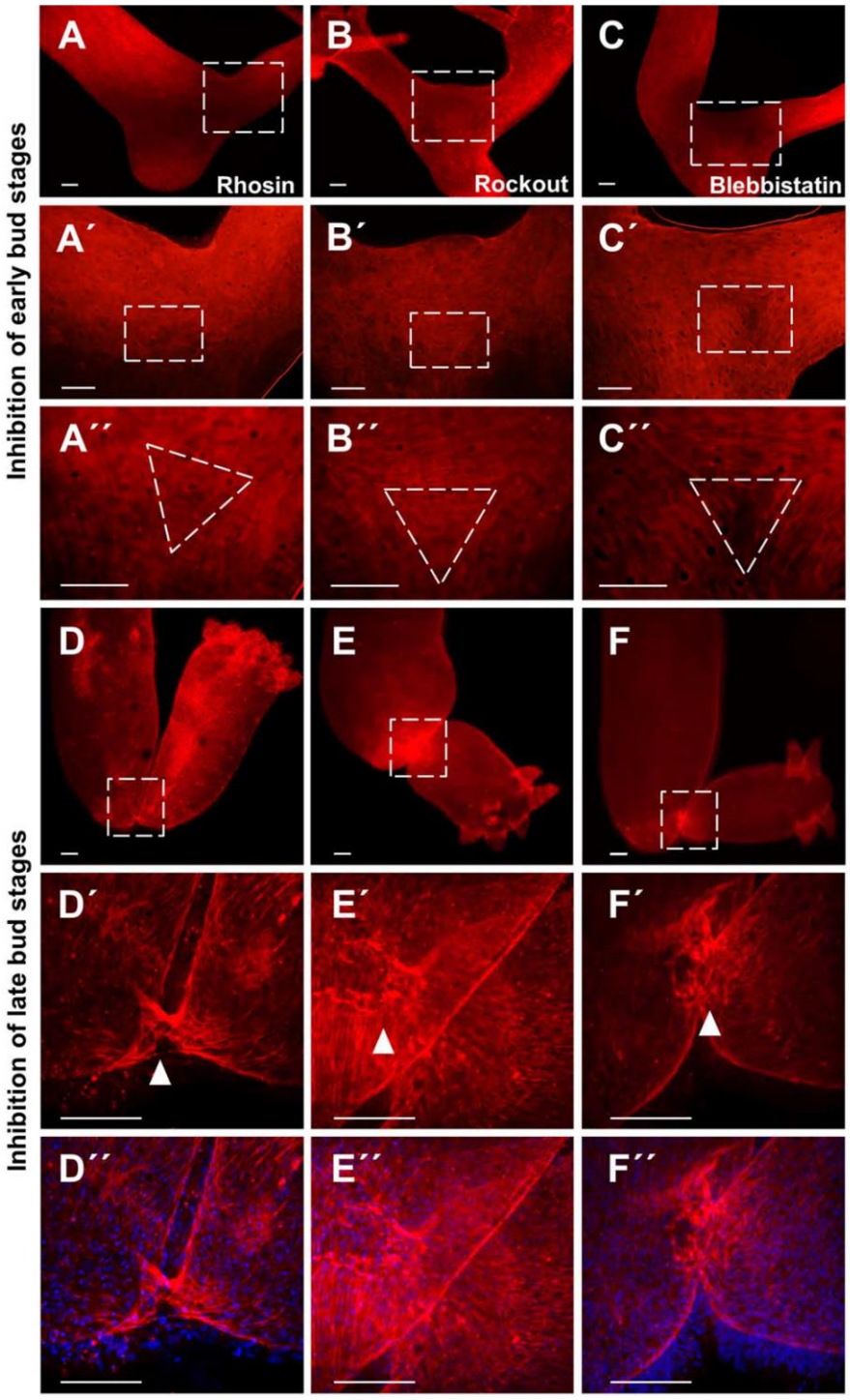

Fig. 8. TRITC-phalloidin staining of early and late budding *Hydra vulgaris* AEP treated with either Rhosin, Rockout or Blebbistatin. Hydra vulgaris AEP (stage 3–5) were subject to inhibitor treatment as indicated in Fig. 7. **A–C′**: Inhibitors: Rhosin (RhoA-specific inhibitor) (A–A′), Rockout (Rho kinase inhibitor) (B–B′), Blebbistatin (myosin II ATPase inhibitor) (C–C′). Treated buds fail to detach and remain attached to the parent with a broad tissue bridge as Y-shaped, branched animals for weeks. A′–A′: The higher magnifications of the branching area shows a triangle of actin filaments at the intersection of parent and bud tissue (A′,B′,C′) (close-up in A′,B′,C′). **D–F′**: Pictures of phenotypes obtained in the experiment leading to Figure 7C. D′,E′,F′: TRITC-phalloidin (red) and DAPI (blue) staining. Treatment of bud stages 5–7 with Rhosin(D–D′), Rockout (E–E′), or Blebbistatin(F–F′) resulted in narrow tissue bridges (white arrowheads) persisting between bud (oriented to the right) and parent. Scale bars = 10 μm in A–C′; 100 μm in D–F.

the EM cells are unable to rearrange their actin cytoskeleton circumferentially along the bud base, if any of the FGFR, Rho-ROCK-myosin II candidate pathway components is inhibited. Instead, the orientation of the F-actin fibers follows and reflects the new orientation of the EM cells along the bud's axis. In late buds (Fig. 8D–F′), a chaotic arrangement of F-actin fibers indicates failure to arrange them properly for final detachment.

In summary, the Rho, ROCK and myosin ATPase inhibitors evoke a morphological phenotype indistinguishable from the FGFR inhibitor SU5402. While phospho-myosin is not detectable in the broad tissue bridges resulting from treatment of early buds, a patch of cells positive for the activated myosin occurs ectodermal at the base of buds treated late.

Discussion

Tissue separation in embryonic systems occurs mostly by mechanical forces generated by apical constriction of cells, which is mediated by actomyosin interactions and often controlled by a pathway using RhoA, ROCK, and myosin (Fagotto, 2014). In *Drosophila*, for example, apical constriction of cells along the midline is essential to internalize gastrulating tissue (Martin et al., 2009). Concomitant with apical constriction the diameter of the central cells decreases, while mechanical tension increases the diameter in cells positioned lateral to the invagination zone (Martin and Goldstein, 2014).

We will discuss similar asymmetric cell shape changes at the *Hydra* bud base and the role of a candidate pathway by means of Rho, ROCK, and myosin II.

Functional Importance of Cell Shape Changes at the Bud Base and in the Tissue Bridge

The occurrence of very small and compact cells at the *Hydra* bud base and large cells with irregular cell membranes in the parent and the tissue bridge resembles similar cell shape and size differences observed during *Drosophila* gastrulation (Martin et al., 2009). Moreover, development of multicellular rosettes, as also found in *Drosophila* (Blankenship et al., 2006), indicates mechanical forces at the detachment site. Tissue sections and phospho-myosin distribution, however, suggest that the mechanisms underlying cell shape changes in *Hydra* are not identical to the ones controlling tissue invagination in *Drosophila*.

In contrast to fly gastrulation, the central bud cells close to the tubular tissue bridge are very small and not just apically constricted. The strong accumulation of F-actin in these cells suggests apicobasal additional to apical and/or lateral constriction. A recent study showed that the ability for apicobasal shortening is an intrinsic property of fully differentiated basal disk cells. It is caused by an apicobasally oriented, intracellular F-actin fiber (Rodrigues et al., 2016). Intracellular apicobasal F-actin fibers would be perfectly suited to weaken cell–matrix interactions at the separation site, when, at the same time, adjacent cells increase their binding to the matrix as in vertebrate tubulogenesis (Burute and Thery, 2012). Whether a change in cell–cell vs. cell–matrix interaction is necessary for bud detachment is an interesting question for future mechanistic studies.

The increase in volume and the apical vesicle accumulation of the exceptionally large, vacuolized EM cells covering the tissue bridge and the adjacent parental body column also distinguishes bud detachment from gastrulation processes. The function of the large cells is unknown, but some speculations may be allowed. Cell enlargement plus vacuolization might serve to passively loosen the tissue bridge and adjacent parental tissue for detachment. Accumulation of apical vesicles, F-actin, and, particularly, of phospho-myosin suggest, however, that these cells contribute actively. We propose three functions for the tissue bridge cells.

First, apical vesicles in EM cells of the body column are known to release glycocalyx components (Bottger et al., 2012). When tissue-bridge cells separate (Fig. 1), a new glycocalyx might be required, either to stiffen the tissue bridge for detachment by sphincter contraction of the bud base (Takahashi et al., 1997) or to enable reintegration of the cells into the body wall following detachment. Cell reintegration has not been investigated in detail, but the detachment site remains morphologically visible for 1–2 hr, in which *FGFRa* expressing cells are detectable in a small, contracting ring and finally in a patch (Sudhop et al., 2004) similar to *FGFe* (Fig. 5K). This coexpression will allow to identify the reintegrating, shrinking cells in future studies.

Second, the coexpression of the matrix metalloprotease *MMPA-3* with *FGFRa* at the bud base and detachment site (Münder et al., 2010) raises the possibility that the large cells secrete MMPA-3, which digests extracellular matrix components in the mesogloea to enable detachment. Third, the final detachment signal is given by myoactive peptides, which activate a sphincter contraction and shedding of the bud (Takahashi et al., 1997). The large cells might contribute to detachment by using their actomyosin to stiffen the tissue by, like in *Drosophila* (Blankenship et al., 2006), forming rosettes, and perhaps supported by an altered glycocalyx.

Taken together, the functions of the small bud base cells as well as of the large cells have to be investigated in detail to elucidate, how the detachment process is finalized.

Role of Ecto- and Endoderm During Tissue Separation

Phospho-myosin was detected in ecto- but not in endodermal cells at the late detachment site, suggesting a leading role for the ectoderm in tissue separation. This feature, interestingly, supports our previous observation, that tissue separation occurs with different kinetics when FGFRa (Kringelchen) is ectopically expressed ecto- or endodermally in transgenic polyps (Hasse et al., 2014). Ectodermal, ectopic Kringelchen-GFP induced a rapid and complete tissue separation within approximately 4 days, corresponding to bud detachment. Endodermal ectopic expression, on the other hand, resulted in a relatively quick endodermal separation, while autotomy of the body column took at least 10 days. Thus, coordination between ecto- and endoderm is possible, either by physical contacts of cells through the mesogloea pores (Shimizu et al., 2008), or by diffusible molecules like FGFs. Whether FGFRa acts effectively in both epithelia or whether FGFRb (Rudolf et al., 2013) assists in tissue separation has to be analyzed as well as the roles of FGFf and FGFe.

In this context, the predominant expression of the two myosin II genes, *st_MyHC* and *nm_MyHC*, in ecto- and endoderm, respectively, is interesting. Their differential expression could be correlated, as in many bilaterians, to the contraction speed of the respective EM cells (Steinmetz et al., 2012). While the *st_MyHC*-expressing, ectodermal cells contract relatively fast (e.g., as escape response after touching), the circular muscle cells expressing *nm_MyHC* contract slowly (predominantly during peristalsis). We found no evidence for the presence of more than two myosin

II genes in *Hydra*. The two myosins are thus not used exclusively for muscle functions in the basal myonemes of the EM cells, but they also function in actomyosin interactions driving cell shape changes.

Given its ectodermal expression, the striated-type, st_MyHC, may be more relevant for tissue separation than the predominantly endodermal nm_MyHC. However, *nm_MyHC* transcription is also upregulated ectodermally close to the detachment site. Recently, *Drosophila* nonmuscle myosin II has been reported to be the essential component for the rate determination of tissue folding (Vasquez et al., 2016). The evaluation of *Hydra* myosin II protein localization and function is necessary to decide this issue.

A Rho–ROCK–Myosin II Candidate Pathway

Ectopic expression of FGFRa causes ectopic tissue separation and targets two pathways: first, a MAPK–dpERK pathway in parental cells close to and within the tissue bridge; second, in a different cell population, a pathway causing F-actin accumulation in cells at the bud base and at ectopic separation sites (Hasse et al., 2014). We, therefore, used gene expression analysis and inhibitor studies to investigate whether a Rho–ROCK–myosin II signaling pathway is required for cell shape changes during bud detachment, and whether it has a link to FGFR signaling. *Hydra* Rho1, 2 (Supplementary Fig. S1B′), Rok (Philipp et al., 2009; Schenkelaars et al., 2016), and the two myosins II (Steinmetz et al., 2012) are structurally conserved to their bilaterian counterparts and, therefore, expected to perform similar functions.

Although physiological side effects of the used inhibitors cannot be excluded, the phenotype of nondetaching buds was consistent with the expression of Rho1, Rok, and the two myosins II.

The fact that drug exposure resulted in a scattered (if any) phospho-myosin pattern in the broad tissue bridge of nondetaching buds likely indicates the presence of normal body column tissue. In contrast, presence of phospho-myosin in the small tissue bridges of buds treated late, suggests that failing detachment is due to the chaotic arrangement of their F-actin fibers (Fig. 8), which might prohibit a coordinated sphincter contraction.

Synexpression with the two *Hydra* FGFRs, two FGFs and α-actinin as well as a phenotype identical to FGFR inhibition suggest a functional relationship between FGFR and the Rho, ROCK, and myosin II pathway. Its function for bud detachment appears equally important as FGFR signaling.

The existence of three members of the RhoABC subgroup turned out interesting. Their sequence features and differential expression indicates that *HvRho1* is the most likely candidate to act within the pathway: Rho1 and Rho2 sequences contain a ROCK-binding site and the interaction site for the Rhosin inhibitor, but only Rho1 is up-regulated at the bud base.

Rho2, expressed in the body ectoderm, might control cell shape changes along the body column, and Rho3 (neither ROCK- nor Rhosin-binding sites), which is expressed in a small cell population surrounding the mouth, might be necessary for shape changes required in the very flexible mouth opening. This function would also be essential at the tentacle base to control the cell shape changes leading to tissue constriction and tubular protrusions. The weak upregulation of Rho1, 2, and Rok at the tentacle bases raises doubts whether the same pathways are active at the bud and tentacle bases, but protein level investigations are missing. There certainly is an additional level of regulation at the bud base, which ensures detachment additional to constriction.

An amino acid exchange in the predicted Blebbistatin binding site of st_MyHC is interesting under functional aspects as it raises the possibility that Blebbistatin interacts differentially with the two *Hydra* myosins II. In *Dictyostelium* myosin II four residues, Ser456 (or Ala), Thr474, Tyr634, and Gln637 are essential for binding the inhibitor (Allingham et al., 2005). These residues are identical in the *Hydra* nm-MyHC. In st-MyHC the position of Tyr634 is changed to a His. Allingham and coauthors showed that replacement of Tyr634 by Phe in skeletal muscle myosin, in myosin Va, and in myosinX increases the $IC_{50} > 150\,\mu m$ and abolishes specificity. Whether the exchange of Tyr to His in *Hydra* st-MyHC causes a decreased affinity to Blebbistatin, has to be investigated by biochemical studies and is essential to decide, which MyHC is essential for detachment. Similar effects and time courses of the inhibitors of FGFR and of the candidate pathway elements suggest a close relationship between them.

A Signaling Network Might be Active at the Bud Base

Invagination during *Drosophila* gastrulation is completely reversible, when the $PI(4,5)P_2$ level is experimentally manipulated (Guglielmi et al., 2015). $PI(4,5)P_2$ is an essential phospholipid, located in the apical domain of the cell membrane and one of the essential elements controlling cell polarity. Upon activation of FGFR, G-protein coupled receptors (GPCR) or noncanonical Wnt signaling (Dailey et al., 2005; Seifert and Mlodzik, 2007), $PI(4,5)P_2$ is hydrolyzed by phospholipase Cγ (PLCγ) yielding the second messengers diacylglycerol (DAG) and IP_3 and activate pathways targeting the actin cytoskeleton.

An involvement of inositol phospholipids in *Hydra* bud detachment is possible as deduced from the fact that lithium ions prevent bud detachment and that this effect is correlated with remarkable changes in the inositol/inositol phosphate levels consistent with the inhibition of inositol mono- and bisphosphatases (Hassel and Berking, 1990; Hassel and Bieller, 1996). Inositol phosphatases ensure inositol recycling, which is essential for the synthesis of inositol lipids, like, $PI(4,5)P_2$. Although LiCl is best known as an activator of canonical Wnt signaling (by inhibiting GSK3β), there is no evidence that canonical Wnt signaling affects bud detachment (own unpublished observations). Noncanonical Wnt signaling, in contrast, which controls bud and tentacle evagination (Philipp et al., 2009) and regulates cell polarity and directed migration in planar polarity signaling in general (for a review see Seifert and Mlodzik, 2007), is able to target the actin cytoskeleton by means of Rho, or by means of a $PI(4,5)P_2$/PLC pathway, just like FGFR (Dailey et al., 2005). In *Hydra, Wnt8* is expressed at the bud base (Philipp et al., 2009), opening the possibility that noncanonical Wnt signaling acts in a network with FGFR and Rho-ROCK-Myosin II.

Conclusions

Despite the possibility that multiple signaling pathways converge on the actin cytoskeleton, we consider it most likely that FGFR signaling plays the major role in the activation of ectodermal Rho-ROCK-myosin II signaling in *Hydra* bud detachment. This conclusion is supported by previous experiments which revealed a direct effect of ectopic FGFR on ectopic F-actin accumulation and tissue separation. It is further supported by the ectodermal synexpression of two FGFs, both FGFRs, Rho1, ROCK, and nonmuscle as well as striated-type MyHC at the detachment site. If

and how endodermal cells contribute to detachment remains an open and interesting questions.

Experimental Procedures

Hydra culture, timing of bud stages and WMISH were performed as described previously (Grens et al., 1996; Sudhop et al., 2004). *Hydra vulgaris AEP* was used throughout the study unless otherwise indicated. For in situ hybridization, sequences for *Hydra* myosin (*nm_MyHC*: XP_012560866; *st_MyHC*: XP_002157926.3), *Hv_α-actinin* (XP_004208576.1), *Hv_Rho1-3* (Supplementary Fig. S1), *HvRok* (NM_001309671.1), the extracellular-domain-encoding sequences of *FGFRa* (XP_002157656) and *FGFRb* (XP_002157686), *HvFGFf and HvFGFe* were used to synthesize digoxigenin (Dig) -labeled RNA sense and antisense probes (Dig-labeling system, ROCHE). The quality of RNA probes was verified by Northern blotting and approximately 300 ng of the respective RNA probe per 0.1 ml was used for standard WMISH.

Deviating from this protocol, proteinase K digestion was prolonged for *Hydra vulgaris AEP* from 10 to 15 min and in situ hybridization required an additional 1:100 (*FGFe* and the two myosins) or 1:5 (*Hv_α-actinin)* dilution of the probe. In case, the in situ hybridization signals in *Hydra vulgaris AEP* were weak (*α-actinin, FGFf*), we used *Hydra magnipapillata* or *Hydra vulgaris, Zürich*, polyps, which yield a better signal-to-noise ratio, as shown previously (Lange et al., 2014). The pattern remained similar. Color development was performed at room temperature and allowed to proceed for 5 to 30 min (*Rho1, myosins, FGFRs, FGFe*, and *α-actinin*) or for up to 3 hr in the dark. All animals (3 to 5 per experiment) showed the same expression pattern.

Tissue Sections, Detection of F-actin/DAPI by Phalloidin, and of Phospho-myosin by MLC20 Antibody Staining

Tissue sections were prepared from normal animals as described (Sudhop et al., 2004) and stained with 1% methylene blue. Whole-mount tetramethylrhodamine (TRITC)-phalloidin and DAPI (4′,6-diamidine-2-phenylidole-dihydrochloride) staining was performed as described previously (Hasse et al., 2014). For phospho-myosin staining, animals were relaxed in 2% urethane for 1 min and fixed overnight in 4% paraformaldehyde (PFA) in 1 × phosphate buffered saline (PBS), pH 7.4 (0.15 M NaCl in 0.01 M sodium-phosphate buffer) at 4° C. Polyps were washed and permeabilized 3 × 20 min in 1 × PBT (1 × PBS containing 0.25% Triton X-100, v/v). Polyps were incubated for at least 7 hrs in blocking buffer (1 × PBT containing 2% BSA). The primary antibody (polyclonal MLC20 (Myosin light chain -phospho S20), Abcam) was diluted 1:400 in blocking buffer and incubated overnight at 4° C. Following 3 × 20 min washing steps in blocking buffer, 3 × 10 min in PBT and again 3 × 20 min in blocking buffer at room temperature, the animals were incubated for 2 hr at room temperature with the secondary antibody (FITC-Affinity Pure goat anti-rabbit (Sigma), diluted 1:750). Unbound antibody was removed by washing 6 × 20 min in PBT followed by an overnight washing step in 1 × PBS, pH 7.4 at 4° C. For MLC20/TRITC-phalloidin double staining, TRITC-phalloidin was incubated in washing buffer for 1 hr following the first washing step. The remaining five washing steps were performed as detailed above. Specimen were embedded in Roti-Mount-Fluorocare and polymerized in the dark. Images were taken on a confocal laser scanning microscope, Leica TCS SP5.

Incubation With Inhibitors

Inhibition with SU5402 (Calbiochem) was performed as described (Sudhop et al., 2004). Optimal concentrations were determined based on published data by evaluating the strongest effects on *Hydra* at low toxicity (Supplementary Fig. S3). For inhibition with Rhosin (Calbiochem, [Shang et al., 2012]) at 100 μM, Rockout (Calbiochem, [Harding and Nechiporuk, 2012]) at 50 and 100 μM; Y-27632 at 5, 20 or 50 μm) or Blebbistatin (Sigma, [Kovacs et al., 2004; Fagotto et al., 2013]) at 2.5 μM, stage 3–5 or stage 5–7 buds (Otto and Campbell, 1977) were selected 24 hrs after the last feeding. Polyps were incubated at 18° C in the dark for 48 hrs in commercially available VOLVIC mineral water containing a final concentration of 1% dimethylsulfoxide (DMSO), 1 mM adenosine triphosphate (ATP) and the corresponding concentration of an inhibitor. As controls, we used untreated polyps carrying the respective bud stages as well as animals incubated in the DMSO/ATP solute without the respective inhibitor. Phenotypes were evaluated 3 days after the end of treatment, when normal buds have detached. Experiments with Rhosin, Rockout, and Blebbistatin were repeated at least six times independently (Rhosin 9x) with a sample size of 10 animals per inhibitor treatment. Y-27632 treatment was carried out once with 10 animals for comparison.

Database Search and Phylogenetic Analysis

To reveal the Rho sequences in *Hydra*, we explored the NCBI databases (http://www.ncbi.nlm.nih.gov/). Annotated human Rho sequences (NP_001655.1 (RhoA), CAA29968.1 (RhoB), AAM21119.1 (RhoC)) were used as query to identify similar sequences in *Hydra* and other animals. The deduced *Hydra* protein sequences were aligned with available protein sequences of the poriferan *Amphimedon queenslandica*, the cnidarian *Nematostella vectensis*, Platyhelminthes, Mollusca, Annelida, Insecta, and Chordata as indicated. Sequences were predicted by automated computational analysis (genomic sequence annotated using gene prediction method: Gnomon, supported by EST evidence). ROCK binding sites in the HvRho proteins were predicted by the NCBI function "Identify conserved domains".

For the phylogenetic tree, sequences were aligned using ClustalX 2.1 (Jeanmougin et al., 1998) with BLOSUM30 alignment matrix and unrooted trees were derived using a Metropolis-coupled Markov Chain Monte Carlo (MrBayes 3.2, ngen=1000000, samplefreq=100). Trees were displayed using FigTRee v1.4.2.

RNA Isolation, cDNA Synthesis, and PCR of Sequences of Interest

The Quickprep Micro Kit (Amersham) was used to harvest poly(A)$^+$ RNA from *Hydra vulgaris AEP*. Poly(A)$^+$ RNA was reverse transcribed using Revert Aid TM Premium First-strand cDNA Synthesis Kit (Fermentas) and diluted 1:100 before PCR amplification of the genes of interest. *Hydra nm_MyHC, HvRho, HvRok*, and *Hv_α-actinin* gene sequences were PCR amplified using the following primer pairs: Primers for *st_MyHC* as in (Steinmetz et al., 2012) ***nm_MyHC*** forward: AGCTGCGTTGCCCGATAATA,

reverse: CGTTGTTGTGCTTCTGCCAA; ***Hv_α-actinin*** forward: TGATCCAGCATGGGAAATGC reverse: ACTGGGCGATTGCTTAA TCG; ***Hv_Rok*** forward: ACACTGCTGTTGGCACTACT, reverse: ATCTGCAACAGCTTGGGCTT; ***HvRho1*** forward: ATTGTTGGTGA TGGTGCTTGTGG, reverse: GCAGCTCTAGTTGCAGTTTCAAATA CC; ***HvRho2*** forward: GCAATTCGCAAGAAATTAGTC; reverse: GCCATCTCACGACCTTGTTCAATC; ***HvRho3*** forward: GAAATCA TCAGAGAGAAGCCC, reverse: TGATATCTTCGAGGTCACGCT. Amplified cDNA fragments were AT-cloned into the pGEM T-Easy vector (Promega). Clone identity was confirmed by sequencing (SeqLab). Promotors used for anti-sense transcription were T7 or SP6 depending on the orientation of the blunt-end cloned cDNAs.

Statistics

In Figure 7, the error bars indicate the standard error of the mean (SEM), which is the standard deviation of the sample mean's estimate of a population mean. The SEM was calculated using the Excel program (Bland and Altman, 1996).

Acknowledgments

We thank two unknown referees for critical comments which improved the manuscript and Eva Frei for polishing the manuscript. Heide Brandtner and Marcel Hemming did an excellent job in caring for our *Hydra* cultures. We are indebted to Helga Kisselbach-Heckmann and Lothar Beck for help with the thin sections. The FGFRb in situ hybridization was performed by Alexander Becker and Dominic Grauer in our MSc course. Without support by the DFG grant HA1732/13 and association of D.A. to GRK 2213, this study would not have been possible.

References

Allingham JS, Smith R, Rayment I. 2005. The structural basis of blebbistatin inhibition and specificity for myosin II. Nat Struct Mol Biol 12:378–379.

Anton-Erxleben F, Thomas A, Wittlieb J, Fraune S, Bosch TC. 2009. Plasticity of epithelial cell shape in response to upstream signals: a whole-organism study using transgenic Hydra. Zoology (Jena) 112:185–194.

Aufschnaiter R, Zamir EA, Little CD, Ozbek S, Munder S, David CN, Li L, Sarras MP Jr, Zhang X. 2011. In vivo imaging of basement membrane movement: ECM patterning shapes Hydra polyps. J Cell Sci 124:4027–4038.

Beckmann A, Ozbek S. 2012. The nematocyst: a molecular map of the cnidarian stinging organelle. Int J Dev Biol 56:577–582.

Bland JM, Altman DG. 1996. Statistics notes. Logarithms. BMJ 312:700.

Blankenship JT, Backovic ST, Sanny JS, Weitz O, Zallen JA. 2006. Multicellular rosette formation links planar cell polarity to tissue morphogenesis. Dev Cell 11:459–470.

Bottger A, Doxey AC, Hess MW, Pfaller K, Salvenmoser W, Deutzmann R, Geissner A, Pauly B, Altstatter J, Munder S, Heim A, Gabius HJ, McConkey BJ, David CN. 2012. Horizontal gene transfer contributed to the evolution of extracellular surface structures: the freshwater polyp Hydra is covered by a complex fibrous cuticle containing glycosaminoglycans and proteins of the PPOD and SWT (sweet tooth) families. PLoS One 7:e52278.

Bottger A, Hassel M. 2012. Hydra, a model system to trace the emergence of boundaries in developing eumetazoans. Int J Dev Biol 56:583–591.

Boureux A, Vignal E, Faure S, Fort P. 2007. Evolution of the Rho family of ras-like GTPases in eukaryotes. Mol Biol Evol 24: 203–216.

Burute M, Thery M. 2012. Spatial segregation between cell-cell and cell-matrix adhesions. Curr Opin Cell Biol 24:628–636.

Buzgariu W, Al Haddad S, Tomczyk S, Wenger Y, Galliot B. 2015. Multi-functionality and plasticity characterize epithelial cells in Hydra. Tissue Barriers 3:e1068908.

Chapman JA, Kirkness EF, Simakov O, Hampson SE, Mitros T, Weinmaier T, Rattei T, Balasubramanian PG, Borman J, Busam D, Disbennett K, Pfannkoch C, Sumin N, Sutton GG, Viswanathan LD, Walenz B, Goodstein DM, Hellsten U, Kawashima T, Prochnik SE, Putnam NH, Shu S, Blumberg B, Dana CE, Gee L, Kibler DF, Law L, Lindgens D, Martinez DE, Peng J, Wigge PA, Bertulat B, Guder C, Nakamura Y, Ozbek S, Watanabe H, Khalturin K, Hemmrich G, Franke A, Augustin R, Fraune S, Hayakawa E, Hayakawa S, Hirose M, Hwang JS, Ikeo K, Nishimiya-Fujisawa C, Ogura A, Takahashi T, Steinmetz PR, Zhang X, Aufschnaiter R, Eder MK, Gorny AK, Salvenmoser W, Heimberg AM, Wheeler BM, Peterson KJ, Bottger A, Tischler P, Wolf A, Gojobori T, Remington KA, Strausberg RL, Venter JC, Technau U, Hobmayer B, Bosch TC, Holstein TW, Fujisawa T, Bode HR, David CN, Rokhsar DS, Steele RE. 2010. The dynamic genome of Hydra. Nature 464:592–596.

Dailey L, Ambrosetti D, Mansukhani A, Basilico C. 2005. Mechanisms underlying differential responses to FGF signaling. Cytokine Growth Factor Rev 16:233–247.

Fagotto F. 2014. The cellular basis of tissue separation. Development 141:3303–3318.

Fagotto F, Rohani N, Touret AS, Li R. 2013. A molecular base for cell sorting at embryonic boundaries: contact inhibition of cadherin adhesion by ephrin/ Eph-dependent contractility. Dev Cell 27:72–87.

Foley KS, Young PW. 2014. The non-muscle functions of actinins: an update. Biochem J 459:1–13.

Graf L, Gierer A. 1980. Size, shape and orientation of cells in budding Hydra and regulation of regeneration in cell aggregates. Wilhelm Roux Arch Dev Biol 188:141–151.

Grens A, Gee L, Fisher DA, Bode HR. 1996. CnNK-2, an NK-2 homeobox gene, has a role in patterning the basal end of the axis in hydra. Dev Biol 180:473–488.

Guglielmi G, Barry JD, Huber W, De Renzis S. 2015. An optogenetic method to modulate cell contractility during tissue morphogenesis. Dev Cell 35:646–660.

Harding MJ, Nechiporuk AV. 2012. Fgfr-Ras-MAPK signaling is required for apical constriction via apical positioning of Rho-associated kinase during mechanosensory organ formation. Development 139:3130–3135.

Hasse C, Holz O, Lange E, Pisowodzki L, Rebscher N, Christin Eder M, Hobmayer B, Hassel M. 2014. FGFR-ERK signaling is an essential component of tissue separation. Dev Biol 395:154–166.

Hassel M, Berking S. 1990. Lithium ions interfere with pattern control in hydra-vulgaris. Roux Arch Dev Biol 198:382–388.

Hassel M, Bieller A. 1996. Stepwise transfer from high to low lithium concentrations increases the head-forming potential in Hydra vulgaris and possibly activates the PI cycle. Dev Biol 177:439–448.

Hobmayer B, Jenewein M, Eder D, Eder MK, Glasauer S, Gufler S, Hartl M, Salvenmoser W. 2012. Stemness in Hydra - a current perspective. Int J Dev Biol 56:509–517.

Hobmayer B, Rentzsch F, Kuhn K, Happel CM, von Laue CC, Snyder P, Rothbacher U, Holstein TW. 2000. WNT signalling molecules act in axis formation in the diploblastic metazoan Hydra. Nature 407:186–189.

Jeanmougin F, Thompson JD, Gouy M, Higgins DG, Gibson TJ. 1998. Multiple sequence alignment with Clustal X. Trends Biochem Sci 23:403–405.

Kovacs M, Toth J, Hetenyi C, Malnasi-Csizmadia A, Sellers JR. 2004. Mechanism of blebbistatin inhibition of myosin II. J Biol Chem 279:35557–35563.

Kroening S, Stix J, Keller C, Streiff C, Goppelt-Struebe M. 2010. Matrix-independent stimulation of human tubular epithelial cell migration by Rho kinase inhibitors. J Cell Physiol 223:703–712.

Lange E, Bertrand S, Holz O, Rebscher N, Hassel M. 2014. Dynamic expression of a Hydra FGF at boundaries and termini. Dev Genes Evol 224:235–244.

Levayer R, Lecuit T. 2012. Biomechanical regulation of contractility: spatial control and dynamics. Trends Cell Biol 22:61–81.

Martin AC, Goldstein B. 2014. Apical constriction: themes and variations on a cellular mechanism driving morphogenesis. Development 141:1987–1998.
Martin AC, Kaschube M, Wieschaus EF. 2009. Pulsed contractions of an actin-myosin network drive apical constriction. Nature 457:495–499.
Münder S, Käsbauer T, Prexl A, Aufschnaiter R, Zhang X, Towb P, Böttger A. 2010. Notch signalling defines critical boundary during budding in Hydra. Dev Biol 344:331–345.
Munder S, Tischer S, Grundhuber M, Buchels N, Bruckmeier N, Eckert S, Seefeldt CA, Prexl A, Kasbauer T, Bottger A. 2013. Notch-signalling is required for head regeneration and tentacle patterning in Hydra. Dev Biol 383:146–157.
Nakamura Y, Tsiairis CD, Özbek S, Holstein TW. 2011. Autoregulatory and repressive inputs localize Hydra Wnt3 to the head organizer. Proc Natl Acad Sci U S A 108:9137–9142.
Niehrs C, Pollet N. 1999. Synexpression groups in eukaryotes. Nature 402:483–487.
Otto J, Campbell R. 1977. Budding in Hydra attenuata: bud stages and fate map. J Exp Zool 200:417–428.
Philipp I, Aufschnaiter R, Ozbek S, Pontasch S, Jenewein M, Watanabe H, Rentzsch F, Holstein TW, Hobmayer B. 2009. Wnt/beta-catenin and noncanonical Wnt signaling interact in tissue evagination in the simple eumetazoan Hydra. Proc Natl Acad Sci U S A 106:4290–4295.
Rodrigues M, Ostermann T, Kremeser L, Lindner H, Beisel C, Berezikov E, Hobmayer B, Ladurner P. 2016. Profiling of adhesive-related genes in the freshwater cnidarian Hydra magnipapillata by transcriptomics and proteomics. Biofouling 32:1115–1129.
Rudolf A, Huubinger C, Huusken K, Vogt A, Rebscher N, Oel SF, Renkawitz-Pohl R, Hassel M. 2013. The Hydra FGFR, Kringelchen, partially replaces the Drosophila Heartless FGFR. Dev Genes Evol 223:159–169.
Sarras MP Jr. 2012. Components, structure biogenesis and function of the Hydra extracellular matrix in regeneration, pattern formation and cell differentiation. Int J Dev Biol 56:567–576.
Schenkelaars Q, Quintero O, Hall C, Fierro-Constain L, Renard E, Borchiellini C, Hill AL. 2016. ROCK inhibition abolishes the establishment of the aquiferous system in Ephydatia muelleri (Porifera, Demospongiae). Dev Biol 412:298–310.
Schwayer C, Sikora M, Slovakova J, Kardos R, Heisenberg CP. 2016. Actin Rings of Power. Dev Cell 37:493–506.
Seifert JR, Mlodzik M. 2007. Frizzled/PCP signalling: a conserved mechanism regulating cell polarity and directed motility. Nat Rev Genet 8:126–138.
Seybold A, Salvenmoser W, Hobmayer B. 2016. Sequential development of apical-basal and planar polarities in aggregating epitheliomuscular cells of Hydra. Dev Biol 412:148–159.
Shang X, Marchioni F, Sipes N, Evelyn CR, Jerabek-Willemsen M, Duhr S, Seibel W, Wortman M, Zheng Y. 2012. Rational design of small molecule inhibitors targeting RhoA subfamily Rho GTPases. Chem Biol 19:699–710.
Shimizu H, Aufschnaiter R, Li L, Sarras MP Jr, Borza DB, Abrahamson DR, Sado Y, Zhang X. 2008. The extracellular matrix of hydra is a porous sheet and contains type IV collagen. Zoology (Jena) 111:410–418.
Shimizu H, Zhang X, Zhang J, Leontovich A, Fei K, Yan L, Sarras MP Jr. 2002. Epithelial morphogenesis in hydra requires de novo expression of extracellular matrix components and matrix metalloproteinases. Development 129:1521–1532.
Sjoblom B, Salmazo A, Djinovic-Carugo K. 2008. Alpha-actinin structure and regulation. Cell Mol Life Sci 65:2688–2701.
Steinmetz PR, Kraus JE, Larroux C, Hammel JU, Amon-Hassenzahl A, Houliston E, Worheide G, Nickel M, Degnan BM, Technau U. 2012. Independent evolution of striated muscles in cnidarians and bilaterians. Nature 487:231–234.
Sudhop S, Coulier F, Bieller A, Vogt A, Hotz T, Hassel M. 2004. Signalling by the FGFR-like tyrosine kinase, Kringelchen, is essential for bud detachment in Hydra vulgaris. Development 131:4001–4011.
Takahashi T, Muneoka Y, Lohmann J, Lopez de Haro M, Solleder G, Bosch T, David C, Bode H, Koizumi O, Shimizu H, Hatta M, Fujisawa T, Sugiyama T. 1997. Systematic isolation of peptide signal molecules regulating development in hydra: LWamide and PW families. Proc Natl Acad Sci U S A 94:1241–1246.
Vasquez CG, Heissler SM, Billington N, Sellers JR, Martin AC. 2016. Drosophila non-muscle myosin II motor activity determines the rate of tissue folding. Elife 5.
Wheeler AP, Ridley AJ. 2004. Why three Rho proteins? RhoA, RhoB, RhoC, and cell motility. Exp Cell Res 301:43–49.

Chapter 2

Holz et al., 2020

Alternative pathways control actomyosin contractility in epitheliomuscle cells during morphogenesis and body contraction

Developmental Biology 463 (2020) 88-98

DOI: 10.1016/j.ydbio.2020.04.001

3.1 Introduction to Chapter 2

In Chapter II (Holz et al., 2020) the main approach was to elucidate how the detachment process of the buds takes place mechanistically and which subcellular compartments of the epitheliomuscle cells were used during bud base morphogenesis. To obtain a full picture of MRLC localization in *Hydra*, gene expression analysis and immunohistological analysis with an antibody against the unphosphorylated RLC protein (MYL9) were carried out. Furthermore it was addressed whether basal contractility as well as morphogenetic processes was regulated by independent signaling pathways. To answer these questions, detailed analysis of cLSM stacks were performed to analyze subcellular localization of pMLC20 in constricting bud base cells. To gain insights into potential signaling processes during body contractility and morphogenesis, inhibitor experiments were carried out, followed by immunohistological and western blot analysis.

The data revealed that *Hv_MRLC12B-like* is expressed in the whole body column of the polyp and is upregulated in morphogenetic active regions, which coincides with the localization of MYL9. Interestingly, MYL9 can be detected both ectodermal and endodermal while pMLC20 is restricted to an ectodermal localization. The detailed analysis of pMLC20 at the late bud base revealed that the entire cellular cortex of the epitheliomuscle cells is used during bud morphogenesis. The inhibitor experiments have shown that the basal contractility and morphogenetic processes are regulated independently. The contractility is controlled by MLCK signaling while morphogenesis is Rho-ROCK dependent.

My part in this publication was the implementation and evaluation of all experiments mentioned as well as the compilation of the data of the publication

The quantitative evaluation of the Western blot analysis was carried out by Dr. David Apel. The Supplementary video material was created by Prof. Dr. Monika Hassel and edited by Dr. David Apel.

Developmental Biology 463 (2020) 88–98

Contents lists available at ScienceDirect

Developmental Biology

journal homepage: www.elsevier.com/locate/developmentalbiology

Alternative pathways control actomyosin contractility in epitheliomuscle cells during morphogenesis and body contraction

Oliver Holz [a], David Apel [a,b], Monika Hassel [a,*]

[a] Philipps University Marburg, Faculty of Biology, Morphology and Evolution of Invertebrates, D-35039 Marburg, Germany
[b] DFG Research Training Group, Membrane Plasticity in Tissue Development and Remodeling, GRK 2213, Philipps-Universität Marburg, Germany

ARTICLE INFO

Keywords:
Movement
Tissue separation
Rock
MLCK
Cnidaria

ABSTRACT

In adult *Hydra*, epitheliomuscle cells form the monolayered ecto- and endodermal epithelia. Their basal myonemes function as a longitudinal and circular muscle, respectively. Based on the observation that a Rho/Rock pathway, controlling the cell shape changes during detachment of *Hydra* buds, is not involved in body movement, at least two actomyosin compartments must exist in these cells: a basal one for body movement and a cortical one for cell shape changes. We therefore analyzed the regional and subcellular localization of the Ser19-phosphorylated myosin regulatory light chain (pMLC20). Along the body column, pMLC20 was detected strongly in the basal myonemes and weakly in the apical cell compartments of ectodermal epitheliomuscle cells. In cells of the bud base undergoing morphogenesis, pMLC20 was localized to intracellular stress fibers as well as to the apical and additionally to the lateral cortical compartment. Pharmacological inhibition revealed that pMLC20 is induced in these compartments by at least two independent pathways. In myonemes, MLC is phosphorylated mainly by myosin light chain kinase (MLCK). In contrast, the cortical apical and lateral MLC phosphorylation in constricting ectodermal cells of the bud base is stimulated via the Rho/ROCK pathway.

1. Introduction

Apical constriction is an evolutionary conserved mechanism that occurs in a variety of morphogenetic processes during embryogenesis (Pearl et al., 2017). It requires the reorganization of the cortical actin cytoskeleton and actomyosin interactions (Martin and Goldstein, 2014; Martin et al., 2009). Cortical actomyosin consists of a complex of actin filaments, non-muscle myosin II and a variety of other proteins which modulate actomyosin network organization and stability (Martin, 2016). The non-muscle myosin II fulfills several cellular functions. It acts as a motor protein to generate contractile forces and acts additionally as an important cross-linker between actin filaments (Ma et al., 2012; Martin, 2016; Schwayer et al., 2016). Phosphorylation of the myosin regulatory light chain (MLC) is a precondition to generate contractile forces. It ensures myosin II activity and actomyosin network formation (Somlyo and Somlyo, 2003; Watanabe et al., 2007). Five regulatory phosphorylation sites at the N-terminus of MLC, Ser1, Ser2 and Thr10, inhibit MLC, while phosphorylation of Thr18 and Ser19 is essential and synergistic for myosin activation and the formation and stability of contractile actomyosin bundles (Ikebe and Hartshorne, 1985; Ikebe et al., 1987; Komatsu and Ikebe, 2007; Vicente-Manzanares et al., 2008; Watanabe et al., 2007). A variety of signaling pathways converge on MLC phosphorylation and modulate the intensity of network formation and contractility (Newell-Litwa et al., 2015; Vicente-Manzanares et al., 2008). The two main pathways for MLC phosphorylation are via myosin light chain kinase (MLCK) and via Rho signaling (Betapudi, 2014; Levayer and Lecuit, 2012). MLCK phosphorylates MLC in a calcium dependent manner at Thr18 and/or Ser19. The phosphorylation level is balanced by myosin light chain phosphatase (MLCP) which decreases actomyosin network formation and therewith contractility (Watanabe et al., 2007).

Rho signaling, in contrast, stabilizes high MLC phosphorylation levels mainly by inhibiting MLC phosphatase, MLCP (Hartshorne et al., 1998; Kimura et al., 1996; Zhang et al., 2015). The small GTPase activates Rho-associated-kinase (Rock) and functions as a switch: it prevents MLC dephosphorylation by blocking MLCP and additionally phosphorylates MLC directly at the activation sites (Bresnick, 1999; Sellers, 1991). Rho-mediated signaling therefore stabilizes a strong actomyosin network and stress fiber formation (Martin and Goldstein, 2014; Newell-Litwa et al., 2015; Watanabe et al., 2007). Furthermore, Rho signaling is essential for the apical enrichment of actomyosin complexes which is a prerequisite for apical constriction during morphogenesis of vertebrate and insect embryos (Borges et al., 2011; Pearl et al., 2017).

* Corresponding author. Philipps University, FB 17 Biology, Molecular Zoology. Karl von Frisch Str. 8, 35039 Marburg, Germany.
E-mail address: hassel@biologie.uni-marburg.de (M. Hassel).

https://doi.org/10.1016/j.ydbio.2020.04.001
Received 16 October 2019; Received in revised form 10 March 2020; Accepted 14 April 2020
Available online 1 May 2020

Under the aspects of functional evolution of Rho signaling and actomyosin contractility, the freshwater polyp *Hydra* is an interesting system. Due to permanent cell proliferation, tissue constantly shifts towards the apical and basal ends and undergoes morphogenesis to maintain the apical head with its mouth opening and tentacles as well as the basal disc (foot) for attachment. Additionally, excess tissue evaginates into lateral buds which detach as fully grown young polyps 4 days later from the parent's flank (Otto and Campbell, 1977). Bud detachment in *Hydra* is unique compared to other tissue separation processes. The two monolayered epithelia with their intermitting acellular extracellular matrix (called mesogloea in Cnidaria) constrict and separate between parent and bud without a wound or apoptosis. The ectoderm takes the leading role by activating an FGFR-induced Rho/Rock-dependent pathway which controls cell shape changes and the localized accumulation of cortical actomyosin in the bud base ectoderm and in adjacent parental tissue (Hasse et al., 2014; Holz et al., 2017).

The fact that the inhibition of Rho/Rock signaling prohibited these cell shape changes and the formation of local actomyosin complexes, but did not interfere with body contractions, attracted our interest. *Hydra* lacks true muscle cells for movement. Instead, the monolayered *Hydra* epithelia (ecto- and endoderm) are formed by epitheliomuscle cells which unite epithelial functions in their apical part and muscle function in their basal compartments (Leclere and Rottinger, 2016). The epitheliomuscle cells send basal contractile processes (myonemes) along the extracellular matrix. These act as functional antagonists in body contraction and elongation because the ectodermal myonemes run longitudinally and the endodermal ones circularly (Aufschnaiter et al., 2017). Since morphogenesis, but not movement of the *Hydra* body was impaired by pharmacological inhibition of Rho and Rock signaling, we investigated whether different signaling systems act in the basal and in the cortical compartments of the epitheliomuscle cells. Our study revealed a clear correlation between Rho/Rock activation and morphogenesis during which pMLC20 is localized in the apical and lateral compartments of ectodermal bud base cells. In body column tissue, pMLC20 was located mainly in the myonemes being related to body movement. MLCK activity, but not Rho/Rock signaling, controls pMLC20 in this compartment. Our data elucidate part of the physiological background of epitheliomuscle function in morphogenesis.

2. Materials and methods

2.1. Hydra culture

Hydra cultures were raised as summarized in (Klimovich et al., 2019).

2.2. In situ hybridization and immunofluorescence

Whole mount *in situ* hybridization was performed as described previously (Sudhop et al., 2004). Detection of pMLC20 (abcam: ab2480, dilution 1:400), MYL9 (abcam: ab64161, dilution 1:200) and F-actin were performed according to (Holz et al., 2017). TRITC-phalloidin staining was carried out as described in (Hasse et al., 2014). Detection of Thr18 plus Ser19 using the Phospho-Myosin Light Chain 2 (Thr18/Ser19) Antibody #3674 of CST (1:100) yielded neither a signal in the Western Blot nor in *Hydra* tissue.

2.3. Western Blot

The inhibited polyps were collected and the amount of tissue was quantified by weight. The protein concentration was quantified in a previous series using the bicinchonic acid protein assay kit (SIGMA) and ten samples of three equally sized polyps, each. The polyps were dissolved by adding 20 parts (v/w) of the bicinchonic acid reagent A solution containing 2% SDS and dissolved after 10 min by pipetting up and down. Standards samples were treated in a similar way. Solution B was added and the concentration determined according to the manufacturer's recommendation using a BSA standard curve. Ten independent determinations of the protein concentration showed less than 7% deviation. We therefore routinely use three *Hydra* of similar size per sample for Western Blot analysis and a standard internal loading control (the anti-tubulin antibody in this study). *Hydra* tissue was boiled for 5 min in 25 µl of 2x sample buffer (Laemmli, 1970). Samples were quickly cooled on ice and subjected to denaturing PAGE. A Western blot was carried out following standard procedures on a PVDF membrane. The primary anti-pMLC antibody (rabbit polyclonal, Phospho Myosin Light Chain S20, abcam) was used 1:2000 diluted in PBT (0,1% Tween 20) with 2% bovine serum albumin (BSA fraction V). A single band was detected at about 20 kd using a peroxidase coupled anti-rabbit antibody and the ECL system. As an internal loading control we used an anti-Tubulin antibody (monoclonal, anti-α-Tubulin, Sigma) in a 1:5000 dilution in PBT (0,1% Tween 20) with 2% bovine serum albumin (BSA fraction V). The ECL (Pierce) chemiluminescence signal was documented by using the LI-COR Odyssey Fc System and images processed by the Image Studio ™ (5.2, LI-COR® Biotechnology) software. Band intensity was determined using the FIJI (ImageJ) Gel analyzing tools. The relative signal intensity in each lane (ratio of sample signal (ROI) to tubulin signal) was calculated and the resulting value compared to the control as a percent value.

2.4. Incubation with inhibitors

Inhibition with Rhosin, Rockout and Blebbistatin was performed as described previously (Holz et al., 2017). Optimal concentrations of freshly prepared inhibitor solutions (ML7 at 1–5 µM, Calyculin A at 40 nM and Cytochalasin B at 10 µg/ml) were based on published data and by evaluating the strongest effects at low toxicity: for immunodetection and Western blot analysis of pMLC, polyps carrying a stage 5–7 bud were selected 24 h after the last feeding. Polyps were incubated at 18 °C for 16 h in the dark in VOLVIC mineral water containing a final concentration of 1% dimethylsulfoxide (DMSO), 1 mM adenosine triphosphate (ATP) and the respective concentration of the inhibitor. ATP was added to avoid kinase inhibition caused by leakage of the triphosphate from the DMSO-treated polyps. After incubation, polyps were directly fixed in 4% PFA or suspended in 2x Laemmli sample buffer for Western blot. For phalloidin staining animals were incubated for 6 h and fixed in 4% PFA prior to staining. Since the polyps reacted very sensitive to the ML7 inhibitor, the long term incubation (16 h) was performed in 1 µM, 2,5 or 5 µM (Western blot), tissue analysis and immunodetection were done at 1 µM and 2,5 µM, respectively, and movies taken using 2,5 or 5 µM ML7. The sensitivity to ML7 concentration varied over time (9 months) and had to be adjusted for each inhibitor batch. To obtain the loss-of-tentacles phenotype, polyps had to be incubated in the freshly prepared inhibitor. In five experimental series polyps incubated in 2,5 or 5 µM ML7 reacted with the typical tentacle shedding (see movies), however after 1,5 to 6 h. Incubations in 5 µM ML7 for 16 h either reduced the polyps to small tissue chunks, while polyps in 1 and 2,5 µM were smaller but well recognizable as tentacle-less *Hydra*. In other experiments, the response shifted to higher concentrations with 1 µM ML7 having no visible effect.

A long term treatment (e.g. 16 hrs) with Cytochalasin B lead to complete tissue disintegration. Therefore, under standard conditions, polyps were incubated for 6 h in the respective inhibitor (see Fig. 6).

2.5. RNA isolation, cDNA synthesis, PCR and probe synthesis

The RNA easy Mini Kit (Qiagen) was used to isolate the total RNA from *Hydra vulgaris AEP*. RNA was reverse transcribed using Revert Aid First-strand cDNA Synthesis Kit (Fermentas). The synthesized cDNA was used in a 1:100 dilution to amplify the gene of interest by PCR. *Hv-MRLC12B-like* gene sequences were PCR amplified using the following primer pair: *Hv-MRLC12B-like* forward: GCAAGAAAAGAGCCCAAAGAGC, *Hv-MRLC12B-like* reverse: TGCAACACACAGGTATTGGC. The amplified *Hv-MRLC12B-like* fragment was cloned into the pGEM T-Easy vector (Promega). Clone identity was confirmed by sequencing (SeqLab).

Flanking promotors (SP6 and T7) were used for anti-sense and sense probe transcription.

2.6. Microscopy and image manipulation

Images were taken on a confocal laser scanning microscope, Leica TCS SP5. The fluorescence intensity of TRITC-phalloidin and pMLC20 labelling was determined using the free imaging software FIJI (v1.52i) (Schindelin et al., 2012). Further image manipulations were performed by GIMP (GNU Image Manipulation Program).

Body movement of *Hydra* polyps with or without the MLCK inhibitor ML7 was recorded digitally with the Nikon SMZ800 dissection microscope and NIS software. For short term movies 20 s to 1 min were recorded with 25 frames per second (fps). 3–5 animals with a bud were kept at 18 °C in 6-well plates containing 4–8 ml of *Hydra* medium (control). The solute control contained additionally 1% DMSO and 1 mM ATP and the assays ML7 (5 μM in 1% DMSO, 1 mM ATP). The animals were examined every 10–30 min and pinched with a metal forceps to monitor whether they were able to contract their body column. Spontaneous movement was monitored by long term movies of control and ML7-treated polyps at 18–22 °C taking a picture every 10 s (0,1 fps) for a maximum of 3:30 h. The movies were compressed suing FIJI and VLC Media player.

3. Results

Since cell-shape-related contractile forces are generated by a highly dynamic actomyosin network in the cellular cortex and mainly regulated by phosphorylation of the myosin regulatory light chain (MLC), we first analyzed the distribution of pMLC20 and F-actin in whole *Hydra*.

3.1. Characteristic distribution of the myosin regulatory light chain gene and the (phosphorylated) protein in cells undergoing morphogenesis

In the genome of *Hydra,* only a single *MRLC* gene (*Hv_MRLC12B-like gene;* CDG72090.1 protein) (Steinmetz et al., 2012; Wenger and Galliot, 2013) is annotated. The gene expression domains of *Hv_MRLC12B-like* were identified by whole mount *in situ* hybridisation (Fig. 1). While the sense probe yielded no signal (data not shown), the antisense probe revealed a constitutive, strong endodermal and, mostly weak, ectodermal expression along the body column. In the apical-most region of the hypostome, in the peduncle and the basal disc, gene expression was much weaker. Color development of the specimen shown in Fig. 1 was not run to completion but optimized for the visibility of these differences. Elevated ectodermal expression was detected at the tentacle bases (Fig. 1 B) in sprouting bud tentacles and at the constricting bud base (Fig. 1 A, C).

The gene expression pattern of *Hv_MRLC12B-like* was reflected by the immunoreactivity of the MYL9 antibody (Fig. 2 A, B) which recognizes the highly conserved MLC (Fig. 2 G). The MYL9 signal was located mainly in the myonemes of ecto- and endodermal cells and weak in their cell bodies (Fig. 2 A′). It was enriched in the tentacles bases (Fig. 2 A) as well as at the bud detachment site (Fig. 2 B). Additionally, MYL9 was detected strongly in a ring of terminally differentiated cells around the mouth where the *MLC* mRNA was not (or no longer) detectable (Fig. 2 A). The *Hv_MRLC12B-like* transcript and MLC protein distribution partially overlapped with the localization of MLC phosphorylated at Ser19 (pMLC20(Ser19) antibody) (Fig. 2C–F). Conspicuous was a strong signal of pMLC20 at the mature tentacle bases (Fig. 2 C) and in the sprouting tentacles of buds, both ectodermal as indicated by the longitudinal fibres (Fig. 2 D, D′). Along the body column ectoderm, pMLC20(Ser19) was detected in variable patterns in the myonemes and, rarely, also the basal cell body of scattered single or clustered ectodermal cells (Fig. 2 E). This variability might reflect the individual phosphorylation status of MLC in single cells. In endodermal cells only a very weak, cortical signal was detectable, but the circular myonemes could not be detected close to the mesogloea (Fig. 2 E'). The strongest signal was located at the constricting bud base (Fig. 2 F) as reported previously (Holz et al., 2017).

A detailed analysis of the pMLC20 distribution in mid and late bud stages revealed a dynamic MLC phosphorylation pattern in the ectoderm

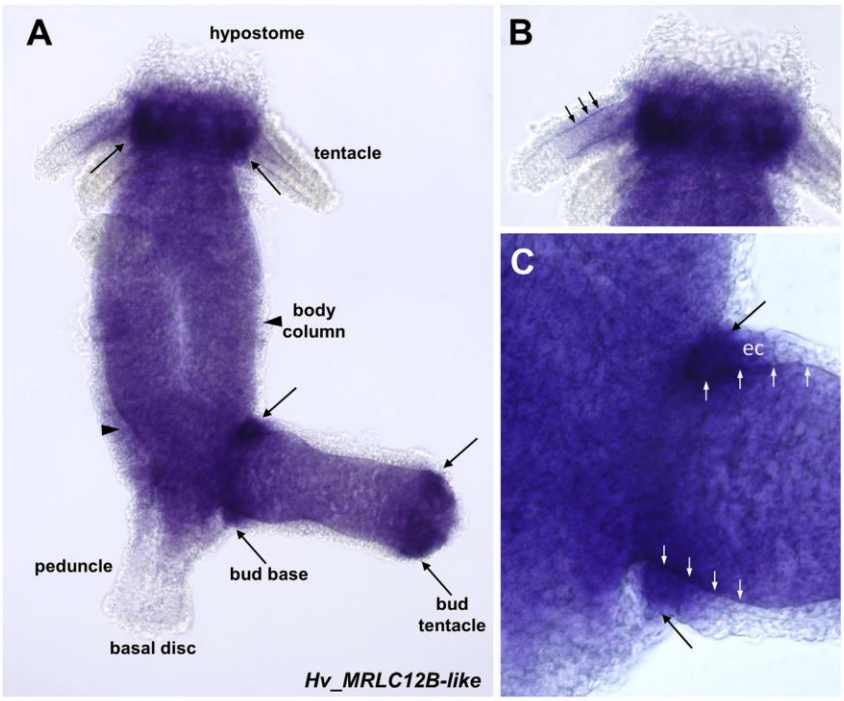

Fig. 1. Distribution of the myosin regulatory light chain mRNA *(Hv_RLC12B-like)*. (A) *Hv_RLC12B-like* gene expression pattern as detected by *in situ* hybridization in a polyp carrying a stage 6 bud. Elevated expression in ectodermal cells of the bud base, tentacle base and in tentacle buds (black arrows) as well as weaker expression in the body column ectoderm is indicated by arrowheads). **(B)** Magnification of the head: short arrows indicate a strong staining at the interface between ecto- and endoderm, which is likely due to mRNA enriched in the myonemes and cell anchors, which reach into the mesogloea. (C) The strong ectodermal staining at the bud base is indicated by black arrows. Short white arrows demarcate the mesogloea.

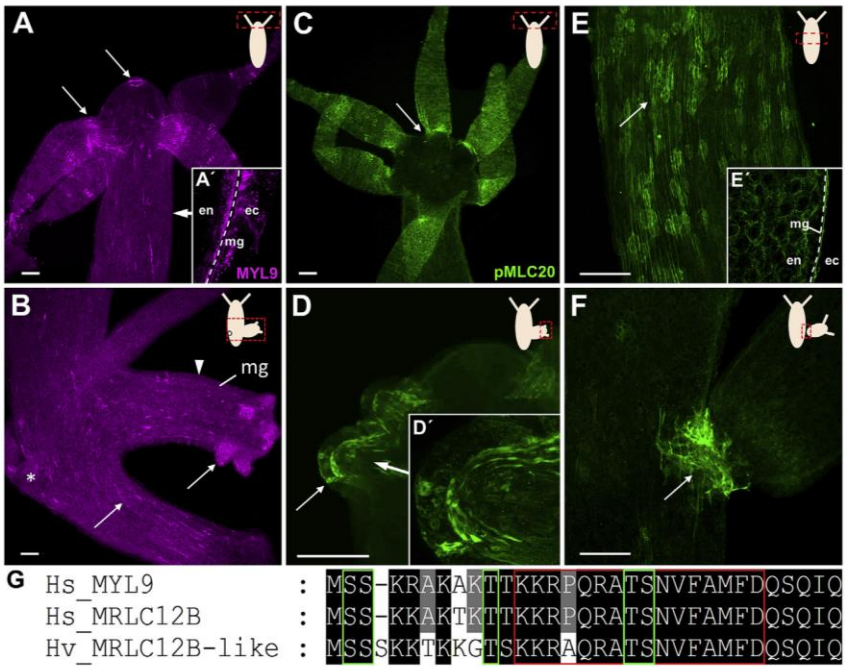

Fig. 2. Distribution of the unphosphorylated and the phosphorylated MLC protein in whole *Hydra*. **(A, B)** Immunofluorescence detection of the unphosphorylated myosin regulatory light chain with the MYL9 and a FITC-coupled secondary antibody (color set to magenta). (A) Head; MYL9 yields a strong signal at the tentacle bases and the mouth opening (arrows). (A′) Closeup of the body wall; MLC is detected mostly basal in ecto- and endodermal cells, the mesogloea (mg) is indicated by a dotted line. (B) Body column: MLC in myonemes and sprouting tentacles (arrows) and at the bud detachment site (asterisk) show a stronger signal. Arrowheads indicate ectodermal staining. **(C–F)** Immunofluorescence detection of the phosphorylated myosin regulatory light chain with the pMLC20(Ser19) and a FITC-coupled secondary antibody (green). Arrows indicate strongly pMLC20-positive myonemes and cells. **(C)** Tentacle base, **(D, D′)** evaginating tentacle buds, **(E)** body column: single cells or small cell clusters with myonemes, **(E′)** Closeup showing a very weak staining of the endodermal cell cortex. **(F)** late bud base (stage 9). The insets depict the respective position along the *Hydra* body column. **(G)** Alignment of the N-terminal region of the myosin regulatory light chain of *Homo sapiens* Hs_MYL9 (NCBI: CAG33124.1) and Hs_MRLC12B (NCBI: NP_001138417.1) with *Hydra vulgaris* myosin regulatory light chain (Hv_MRLC12B-like, NCBI: CDG72090.1). The red box indicates the pMLC20(Ser19) antibody epitope (abcam), green boxes indicate the phosphorylation sites. ec ectodermal, en endodermal, mg mesogloea. Scale bar 100 μm.

of constricting and detaching bud base tissue as well as in the developing bud tentacles (Fig. 3). Up to bud stage 6, the pMLC20 pattern in bud tissue was indistinguishable from parent polyps (Fig. 3B–D). In stage 6, the pMLC20 signal increased significantly in early sprouting tentacle tips (Fig. 3 C, K-L). Cells in the centre of these tentacle evaginations as well as the cells surrounding the tentacle evagination zone had reduced myonemes and a ring of F-actin-enriched cells framed the sprouting tentacle (Fig. 3 L) as described by (Anton-Erxleben et al., 2009; Aufschnaiter et al., 2017). Our data additionally revealed a strong pMLC20 signal in an irregularly shaped central patch of cells in the evaginating tissue tip (Fig. 3 K', L′).

From stage 7 onwards, the characteristic ring of pMLC20-positive ectodermal cells developed at the bud base and demarcated the later constriction site (Fig. 3E–H). Formation of the ring started in cells at the upper border of the stage 7 bud base, directed towards the parent's head (Fig. 3 E), and proceeded from both sides until it enclosed the bud base in stage 8 (Fig. 3 G, H). At the same time, tissue constriction proceeded (Fig. 3 I, J; Fig. S1 A, B).

A closer view to the late detachment zone revealed a sharply demarcated, mostly parental, cluster of pMLC20-positive ectodermal cells surrounding the constricting site (Fig. 4). These cells were flanked by either parental or bud cells in which F-actin but not pMLC20 had strongly accumulated (Fig. 4 A – D). The pMLC20-positive ring of cells decreased its diameter from about 40 cells in stage 9 to about 10 cells in stage 10 (Fig. 4) and persisted around the almost closed aboral pore of the bud's basal disc (Fig. 4 C, D). In the tissue lateral to this site, a few big parental and much smaller bud cells retained a weak pMLC20 signal. Remarkable was the very weak actin staining in cells strongly positive for pMLC20 (Fig. 4 A; Fig. S2 B, B′, C, C′). Since in single TRITC-phalloidin staining reactions (Fig. S2 A, A′) a strong signal was detected in all bud base cells, this effect might be due to a potential steric hindrance of TRITC-phalloidin binding to F-actin by the bound pMLC20 antibody.

Taken together, pMLC20 is readily detected in scattered ectodermal epitheliomuscle cells and myonemes throughout the body column of *Hydra* which might reflect the individual phosphorylation status of single cells. The phosphorylated myosin light chain is significantly increased in ectodermal cells of regions undergoing morphogenesis, like in the tentacle bases and at the bud detachment site.

3.2. *Compartmentalized signaling pathways for MLC phosphorylation in epitheliomuscle cells*

Our previous studies had shown that a Rho-dependent pathway is essential to activate ectodermal pMLC20 (Ser19) phosphorylation in *Hydra* morphogenesis (Holz et al., 2017). The canonical pathway to control smooth muscle activity in animals, however, is phosphorylation via MLCK. We therefore, next, investigated on the protein level by specific pharmacological interference, whether MLC is phosphorylated in *Hydra* by MLCK additional to or independent of phosphorylation induced via the Rho-dependent pathway (Fig. 5 A).

Western blot analysis (Fig. 5 B) revealed that the inhibitors Rhosin (inhibiting RhoA), Rockout (blocking Rock activity) and ML7 (MLCK inhibitor) reduced pMLC20 to 56%, 44% and 46%. A further concentration-dependent but saturated loss of phosphorylation occurred in 2,5 μM (18%) and 5 μM ML7 (14%). In a combined treatment, an additive effect of ML7 and Rhosin became obvious and the signal intensity was reduced from 46% (1 μM ML7) and 44% (Rhosin, 100 μM) to just 19%. This latter feature indicates a separate targeting of MLC phosphorylation by MLCK and Rho-dependent pathways.

In a second set of experiments, the effects of Rhosin and ML7 were monitored with respect to the subcellular distribution of pMLC20 and actomyosin distribution in *Hydra* tissue (Fig. 5C–K). The typical pattern of stained myonemes, scattered cells in the body column and a strong signal at the bud base of control polyps (Fig. 5C–E) was further analyzed by optical sections of the bud base cells. Here, pMLC20 was found strongly enriched in the apical, lateral and basal compartments of ectodermal cells (Fig. 5 E). These cells were flanked by cells with a strong F-actin signal (Fig. 7 B, C). Following Rhosin treatment, the level of

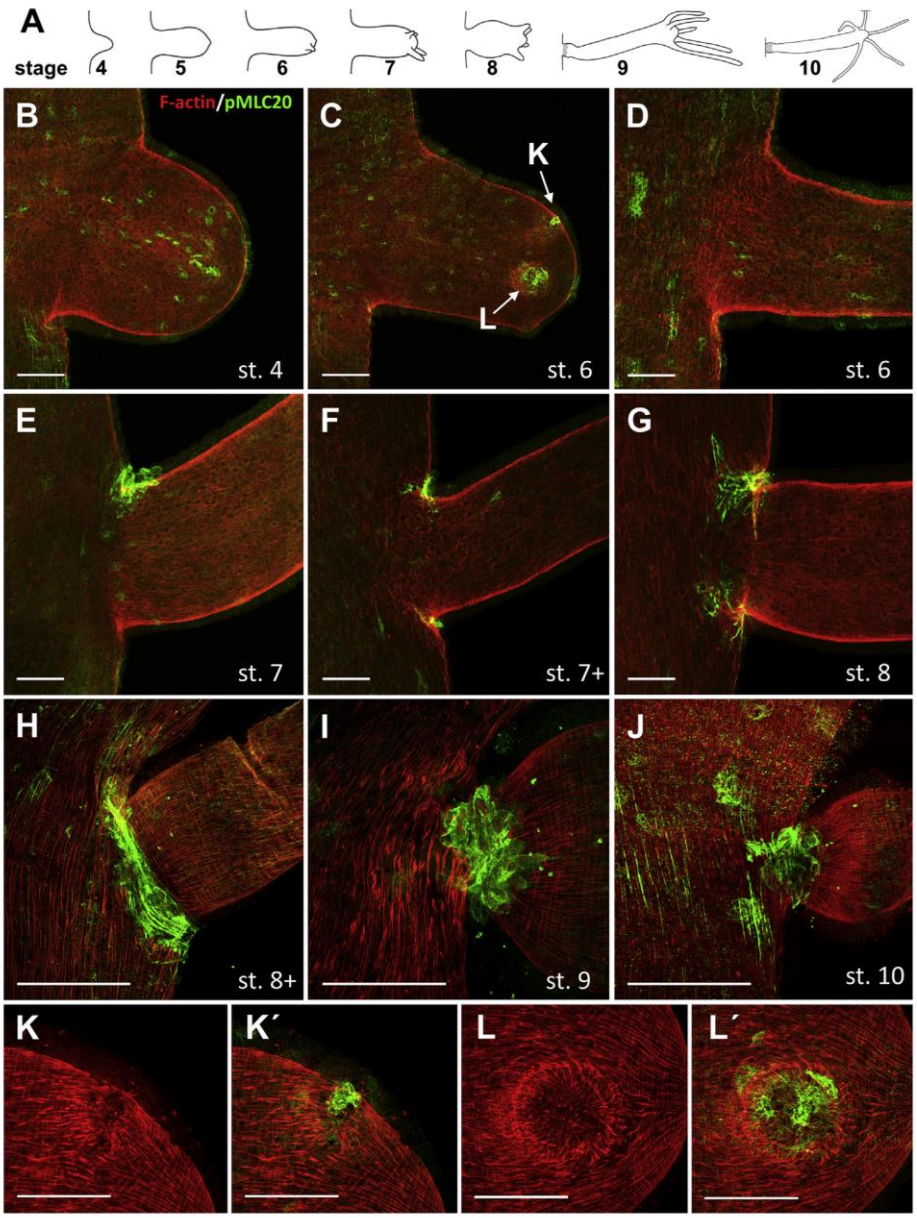

Fig. 3. Detection of F-actin by phalloidin and of the phosphorylated regulatory myosin light chain by the pMLC20 antibody in *Hydra* buds. (A) Scheme of bud stages 4 to 10 (Otto and Campbell, 1977). **(B–J)** Buds in different stages stained with phalloidin-TRITC (red) and anti-pMLC20 detected by a FITC-coupled secondary antibody (green). Maximum projection of a cLSM stacks each. **(B)** Bud stage 4: scattered pMLC-positive cells in the parent and bud, **(C, D)** stage 6: the sprouting tentacles of the bud show an increased level of pMLC20 and the parent and bud body column an irregular pattern of pMLC-positive cells, **(E)** stage 7: pMLC20 at the bud base comes up first in cells directed towards the parent's head, **(F)** stage 7+: pMLC20 at the upper and lower borders of the bud base, **(G, H)** stage 8: pMLC-positive, mostly parental,cells increase in number and form a ring surrounding the bud base concomitant with the onset of constriction. **(I)** stage 9: cells of the constriction site contain a high level of pMLC20, **(J)** stage 10: the number of pMLC20-positive cells at the bud base is low when constriction comes to an end. **(K–L)** Evaginating tentacles sprout from a placode-like cluster of pMLC20-positive cells. Scale bar 100 μm.

pMLC20 in myonemes remained stable (Fig. 5 F - H), but the apical and lateral enrichment of pMLC20 at the detachment site was abolished. ML7 treatment (2,5 μM, 6 h) strongly diminished MLC phosphorylation in the whole body (Fig. 5 I – K). At the bud base, apical staining persisted in a few cells (Fig. 5 J, K), but neither stress fibres nor lateral pMLC20 were detectable. Weakly stained short fibres and globular conglomerates persisted and were enriched at the bud base (compare Fig. 5 C – E and I – K).

Given the extremely weak pMLC signal in endodermal cells (Fig. 2 E') and its apparent lack in endodermal myonemes, we attempted to detect both activating residues in pMLC20 using an antibody recognizing both activating residues, Thr18 as well as Ser19 (CST). This experiment was, unfortunately, not successful (Western Blot, immunofluorescence).

Based on these data, Rho/Rock signaling is necessary for the apical and lateral localization of pMLC20(Ser19) in cells of the detachment site, while MLCK acts mainly in the basal compartment of the body column.

3.3. Tissue contractility and integrity under the effect of inhibitors interfering with actomyosin network formation

To evaluate the importance of MLC phosphorylation for tissue contractility and proper actomyosin network formation, we compared the effects of Rhosin, Rockout and ML7 to effects of inhibitors interfering more directly with actomyosin network formation (Fig. 6). The additional inhibitors were Calyculin A to inhibit the MLC phosphatase (MLCP), Cytochalasin B which prevents the nucleation of monomeric actin to form F-actin fibers (Theodoropoulos et al., 1994), and Blebbistatin, which inhibits the myosin ATPase and therewith the interaction of F-actin and myosin II (Kovacs et al., 2004).

Aberrant morphology or behavioral responses to pinching with a forceps were not observed in Rhosin-, Rockout or Calyculin A - treated polyps for up to 16 h, they reacted like control polyps (Fig. S3 B–C′ and movie 1). In contrast, Cytochalasin B and Blebbistatin - treated *Hydra* lost

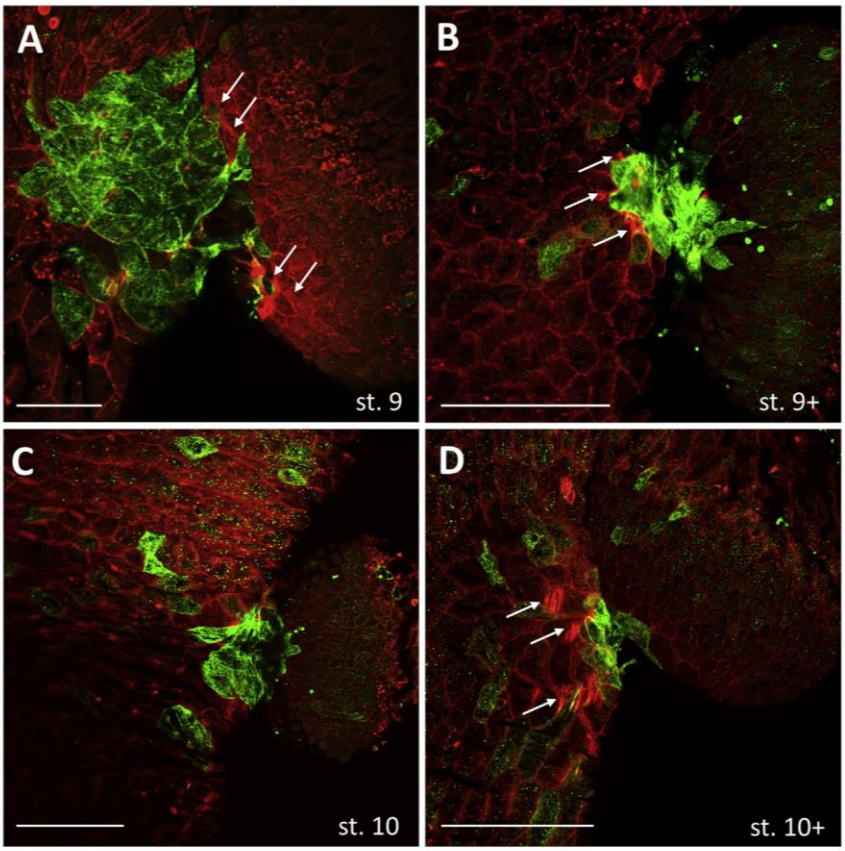

Fig. 4. A cluster of pMLC20-positive cells at the bud base accompanies morphogenesis in the final bud stages. (A–D) Single optical sections taken from the surface of the late bud base (stages 9 and 10). Arrows indicate the accumulation of F-actin (red) in cells neighboring the pMLC20-positive cells (green) at the detaching bud base. (C, D) The cytoplasm of scattered cells in parental and bud tissue close to the detachment site is pMLC20-positive when constriction comes to an end. Scale bar 50 μm.

their contractility within 2 h (Fig. S3 E-F') and their body column started to disintegrate after 8–16 h of incubation.

Remarkable was in ML7 treated animals the transient unusual elongation, the thickening of the head and the cell by cell loss of tentacles from the apex to the basis in five independent experiments which occurred with none of the other inhibitors (Fig. S3 D, D' and movie 2 and 5). The tentacle loss was particularly remarkable. Mature tentacles contracted in their apical part taking a broad, spatula-like form above a slim base (see movie 2 and 5). The broad part then started to disintegrate cell by cell down to the slim part. Body column tissue as well as the tentacles of buds remained unaffected for about 1 more hour. Removal of the inhibitor during or after tentacle disintegration quickly restored tissue integrity with about 40 min, the tentacle surface smoothened and tentacles started to regenerate. The effects on tentacles were not further analyzed.

Supplementary video related to this article can be found at https://doi.org/10.1016/j.ydbio.2020.04.001

Tissue contractility was affected by ML7 to various extent. In three of the five experiments an almost complete inhibition of movement to pinching was transiently reached between 2,5 – 3,5 h after the start of incubation (movie 5). Only a very restricted, local reaction occurred and the body column thickened forming a bubble-like structure. Thereafter, the animals shortened and movement was restored indicating a loss of inhibitor effects. Long term recording revealed, surprisingly, that the spontaneous contractions persisted (movie 2).

The inhibitor effects on the actin cytoskeleton and *Hydra* tissue integrity were evaluated using TRITC-phalloidin as a marker for F-actin in polyps treated for 6 h (Fig. 6). In control polyps, F-actin localized to the apical and cortical compartments with clearly defined cell boundaries (Fig. 6 A) and the myonemes were readily detectable (Fig. 6 A″).

Treatment with Rhosin or Calyculin A had no effect. Like in the controls, well-defined, sharp cell borders were visible (Fig. 6 B, C and B′, C′), the myonemes (Fig. 6 B″, C″) and the level of F-actin network formation seemed unaffected. In Calyculin A – treated polyps, the cell borders appeared even more pronounced than in the control (Fig. 6 C and C′). Decreased dephosphorylation is thought to increase the level of pMLC20 and therewith to cause a rigid cell cortex as long as the system is not saturated.

The MLCK inhibitor ML7 (2,5 μM), in contrast, dramatically affected the F-actin network. Cell boundaries appeared fuzzy (Fig. 6 D and D′) and only short, discontinuous fibres were detectable instead of long myonemes (Fig. 6 D″; Fig. 5 I). The tentacle phenotype (Fig. S3 D, D' and movies) was fully expressed. Inhibition of MLC phosphorylation is thought to disturb the crosslinking between F-actin fibers.

An even more pronounced phenotype was evoked by Cytochalasin B and Blebbistatin (Fig. 6 E and F). Disordered cell boundaries (Fig. 6 E′, F′) and dramatically shortened basal actin fibers and actin clumps resulted (Fig. 6 E″, F″). The actomyosin network collapse is likely due to destabilized F-actin fibers. It matches the lack of actomyosin interactions and therewith the loss of an ordered network.

To sum up, the actomyosin network and phosphorylation of MLC are not simply necessary for *Hydra* body contractility and morphogenesis but as well for tissue stability and integrity.

4. Discussion

In Bilateria, body contractions are performed by specialized muscle cells, while morphogenesis requires cell shape changes of epithelial and/or myoepithelial cells. Contractility depends on actomyosin interactions and the phosphorylation of several myosin regulatory light chains (MLC)

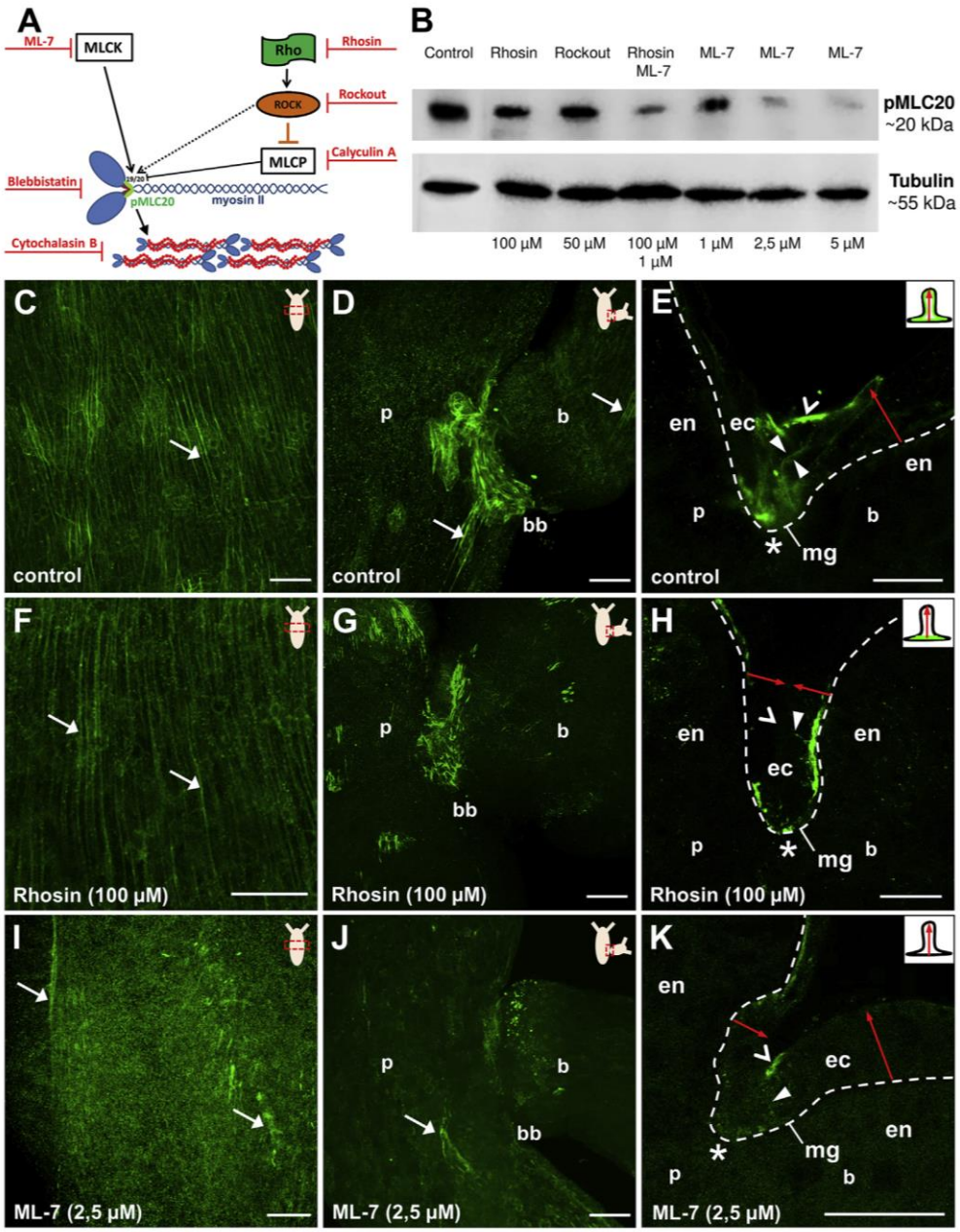

Fig. 5. Differential phosphorylation of MLC at Ser19 by Rho- and MLCK- dependent pathways. (A) Schematic representation of the MLCK and Rho-mediated alternative pathways for MLC phosphorylation and depiction of targets for inhibition of phosphorylation, actomyosin interactions and network formation. **(B)** Western Blot analysis to visualize the pMLC20 level after inhibition for 6 h. Tubulin immunoreactivity served as a loading control. **(C–K)** Immunofluorescence using the pMLC20 and a FITC-coupled secondary antibody. Maximum projection of cLSM stacks taken in the body column **(C, F, I)** or at the bud base **(D, G, J)**. Insets indicate the position within the polyp and arrows the pMLC20-positive myonemes. **(E, H, K)** Optical section (0.5 µm) within the constriction zone of the normal and Rho-inhibited bud base (lateral view). The basal-to-apical orientation of the cells is indicated by red arrows. Strong pMLC20 is indicated in the apical (open arrowhead), lateral (arrowhead) and basal compartments (asterisk). **(F–H)** Following Rho inhibition, the basal signal persists in the ectodermal myonemes (asterisk). **(I–K)** In polyps treated with ML7 (2,5 µM) for 6 h, only short pMLC20-positive fibers persist. Abbreviations: bb bud base; b bud; ec ectoderm; en endoderm; mg mesogloea, p parent. Scale bar 50 µm.

regulated by several independent pathways (Watanabe et al., 2007).

The prebilaterian *Hydra*, instead, uses the epitheliomuscle cell which is bifunctional with respect to mediating body movement and morphogenesis (Leclere and Rottinger, 2016). Only a single MLC is known (Steinmetz et al., 2012; Wenger and Galliot, 2013) and the physiological pathways activating MLC have not been investigated in detail. We here discuss the implications of two pathways mediating MLC phosphorylation. One acts via Rho and Rock in the lateral and apical compartments of epitheliomuscle cells during morphogenesis of the bud base, the other via MLCK in the basal, myonemal cell compartment (Fig. 7).

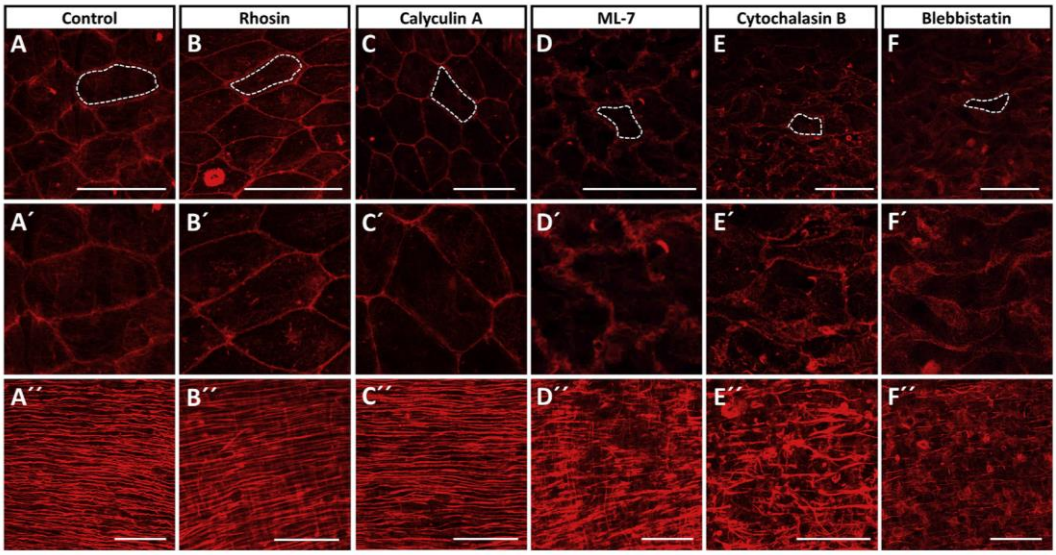

Fig. 6. Effects of various inhibitors affecting the actin cytoskeleton and myosin function. Polyps were treated for 6 h with ML7 (2,5 μM), Rhosin (100 μM), Rockout (50 μM), Cytochalasin B (10 μg/ml), Calyculin A (20 nM) or Blebbistatin (5 μM) as indicated. TRITC- Phalloidin as used as a marker for F-actin. **(A–E)** Optical sections within the apical region of ectodermal epitheliomuscle cells in the body column. **(A′- E′)** Digital magnification of (A–E), apical cell compartment including the apical cell-cell contacts. **(A″- E″)** Maximum projection of a cLSM stack focused on the basal compartment of ectodermal cells with their longitudinal myonemes. Scale bar 50 μm.

4.1. Bud detachment requires actomyosin regulation by Rho/Rock signaling in the apical and lateral compartments of epitheliomuscle cells

Consistent with the inhibitory action of Rho and Rock inhibitors on bud morphogenesis (Holz et al., 2017), we here show that Rhosin and Rockout significantly reduce the pMLC20 protein (Fig. 5 B), particularly in stress fibres of the lateral and apical cell compartments of constricting ectodermal epitheliomuscle cells (Fig. 5 F - H).

Mechanistically interesting is the neighborhood of central, strongly pMLC20-positive cells and lateral cells on either parental and bud's side which strongly accumulate F-actin (Fig. 7 B, C). This constellation of a dynamic phosphomyosin-rich center and lateral F-actin-rich cells is similar to and typical for morphogenetic processes in vertebrate and fly where lateral stiffening (by F-actin) supports tissue separation (Fagotto, 2014). Tension and stiffness can generate the forces for separation of bud and parent, but the neighboring cells must simultaneously loosen their lateral cell-cell-contacts by e.g. reducing cadherin interactions and strengthen their anchor in the extracellular matrix, by e.g. integrins (Burute and Thery, 2012; Case and Waterman, 2015). Based on the arrangement of F-actin and pMLC20 at the detachment site, we propose a model in which the pMLC20-positive cells generate tension to drive morphogenesis and finally cell-cell separation, while the neighboring cells increase tissue stiffness by accumulating F-actin in lateral and apical patches and stress fibers (Fig. 7 B′, C′). How *Hydra* epitheliomuscle cells finally manage the separation process remains an open question. The here-described side-by-side localization of pMLC20 and F-actin cushions indicates an actomyosin-based mechanism, but the role of signaling pathways targeting adhesion molecules remains to be elucidated.

4.2. Body movement and myosin light chain regulation by MLCK in the basal compartment of epitheliomuscle cells

Longitudinal body movement is likely regulated by MLCK (Fig. 7A) and it is interesting to note that the inhibition of MLCK by ML7 evoked several biological responses. In the first phase of treatment polyps elongated, developed a bulging head and mature tentacles were lost cell by cell from the apex towards the basis. A transient, almost complete immobilization followed, in which the fast contractions induced by pinching were abolished. Thereafter, the polyps shortened. Interesting is the persisting typical spontaneous longitudinal contractility, despite the strongly reduced reaction to pinching. It suggests an independent, ML7-insensitive mechanism of the phasic, oscillatory movement compared to escape reactions in at least some of the cells.

Based on these multiple effects, we propose that ML7 acts differentially on several targets. Early, it seems to impair the contractility of, at least part of, the ectodermal longitudinal myonemes, without affecting the endodermal, circular ones and without affecting the spontaneous oscillatory movement. Provided, the endodermal myonemes keep a certain tonus, body elongation would result - interrupted by the spontaneous body contractions. A bulging head would form when endodermal contractility is lost slowly in the apical region. Finally, when the endodermal myonemes in the body relax, shortening of the polyps would occur.

The hypothesis of a differential reaction of ecto- and endodermal cells is supported by (i) a different morphology of their myonemes and (ii) their different characteristics of contractility. Recently, a detailed analysis of epitheliomuscle cells has revealed that ectodermal epitheliomuscle cells possess a few thick myonemes, but endodermal ones multiple thin myonemes (Aufschnaiter et al., 2017; Seybold et al., 2016). Both cell types mediate a different mode of contraction: ectodermal longitudinal contractions occur fast - either as spontaneous, oscillatory ones (Murillo-Rincon et al., 2017) or as escape reactions to mechanical stimuli. In contrast, elongation of polyps effected by endodermal circular contractions occurs slowly, e.g. when *Hydra* tries to reach prey or elongates following fast contractions. Ectodermal muscle fibres, therefore, seem to react mainly phasic and endodermal ones mainly tonic.

Interestingly, only the thick, cable-like ectodermal myonemes which perform the fast, phasic twitching, react with the pMLC20(Ser19) antibody. In contrast, the multiple thin endodermal fibres lack a substantial pMLC20 signal, although they strongly express the *MLC* gene and although the MYL9 antibody detects the unphosphorylated MLC ecto-as well as endodermally. It is therefore unlikely that MLC should not be used in endodermal epitheliomuscle cells.

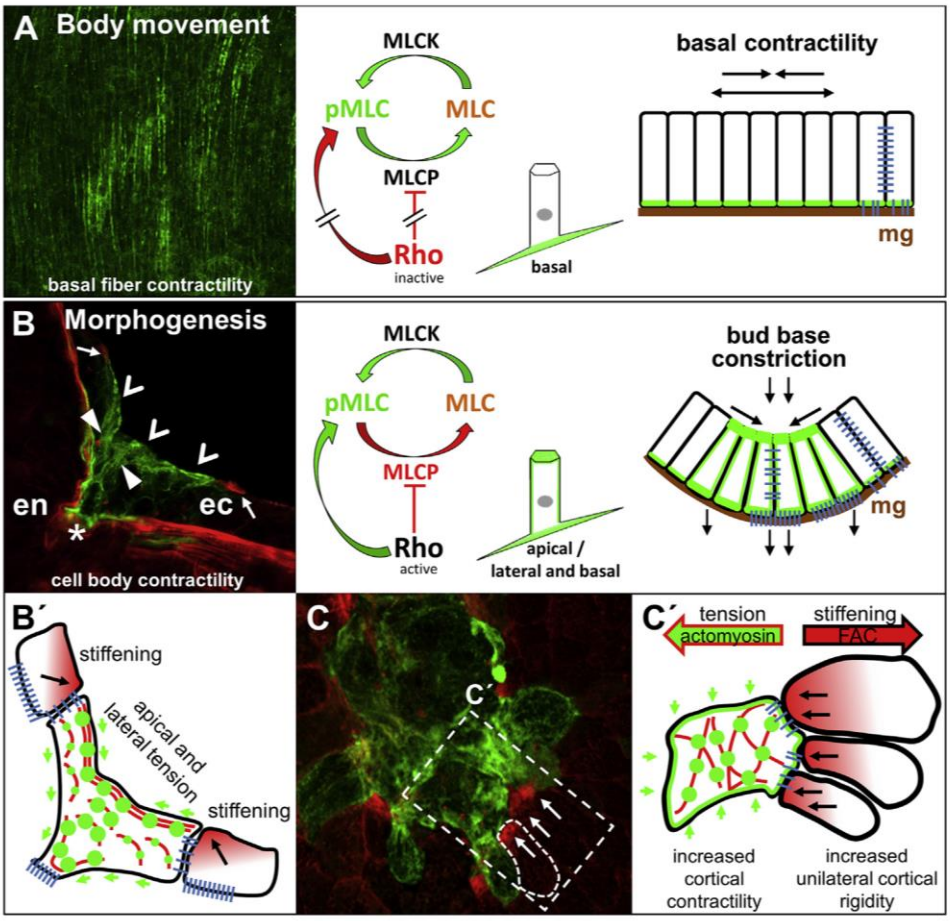

Fig. 7. Movement versus morphogenesis: a hypothesis for at least two signaling pathways controlling the differential phosphorylation of pMLC20. (A–B) Data, schemes and models depicting the pathways and subcellular localization of pMLC20 in ectodermal epithelial cells used for movement or localized contractility during morphogenesis. **(A)** Body column: pMLC20 is located in the myonemes of ectodermal epithelial cells and ensures body contractility. MLCK and MLCP together determine an intermediate level of actomyosin network formation, signaling via Rho plays a minor role. Columnar cells of the epithelium carry pMLC20 in their basal compartment, are anchored in the mesogloea (brown) and connected by cell-cell and cell-matrix adhesion molecules (blue). **(B)** Bud detachment (lateral view): pMLC is located in a cluster of constricting cells at the bud base and detectable in their basal, lateral and apical regions. Neighboring cells strongly accumulate F-actin unilaterally. Active Rho signaling blocks the dephosphorylation by MLCP and phosphorylates MRLC, increasing the level of pMLC. Rho signaling ensures the apical and lateral enrichment of actomyosin additional to the basal one. Color code as in (A). **(B′)** Model (lateral view) of the pMLC20 (green) and localized F-actin (red) generating tensional forces (green arrows). Anchors in the mesogloea tighten while lateral adhesion of cells is reduced (blue bars). **(C)** Side-by-side localization (surface view) of unilateral F-actin patches and apical pMLC20 in adjacent cells at the bud base. **(C′)** Model (surface view) for the tensional forces and reduced lateral contacts.

4.3. Alternative MLC phosphorylation sites might be used in ecto- and endodermal cells

An obvious possibility to explain this discrepancy would be the activation of endodermal MLC by alternative phosphorylation sites which are not or only weakly detected by the pMLC20 antibody.

Cnidarian (epithelio)muscle cells are thought to be homologous to smooth muscle of Bilateria (Leclere and Rottinger, 2016; Steinmetz et al., 2012), and these use Thr18 additional to Ser19 to either modulate or fully activate MLC by double phosphorylation (Vicente-Manzanares et al., 2008). While Ser19 is phosphorylated fast and mostly in initial phasic contractions, Thr18 is phosphorylated at slower rates and mostly in tonic muscle. The Thr18/Ser19 pair is typically found phosphorylated during sustained contractions, Thr18 is additionally involved in secretion processes (Getz et al., 2010; Harnett et al., 2005; Murthy, 2006). The regulation of Thr18/Ser19 phosphorylation in phasic and tonic contractions in e.g. the vertebrate esophagus is complex and controlled by multiple kinase pathways (Harnett et al., 2005).

Hydra MLC possesses all of the N-terminal phosphorylation sites for myosin regulation identified in Bilateria (Fig. 2), and it is likely that besides Rho/Rock and MLCK also other kinases act in epitheliomuscle cells. The pMLC20 antibody (abcam) used in our study detects Ser19, and there is no information, whether it crossreacts with Thr18 or the double phosphorylated site. Experiments with an antibody detecting the double phosphorylated MLC were not successful, but the analysis of Thr18 is important in the future to obtain a full picture.

4.4. Loss of tentacles - a function of MLCK in tissue integrity and cell-cell adhesion

Besides controlling body movement in *Hydra*, MLCK also seems to be involved in the regulation of tissue integrity which is severely affected in the tentacles by ML7 treatment. The rapid cell by cell loss of tentacles within 1–3 h of treatment is particularly remarkable, because tentacles usually are very resistant to shearing, dissociation or chemical maceration (David, 1973; Gierer et al., 1972). One reason for the quick loss of tentacle tissue might be the essential role of MLCK described in bilaterian tight junction regulation where MLCK phosphorylation regulates the ZO-1 (Zonula occludens-1), occludin and claudin proteins and therewith the barrier function of epithelia (Cheng et al., 2015; Cunningham and Turner, 2012; Shen, 2012). Invertebrates instead have septate junctions. ZO-1 as well as claudin are encoded in the *Hydra* genome (Chapman et al., 2010), but whether these proteins are regulated by MLCK in *Hydra* is unknown. The failing regulation of adhesive cell-cell junctions (septate or adherens type) plus reduction of attachment to the ECM are the most likely reason for the dramatic loss of tissue integrity following ML7 exposure and would link *Hydra* MLCK also to the lateral compartment of the cells. An involvement of the ECM seems likely as well, because bud

tentacles are more resistant to ML7 than mature ones. Bud cells are anchored in a newly synthesized ECM (Aufschnaiter et al., 2011), which might be better suited to fix the cells.

5. Conclusion

Our data provide new insights into the role of MLC phosphorylation by either MLCK or a Rho pathway in three differentially controlled compartments of the *Hydra* epitheliomuscle cells. Despite some evidence that other serine/threonine kinases phosphorylate MLC as well, we propose that, in *Hydra*, MLCK is a main player to control cellular contractility in body movement. FGFR-dependent Rho signaling, in contrast, is essential for MLC phosphorylation during morphogenesis to achieve bud detachment. To further elucidate the mechanisms of morphogenetic movements and actomyosin interactions in epitheliomuscle cells of *Hydra,* studies on MLC function are required. Questions to address are particularly the signaling network in these bifunctional cells and the interplay between cell-cell and cell-matrix adhesion to understand how the tissue separation between *Hydra* and its buds works.

Acknowledgement and Funding

We thank the Deutsche Forschungsgemeinschaft (grant HA1732-13) for support. D.A. was associated to the DFG Research Training Group ‘Membrane Plasticity in Tissue Development and Remodeling’ (GRK 2213).

Appendix A. Supplementary data

Supplementary data to this article can be found online at https://doi.org/10.1016/j.ydbio.2020.04.001.

References

Anton-Erxleben, F., Thomas, A., Wittlieb, J., Fraune, S., Bosch, T.C., 2009. Plasticity of epithelial cell shape in response to upstream signals: a whole-organism study using transgenic Hydra. Zoology (Jena) 112, 185–194.
Aufschnaiter, R., Wedlich-Soldner, R., Zhang, X., Hobmayer, B., 2017. Apical and basal epitheliomuscular F-actin dynamics during Hydra bud evagination. Biology open 6 (8), 1137–1148.
Aufschnaiter, R., Zamir, E.A., Little, C.D., Ozbek, S., Munder, S., David, C.N., Li, L., Sarras Jr., M.P., Zhang, X., 2011. In vivo imaging of basement membrane movement: ECM patterning shapes Hydra polyps. J. Cell Sci. 124, 4027–4038.
Betapudi, V., 2014. Life without double-headed non-muscle myosin II motor proteins. Front. Chem. 2, 45.
Borges, R.M., Lamers, M.L., Forti, F.L., Santos, M.F., Yan, C.Y., 2011. Rho signaling pathway and apical constriction in the early lens placode. Genesis 49, 368–379.
Bresnick, A.R., 1999. Molecular mechanisms of nonmuscle myosin-II regulation. Curr. Opin. Cell Biol. 11, 26–33.
Burute, M., Thery, M., 2012. Spatial segregation between cell-cell and cell-matrix adhesions. Curr. Opin. Cell Biol. 24, 628–636.
Case, L.B., Waterman, C.M., 2015. Integration of actin dynamics and cell adhesion by a three-dimensional, mechanosensitive molecular clutch. Nat. Cell Biol. 17, 955–963.
Chapman, J.A., Kirkness, E.F., Simakov, O., Hampson, S.E., Mitros, T., Weinmaier, T., Rattei, T., Balasubramanian, P.G., Borman, J., Busam, D., Disbennett, K., Pfannkoch, C., Sumin, N., Sutton, G.G., Viswanathan, L.D., Walenz, B., Goodstein, D.M., Hellsten, U., Kawashima, T., Prochnik, S.E., Putnam, N.H., Shu, S., Blumberg, B., Dana, C.E., Gee, L., Kibler, D.F., Law, L., Lindgens, D., Martinez, D.E., Peng, J., Wigge, P.A., Bertulat, B., Guder, C., Nakamura, Y., Ozbek, S., Watanabe, H., Khalturin, K., Hemmrich, G., Franke, A., Augustin, R., Fraune, S., Hayakawa, E., Hayakawa, S., Hirose, M., Hwang, J.S., Ikeo, K., Nishimiya-Fujisawa, C., Ogura, A., Takahashi, T., Steinmetz, P.R., Zhang, X., Aufschnaiter, R., Eder, M.K., Gorny, A.K., Salvenmoser, W., Heimberg, A.M., Wheeler, B.M., Peterson, K.J., Bottger, A., Tischler, P., Wolf, A., Gojobori, T., Remington, K.A., Strausberg, R.L., Venter, J.C., Technau, U., Hobmayer, B., Bosch, T.C., Holstein, T.W., Fujisawa, T., Bode, H.R., David, C.N., Rokhsar, D.S., Steele, R.E., 2010. The dynamic genome of Hydra. Nature 464, 592–596.
Cheng, X., Wang, X., Wan, Y., Zhou, Q., Zhu, H., Wang, Y., 2015. Myosin light chain kinase inhibitor ML7 improves vascular endothelial dysfunction via tight junction regulation in a rabbit model of atherosclerosis. Mol. Med. Rep. 12, 4109–4116.
Cunningham, K.E., Turner, J.R., 2012. Myosin light chain kinase: pulling the strings of epithelial tight junction function. Ann. N. Y. Acad. Sci. 1258, 34–42.
David, C.N., 1973. A quantitative method for maceration of *Hydra* tissue. Willielm Roux Arch. EntwMech. Org 171, 259–268.
Fagotto, F., 2014. The cellular basis of tissue separation. Development 141, 3303–3318.
Getz, T.M., Dangelmaier, C.A., Jin, J., Daniel, J.L., Kunapuli, S.P., 2010. Differential phosphorylation of myosin light chain (Thr)18 and (Ser)19 and functional implications in platelets. J. Thromb. Haemostasis 8, 2283–2293.
Gierer, A., Berking, S., Bode, H., David, C.N., Flick, K., Hansmann, G., Schaller, H., Trenkner, E., 1972. Regeneration of hydra from reaggregated cells. Nat. N. Biol. 239, 98–101.
Harnett, K.M., Cao, W., Biancani, P., 2005. Signal-transduction pathways that regulate smooth muscle function I. Signal transduction in phasic (esophageal) and tonic (gastroesophageal sphincter) smooth muscles. Am. J. Physiol. Gastrointest. Liver Physiol. 288, G407–G416.
Hartshorne, D.J., Ito, M., Erdodi, F., 1998. Myosin light chain phosphatase: subunit composition, interactions and regulation. J. Muscle Res. Cell Motil. 19, 325–341.
Hasse, C., Holz, O., Lange, E., Pisowodzki, L., Rebscher, N., Christin Eder, M., Hobmayer, B., Hassel, M., 2014. FGFR-ERK signaling is an essential component of tissue separation. Dev. Biol. 395 (1), 154–166.
Holz, O., Apel, D., Steinmetz, P., Lange, E., Hopfenmuller, S., Ohler, K., Sudhop, S., Hassel, M., 2017. Bud detachment in hydra requires activation of fibroblast growth factor receptor and a Rho/Rock-myosin II signaling pathway to ensure formation of a basal constriction. Dev. Dynam. 246, 502–516 an official publication of the American Association of Anatomists.
Ikebe, M., Hartshorne, D.J., 1985. Phosphorylation of smooth muscle myosin at two distinct sites by myosin light chain kinase. J. Biol. Chem. 260, 10027–10031.
Ikebe, M., Hartshorne, D.J., Elzinga, M., 1987. Phosphorylation of the 20,000-dalton light chain of smooth muscle myosin by the calcium-activated, phospholipid-dependent protein kinase. Phosphorylation sites and effects of phosphorylation. J. Biol. Chem. 262, 9569–9573.
Kimura, K., Ito, M., Amano, M., Chihara, K., Fukata, Y., Nakafuku, M., Yamamori, B., Feng, J., Nakano, T., Okawa, K., Iwamatsu, A., Kaibuchi, K., 1996. Regulation of myosin phosphatase by Rho and rho-associated kinase (Rho-kinase). Science 273, 245–248.
Klimovich, A., Wittlieb, J., Bosch, T.C.G., 2019. Transgenesis in Hydra to characterize gene function and visualize cell behavior. Nat. Protoc. 14, 2069–2090.
Komatsu, S., Ikebe, M., 2007. The phosphorylation of myosin II at the Ser1 and Ser2 is critical for normal platelet-derived growth factor induced reorganization of myosin filaments. Mol. Biol. Cell 18, 5081–5090.
Kovacs, M., Toth, J., Hetenyi, C., Malnasi-Csizmadia, A., Sellers, J.R., 2004. Mechanism of blebbistatin inhibition of myosin II. J. Biol. Chem. 279, 35557–35563.
Laemmli, U.K., 1970. Cleavage of structural proteins during the assembly of the head of bacteriophage T4. Nature 227, 680–685.
Leclere, L., Rottinger, E., 2016. Diversity of Cnidarian muscles: function, anatomy, development and regeneration. Front. Cell Dev. Biol. 4, 157.
Levayer, R., Lecuit, T., 2012. Biomechanical regulation of contractility: spatial control and dynamics. Trends Cell Biol. 22, 61–81.
Ma, X., Kovacs, M., Conti, M.A., Wang, A., Zhang, Y., Sellers, J.R., Adelstein, R.S., 2012. Nonmuscle myosin II exerts tension but does not translocate actin in vertebrate cytokinesis. Proc. Natl. Acad. Sci. U. S. A. 109, 4509–4514.
Martin, A.C., Goldstein, B., 2014. Apical constriction: themes and variations on a cellular mechanism driving morphogenesis. Development 141, 1987–1998.
Martin, A.C., Kaschube, M., Wieschaus, E.F., 2009. Pulsed contractions of an actin-myosin network drive apical constriction. Nature 457, 495–499.
Martin, S.G., 2016. Role and organization of the actin cytoskeleton during cell-cell fusion. Semin. Cell Dev. Biol. 60, 121–126.
Murillo-Rincon, A.P., Klimovich, A., Pemoller, E., Taubenheim, J., Mortzfeld, B., Augustin, R., Bosch, T.C.G., 2017. Spontaneous body contractions are modulated by the microbiome of Hydra. Sci. Rep. 7, 15937.
Murthy, K.S., 2006. Signaling for contraction and relaxation in smooth muscle of the gut. Annu. Rev. Physiol. 68, 345–374.
Newell-Litwa, K.A., Horwitz, R., Lamers, M.L., 2015. Non-muscle myosin II in disease: mechanisms and therapeutic opportunities. Dis. Model Mech. 8, 1495–1515.
Otto, J., Campbell, R., 1977. Budding in Hydra attenuata: bud stages and fate map. J. Exp. Zool. 200, 417–428.
Pearl, E.J., Li, J., Green, J.B., 2017. Cellular systems for epithelial invagination. Philos. Trans. R. Soc. Lond. Ser. B Biol. Sci. 372.
Schindelin, J., Arganda-Carreras, I., Frise, E., Kaynig, V., Longair, M., Pietzsch, T., Preibisch, S., Rueden, C., Saalfeld, S., Schmid, B., Tinevez, J.Y., White, D.J., Hartenstein, V., Eliceiri, K., Tomancak, P., Cardona, A., 2012. Fiji: an open-source platform for biological-image analysis. Nat. Methods 9, 676–682.
Schwayer, C., Sikora, M., Slovakova, J., Kardos, R., Heisenberg, C.P., 2016. Actin rings of power. Dev. Cell 37, 493–506.
Sellers, J.R., 1991. Regulation of cytoplasmic and smooth muscle myosin. Curr. Opin. Cell Biol. 3, 98–104.
Seybold, A., Salvenmoser, W., Hobmayer, B., 2016. Sequential development of apical-basal and planar polarities in aggregating epitheliomuscular cells of Hydra. Dev. Biol. 412, 148–159.
Shen, L., 2012. Tight junctions on the move: molecular mechanisms for epithelial barrier regulation. Ann. N. Y. Acad. Sci. 1258, 9–18.
Somlyo, A.P., Somlyo, A.V., 2003. Ca2+ sensitivity of smooth muscle and nonmuscle myosin II: modulated by G proteins, kinases, and myosin phosphatase. Physiol. Rev. 83, 1325–1358.
Steinmetz, P.R., Kraus, J.E., Larroux, C., Hammel, J.U., Amon-Hassenzahl, A., Houliston, E., Worheide, G., Nickel, M., Degnan, B.M., Technau, U., 2012.

Independent evolution of striated muscles in cnidarians and bilaterians. Nature 487, 231–234.
Sudhop, S., Coulier, F., Bieller, A., Vogt, A., Hotz, T., Hassel, M., 2004. Signalling by the FGFR-like tyrosine kinase, Kringelchen, is essential for bud detachment in Hydra vulgaris. Development 131, 4001–4011.
Theodoropoulos, P.A., Gravanis, A., Tsapara, A., Margioris, A.N., Papadogiorgaki, E., Galanopoulos, V., Stournaras, C., 1994. Cytochalasin B may shorten actin filaments by a mechanism independent of barbed end capping. Biochem. Pharmacol. 47, 1875–1881.
Vicente-Manzanares, M., Koach, M.A., Whitmore, L., Lamers, M.L., Horwitz, A.F., 2008. Segregation and activation of myosin IIB creates a rear in migrating cells. J. Cell Biol. 183, 543–554.
Watanabe, T., Hosoya, H., Yonemura, S., 2007. Regulation of myosin II dynamics by phosphorylation and dephosphorylation of its light chain in epithelial cells. Mol. Biol. Cell 18, 605–616.
Wenger, Y., Galliot, B., 2013. RNAseq versus genome-predicted transcriptomes: a large population of novel transcripts identified in an Illumina-454 Hydra transcriptome. BMC Genom. 14, 204.
Zhang, W., Huang, Y., Wu, Y., Gunst, S.J., 2015. A novel role for RhoA GTPase in the regulation of airway smooth muscle contraction. Can. J. Physiol. Pharmacol. 93, 129–136.

Chapter 3

Additional unpublished data on myosin and actomyosin localization and their potential functions in other body regions of *Hydra*

4.1 Introduction to Chapter 3

Chapter 3 summarizes unpublished data of myosin and actomyosin, partly from pilot projects in which I investigated and answered the questions: (i) how many myosins are available in the genome of *Hydra*, (ii) whether *nm-MyHC* and *st-MyHC* are detectable by double *in situ* hybridization and (iii) whether actomyosin and especially pMLC20 play a role in other epitheliomuscle cell functions such as regeneration and the maturation of testicles. To address these issues, database analysis as well as phylogenetic analysis were performed to identify different myosins in *Hydra* and to characterize them phylogenetically. To clarify the spatial separated expression of both class II myosins in *Hydra* double *in situ* hybridization was performed. To receive a full picture of pMLC20 function and localization during morphogenetic processes in *Hydra*, immunohistological analysis was performed using regenerating polyps and polyps carrying multiple testes.

The data revealed a total number of 10 different myosins in *Hydra* which group phylogenetically into the existing myosin classes. The double *in situ* hybridization confirmed that *st-MyHC* is expressed in the ectoderm and *nm-MyHC* in the endoderm. The pMLC20 investigations on the other morphological processes showed that actomyosin is also involved in wound closure during regeneration as well as testes formation.

My part in this chapter was the database analysis to identify different myosins in *Hydra*, the structural domain analysis as well as the phylogenetic analysis. In addition, the further analysis of the pMLC20 localization in other morphogenetic regions was carried out by me.

The double *in situ* hybridization was carried out by Belinda Rotta, supervised by me during her bachelor thesis.

4.2 Identification of different myosins in *Hydra*

Myosins belong to a superfamily of actin based molecular motor proteins and generate contractile forces for diverse processes inside the cell (Syamaladevi et al., 2012). The superfamily comprises at least 24 classes which are divided based on the head domain sequence similarity and domain organization (Richards and Cavalier-Smith, 2005; Goodson and Spudich, 1993). In order to clarify how many myosin subtypes are present in the genome of *Hydra*, database analysis were carried out in NCBI database. This analysis revealed that at least 10 different myosin subtypes exist in *Hydra* based on the NCBI database (Table 1). The identified myosin subtypes include class specific domains, which are evaluated by using the domain prediction tool of NCBI (Table 1).

Table 1: Different myosins exist in *Hydra*

Name	Myosin class	Predicted domains (including Motor domain)	putative structure (Hodge and Cope 2000)	Acc. No
Myosins				
unconventional myosin-Ie-like	I	Myosin_TH1, SH3-Myole		XP_012564396.1
myosin heavy chain striated-type	II	Myosin_tail_1, Cep57_CLD, OmpH		XP_002157926.3
myosin 10-like		Myosin_tail_1 **(Inhibitor: blebbistatin)**		XP_012560866
myosin-IIIb-like	III		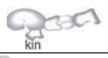	XP_012562223.1
unconventional myosin-Va	V	Taxilin, Myo5_CBD	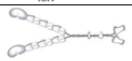	XP_012559760.1
unconventional myosin-VI-like	VI	PhaB_Bmeg		XP_012554391.1
myosin-VIIa-like	VII	MyTH4, FERM_C1, FERM_C2, SH3	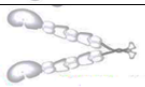	XP_012559202.1
unconventional myosin-IXa-like	IX	RhoGAP		XP_012560393.1
unconventional myosin-X-like (partial)	X	tolA_full, PH2_MyoX, Nyd-SP28, PH-like	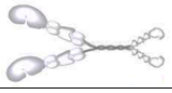	XP_012559254.1
unconventional myosin -XVIIIa-like	XII / XVII	Cast, DUF342		XP_012560559.1

In order to elucidate whether the identified subtypes in *Hydra* group phylogenetically into the correct class, a myosin superfamily tree analysis was performed. The required set of sequence data was taken from (Hodge and Cope, 2000: www.mrc-lmb.cam.ac.uk/myosin/), and the newly identified *Hydra* sequences were added. The alignment data compare the core motor domain of each myosin. In Fig. 2.1, an unrooted phylogenetic tree was created by using distance matrix analysis performed with ClustalW (Hodge and Cope, 2000).

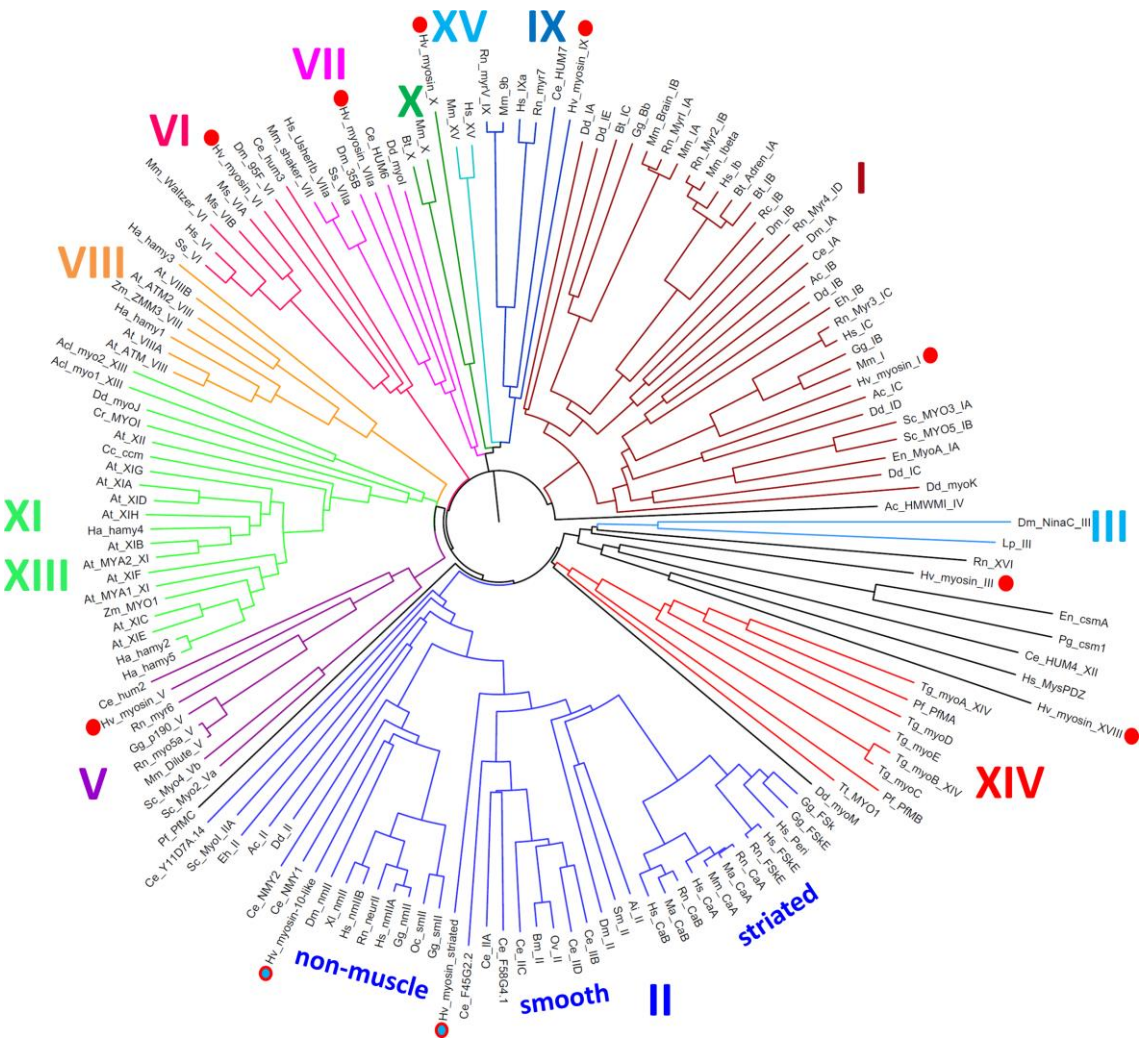

Figure 2.1: Phylogenetic tree of myosin motor-domains in *Hydra* and Bilateria. The phylogenetic tree comprises a large number of different myosins including the ten predicted *Hydra* myosins. Class II myosins (red/blue dots), other *Hydra* myosins containing a myosin specific motor domain (red dots). The blue lines highlight *Hydra* class II myosins for which whole mount expression patterns are known (Holz et al. 2017). **Abbrevations:** Species: Ac: *Acanthamoeba castellanii*, Acl: *Acetabularia cliftonii,* Ai: *Aequipecten irradians,* At: *Arabidopsis thaliana,* Bm: *Brugia malayi,* Bt: *Bos taurus*, Cc: *Chara corallina,* Ce: *Caenorhabditis elegans*, Cr: *Chlamydomonas reinhardtii*, Dd: *Dictyostelium discoidium*, Dm: *Drosophila melanogaster,* En: *Emiricella nidulans,* Eh: *Entamoeba histolytica*, Gg: *Gallus gallus*, Ha: *Helianthus annus*, Hs: *Homo sapiens*, Hv: *Hydra vulgaris* (red dots), Lp: *Limulus polyphemus*, Ma: *Mesocricetus auratus*, Mm: *Mus musculus*, Oc: *Oryctolagus cuniculus,* Ov: *Onchocerca volvulus*, Pf: *Plasmodium falciparum*, Pg: *Pyricularia grisea*, Rc: *Rana catesbeiana,* Rn: *Rattus norvegicus*, Sc: *Saccharomyces cerevisiae*, Sm: *Schistosoma mansoni*, Ss: *Sus scrofa domestica*, Tg: *Toxoplasma gondii,* Tt: *Tetrahymena thermophila,* XlX: *enopus laevis*, Zm: *Zea mays;* **myosin subtypes:** Adren: Bovine Adrenal (myosin I), Bb: Brush Border Myosin, ICaA: Cardiac alpha (myosin II), CaB: Cardiac beta (myosin II), csm: Chitin synthase-myosin FSk: Fast Skeletal (myosin II) = striated, FSkE: Embryonic Fast Skeletal (myosin II), HMWMI: High Molecular Weight Myosin I, neur: Neuronal (myosin II), nm: Non-muscle (myosin II), PDZ: Human myosin with a PDZ domain, Peri: Perinatal (myosin II), sm: Smooth muscle (myosin II)
(Sequence data and parameters according to Hodge and Cope, 2000)

The phylogenetic analysis revealed, that all myosin subtypes identified in *Hydra* group to specific known classes within the superfamily tree (Fig. 2.1). The red dots clarify the *Hydra* myosins. The red/blue dots mark the class II myosins in *Hydra* which are of particular importance for the question addressed in the present work, since class II myosins represent the conventional myosins for cellular and muscle contractility.

The gene expression data showed that *st-MyHC* (Hv_myosin-striated) and *nm-MyHC* (Hv_myosin-10-like) are expressed separately in both the ecto- and endoderm (Holz et al., 2017). To illustrate this different expression pattern, a double *in situ* hybridization was performed.

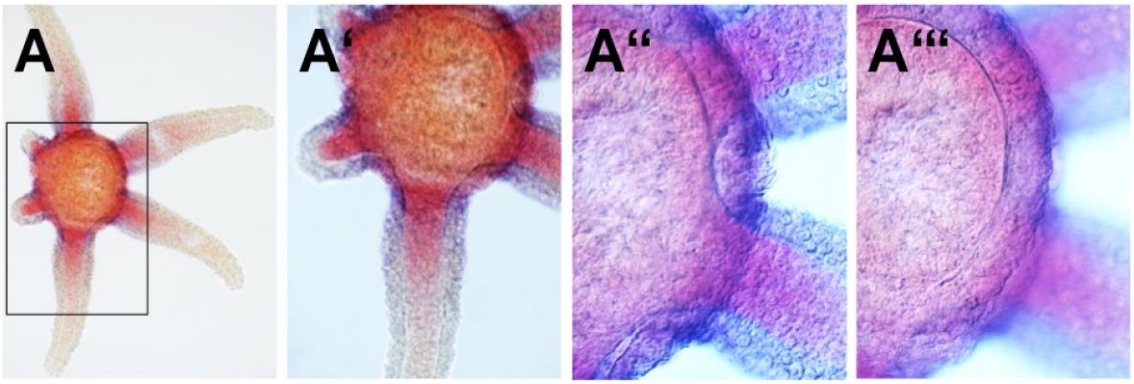

Figure 2.2: *st-MyHC* and *nm-MyHC* double ISH of the head. *st-MyHC* was digoxigenin labelled and detected in blue, *nm_MyHC* was fluorescein labelled and detected in red. (A) *st-MyHC* was detected in the ectoderm, while *nm-MyHC* was detected in the endoderm (10x magnification) (A´) 20x magnification (A´´ and A´´´) 40x magnification in different optical layers with focus on the mesogloea. (Image taken from the Bachelor thesis project of Belinda Rotta, 2017, supervised by me)

The *Hydra* head was chosen to illustrate and compare the two expression patterns because it showed a consistent expression pattern of both myosins. The double *in situ* hybridization confirmed that both myosin subtypes are expressed separately in head tissue of normal adult polyps as well as in body tissue (not shown) in ectoderm (*st-MyHC*, blue) and endoderm (*nm-MyHC*, red) (Fig. 2.2 A and A´). The separation becomes visible bydistinctly by focussing the mesogloea (Fig. 2.2 A´´ and A´´´). The violet colour (usually indicating coexpression) is based on the overlap of the epithelial layers.

4.3 Distribution of pMLC20 during other morphogenetic processes

The phosphorylation of RLC is crucial for generation of contractile forces and formation of contractile networks which in turn is essential for several cellular processes like e.g. morphogenesis (Sutherland and Lesko, 2020). It has been reported that pMLC20 is involved during bud detachment as well as tentacle evagination (Holz et al., 2017; Holz et al., 2020). Besides budding and bud detachment there are still other morphogenetic processes taking place in *Hydra* like testis formation during sexual reproduction or regeneration after an injury.

4.3.1 Involvement of actomyosin complexes during testis formation in *Hydra*

The cnidarian *Hydra* usually propagates asexual by budding which represents the primary reproduction form. Caused by starvation or temperature drop the polyps undergo sexual phases where egg and sperm are differentiated (Kuznetsov et al., 2001). The germ cells are derived from multipotent interstitial stem cells while the testis structure is built exclusively by ectodermal epitheliomuscle cells (Fig. 2.3) (Bosch and David, 1986; Tardent, 1974).

Figure 2.3: The anatomy of the testis in *Hydra.* Shown is a histological cross-section of a mature testis stained with methylene blue/basic fuchsin/borax. Cellular structures and the mesogloea are visible in pink and maturing sperm in blue. Abbreviations: mg: mesogloea, ec: ectoderm, en: endoderm, ch: chamber, c-ec: columnar like elongated ectodermal cells. The dotted line indicates such a chamber for sperm maturing formed by strongly elongated ectodermal cells.

(Modified after: Kuznetsov et al., 2001)

To elucidate whether pMLC20 is involved during testis formation, pMLC20/phalloidin staining was performed on polyps carrying multiple testes. The data revealed that developing testes are strongly positive for the pMLC20 protein. The stage 3 as well as the stage 4 testes indicated a strong pMLC20 signal (Fig. 2.5 A).

Interestingly, the stage 3 (Fig. 2.5 A, left testis) testis did not show such structures (chambers) and no developmental sperm stages (Fig. 2.4). The apical region contained big cells positive for pMLC20 (Fig. 2.4 A). In the mid region as well as in the maximum projection disordered, irregularly fibers were detectable (Fig. 2.4 B and C). The lumen of the testis is filled with immature spermatogonia or spermatocytes (Fig. 2.4 B).

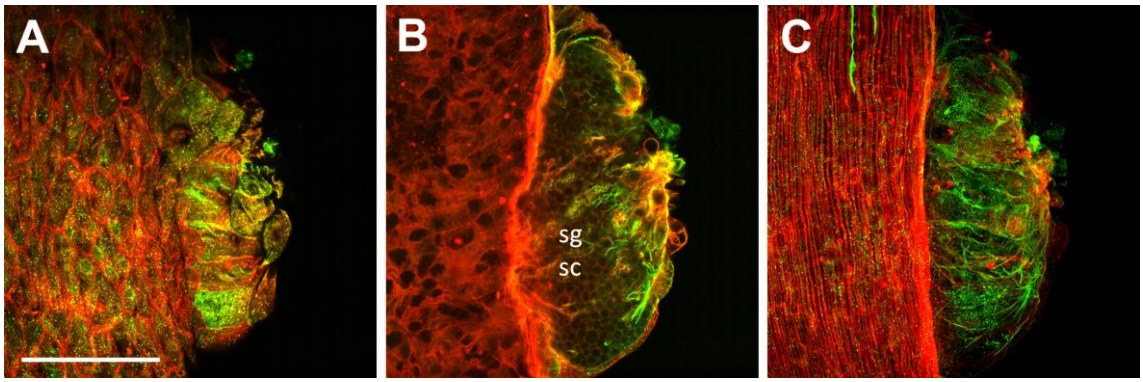

Figure 2.4: Detailed view of a stage 3 testis (Fig. 2.5 A, left testis). The orientation was changed. (A – C) Merged channels of F-actin and pMLC20. (A) Optical section in the apical region. (B) Optical section in the mid region. Maturing sperm are recognizable (sg, sc). (C) Maximum projection. Abbreviations: sg: spermatogonia, sc: spermatocytes. Scale bar: 100 µm

Detailed analysis of the double labelling (pMLC20/phalloidin) revealed several structures within the stage 4 testis (Fig. 2.5 B – J). In the apical region the actin labelling revealed that the testis if formed by big regular shaped ectodermal cells (Fig. 2.5 B). The mid region showed the typical chambers that support spermatogenesis and subdivide the testis lumen into different compartments. A stronger signal is observed at the apical opening (Fig. 2.5 E). Furthermore the different stages of maturing sperms were recognizable (Fig. 2.5 E). The maximum projection showed that F-actin is mainly located in the cellular cortex of ectodermal cells while the typical strong basal F-actin bundles are absent (Fig. 2.5 H).

In the apical region pMLC20 is strongly located in disordered, isolated cells (Fig. 2.5 C). In the mid region, comparable to actin, the chambers were detected (Fig. 2.5 F). These structures are highlighted by a dotted line (Fig. 2.5 G). The maximum projection revealed that pMLC20 is present in irregular disordered fibers within the testis (Fig. 2.5 I) with a stronger localization at the apical opening (Fig. 2.5 G and J).

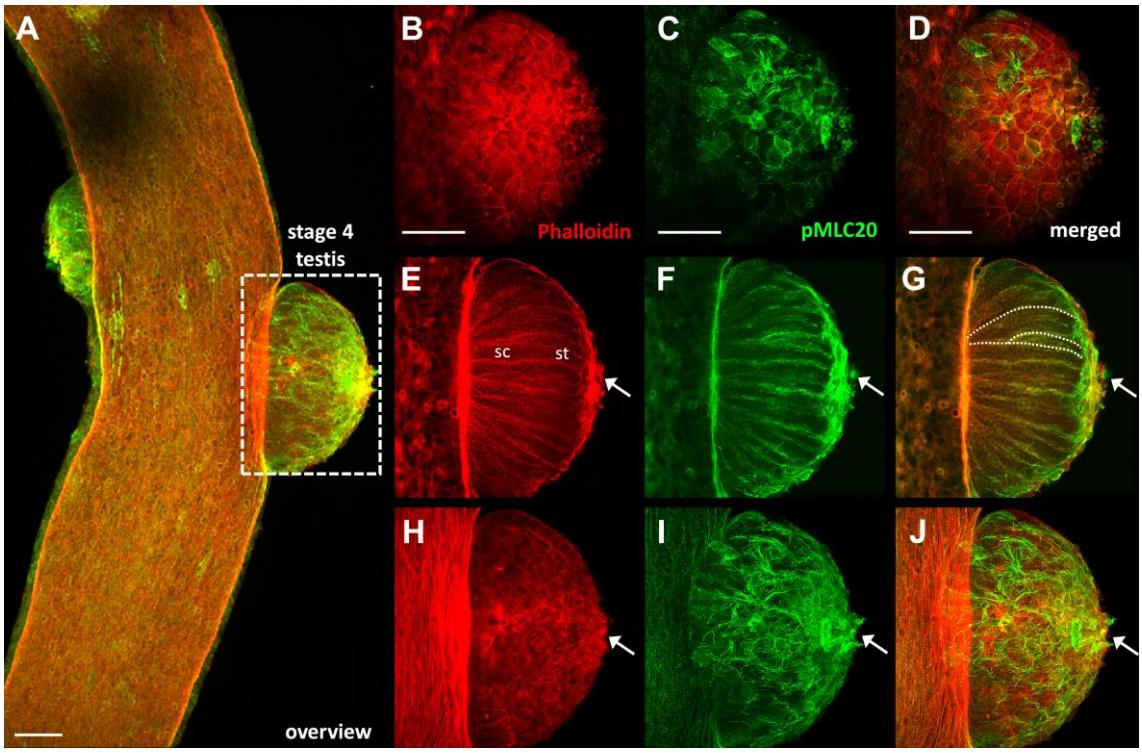

Figure 2.5: Distribution of pMLC20 during testes development in *Hydra*. (A) Polyp carrying 2 testes. Stage 3 testis on the left and stage 4 testis on the right. (B – J) Detailed view of the stage 4 testis. (B – D) Optical section of the apical region of the respective channel as well as a merged image. (E – G) Optical section within the mid region of the respective channel as well as a merged image. Arrows indicate the apical opening. The dotted line marks exemplary the stabilizing structures. (H – J) Maximum projection of the respective channel as well as a merged image. Arrows indicate the apical opening (Testes stages according to: Rentzsch et al. 2005) Scale bar: 100 µm. Abbreviations: sc: spermatocytes, st: spermatids

Since the lateral view indicated a strong localization of F-actin as well as pMLC20 (Fig. 2.5 E-G) the question arose whether actomyosin complexes surround the apical opening. This issue is addressed in Fig. 2.6 which showed a polyp carrying two matured testis in stage 4 (Fig. 2.6 A´). The right one (Fig. 2.6 A´) is slightly tilted which allowed a top view of the apical opening. Indeed the apical opening is clearly surrounded by actomyosin (Fig. 2.6 A – C).

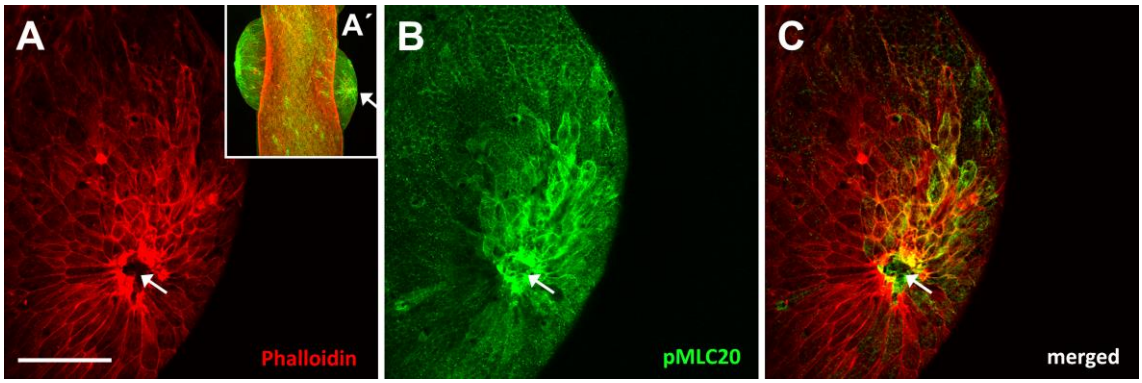

Figure 2.6: Detailed view of a tilted stage 4 testis which allows an on top view of the apical opening. (A´) Overview, arrow indicates the tilted testis. (A) Phalloidin (B) pMLC20 (C) merged; each in the maximum projection. The arrow indicates the apical opening. Scale bar: 100 µm

Although testes development is a rare stress induced process in the ancestral cnidarian *Hydra,* the process is well organized. The outer structure derived by bulged ectodermal epitheliomuscle cells which revealed an atypical distribution of actomyosin complexes in the cells but also in the typical cellular structures for the chambers. Unexpected, but quite clearly, the apical opening is strongly surrounded by actomyosin.

4.3.2 Involvement of actomyosin complexes during wound closure in *Hydra*

Hydra exhibits a remarkable ability to regenerate and lost structures are regenerated completely. When *Hydra* polyps are bisected at 50 % body length, the head and foot regenerate within a few days (Holstein et al., 2003). This regeneration of lost or damaged body parts is necessary for survival of the organism (Reddy et al., 2019). The mechanism for regeneration and wound healing in *Hydra* is called morphallaxis, because lost body parts are reorganized in concert with already existing tissue into the new structures without cell proliferation (Holstein et al., 2003).

To address whether contractile forces induced by RLC phosphorylation are involved in wound closure during regeneration in *Hydra*, regeneration experiments were carried out. The polyps were cut at 50 % body lengths and cohorts fixed every hour from 1 to 6 hours of regeneration.

Preliminary data revealed that pMLC20 accumulates in the area of wound closure (Fig. 2.7 B and C). No matter whether the head or the foot region was evaluated, wound closure was completed after 5 hrs (Fig. 2.7 B). At the head region as well as the foot region, pMLC20 spots are in both cases directly located at the closing wound (Fig. 2.7 B and C).

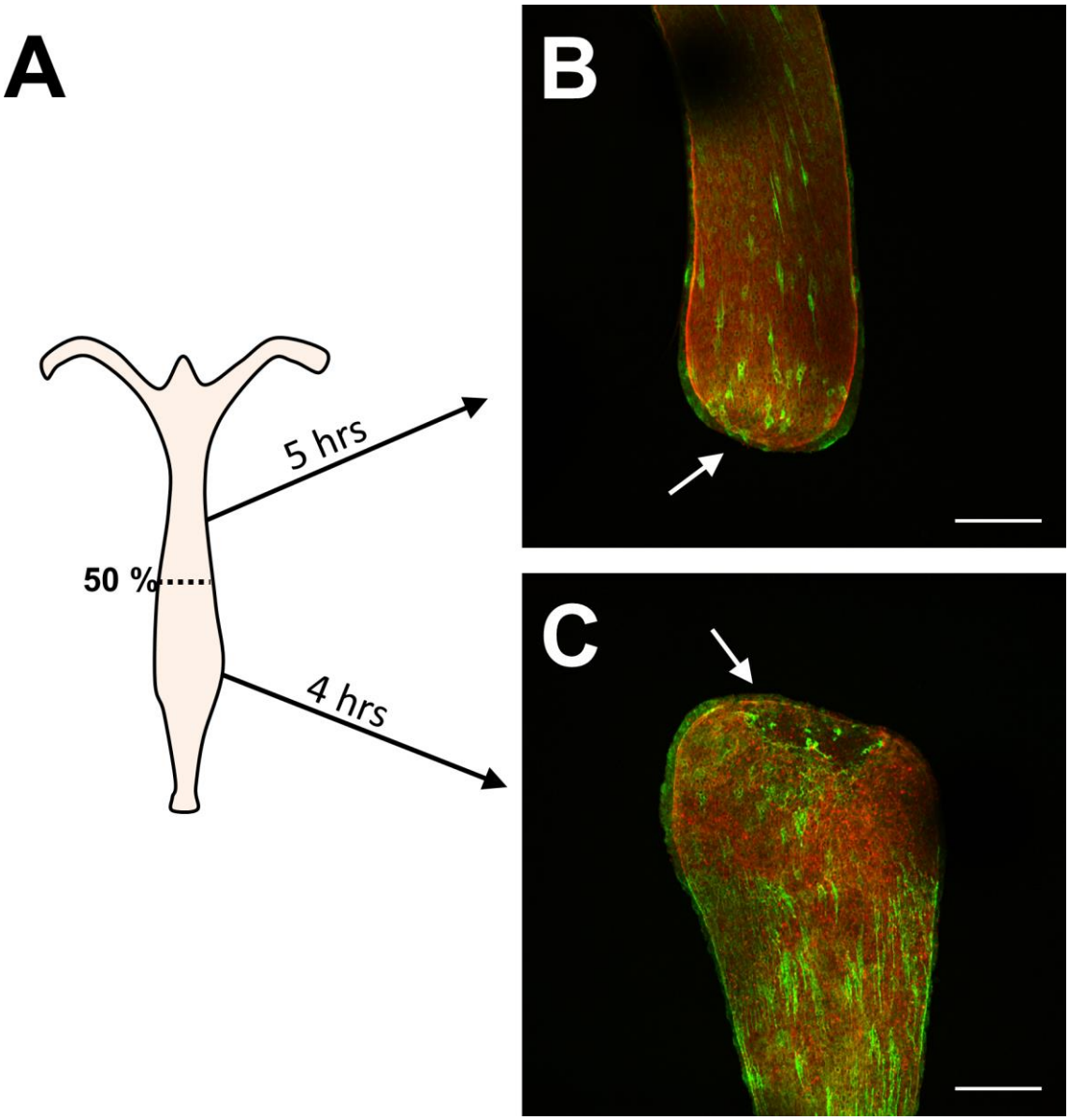

Figure 2.7: pMLC20 in regenerating *Hydra* tissue. (A) Scheme of regeneration experiment. Polyps were cut at 50% body length. (B) Head region after 5 hrs of regeneration and (C) Foot region after 4 hrs of regeneration. The wound site is indicated by arrows. Scale bar: 250 µm

As expected, pMLC20 and therefore contractile actomyosin seems to be involved in wound closure during regeneration in *Hydra*.

5 General discussion

The freshwater polyp *Hydra* exhibits a simple body plan consisting of a diploblastic tissue. The epithelial cells of the ecto- and endodermal monolayers combine an apical epithelial function plus a muscle function, with their basal myonemes ensuring contractility of the polyp (Leclere and Röttinger, 2016).

Various morphogenetic processes, such as tentacle development, bud formation and bud detachment are managed by the ectodermal epitheliomuscle cells. The present work revealed two pathways targeting the formation of actomyosin complexes which are activated (a) by a Rho-ROCK dependent pathway for morphogenetic processes and (b) by MLCK signaling for contractility of the body. Regulation of MRLC phosphorylation also seems to be decisive for tissue integrity in the diploblastic tissue (Holz et al., 2017, Holz et al., 2020). Both pathways act in different subcellular compartments. The implication of these pathways for *Hydra* biology and the specific roles of epitheliomuscle cells in morphogenesis will be discussed.

5.1 A highly conserved molecular toolkit for contractility-based morphogenesis in *Hydra*

A first indication that *Hydra* possesses the whole molecular toolkit for a Rho dependent regulation of contractility (Fig. 3.1 B) was given by the expression of its elements in overlapping regions during bud morphogenesis (Holz et al., 2017; Holz et al., 2020). It is revealed that *Hydra* uses this signaling pathway for tissue separation, since inhibition of each element of the pathway resulted in failure of bud detachment (Holz et al., 2017) (Fig. 3.1 C).

An interesting aspect is the dramatic difference of inhibitor effects depending on the developmental stage of the treated bud. While early inhibition (stage 3-4) leads to the phenotype shown in Fig. 3.1 C, late inhibition (stage 4-6) leads to animals that form a constriction at the bud base, but final detachment is prevented (Holz et al., 2017, Fig. 7 G-I; Fig. 8 D-F). The same effect is observed by FGFR inhibition with SU5402 (Sudhop et al., 2004), and is comparable to the one observed in *Hydra* lines transgenic for a truncated FGFR (Hasse et al., 2014). The reason for this effect is unknown, but suggests that the fate of the cells is already determined at an early stage of bud development. From this point of view the dynamic recruitment of parental tissue into the bud by concentric rings is interesting (Otto and Campbell, 1977; Berking, 2003). The schematic representation of these concentric rings, in fact, coincides partially with the expression of *FGFRa* (*kringelchen*). The expression of *FGFRa* already starts in

stage 4 of the bud as a broad, proximal ring. This is about 3 days before the bud detaches and therefore, suggests that early FGFRa signaling instructs these cells for later detachment. The time point of *FGFRa* expression at the bud base overlaps with the required beginning of the Rho, ROCK and myosin II inhibitor exposure to achieve a high number of non-detaching phenotypes. In this case, disturbation of FGFR dependent signaling via Rho, ROCK and myosin II in an early developmental stage prevents detachment indicating an essential role of this pathway for the early determination of cells for later formation of the constriction and detachment (Fig. 3.1 C). Since the late inhibitor exposure has much weaker effects, we propose a reduced level of signaling that allows constriction of the bud base but is not strong or persistent enough for final detachment (Sudhop et al., 2004, Hasse et al., 2014; Holz et al., 2017).

5.1.1 Actin binding proteins as decisive factors for contractile network properties

Besides the activation of contractility, the composition of the network is important for its properties (Pellegrin and Mellor, 2007). The decisive factor here is the fine-tuning by actin-binding proteins, which characterize the dynamics and organization of the contractile network. Typical for a network with low dynamics but high contractility (Pellegrin and Mellor, 2007) is an involvement of α-actinin in actomyosin network formation. The strong expression of *Hydra* α-actinin at the late, constricting bud base (Holz et al., 2017) therefore, suggests a constellation in which a relatively stiff actin network generates high tension forces.

Taken together, all components of a Rho dependent signaling pathway, as well as additional components for activation and network architecture, are expressed in overlapping regions that undergo morphogenetic changes. The fact that inhibition of all components within a Rho dependent pathway leads to non-detaching, Y-shaped phenotypes identified a Rho-ROCK pathway essential for bud detachment.

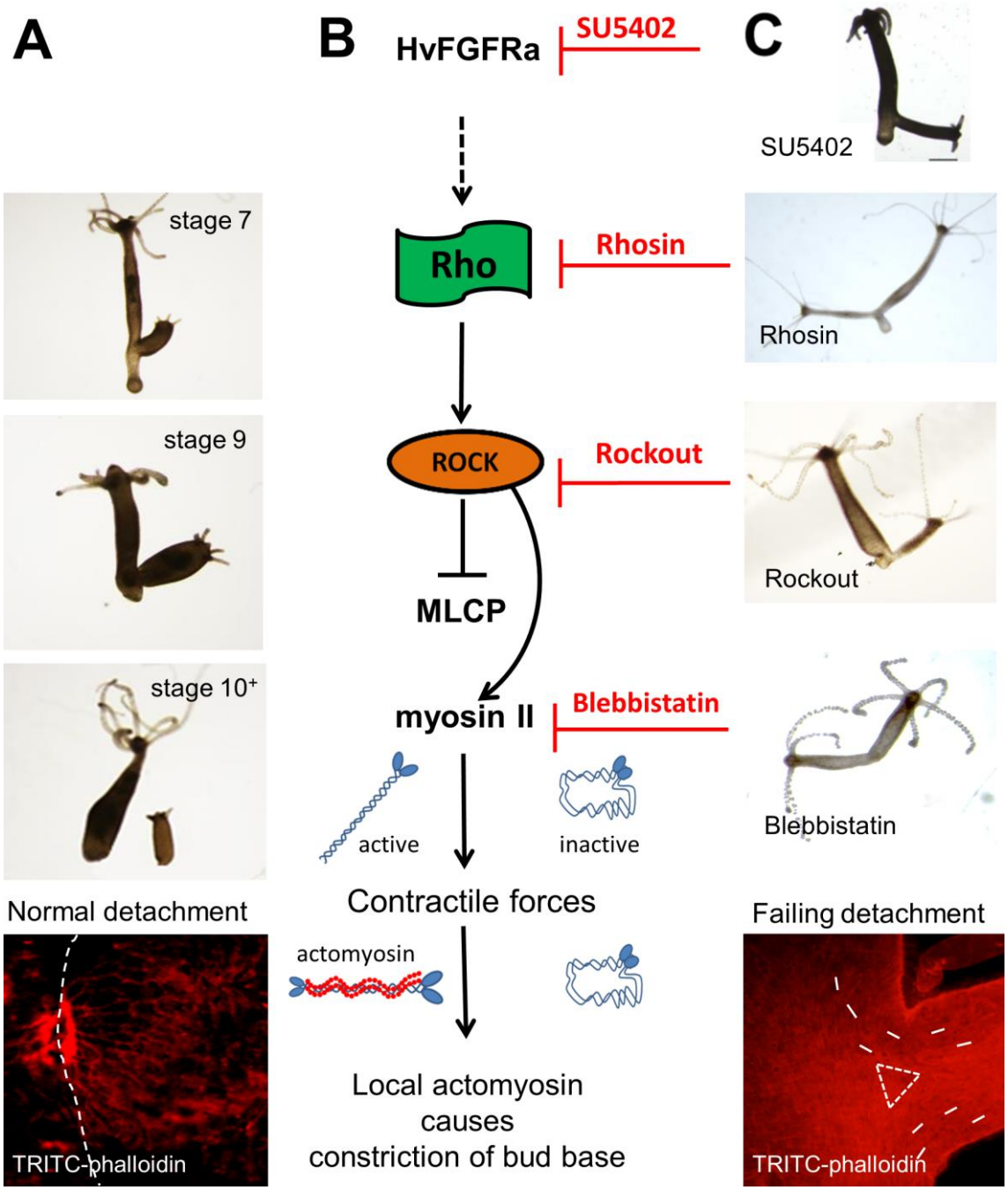

Figure 3.1: Graphical summary for FGFR-Rho-ROCK dependent bud detachment in *Hydra*
(A) Normal bud detachment is accompanied by an accumulation of F-actin at the bud base and is characterized by a constriction from stage 8 onwards. (B) Candidate pathway downstream of FGFR for F-actin reorganization and thus for proper bud detachment. A Rho dependent pathway is essential to initiate contractile forces for bud base constriction. The signaling pathway is manipulated by various inhibitors (red bars). (C) Inhibition of each component within the pathway prevents bud detachment in a similar way and leads to a non-detaching phenotype (Y-shaped animals). During this failing detachment, F-actin accumulation at the bud base is prevented.

5.1.2 A single RLC for the potential regulation of two differently expressed myosins

In *Hydra*, only two class II myosins (nm_MyHC, st_MyHC) are known (Steinmetz et al., 2012; Holz et al., 2017). The activity and activation of non-muscle myosin II is typically controlled by RLCs (Vincente-Manzanares et al., 2009, Park et al., 2011), while the activation of striated myosin II is a calcium dependent process (Gordon et al., 2000). In the genome of *Hydra,* only one regulatory light chain is predicted/annotated (*RLC12B*, Wenger and Galliot, 2013), and the question arises whether in the prebilaterian *Hydra* MRLC acts similar to bilaterian RLCs. Although we did not further investigate this issue, presence of the canonical inhibitory phosphorylation sites, Ser2, Ser3, and Thr10, suggests that *Hydra* MRLC is regulated like bilaterian RLCs to turn off network formation and reorganization (Komatsu and Ikebe, 2007). As well, presence of the essential canonical activatory phosphorylation sites, Thr19 and Ser20 (Newell-Litwa et al., 2015), suggests that RLC activation in *Hydra* occurs by a similar mechanism as in bilateria. I have obtained a complex picture of MRLC distribution in *Hydra* either by gene expression data as well as by two antibodies. The localization of the mRNA by i*n situ* hybridization directly correlates with that of the antibody against MRLC (MYL9), while an antibody against the phosphorylated MRLC (pMLC20) is exclusively restricted to the ectoderm (Holz et al., 2020). This is somewhat controversy, since the nm-myosin which is normally regulated by RLCs is expressed in the endoderm. This might be managed due to differential phosphorylation at Thr19 but has to be investigated in further studies, since MYL9 is also present in the endoderm as well as the mRNA. RLCs are myosin associated proteins that binds to a highly conserved IQ-motif (IQxxxRGxxxR) within the neck region of the myosin heavy chain (MHC) (Bähler and Rhoads, 2002). Both class II myosins in *Hydra* contain an IQ-motif inside the neck region of MyHC for RLC interaction (Supplement Fig. S 2). Which myosin in *Hydra* is regulated by the RLC requires further investigation. Another unsolved issue is, whether the definition of non-muscle and striated-type myosins is useful and applicable in this case. Based on the absence of specialized muscle cells in *Hydra,* the polyps likely use both myosin II isoforms as non-muscle myosin subtypes, independent from each other in the endoderm or ectoderm.

5.2 pMLC20 is located in different cellular compartments during several morphogenetic processes

The epithelial tissue in *Hydra* is subject to permanent proliferation and therefore shifts to the apical and basal termini (Hobmayer et al., 2012). There cells differentiate and have to change their shape in e.g. cnidarian specific battery cells. In the polyp are different, complex patterns that have to be formed. Most of them occur during the asexual budding process like the evagination and maintenance of tentacles or the constriction at the late bud base where a strongly RLC phosphorylation (pMLC20) accompanies bud detachment (Holz et al., 2020). Additional data provides, that all regions that undergo morphogenetic changes revealed pMLC20 in different subcellular compartments with potential different properties.

5.2.1 pMLC20 is involved in early tentacle evagination and stabilization

The pMLC20 analysis revealed that actomyosin is involved in early evaginating tentacle buds which depend on non-canonical and canonical WNT signaling (Philipp et al., 2009). During early tentacle evagination the ectoderm is thickened in which central cells showed a cortical localization of pMLC20 (Fig. 3.2 A, A´). This early evagination occurs similarly in the anthozoan *Nematostella vectensis*, where tentacle evagination starts by even a thickening of ectodermal epithelial cells. Based on the circular reorganization of the actin cytoskeleton at evaginating tentacles (Philipp et al., 2009, Holz et al., 2020) as well as during bud evagination (Aufschnaiter et al., 2017) it would be likely, that at least the early evagination process in both is comparable, although pMLC20 data are missing for bud evagination. Later on pMLC20 accumulated in unusually short and thick fibres at the base of ectodermal cells as well as in the centre of a few cells of the lateral tentacle tip (Fig. 3.2 B). The central position of the cells with pMLC20 corresponds to a region which is supposed to mechanically stabilize the evaginating tentacles. To this end, a persistent control of contractility is required (Katoh et al., 2011). In contrast to usual apical constriction in bilaterian invagination morphogenesis, e.g. in neurulation (Butler et al., 2019), the evaginating ectodermal *Hydra* tentacle bud cells seem to undergo a basal constriction (Fig. 3.2 B, C). While apical constriction generates tensional forces to initiate invagination of the epithelium, increased basal ectodermal forces in the tentacle buds might be appropriate to push out the ectodermal cells for tissue evagination. The basal constriction of ectodermal cells might force the tissue bilayer to evaginate (Fig. 3.2 B, C). My data suggest that pMLC20 promotes early evagination by basal constriction accompanied by a stabilizing function in early already evaginated tentacle. Such a basal stabilizing is similar to one described in *Nematostella* gastrulation, where invaginating cells constrict apically while

surrounding cells constrict basally to support this morphogenetic process (Pukhlyakova et al., 2018). Whether basal constriction in *Hydra* is necessary for evagination or takes over a stabilizing function requires further investigations.

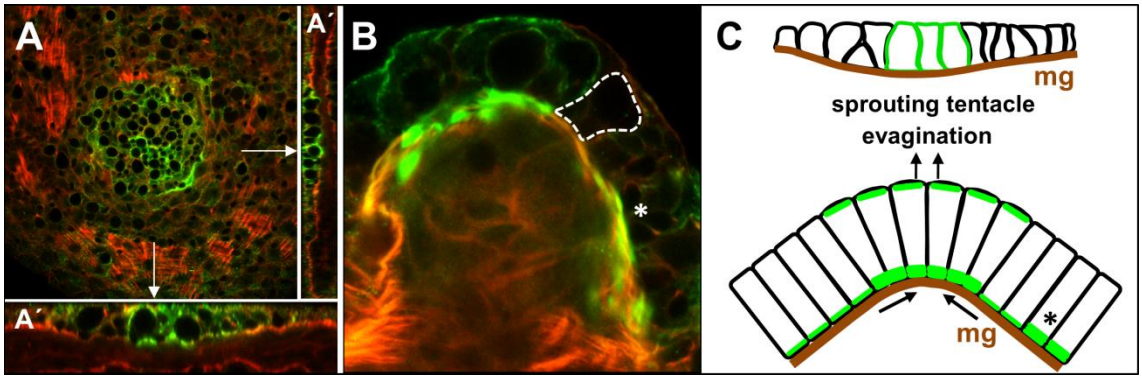

Figure 3.2: Involvement of actomyosin during tentacle evagination. (A) Early evaginating tentacle, (A´) orthogonal optical sections. (B) Later tentacle after evagination. The dotted line indicates an ectodermal cell. The asterisk indicates lateral located basal fibers. (C) Schematic model for tentacle evagination. In early evagination, the ectoderm thickens and central cells have a high level of pMLC in the cellular cortex. In later tentacles, pMLC in the basal compartment in the tip of the tentacle as well as in lateral regions (asterisk) stabilizes tissue evagination.

5.2.2 pMCL20 is involved in testes formation and wound closure during regeneration

Besides pattern formation during development, there are stress - induced morphogenetic processes, such as testes formation and regeneration. During testes formation pMLC20 as well as phalloidin staining revealed a complex disordered meshwork of thin fibres and a strong localization in the strongly elongated columnar like cells that might stabilize the structure of the testes. In general, the detailed analysis of the testes revealed some unexpected details. The epitheliomuscle cells from which the testes are formed offered that the typical basal myonemes are missing. Since the testes do not have to contract, this is not a functional disadvantage, but it does open up a completely new picture of the ectodermal epitheliomuscle cells. Also the strong localization surrounding the apical opening is unusual, since nothing comparable is observed in the polyp for e.g. at the mouth opening. For this issue I propose that actomyosin complexes in testes take over a primarily stabilizing function within the cells as well as in the columnar like cells which form the chambers. This supporting structures converge around the apical opening what results in these unexpected, strong accumulation.

Furthermore, pMLC20, i.e. actomyosin, is involved in wound closure during regeneration. However, it seems to be obvious that *Hydra* uses this contractile mechanism for wound closure during regeneration, since contractile forces are required to close the ,,epithelial gap".

To sum up, phosphorylation of RLC and thus contractile forces occur in all morphogenetic processes in *Hydra*. However, it remains still unclear whether these structures are used exclusively to generate contractility or also takes over stabilizing functions for rigidity. These functional differences might be a result of different signaling pathways that influence actomyosin activation as well as network formation. This hypothesis is supported by at least differential gene expression patterns in varying morphogenetic active regions. In particular during bud detachment, a strong, consistent phosphorylation could be described, which accompanies the entire detachment process and essential for contractile forces.

5.3 Parental ectodermal tissue takes over the leading role during bud base morphogenesis

The bud base is initially a dynamic region where tissue is recruited and moves into the newly formed bud. In stage 6 bud tissue becomes static and tissue flow stops concomitant with detachment morphogenesis (Otto and Campbell, 1977; Berking, 2003). Histological sections revealed that cells within the bud base constriction change their morphological properties while adjacent cells in the parental tissue are normal whereas cells on the bud side are small and constricted (Holz et al., 2017; Fig. 3.3 A). This observation was confirmed by phalloidin staining. Recently published data by detailed pMLC20 analysis add to this finding and clearly show that the actomyosin complexes are located to the parental rather than bud tissue (Holz et al., 2020). Based on the collected data, I propose that the parental tissue is the active part during bud base constriction (Fig. 3.3 B) and bud tissue is pulled off passively by tensile forces and increasing stiffness due to a unilateral actin accumulation (Holz et al., 2020).

5.3.1 Persistent pMLC20 accompanies bud base morphogenesis

The process of bud detachment is highly dynamic and passes different stages becomes visible due to pMLC20. Based on that, the detachment phase is subdivided in: a) unilateral establishment of a contractile actomyosin ring of cells; b) constriction (Fig. 3.3 C, C´); c) closure of the epithelial gap between parent and bud (Fig. 3.3 D, D´); d) detachment (Fig. 3.3 E, E´). At this point, it seems to be likely, that this local accumulation of contractile elements represents the ,,sphincter'' for final detachment (Takahashi et al., 1997; Fig. 3.3 E)

In general, the process of bud detachment is more related to an epithelia gap closure than a side-by-side tissue separation, e.g. in a mesodermal boundary formation and separation (Fagotto et al., 2013). Such a unilateral formation of actomyosin around the bud is typical for wound closure (Schwayer et al., 2016; Rothenberg and Fernandez-Gonzales, 2019). During wound closure a cortical ring of actomyosin is established around the epithelial gap and is closed by contractile forces (Brugués et al., 2014). The mechanism of wound closure is not only restricted to the repair of epithelial gaps, it can also take place during developmental processes (Yang and Levine, 2018). During typical side-by-side tissue separation adjacent cells establish unilateral contractile forces to form a boundary to separate from each other (Fagotto et al., 2013). Such an adjacent establishment of actomyosin within the separation boundary cannot be observed in *Hydra* (Holz et al., 2020).

To sum up, the bud base is subdivided into two functional regions during the detachment phase. The parental ectodermal tissue which ensures bud base constriction as well as detachment by active contractile forces and adjacent cells of the bud which differentiate into the foot. Such an asymmetry in adjacent cells presupposes that the cell fate has already been determined.

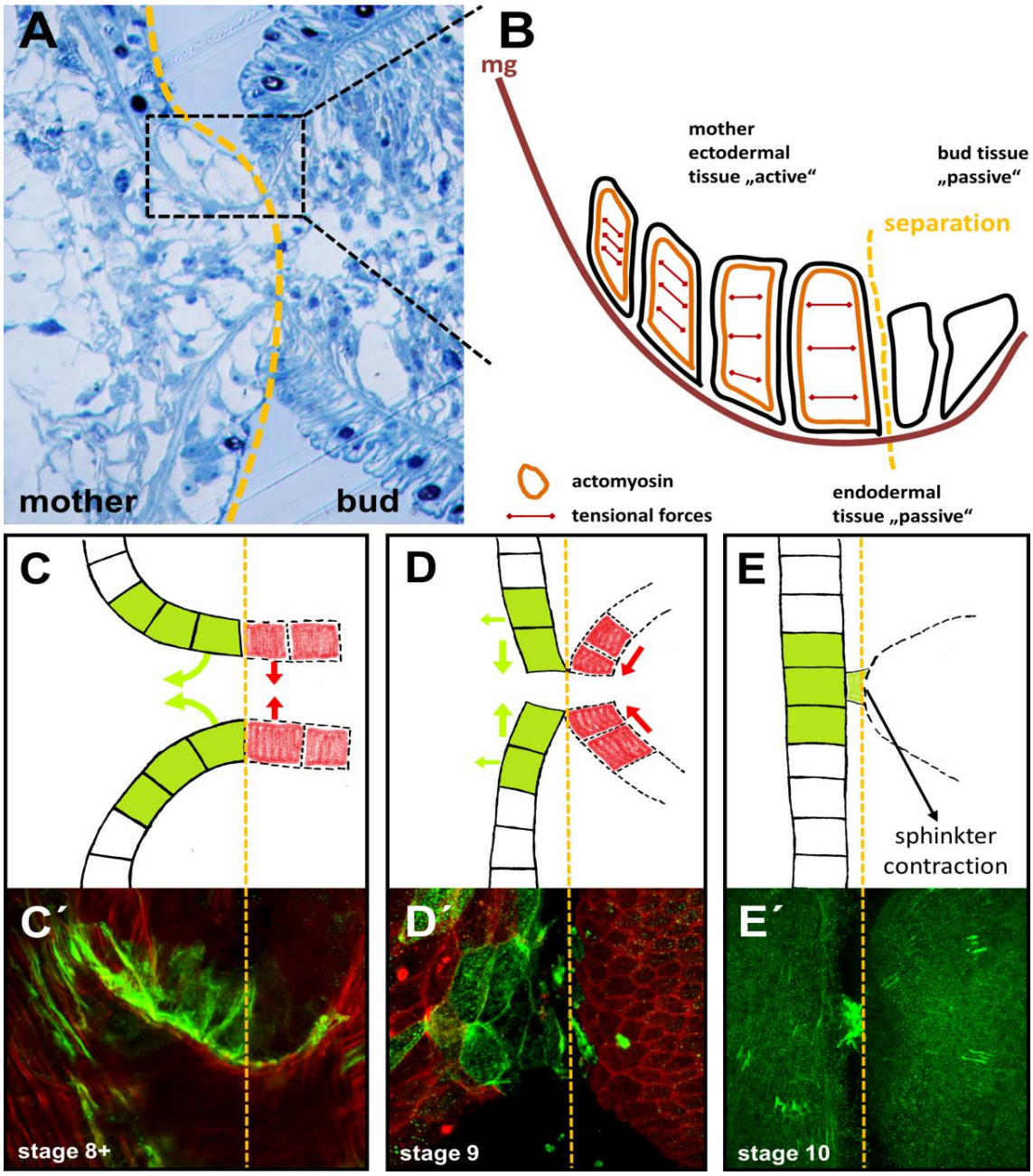

Figure 3.3: Ectodermal contractile forces are generated during detachment on the parent's side rather than in bud tissue. (A) Histological section of the bud base in stage 9 (Holz et al., 2017). (B - E) Schematic summary of contractile events during bud base morphogenesis. Derived from the prevalence of pMLC20 in parental ectodermal tissue is the hypothesis that parental tissue is the active part, while the bud tissue is inactive. (C – E) Scheme of the actomyosin dynamics and direction of contractile forces. Green arrows indicate direction of active contractile forces, while the red arrows show passive tensile forces. (The orange dotted line indicates the separation site).

5.4 The boundary at the late bud base is subdivided in two areas where at least two receptor systems manage bud detachment

The late bud base includes a small area around the boundary between parent and bud. This boundary contains a small population of parental as well as bud cells. This parent-bud boundary is also revealed by several genes encoding signaling elements and being expressed at the bud base (Fig. 3.4 A). Since I assume that active morphogenesis is carried out exclusively by the ectoderm, the focus here is also on ectodermal expressed genes of different receptor systems. A detailed view on subcellular co-factors for signaling, expressed at the late bud base are of great interest but are not considered here, since detailed functions have not been yet described (Suryawanshi et al., 2020). Genes expressed in the subdivided areas at the bud base are summarized in Fig. 3.4 B (Sudhop et al., 2004; Münder et al., 2010; Prexl et al., 2011; Philipp et al., 2009; Tischer et al., 2013; Holz et al., 2017).

5.4.1 Signaling at the bud base might cause functional asymmetry between adjacent cells to ensure detachment

The fact that the parental tissue established unilateral contractile forces indicates a clear functional asymmetry in the cells at the bud base that might be regulated by several signaling pathways.

FGFR signaling is decisive for proper bud detachment (Sudhop et al., 2004; Hasse et al., 2014) and acts upstream of Notch signaling (Münder et al., 2010). However, Notch signaling is just essential to sharpen the FGFR expression which leads to a critical boundary formation at the bud base (Münder et al., 2010). Notch signaling is well known to define developmental boundaries and decides the cell fate by either lateral inhibition or bidirectional signaling (Vazcuez-Ulloa et al., 2018; Henrique and Schweisgut, 2019). In case of boundary formation, Notch is expressed as a stripe, at which adjacent cells undergo cell fate decision (Liao and Oates, 2017) (Fig. 3.4 C). Notch signaling in *Hydra* establish even this parent-bud boundary (Münder et al., 2010) and might support cell fate decisions required to instruct cells for the functional asymmetry. Presence of Ephrin-B1 mRNA (ligand) (Tischer et al., 2013), encoding another component supporting cell fate decision in triploblasts (Wilkinson, 2014), at this boundary. The function of ephrins as well as of non-canonical Wnt signaling during bud detachment, is yet unknown. The presence of FGFR, Notch as well as Ephrin provides a complex regulation of cell fate specification during developmental processes (Perrimon et al., 2012; Haupaix et al., 2013; Wilkinson, 2014).

FGFR signaling is crucial for bud detachment (Sudhop et al., 2004; Hasse et al., 2014) and therefore an interesting candidate for instructing the cells on the parent side for morphogenesis by using potentially different signals.

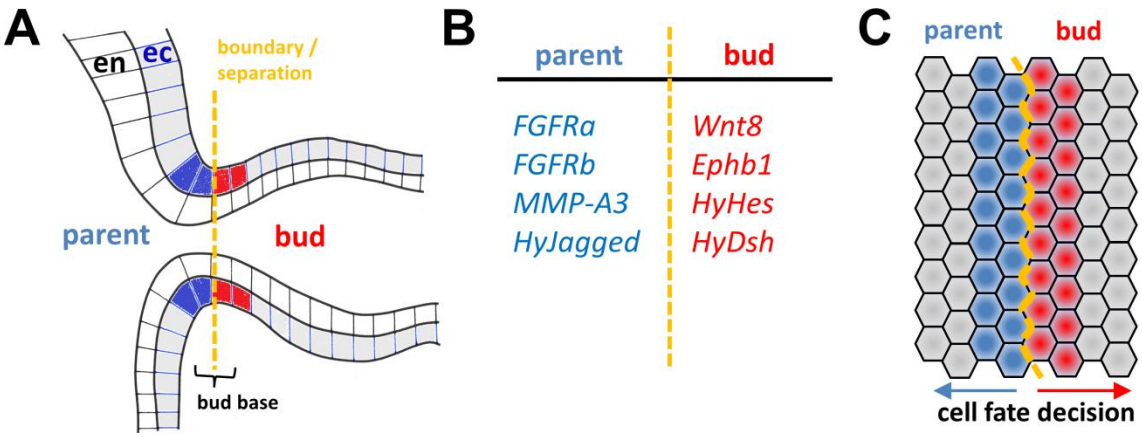

Figure 3.4: Summary of genes expressed at the bud base and a model for the differential control of detachment. (A) Schematic representation of a stage 8 bud with ectoderm (grey) and endoderm (white). Blue labelled cells represent parental expression, red labelled cells expression in the bud. (B) Summary of receptor systems at the bud base. Colour code indicates the area of expression (blue: parent, red: bud). (C) Schematic hypothesis which indicates that the constellation of expression leads to a cell fate decision for proper detachment process. (A – C) The orange dotted line marked the boundary / separation side at the bud base.

5.5 Differential FGFR signaling at the late bud base might unite several cellular downstream reactions

The differential expression of cell fate determination pathways might be related to the presence of two FGFRs in *Hydra*, both of which are expressed at the bud base (Suryawanshi et al., 2020). *FGFRa* is expressed dynamically during the whole budding process and in late stages at the bud base (Sudhop et al., 2004) (Fig 3.5 A), while *FGFRb is* expressed exclusively at the later bud base. FGFRa has been shown to be essential for bud detachment, while the function of FGFRb has not yet been investigated.

Actomyosin as well as dpERK (Fig. 3.5 B) is detected within the *FGFR* expression domain (Fig. 3.5 A) whereby all of these components are located on the parental side. Actomyosin represents the contractile part to enable morphogenesis via a FGFR induced Rho dependent pathway (Holz et al. 2017; Holz et al., 2020). A detailed function of dpERK is not yet known, but inhibition with U0126 leads to a delayed bud detachment which confirms an involvement during the detachment process (Hasse et al., 2014).

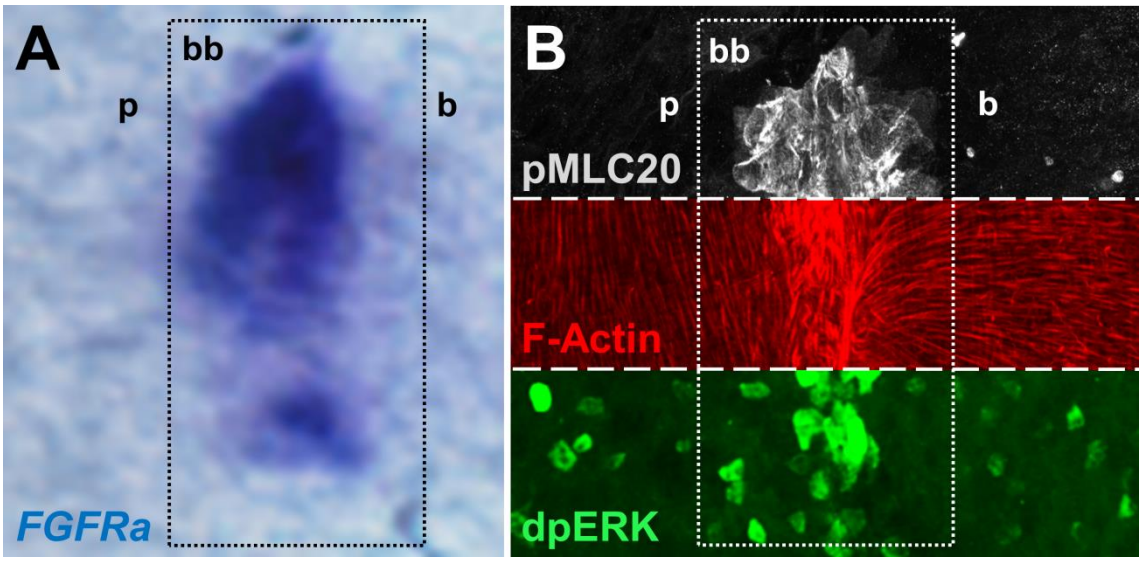

Figure 3.5: Summary of potential targets induced by FGFR signaling during bud detachment in *Hydra* (A) Digital magnification of *FGFRa* expression in a bud stage 9 after *in situ* hybridisation. (B) Compilation of cellular responses at the late bud base. Thereby, pMLC20, the accumulation of actin as well as dpERK are located in an overlapping region at the parental side during bud detachment. Abbreviations: bb: bud base, p: parent, b: bud

5.5.1 FGFR dependent pathways might promote junctional remodelling required for morphogenesis

Rho signaling as well as MAPK/ERK signaling took part during bud detachment. The role of Rho during this process seems clear, but Rho is involved in many aspects of cellular behaviour (Riento and Ridley, 2003). Another main feature of Rho is the regulation of focal adhesion complexes (Ren et al., 2000). Focal adhesion complexes connect actin fibres to the membrane to stabilize and increase stiffening between cells in tissues. Such a reinforced actomyosin network requires an increased cellular focal adhesion complex to transfer tensional forces to e.g. adjacent cells or the ECM (Chang and Kumar, 2013; Kassianidou and Kumar, 2015; Kassianidou *et al.,* 2017; Soiné *et al.,* 2015; Lee and Kumar, 2016). Rho signaling is described to be involved in the recruitment of focal adhesion components to reinforce cellular stiffness (Zhang et al., 2015, Katoh, 2017). Therefore, Rho would be a potential candidate to modulate focal adhesion in *Hydra*, which needs to be investigated.

ERK, where the function in *Hydra* still remains unclear, is involved in several cellular processes. Thus, it can also influence MRLC phosphorylation and in this case it would directly promote the formation of actomyosin for morphogenesis (Betapudi et al, 2013). Furthermore, ERK is known to modulate epithelial cell-cell as well as integrin based cell-matrix adhesion (Fincham et al., 2000). MEK/ERK signaling is directly involved in junctional disruption (Aggarwal et al., 2011) and preventable by treatment with the MEK

inhibitor U0126 (Ray et al., 2007). Bud detachment in polyps treated with U0126 (Hasse et al., 2014) is delayed and the possibility that MEK/ERK signaling is required to disrupt the junctional adhesions an attractive hypothesis. Further studies on ERK function are required to achieve a full understanding of the detachment process. The knowledge of cell-cell as well as cell-matrix adhesion is generally limited in *Hydra.*

Taken together, FGFR dependent pathways might promote Focal adhesion complexes as well as junctional regulation at the bud base. FGFR signaling provides a complex tool kit in *Hydra* that could convey on several intracellular pathways and therefore different functions. As well, it is still unknown where the FGFR proteins are located, which impedes a detailed statement about local functions. Furthermore, several differentially expressed FGF ligands exist, but their function as well as their binding properties are not yet characterized (Lange et al., 2014; Reichart, 2020). And last but not least, intracellular docking and adaptor proteins are differentially expressed at the bud base indicating specificity of FGFR-dependent signaling pathways and representing a versatile toolkit (Suryawanshi et al., 2020). To extend the comprehension of the detachment process further studies on FGFR signaling as well as on the downstream targets are required.

5.6 Hypothesis of morphogenetic regulation in bifunctional epitheliomuscle cells

The present work provided a new, complex picture how epitheliomuscle cells fulfil their dual function as contractile epithelial cells to ensure body contractility as well as manage versatile morphogenetic outcomes. In this context actomyosin complexes are proposed to generate the contractility while the localization in the different cellular compartments is decisive for functionality. Moreover body contractility as well as morphogenetic processes are regulated by at least two independent pathways (Holz et al., 2020). This provided the basic machinery, which enables body contractility such as complex morphogenesis in *Hydra*. However, many questions remained to be unanswered. Recently published data provide that Fat-like cadherins are involved in tissue organization, cell adhesion, and the actin cytoskeleton in *Hydra* (Brooun et al., 2020). These data confirm that the cell-cell adhesion as well as the actin cytoskeleton, actomyosin complexes and tissue integrity are very closely related in the bifunctional epitheliomuscle cells in *Hydra*. This assumption is based on the fact that interference with MLCK signaling (by ML-7) abolished basal F-actin bundles as well as cortical actin while the same is observed by direct interference to actin nucleation by Cytochalasin B (Holz et al., 2020). To obtain full insights into the orchestration of tissue separation by

epitheliomuscle cells further studies, particular on adhesion complexes and cellular junctions are required.

5.6.1 Subcellular compartments of the epitheliomuscle cells ensure versatile morphogenetic outcomes

The epitheliomuscle cells in *Hydra* perform diverse morphogenetic tasks which presumably are regulated by local contractility in different subcellular compartments. Therefore the cell is subdivided into three cellular compartments: a) apical; b) baso-lateral and c) basal (Fig. 3.6 A). Cellular contractility is ensured by myonemes in the basal cellular compartment (Aufschnaiter et al., 2017) (Fig. 3.6 B), which is controlled via MLCK. During morphogenetic processes contractile elements are established in the baso-lateral as well as apical region (Fig. 3.6 C) for e.g. during bud base constriction (Holz et al., 2020). To transfer even this contractility to the surrounding tissue the junctional properties within these morphogenetic regions have to be reorganized.

Cell-cell adhesion as well as tissue integrity is composed by several adhesion complexes in the different cellular compartments in *Hydra* (Seybold et al., 2016) (Fig. 3.6 A, B). Stable cell interactions are required to ensure the structural integrity of tissues, and dynamic changes in cell adhesion take place during morphogenesis of developing tissues (Gumbiner, 1996). I propose that these adhesion complexes have to be reinforced in adjacent cells during bud base constriction to increase stiffness (Fig. 3.6 C). Cells at the separation site loosen their lateral cell-cell-contacts (Fig.3.6 C) by e.g. reducing cadherin - based adhesion and strengthen their anchor in the extracellular matrix by e.g. integrin (Burute and Thery, 2012). The model in Fig. 3.6 B and C summarizes a mechanism by contractile forces as well as cell-cell and cell-matrix adhesion to allow the management at the constricting bud base and last but not least bud detachment.

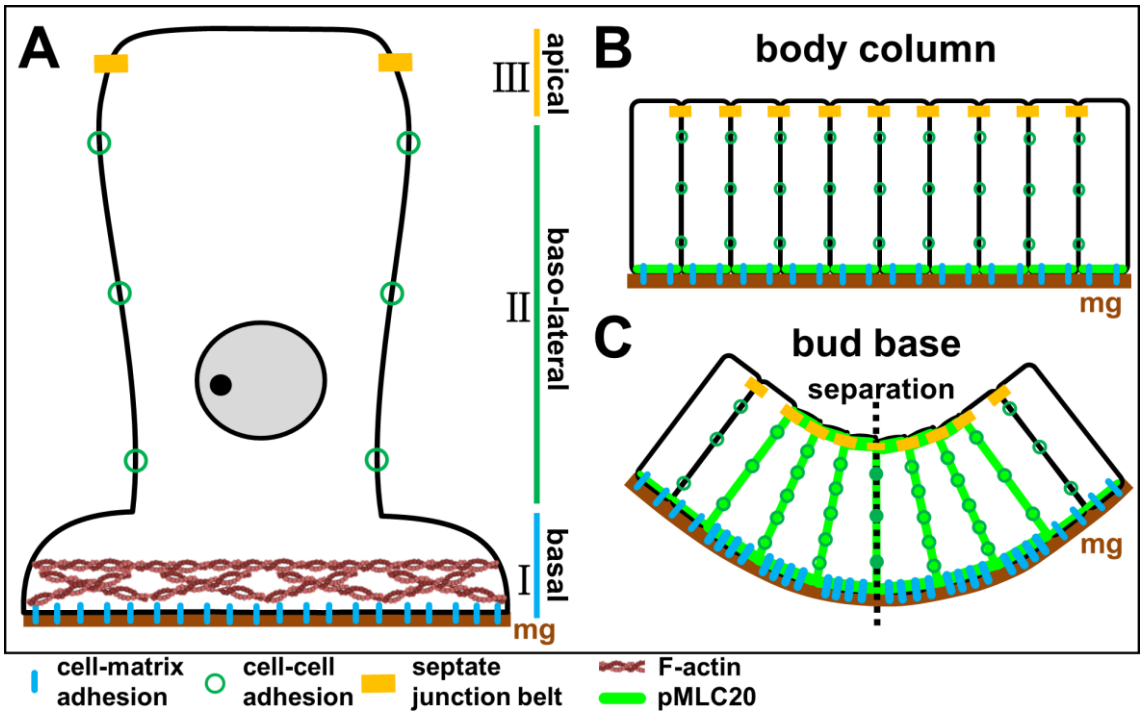

Figure 3.6: Scheme of a mechanism allowing tissue separation using the differential adhesion of ectodermal epitheliomuscle cells. (A) Epitheliomuscle cell with its lateral and basal adhesion sites and contractile elements. (B) Organization of epitheliomuscle cells in the body column ensuring tissue integrity by apical and lateral contact sites and anchoring in the mesogloea by cell-matrix adhesion. (C) Model of the constricting bud base. An increase of cell-matrix adhesion (blue rods) and ectodermal cell adhesion (green dots) between cells flanking the separating cells supports the separation (black dotted line) of parental and bud epithelia in response to traction (pMLC20) and stiffening (actin) of the tissue.

6 Final conclusion and outlook

The cnidarian *Hydra* exhibits a simple body plan. Its diploblastic tissue is formed by epitheliomuscle cells which are known to contribute to several homeostatic functions as well as developmental processes (Buzgariu et al., 2015). The present work provides a new, complex picture how ectodermal epitheliomuscle cells manage morphogenetic processes by actomyosin interactions and their differential occurrence in the subcellular compartments. Furthermore, the data revealed that contractility during body movement and bud base morphogenesis are regulated by independent pathways. Last but not least, the present data strongly suggest multifunctionality of actomyosin in epitheliomuscle cells during morphogenetic processes. Besides the role of actomyosin for contractility in morphogenesis e.g. during bud base constriction, a stabilizing function in testis is very likely and might be regulated by different signaling systems which still have to be identified. The data raise new questions for further investigations that address the dynamics and composition of actomyosin networks. To decipher this complex regulation several actin binding proteins as well as a variety of signaling systems have to be analyzed to gain insight into network properties and describe the difference between a contractile and a stabilizing network. Another interesting aspect is how endodermal epitheliomuscle cells manage their circular contractility, since pMLC20 is clearly restricted to ectodermal cells. Whether an alternative, activating phosphorylation site (Ser18 or Thr19?) of the RLC protein is involved, should be investigated by immunohistological analysis with appropriate antibody. These investigations will add to our knowledge about the properties of the ecto- and endodermal actomyosin network in *Hydra.*

The full orchestration of morphogenetic changes managed by epitheliomuscle cells still remains to be elucidated. Additional studies are required and should address cell-cell adhesion as well as cell-matrix adhesion during morphogenetic processes in *Hydra.* Adhesion molecules have not yet been intensively investigated, but recently published data revealed that Fat-like cadherins are involved in tissue organization, cell adhesion and actin dynamics in *Hydra and therewith take over central roles in the diploblastic tissue (Brooun et al., 2020)*. In future studies, it would be interesting to investigate cell adhesion including the composition of focal adhesion complexes that connect actomyosin with the adhesion molecules to transfer the contractile forces to the adjacent tissue. Initial database analysis revealed that *Hydra* contains a complex toolkit of focal adhesion components (own unpublished data). Besides the cell-cell adhesion, the cell-matrix adhesion has to be investigated to depict the full orchestration.

7 References

Alberts, B., Bray, D., Hopkin, K., Johnson, A., Lewis, J., Raff, M., Roberts, K., Walter, P. (2010) Essential Cell Biology third edition. 590-604. Garland Science, Taylor & Francis Group

Aggarwal, S., Suzuki, T., Taylor, W. L., Bhargava, A., & Rao, R. K. (2011). Contrasting effects of ERK on tight junction integrity in differentiated and under-differentiated Caco-2 cell monolayers. *The Biochemical journal*, *433*(1), 51–63. https://doi.org/10.1042/BJ20100249

Aufschnaiter, R., Wedlich-Söldner, R., Zhang, X., & Hobmayer, B. (2017). Apical and basal epitheliomuscular F-actin dynamics during *Hydra* bud evagination. *Biology open*, *6*(8), 1137–1148. https://doi.org/10.1242/bio.022723

Babina, I. S., & Turner, N. C. (2017). Advances and challenges in targeting FGFR signaling in cancer. *Nature reviews. Cancer*, *17*(5), 318–332. https://doi.org/10.1038/nrc.2017.8

Bähler, M., & Rhoads, A. (2002). Calmodulin signaling via the IQ motif. *FEBS letters*, *513*(1), 107–113. https://doi.org/10.1016/s0014-5793(01)03239-2

Beach, J. R., Shao, L., Remmert, K., Li, D., Betzig, E., & Hammer, J. A., 3rd (2014). Nonmuscle myosin II isoforms coassemble in living cells. *Current biology : CB*, *24*(10), 1160–1166. https://doi.org/10.1016/j.cub.2014.03.071

Berking S. (2003). A model for budding in *Hydra*: pattern formation in concentric rings. *Journal of theoretical biology*, *222*(1), 37–52. https://doi.org/10.1016/s0022-5193(03)00012-2

Betapudi, V., Lominadze, G., Hsi, L., Willard, B., Wu, M., & McCrae, K. R. (2013). Anti-β2GPI antibodies stimulate endothelial cell microparticle release via a nonmuscle myosin II motor protein-dependent pathway. *Blood*, *122*(23), 3808–3817. https://doi.org/10.1182/blood-2013-03-490318

Blanchoin, L., Boujemaa-Paterski, R., Sykes, C., & Plastino, J. (2014). Actin dynamics, architecture, and mechanics in cell motility. *Physiological reviews*, *94*(1), 235–263. https://doi.org/10.1152/physrev.00018.2013

Bode H. R. (2009). Axial patterning in *Hydra*. *Cold Spring Harbor perspectives in biology*, *1*(1), a000463. https://doi.org/10.1101/cshperspect.a000463

Bode H. R. (1996). The interstitial cell lineage of *Hydra*: a stem cell system that arose early in evolution. *Journal of cell science*, *109 (Pt 6)*, 1155–1164.

Boehm, A. M., & Bosch, T. C. (2012). Migration of multipotent interstitial stem cells in *Hydra*. *Zoology (Jena, Germany)*, *115*(5), 275–282. https://doi.org/10.1016/j.zool.2012.03.004

Bosch, T. C., & David, C. N. (1984). Growth regulation in *Hydra*: relationship between epithelial cell cycle length and growth rate. *Developmental biology*, *104*(1), 161–171. https://doi.org/10.1016/0012-1606(84)90045-9

Böttger, A., & Hassel, M. (2012). Hydra, a model system to trace the emergence of boundaries in developing eumetazoans. *The International journal of developmental biology*, *56*(6-8), 583–591. https://doi.org/10.1387/ijdb.113454ab

Bresnick A. R. (1999). Molecular mechanisms of nonmuscle myosin-II regulation. *Current opinion in cell biology*, *11*(1), 26–33. https://doi.org/10.1016/s0955-0674(99)80004-0

Brooun, M., Klimovich, A., Bashkurov, M., Pearson, B. J., Steele, R. E., & McNeill, H. (2020). Ancestral roles of atypical cadherins in planar cell polarity. *Proceedings of the National Academy of Sciences of the United States of America*, *117*(32), 19310–19320. https://doi.org/10.1073/pnas.1917570117

Brugués, A., Anon, E., Conte, V., Veldhuis, J. H., Gupta, M., Colombelli, J., Muñoz, J. J., Brodland, G. W., Ladoux, B., & Trepat, X. (2014). Forces driving epithelial wound healing. *Nature physics*, *10*(9), 683–690. https://doi.org/10.1038/nphys3040

Buker, S. M., Boriack-Sjodin, P. A., & Copeland, R. A. (2019). Enzyme-Inhibitor Interactions and a Simple, Rapid Method for Determining Inhibition Modality. *SLAS discovery : advancing life sciences R & D*, *24*(5), 515–522. https://doi.org/10.1177/2472555219829898

Burnette, D. T., Shao, L., Ott, C., Pasapera, A. M., Fischer, R. S., Baird, M. A., Der Loughian, C., Delanoe-Ayari, H., Paszek, M. J., Davidson, M. W., Betzig, E., & Lippincott-Schwartz, J. (2014). A contractile and counterbalancing adhesion system controls the 3D shape of crawling cells. *The Journal of cell biology*, *205*(1), 83–96. https://doi.org/10.1083/jcb.201311104

Burute, M., & Thery, M. (2012). Spatial segregation between cell-cell and cell-matrix adhesions. *Current opinion in cell biology*, *24*(5), 628–636. https://doi.org/10.1016/j.ceb.2012.07.003

Butler, M. B., Short, N. E., Maniou, E., Alexandre, P., Greene, N., Copp, A. J., & Galea, G. L. (2019). Rho kinase-dependent apical constriction counteracts M-phase apical expansion to enable mouse neural tube closure. *Journal of cell science*, *132*(13), jcs230300. https://doi.org/10.1242/jcs.230300

Buzgariu, W., Al Haddad, S., Tomczyk, S., Wenger, Y., & Galliot, B. (2015). Multi-functionality and plasticity characterize epithelial cells in *Hydra*. *Tissue barriers*, *3*(4), e1068908. https://doi.org/10.1080/21688370.2015.1068908

Chang, C. W., & Kumar, S. (2013). Vinculin tension distributions of individual stress fibers within cell-matrix adhesions. *Journal of cell science*, *126*(Pt 14), 3021–3030. https://doi.org/10.1242/jcs.119032

Christodoulou, N., & Skourides, P. A. (2015). Cell-Autonomous Ca(2+) Flashes Elicit Pulsed Contractions of an Apical Actin Network to Drive Apical Constriction during Neural Tube Closure. *Cell reports*, *13*(10), 2189–2202. https://doi.org/10.1016/j.celrep.2015.11.017

Conti, M. A., & Adelstein, R. S. (2008). Nonmuscle myosin II moves in new directions. *Journal of cell science*, *121*(Pt 1), 11–18. https://doi.org/10.1242/jcs.007112

Courson, D. S., & Rock, R. S. (2010). Actin cross-link assembly and disassembly mechanics for alpha-Actinin and fascin. *The Journal of biological chemistry*, *285*(34), 26350–26357. https://doi.org/10.1074/jbc.M110.123117

Dai, S., Zhou, Z., Chen, Z., Xu, G., & Chen, Y. (2019). Fibroblast Growth Factor Receptors (FGFRs): Structures and Small Molecule Inhibitors. *Cells*, *8*(6), 614. https://doi.org/10.3390/cells8060614

Dickson, C., Spencer-Dene, B., Dillon, C., & Fantl, V. (2000). Tyrosine kinase signaling in breast cancer: fibroblast growth factors and their receptors. *Breast cancer research : BCR*, *2*(3), 191–196. https://doi.org/10.1186/bcr53

Dominguez, R., & Holmes, K. C. (2011). Actin structure and function. *Annual review of biophysics*, *40*, 169–186. https://doi.org/10.1146/annurev-biophys-042910-155359

Downing, T. L., Soto, J., Morez, C., Houssin, T., Fritz, A., Yuan, F., Chu, J., Patel, S., Schaffer, D. V., & Li, S. (2013). Biophysical regulation of epigenetic state and cell reprogramming. *Nature materials*, *12*(12), 1154–1162. https://doi.org/10.1038/nmat3777

Duchesne, L., Tissot, B., Rudd, T. R., Dell, A., & Fernig, D. G. (2006). N-glycosylation of fibroblast growth factor receptor 1 regulates ligand and heparan sulfate co-receptor binding. *The Journal of biological chemistry*, *281*(37), 27178–27189. https://doi.org/10.1074/jbc.M601248200

Duncia, J. V., Santella, J. B., 3rd, Higley, C. A., Pitts, W. J., Wityak, J., Frietze, W. E., Rankin, F. W., Sun, J. H., Earl, R. A., Tabaka, A. C., Teleha, C. A., Blom, K. F., Favata, M. F., Manos, E. J., Daulerio, A. J., Stradley, D. A., Horiuchi, K., Copeland, R. A., Scherle, P. A., Trzaskos, J. M., … Olson, R. E. (1998). MEK inhibitors: the chemistry and biological activity of U0126, its analogs, and cyclization products. *Bioorganic & medicinal chemistry letters*, *8*(20), 2839–2844. https://doi.org/10.1016/s0960-894x(98)00522-8

Fabila, Y., Navarro, L., Fujisawa, T., Bode, H. R., & Salgado, L. M. (2002). Selective inhibition of protein kinases blocks the formation of a new axis, the beginning of budding, in *Hydra*. *Mechanisms of development*, *119*(2), 157–164. https://doi.org/10.1016/s0925-4773(02)00351-9

Falzone, T. T., Lenz, M., Kovar, D. R., & Gardel, M. L. (2012). Assembly kinetics determine the architecture of α-actinin crosslinked F-actin networks. *Nature communications*, *3*, 861. https://doi.org/10.1038/ncomms1862

Fagotto, F., Rohani, N., Touret, A. S., & Li, R. (2013). A molecular base for cell sorting at embryonic boundaries: contact inhibition of cadherin adhesion by ephrin/Eph-dependent contractility. *Developmental cell*, *27*(1), 72–87. https://doi.org/10.1016/j.devcel.2013.09.004

Fagotto F. (2014). The cellular basis of tissue separation. *Development (Cambridge, England)*, *141*(17), 3303–3318. https://doi.org/10.1242/dev.090332

Favata, M. F., Horiuchi, K. Y., Manos, E. J., Daulerio, A. J., Stradley, D. A., Feeser, W. S., Van Dyk, D. E., Pitts, W. J., Earl, R. A., Hobbs, F., Copeland, R. A., Magolda, R. L., Scherle, P. A., & Trzaskos, J. M. (1998). Identification of a novel inhibitor of mitogen-activated protein kinase kinase. *The Journal of biological chemistry*, *273*(29), 18623–18632. https://doi.org/10.1074/jbc.273.29.18623

Fincham, V. J., James, M., Frame, M. C., & Winder, S. J. (2000). Active ERK/MAP kinase is targeted to newly forming cell-matrix adhesions by integrin engagement and v-Src. *The EMBO journal*, *19*(12), 2911–2923. https://doi.org/10.1093/emboj/19.12.2911

Firat-Karalar, E. N., & Welch, M. D. (2011). New mechanisms and functions of actin nucleation. *Current opinion in cell biology*, *23*(1), 4–13. https://doi.org/10.1016/j.ceb.2010.10.007

Fletcher, D. A., & Mullins, R. D. (2010). Cell mechanics and the cytoskeleton. *Nature*, *463*(7280), 485–492. https://doi.org/10.1038/nature08908

Galliot B. (2012). *Hydra*, a fruitful model system for 270 years. *The International journal of developmental biology*, *56*(6-8), 411–423. https://doi.org/10.1387/ijdb.120086bg

Goodson, H. V., & Spudich, J. A. (1993). Molecular evolution of the myosin family: relationships derived from comparisons of amino acid sequences. *Proceedings of the National Academy of Sciences of the United States of America*, *90*(2), 659–663. https://doi.org/10.1073/pnas.90.2.659

Gordon, A. M., Homsher, E., & Regnier, M. (2000). Regulation of contraction in striated muscle. *Physiological reviews*, *80*(2), 853–924. https://doi.org/10.1152/physrev.2000.80.2.853

Gumbiner B. M. (1996). Cell adhesion: the molecular basis of tissue architecture and morphogenesis. *Cell*, *84*(3), 345–357. https://doi.org/10.1016/s0092-8674(00)81279-9

Gunning, P. W., Ghoshdastider, U., Whitaker, S., Popp, D., & Robinson, R. C. (2015). The evolution of compositionally and functionally distinct actin filaments. *Journal of cell science*, *128*(11), 2009–2019. https://doi.org/10.1242/jcs.165563

Hasse, C., Holz, O., Lange, E., Pisowodzki, L., Rebscher, N., Christin Eder, M., Hobmayer, B., & Hassel, M. (2014). FGFR-ERK signaling is an essential component of tissue separation. *Developmental biology*, *395*(1), 154–166. https://doi.org/10.1016/j.ydbio.2014.08.010

Hartshorne, D. J., Ito, M., & Erdödi, F. (1998). Myosin light chain phosphatase: subunit composition, interactions and regulation. *Journal of muscle research and cell motility*, *19*(4), 325–341. https://doi.org/10.1023/a:1005385302064

Harding, M. J., & Nechiporuk, A. V. (2012). Fgfr-Ras-MAPK signaling is required for apical constriction via apical positioning of Rho-associated kinase during mechanosensory organ formation. *Development (Cambridge, England)*, *139*(17), 3130–3135. https://doi.org/10.1242/dev.082271

Haupaix, N., Stolfi, A., Sirour, C., Picco, V., Levine, M., Christiaen, L., & Yasuo, H. (2013). p120RasGAP mediates ephrin/Eph-dependent attenuation of FGF/ERK signals during cell fate specification in ascidian embryos. *Development (Cambridge, England)*, *140*(21), 4347–4352. https://doi.org/10.1242/dev.098756

He, L., Wang, X., Tang, H. L., & Montell, D. J. (2010). Tissue elongation requires oscillating contractions of a basal actomyosin network. *Nature cell biology*, *12*(12), 1133–1142. https://doi.org/10.1038/ncb2124

Heer, N. C., & Martin, A. C. (2017). Tension, contraction and tissue morphogenesis. *Development (Cambridge, England)*, *144*(23), 4249–4260. https://doi.org/10.1242/dev.151282

Heisenberg, C. P., & Bellaïche, Y. (2013). Forces in tissue morphogenesis and patterning. *Cell*, *153*(5), 948–962. https://doi.org/10.1016/j.cell.2013.05.008

Henrique, D., & Schweisguth, F. (2019). Mechanisms of Notch signaling: a simple logic deployed in time and space. *Development (Cambridge, England)*, *146*(3), dev172148. https://doi.org/10.1242/dev.172148

Hobmayer, B., Jenewein, M., Eder, D., Eder, M. K., Glasauer, S., Gufler, S., Hartl, M., & Salvenmoser, W. (2012). Stemness in *Hydra* - a current perspective. *The International journal of developmental biology*, *56*(6-8), 509–517. https://doi.org/10.1387/ijdb.113426bh

Hobmayer, B., Rentzsch, F., Kuhn, K., Happel, C. M., von Laue, C. C., Snyder, P., Rothbächer, U., & Holstein, T. W. (2000). WNT signaling molecules act in axis formation in the diploblastic metazoan *Hydra*. *Nature*, *407*(6801), 186–189. https://doi.org/10.1038/35025063

Holstein, T. W., Hobmayer, E., & Technau, U. (2003). Cnidarians: an evolutionarily conserved model system for regeneration?. *Developmental dynamics : an official publication of the American Association of Anatomists*, *226*(2), 257–267. https://doi.org/10.1002/dvdy.10227

Holz, O., Apel, D., & Hassel, M. (2020). Alternative pathways control actomyosin contractility in epitheliomuscle cells during morphogenesis and body contraction. *Developmental biology*, *463*(1), 88–98. https://doi.org/10.1016/j.ydbio.2020.04.001

Holz, O., Apel, D., Steinmetz, P., Lange, E., Hopfenmüller, S., Ohler, K., Sudhop, S., & Hassel, M. (2017). Bud detachment in *Hydra* requires activation of fibroblast growth factor receptor and a Rho-ROCK-myosin II signaling pathway to ensure formation of a basal constriction. *Developmental dynamics : an official publication of the American Association of Anatomists*, *246*(7), 502–516. https://doi.org/10.1002/dvdy.24508

Ikebe, M., & Hartshorne, D. J. (1985). Phosphorylation of smooth muscle myosin at two distinct sites by myosin light chain kinase. *The Journal of biological chemistry*, *260*(18), 10027–10031.

Ikebe, M., Hartshorne, D. J., & Elzinga, M. (1987). Phosphorylation of the 20,000-dalton light chain of smooth muscle myosin by the calcium-activated, phospholipid-dependent protein kinase. Phosphorylation sites and effects of phosphorylation. *The Journal of biological chemistry*, *262*(20), 9569–9573.

Jena B.P. (2020) Myosin: Cellular Molecular Motor. In: Cellular Nanomachines. Springer, Cham. https://doi.org/10.1007/978-3-030-44496-9_7

Kasza, K. E., Broedersz, C. P., Koenderink, G. H., Lin, Y. C., Messner, W., Millman, E. A., Nakamura, F., Stossel, T. P., Mackintosh, F. C., & Weitz, D. A. (2010). Actin filament length tunes elasticity of flexibly cross-linked actin networks. *Biophysical journal*, *99*(4), 1091–1100. https://doi.org/10.1016/j.bpj.2010.06.025

Kassianidou, E., Hughes, J. H., & Kumar, S. (2017). Activation of ROCK and MLCK tunes regional stress fiber formation and mechanics via preferential myosin light chain phosphorylation. *Molecular biology of the cell*, *28*(26), 3832–3843. https://doi.org/10.1091/mbc.E17-06-0401

Kassianidou, E., & Kumar, S. (2015). A biomechanical perspective on stress fiber structure and function. *Biochimica et biophysica acta*, *1853*(11 Pt B), 3065–3074. https://doi.org/10.1016/j.bbamcr.2015.04.006

Kassianidou, E., Brand, C. A., Schwarz, U. S., & Kumar, S. (2017). Geometry and network connectivity govern the mechanics of stress fibers. *Proceedings of the National Academy of Sciences of the United States of America*, *114*(10), 2622–2627. https://doi.org/10.1073/pnas.1606649114

Katoh, K., Kano, Y., & Noda, Y. (2011). Rho-associated kinase-dependent contraction of stress fibres and the organization of focal adhesions. *Journal of the Royal Society, Interface*, *8*(56), 305–311. https://doi.org/10.1098/rsif.2010.0419

Katoh K. (2017). Activation of Rho-kinase and focal adhesion kinase regulates the organization of stress fibers and focal adhesions in the central part of fibroblasts. *PeerJ*, *5*, e4063. https://doi.org/10.7717/peerj.4063

Kimura, K., Ito, M., Amano, M., Chihara, K., Fukata, Y., Nakafuku, M., Yamamori, B., Feng, J., Nakano, T., Okawa, K., Iwamatsu, A., & Kaibuchi, K. (1996). Regulation of myosin phosphatase by Rho and Rho-associated kinase (Rho-kinase). *Science (New York, N.Y.)*, *273*(5272), 245–248. https://doi.org/10.1126/science.273.5272.245

Klimovich, A., Wittlieb, J., & Bosch, T. (2019). Transgenesis in *Hydra* to characterize gene function and visualize cell behavior. *Nature protocols*, *14*(7), 2069–2090. https://doi.org/10.1038/s41596-019-0173-3

Komatsu, S., & Ikebe, M. (2007). The phosphorylation of myosin II at the Ser1 and Ser2 is critical for normal platelet-derived growth factor induced reorganization of myosin filaments. *Molecular biology of the cell*, *18*(12), 5081–5090. https://doi.org/10.1091/mbc.e06-12-1076

Kovács, M., Tóth, J., Hetényi, C., Málnási-Csizmadia, A., & Sellers, J. R. (2004). Mechanism of blebbistatin inhibition of myosin II. *The Journal of biological chemistry*, *279*(34), 35557–35563. https://doi.org/10.1074/jbc.M405319200

Kroening, S., Stix, J., Keller, C., Streiff, C., & Goppelt-Struebe, M. (2010). Matrix-independent stimulation of human tubular epithelial cell migration by Rho kinase inhibitors. *Journal of cellular physiology*, *223*(3), 703–712. https://doi.org/10.1002/jcp.22079

Kuznetsov, S., Lyanguzowa, M., & Bosch, T. C. (2001). Role of epithelial cells and programmed cell death in *Hydra* spermatogenesis. *Zoology (Jena, Germany)*, *104*(1), 25–31. https://doi.org/10.1078/0944-2006-00005

Lange, E., Bertrand, S., Holz, O., Rebscher, N., & Hassel, M. (2014). Dynamic expression of a *Hydra* FGF at boundaries and termini. *Development genes and evolution*, *224*(4-6), 235–244. https://doi.org/10.1007/s00427-014-0480-1

Leclère, L., & Röttinger, E. (2017). Diversity of Cnidarian Muscles: Function, Anatomy, Development and Regeneration. *Frontiers in cell and developmental biology*, *4*, 157. https://doi.org/10.3389/fcell.2016.00157

Lecuit, T., & Le Goff, L. (2007). Orchestrating size and shape during morphogenesis. *Nature*, *450*(7167), 189–192. https://doi.org/10.1038/nature06304

Leckband, D. E., & de Rooij, J. (2014). Cadherin adhesion and mechanotransduction. *Annual review of cell and developmental biology*, *30*, 291–315. https://doi.org/10.1146/annurev-cellbio-100913-013212

Lee, S., & Kumar, S. (2016). Actomyosin stress fiber mechanosensing in 2D and 3D. *F1000Research*, *5*, F1000 Faculty Rev-2261. https://doi.org/10.12688/f1000research.8800.1

Levayer, R., & Lecuit, T. (2012). Biomechanical regulation of contractility: spatial control and dynamics. *Trends in cell biology*, *22*(2), 61–81. https://doi.org/10.1016/j.tcb.2011.10.001

Liao, B. K., & Oates, A. C. (2017). Delta-Notch signaling in segmentation. *Arthropod structure & development*, *46*(3), 429–447. https://doi.org/10.1016/j.asd.2016.11.007

Lv, Z., & Großhans, J. (2016). A Radial Actin Network in Apical Constriction. *Developmental cell*, *39*(3), 280–282. https://doi.org/10.1016/j.devcel.2016.10.017

Machesky, L. M., Atkinson, S. J., Ampe, C., Vandekerckhove, J., & Pollard, T. D. (1994). Purification of a cortical complex containing two unconventional actins from Acanthamoeba by affinity chromatography on profilin-agarose. *The Journal of cell biology*, *127*(1), 107–115. https://doi.org/10.1083/jcb.127.1.107

Martínez, D. E., & Bridge, D. (2012). *Hydra*, the everlasting embryo, confronts aging. *The International journal of developmental biology*, *56*(6-8), 479–487. https://doi.org/10.1387/ijdb.113461dm

Martin, V. J., Littlefield, C. L., Archer, W. E., & Bode, H. R. (1997). Embryogenesis in *Hydra*. *The Biological bulletin*, *192*(3), 345–363. https://doi.org/10.2307/1542745

Martin, A. C., & Goldstein, B. (2014). Apical constriction: themes and variations on a cellular mechanism driving morphogenesis. *Development (Cambridge, England)*, *141*(10), 1987–1998. https://doi.org/10.1242/dev.102228

Martin, A. C., Kaschube, M., & Wieschaus, E. F. (2009). Pulsed contractions of an actin-myosin network drive apical constriction. *Nature*, *457*(7228), 495–499. https://doi.org/10.1038/nature07522

Martin S. G. (2016). Role and organization of the actin cytoskeleton during cell-cell fusion. *Seminars in cell & developmental biology*, *60*, 121–126. https://doi.org/10.1016/j.semcdb.2016.07.025

Menke, A., & Giehl, K. (2012). Regulation of adherens junctions by Rho GTPases and p120-catenin. *Archives of biochemistry and biophysics*, *524*(1), 48–55. https://doi.org/10.1016/j.abb.2012.04.019

Meyer, R. K., & Aebi, U. (1990). Bundling of actin filaments by alpha-actinin depends on its molecular length. *The Journal of cell biology*, *110*(6), 2013–2024. https://doi.org/10.1083/jcb.110.6.2013

Mohammadi, M., McMahon, G., Sun, L., Tang, C., Hirth, P., Yeh, B. K., Hubbard, S. R., & Schlessinger, J. (1997). Structures of the tyrosine kinase domain of fibroblast growth factor receptor in complex with inhibitors. *Science (New York, N.Y.)*, *276*(5314), 955–960. https://doi.org/10.1126/science.276.5314.955

Münder, S., Käsbauer, T., Prexl, A., Aufschnaiter, R., Zhang, X., Towb, P., & Böttger, A. (2010). Notch signaling defines critical boundary during budding in *Hydra*. *Developmental biology*, *344*(1), 331–345. https://doi.org/10.1016/j.ydbio.2010.05.517

Newell-Litwa, K. A., Horwitz, R., & Lamers, M. L. (2015). Non-muscle myosin II in disease: mechanisms and therapeutic opportunities. *Disease models & mechanisms*, *8*(12), 1495–1515. https://doi.org/10.1242/dmm.022103

Nishikawa, M., Sellers, J. R., Adelstein, R. S., & Hidaka, H. (1984). Protein kinase C modulates in vitro phosphorylation of the smooth muscle heavy meromyosin by myosin light chain kinase. *The Journal of biological chemistry*, *259*(14), 8808–8814.

Ong, K., Collier, C., & DiNardo, S. (2019). Multiple feedback mechanisms fine-tune Rho signaling to regulate morphogenetic outcomes. *Journal of cell science*, *132*(8), jcs224378. https://doi.org/10.1242/jcs.224378

Ornitz, D. M., & Itoh, N. (2015). The fibroblast growth factor signaling pathway. *Wiley Interdisciplinary Reviews: Developmental Biology*, *4*(3), 215–266. https://doi.org/10.1002/wdev.176

Ornitz, D. M., & Itoh, N. (2001). Fibroblast growth factors. *Genome biology*, *2*(3), REVIEWS3005. https://doi.org/10.1186/gb-2001-2-3-reviews3005

Otto, J. J., & Campbell, R. D. (1977). Budding in *Hydra* attenuata: bud stages and fate map. *The Journal of experimental zoology*, *200*(3), 417–428. https://doi.org/10.1002/jez.1402000311

Park, I., Han, C., Jin, S., Lee, B., Choi, H., Kwon, J. T., Kim, D., Kim, J., Lifirsu, E., Park, W. J., Park, Z. Y., Kim, D. H., & Cho, C. (2011). Myosin regulatory light chains are required to maintain the stability of myosin II and cellular integrity. *The Biochemical journal*, *434*(1), 171–180. https://doi.org/10.1042/BJ20101473

Perrimon, N., Pitsouli, C., & Shilo, B. Z. (2012). Signaling mechanisms controlling cell fate and embryonic patterning. *Cold Spring Harbor perspectives in biology*, *4*(8), a005975. https://doi.org/10.1101/cshperspect.a005975

Philipp, I., Aufschnaiter, R., Ozbek, S., Pontasch, S., Jenewein, M., Watanabe, H., Rentzsch, F., Holstein, T. W., & Hobmayer, B. (2009). Wnt/beta-catenin and noncanonical Wnt signaling interact in tissue evagination in the simple eumetazoan *Hydra*. *Proceedings of the National Academy of Sciences of the United States of America*, *106*(11), 4290–4295. https://doi.org/10.1073/pnas.0812847106

Pearl, E. J., Li, J., & Green, J. B. (2017). Cellular systems for epithelial invagination. *Philosophical transactions of the Royal Society of London. Series B, Biological sciences*, *372*(1720), 20150526. https://doi.org/10.1098/rstb.2015.0526

Pellegrin, S., & Mellor, H. (2007). Actin stress fibres. *Journal of cell science*, *120*(Pt 20), 3491–3499. https://doi.org/10.1242/jcs.018473

Pollard T. D. (2016). Actin and Actin-Binding Proteins. *Cold Spring Harbor perspectives in biology*, *8*(8), a018226. https://doi.org/10.1101/cshperspect.a018226

Prager-Khoutorsky, M., Lichtenstein, A., Krishnan, R., Rajendran, K., Mayo, A., Kam, Z., Geiger, B., & Bershadsky, A. D. (2011). Fibroblast polarization is a matrix-rigidity-dependent process controlled by focal adhesion mechanosensing. *Nature cell biology*, *13*(12), 1457–1465. https://doi.org/10.1038/ncb2370

Prexl, A., Münder, S., Loy, B., Kremmer, E., Tischer, S., & Böttger, A. (2011). The putative Notch ligand HyJagged is a transmembrane protein present in all cell types of adult *Hydra* and upregulated at the boundary between bud and parent. *BMC cell biology*, *12*, 38. https://doi.org/10.1186/1471-2121-12-38

Pukhlyakova, E., Aman, A. J., Elsayad, K., & Technau, U. (2018). β-Catenin-dependent mechanotransduction dates back to the common ancestor of Cnidaria and Bilateria. *Proceedings of the National Academy of Sciences of the United States of America*, *115*(24), 6231–6236. https://doi.org/10.1073/pnas.1713682115

Pulido Companys, P., Norris, A., & Bischoff, M. (2020). Coordination of cytoskeletal dynamics and cell behaviour during *Drosophila* abdominal morphogenesis. *Journal of cell science*, *133*(6), jcs235325. https://doi.org/10.1242/jcs.235325

Rauzi, M., Lenne, P. F., & Lecuit, T. (2010). Planar polarized actomyosin contractile flows control epithelial junction remodelling. *Nature*, *468*(7327), 1110–1114. https://doi.org/10.1038/nature09566

Ray, R. M., Vaidya, R. J., & Johnson, L. R. (2007). MEK/ERK regulates adherens junctions and migration through Rac1. *Cell motility and the cytoskeleton*, *64*(3), 143–156. https://doi.org/10.1002/cm.20172

Rebscher, N., Deichmann, C., Sudhop, S., Fritzenwanker, J. H., Green, S., & Hassel, M. (2009). Conserved intron positions in FGFR genes reflect the modular structure of FGFR and reveal stepwise addition of domains to an already complex ancestral FGFR. *Development genes and evolution*, *219*(9-10), 455–468. https://doi.org/10.1007/s00427-009-0309-5

Reddy, P. C., Gungi, A., & Unni, M. (2019). Cellular and Molecular Mechanisms of *Hydra* Regeneration. *Results and problems in cell differentiation*, *68*, 259–290. https://doi.org/10.1007/978-3-030-23459-1_12

Reichart, L (2020). Functional analysis of siRNA mediated knockdowns of fibroblast growth factors in *Hydra* vulgaris https://doi.org/10.17192/z2021.0051

Ren, X. D., Kiosses, W. B., Sieg, D. J., Otey, C. A., Schlaepfer, D. D., & Schwartz, M. A. (2000). Focal adhesion kinase suppresses Rho activity to promote focal adhesion turnover. *Journal of cell science*, *113 (Pt 20)*, 3673–3678.

Rentzsch, F., Hobmayer, B., & Holstein, T. W. (2005). Glycogen synthase kinase 3 has a proapoptotic function in *Hydra* gametogenesis. *Developmental biology*, *278*(1), 1–12. https://doi.org/10.1016/j.ydbio.2004.10.007

Richards, T. A., & Cavalier-Smith, T. (2005). Myosin domain evolution and the primary divergence of eukaryotes. *Nature*, *436*(7054), 1113–1118. https://doi.org/10.1038/nature03949

Riento, K., & Ridley, A. J. (2003). Rocks: multifunctional kinases in cell behaviour. *Nature reviews. Molecular cell biology*, *4*(6), 446–456. https://doi.org/10.1038/nrm1128

Roh-Johnson, M., Shemer, G., Higgins, C. D., McClellan, J. H., Werts, A. D., Tulu, U. S., Gao, L., Betzig, E., Kiehart, D. P., & Goldstein, B. (2012). Triggering a cell shape change by exploiting preexisting actomyosin contractions. *Science (New York, N.Y.)*, *335*(6073), 1232–1235. https://doi.org/10.1126/science.1217869

Rothenberg, K. E., & Fernandez-Gonzalez, R. (2019). Forceful closure: cytoskeletal networks in embryonic wound repair. *Molecular biology of the cell*, *30*(12), 1353–1358. https://doi.org/10.1091/mbc.E18-04-0248

Rudolf, A., Hübinger, C., Hüsken, K., Vogt, A., Rebscher, N., Onel, S. F., Renkawitz-Pohl, R., & Hassel, M. (2013). The *Hydra* FGFR, Kringelchen, partially replaces the Drosophila Heartless FGFR. *Development genes and evolution*, *223*(3), 159–169. https://doi.org/10.1007/s00427-012-0424-6

Salbreux, G., Charras, G., & Paluch, E. (2012). Actin cortex mechanics and cellular morphogenesis. *Trends in cell biology*, *22*(10), 536–545. https://doi.org/10.1016/j.tcb.2012.07.001

Sarras M. P., Jr (2012). Components, structure, biogenesis and function of the *Hydra* extracellular matrix in regeneration, pattern formation and cell differentiation. *The International journal of developmental biology*, *56*(6-8), 567–576. https://doi.org/10.1387/ijdb.113445ms

Schmoller, K. M., Lieleg, O., & Bausch, A. R. (2008). Cross-linking molecules modify composite actin networks independently. *Physical review letters*, *101*(11), 118102. https://doi.org/10.1103/PhysRevLett.101.118102

Schwayer, C., Sikora, M., Slováková, J., Kardos, R., & Heisenberg, C. P. (2016). Actin Rings of Power. *Developmental cell*, *37*(6), 493–506. https://doi.org/10.1016/j.devcel.2016.05.024

Sekine T, Yamaguchi M (1963). Effect of ATP on the binding of N-ethylmaleimide to SH groups in the active site of myosin ATPase. *Journal of biochemistry* 54, 196–198.

Sellers J. R. (1991). Regulation of cytoplasmic and smooth muscle myosin. *Current opinion in cell biology*, *3*(1), 98–104. https://doi.org/10.1016/0955-0674(91)90171-t

Seybold, A., Salvenmoser, W., & Hobmayer, B. (2016). Sequential development of apical-basal and planar polarities in aggregating epitheliomuscular cells of *Hydra*. *Developmental biology*, *412*(1), 148–159. https://doi.org/10.1016/j.ydbio.2016.02.022

Shang, X., Marchioni, F., Sipes, N., Evelyn, C. R., Jerabek-Willemsen, M., Duhr, S., Seibel, W., Wortman, M., & Zheng, Y. (2012). Rational design of small molecule inhibitors targeting RhoA subfamily Rho GTPases. *Chemistry & biology*, *19*(6), 699–710. https://doi.org/10.1016/j.chembiol.2012.05.009

Shimizu, H., Aufschnaiter, R., Li, L., Sarras, M. P., Jr, Borza, D. B., Abrahamson, D. R., Sado, Y., & Zhang, X. (2008). The extracellular matrix of *Hydra* is a porous sheet and contains type IV collagen. *Zoology (Jena, Germany)*, *111*(5), 410–418. https://doi.org/10.1016/j.zool.2007.11.004

Soiné, J. R., Brand, C. A., Stricker, J., Oakes, P. W., Gardel, M. L., & Schwarz, U. S. (2015). Model-based traction force microscopy reveals differential tension in cellular actin bundles. *PLoS computational biology*, *11*(3), e1004076. https://doi.org/10.1371/journal.pcbi.1004076

Steele R. E. (2002). Developmental signaling in *Hydra*: what does it take to build a "simple" animal?. *Developmental biology*, *248*(2), 199–219. https://doi.org/10.1006/dbio.2002.0744

Steinmetz, P. R., Kraus, J. E., Larroux, C., Hammel, J. U., Amon-Hassenzahl, A., Houliston, E., Wörheide, G., Nickel, M., Degnan, B. M., & Technau, U. (2012). Independent evolution of striated muscles in cnidarians and bilaterians. *Nature*, *487*(7406), 231–234. https://doi.org/10.1038/nature11180

Sudhop, S., Coulier, F., Bieller, A., Vogt, A., Hotz, T., & Hassel, M. (2004). Signaling by the FGFR-like tyrosine kinase, Kringelchen, is essential for bud detachment in *Hydra* vulgaris. *Development (Cambridge, England)*, *131*(16), 4001–4011. https://doi.org/10.1242/dev.01267

Suryawanshi, A., Schaefer, K., Holz, O., Apel, D., Lange, E., Hayward, D. C., Miller, D. J., & Hassel, M. (2020). What lies beneath: *Hydra* provides cnidarian perspectives into the evolution of FGFR docking proteins. *Development genes and evolution*, *230*(3), 227–238. https://doi.org/10.1007/s00427-020-00659-4

Sutherland, A., & Lesko, A. (2020). Pulsed actomyosin contractions in morphogenesis. *F1000Research*, *9*, F1000 Faculty Rev-142. https://doi.org/10.12688/f1000research.20874.1

Svitkina T. (2018). The Actin Cytoskeleton and Actin-Based Motility. *Cold Spring Harbor perspectives in biology*, *10*(1), a018267. https://doi.org/10.1101/cshperspect.a018267

Syamaladevi, D. P., Spudich, J. A., & Sowdhamini, R. (2012). Structural and functional insights on the Myosin superfamily. *Bioinformatics and biology insights*, *6*, 11–21. https://doi.org/10.4137/BBI.S8451

Takahashi, T., Muneoka, Y., Lohmann, J., Lopez de Haro, M. S., Solleder, G., Bosch, T. C., David, C. N., Bode, H. R., Koizumi, O., Shimizu, H., Hatta, M., Fujisawa, T., & Sugiyama, T. (1997). Systematic isolation of peptide signal molecules regulating development in *Hydra*: LWamide and PW families. *Proceedings of the National Academy of Sciences of the United States of America*, *94*(4), 1241–1246. https://doi.org/10.1073/pnas.94.4.1241

Tamada, M., Perez, T. D., Nelson, W. J., & Sheetz, M. P. (2007). Two distinct modes of myosin assembly and dynamics during epithelial wound closure. *The Journal of cell biology*, *176*(1), 27–33. https://doi.org/10.1083/jcb.200609116

Tambe, D. T., Hardin, C. C., Angelini, T. E., Rajendran, K., Park, C. Y., Serra-Picamal, X., Zhou, E. H., Zaman, M. H., Butler, J. P., Weitz, D. A., Fredberg, J. J., & Trepat, X. (2011). Collective cell guidance by cooperative intercellular forces. *Nature materials*, *10*(6), 469–475. https://doi.org/10.1038/nmat3025

Tardent, P (1974) Gametogenesis in the Genus *Hydra*, *American Zoologist*, Volume 14, Issue 2, Pages 447–456, https://doi.org/10.1093/icb/14.2.447

Technau, U., & Steele, R. E. (2011). Evolutionary crossroads in developmental biology: Cnidaria. *Development (Cambridge, England)*, *138*(8), 1447–1458. https://doi.org/10.1242/dev.048959

Thisse, B., & Thisse, C. (2005). Functions and regulations of fibroblast growth factor signaling during embryonic development. *Developmental biology*, *287*(2), 390–402. https://doi.org/10.1016/j.ydbio.2005.09.011

Tischer, S., Reineck, M., Söding, J., Münder, S., & Böttger, A. (2013). Eph receptors and ephrin class B ligands are expressed at tissue boundaries in *Hydra* vulgaris. *The International journal of developmental biology*, *57*(9-10), 759–765. https://doi.org/10.1387/ijdb.130158ab

Tojkander, S., Gateva, G., & Lappalainen, P. (2012). Actin stress fibers--assembly, dynamics and biological roles. *Journal of cell science*, *125*(Pt 8), 1855–1864. https://doi.org/10.1242/jcs.098087

Vázquez-Ulloa, E., Lizano, M., Sjöqvist, M., Olmedo-Nieva, L., & Contreras-Paredes, A. (2018). Deregulation of the Notch pathway as a common road in viral carcinogenesis. *Reviews in medical virology*, *28*(5), e1988. https://doi.org/10.1002/rmv.1988

Vicente-Manzanares, M., Ma, X., Adelstein, R. S., & Horwitz, A. R. (2009). Non-muscle myosin II takes centre stage in cell adhesion and migration. *Nature reviews. Molecular cell biology*, *10*(11), 778–790. https://doi.org/10.1038/nrm2786

Wachsstock, D. H., Schwartz, W. H., & Pollard, T. D. (1993). Affinity of alpha-actinin for actin determines the structure and mechanical properties of actin filament gels. *Biophysical journal*, *65*(1), 205–214. https://doi.org/10.1016/S0006-3495(93)81059-2

Wachsstock, D. H., Schwarz, W. H., & Pollard, T. D. (1994). Cross-linker dynamics determine the mechanical properties of actin gels. *Biophysical journal*, *66*(3 Pt 1), 801–809. https://doi.org/10.1016/s0006-3495(94)80856-2

Wittlieb, J., Khalturin, K., Lohmann, J. U., Anton-Erxleben, F., & Bosch, T. C. (2006). Transgenic *Hydra* allow in vivo tracking of individual stem cells during morphogenesis. *Proceedings of the National Academy of Sciences of the United States of America*, *103*(16), 6208–6211. https://doi.org/10.1073/pnas.0510163103

Wang, A. T., Deng, L., & Liu, H. T. (2012). A new species of *Hydra* (Cnidaria: Hydrozoa: Hydridae) and molecular phylogenetic analysis of six congeners from China. *Zoological science*, *29*(12), 856–862. https://doi.org/10.2108/zsj.29.856

Watanabe, T., Hosoya, H., & Yonemura, S. (2007). Regulation of myosin II dynamics by phosphorylation and dephosphorylation of its light chain in epithelial cells. *Molecular biology of the cell*, *18*(2), 605–616. https://doi.org/10.1091/mbc.e06-07-0590

Welch, M. D., DePace, A. H., Verma, S., Iwamatsu, A., & Mitchison, T. J. (1997). The human Arp2/3 complex is composed of evolutionarily conserved subunits and is localized to cellular regions of dynamic actin filament assembly. *The Journal of cell biology*, *138*(2), 375–384. https://doi.org/10.1083/jcb.138.2.375

Wendt, T., Taylor, D., Trybus, K. M., & Taylor, K. (2001). Three-dimensional image reconstruction of dephosphorylated smooth muscle heavy meromyosin reveals asymmetry in the interaction between myosin heads and placement of subfragment 2. *Proceedings of the National Academy of Sciences of the United States of America*, *98*(8), 4361–4366. https://doi.org/10.1073/pnas.071051098

Wenger, Y., & Galliot, B. (2013). RNAseq versus genome-predicted transcriptomes: a large population of novel transcripts identified in an Illumina-454 *Hydra* transcriptome. *BMC genomics*, *14*, 204. https://doi.org/10.1186/1471-2164-14-204

Wheeler, A. P., & Ridley, A. J. (2004). Why three Rho proteins? RhoA, RhoB, RhoC, and cell motility. *Experimental cell research*, *301*(1), 43–49. https://doi.org/10.1016/j.yexcr.2004.08.012

Wilkinson D. G. (2014). Regulation of cell differentiation by Eph receptor and ephrin signaling. *Cell adhesion & migration*, *8*(4), 339–348. https://doi.org/10.4161/19336918.2014.970007

Xie, Y., Su, N., Yang, J., Tan, Q., Huang, S., Jin, M., Ni, Z., Zhang, B., Zhang, D., Luo, F., Chen, H., Sun, X., Feng, J. Q., Qi, H., & Chen, L. (2020). FGF/FGFR signaling in health and disease. *Signal transduction and targeted therapy*, *5*(1), 181. https://doi.org/10.1038/s41392-020-00222-7

Yang, C., Czech, L., Gerboth, S., Kojima, S., Scita, G., & Svitkina, T. (2007). Novel roles of formin mDia2 in lamellipodia and filopodia formation in motile cells. *PLoS biology*, *5*(11), e317. https://doi.org/10.1371/journal.pbio.0050317

Yang, Y., & Levine, H., (2018). Role of the supracellular actomyosin cable during epithelial wound healing. *Soft matter*, *14*(23), 4866–4873. https://doi.org/10.1039/c7sm02521a

Zhang, W., Huang, Y., Wu, Y., & Gunst, S. J. (2015). A novel role for RhoA GTPase in the regulation of airway smooth muscle contraction. *Canadian journal of physiology and pharmacology*, *93*(2), 129–136. https://doi.org/10.1139/cjpp-2014-0388

8 Supplementary Information

8.1 Weitere Publikationen

Suryawanshi et al., 2020

What lies beneath: *Hydra* provides cnidarian perspectives into the evolution of FGFR docking proteins

Development Genes and Evolution 230(3):227-238, 2020

DOI: 10.1007/s00427-020-00659-4.

Development Genes and Evolution
https://doi.org/10.1007/s00427-020-00659-4

ORIGINAL ARTICLE

What lies beneath: *Hydra* provides cnidarian perspectives into the evolution of FGFR docking proteins

Ashwini Suryawanshi[1] · Karolin Schaefer[1] · Oliver Holz[1] · David Apel[1,2] · Ellen Lange[1] · David C. Hayward[3] · David J. Miller[4] · Monika Hassel[1]

Received: 24 October 2019 / Accepted: 27 February 2020

Abstract

Across the Bilateria, FGF/FGFR signaling is critical for normal development, and in both *Drosophila* and vertebrates, docking proteins are required to connect activated FGFRs with downstream pathways. While vertebrates use Frs2 to dock FGFR to the RAS/MAPK or PI3K pathways, the unrelated protein, downstream of FGFR (Dof/stumps/heartbroken), fulfills the corresponding function in *Drosophila*. To better understand the evolution of the signaling pathway downstream of FGFR, the available sequence databases were screened to identify Frs2, Dof, and other key pathway components in phyla that diverged early in animal evolution. While Frs2 homologues were detected only in members of the Bilateria, canonical Dof sequences (containing Dof, ankyrin, and SH2/SH3 domains) were present in cnidarians as well as bilaterians (but not in other animals or holozoans), correlating with the appearance of FGFR. Although these data suggested that Dof coupling might be ancestral, gene expression analysis in the cnidarian *Hydra* revealed that *Dof* is not upregulated in the zone of strong *FGFRa* and *FGFRb* expression at the bud base, where FGFR signaling controls detachment. In contrast, transcripts encoding other, known elements of FGFR signaling in Bilateria, namely the FGFR adaptors Grb2 and Crkl, which are acting downstream of Dof (and Frs2), as well as the guanyl nucleotide exchange factor Sos, and the tyrosine phosphatase Csw/Shp2, were strongly upregulated at the bud base. Our expression analysis, thus, identified transcriptional upregulation of known elements of FGFR signaling at the *Hydra* bud base indicating a highly conserved toolkit. Lack of transcriptional *Dof* upregulation raises the interesting question, whether *Hydra* FGFR signaling requires either of the docking proteins known from Bilateria.

Keywords Receptor tyrosine kinase · Adapter protein · Grb2 · Crkl · Dof

Communicated by Mark Q. Martindale

Electronic supplementary material The online version of this article (https://doi.org/10.1007/s00427-020-00659-4) contains supplementary material, which is available to authorized users.

✉ Monika Hassel
hassel@staff.uni-marburg.de

Ashwini Suryawanshi
ashwiniacs@gmail.com

Karolin Schaefer
karolin.schaefer@biologie.uni-marburg.de

Oliver Holz
oliver.holz@biologie.uni-marburg.de

David Apel
David.apel@biologie.uni-marburg.de

Ellen Lange
ellen.lange.bio@web.de

David C. Hayward
david.hayward@anu.edu.au

David J. Miller
david.miller@jcu.edu.au

[1] Morphology and Evolution of Invertebrates, Philipps University, FB17, Karl von Frisch Str. 8, 35032 Marburg, Germany

[2] DFG Research Training Group, Membrane Plasticity in Tissue Development and Remodeling, GRK 2213, Philipps-Universität Marburg, Marburg, Germany

[3] Research School of Biology, Australian National University, Canberra, ACT 0200, Australia

[4] ARC Centre of Excellence for Coral Reef Studies, James Cook University, Townsville, Queensland 4811, Australia

Published online: 20 March 2020

Introduction

Across the Bilateria, fibroblast growth factor receptors (FGFR) and their ligands control embryonic as well as adult morphogenesis. Although the receptor tyrosine kinase (RTK) superfamily has earlier origins, the FGF/FGFR signaling system is thought to have evolved in Ureumetazoa, the last common ancestor of Cnidaria and Bilateria (Babonis and Martindale 2017; Bertrand et al. 2014; Lange et al. 2014; Oulion et al. 2012; Rebscher et al. 2009). Little is known about the evolution of signaling elements downstream of this specific family of receptor tyrosine kinases. In both the fly and vertebrates, docking proteins are essential to specifically transduce the signal of an activated (trans-phosphorylated) FGFR dimer into the cell (Brummer et al. 2010; Lemmon and Schlessinger 2010).

One specific issue of interest is the nature of the ancestral mechanism by which the activated FGFR is coupled to downstream signaling pathways, as vertebrates, *Drosophila* and the nematode *C. elegans* use completely unrelated proteins to fulfill this task. In vertebrates, Frs2 (FGF receptor **s**ubstrate **2**), a member of the membrane-linked protein (MLP) family, connects FGFR to the PI3 kinase and RAS/ERK1/2 signaling pathways (Gotoh 2008). In *Drosophila,* Dof (downstream **o**f FGFR, also known as stumps or heartbroken), is essential for FGFR signaling and connects the heartless and breathless FGFRs to the RAS/MAPK or PI3 kinase signaling pathways (Csiszar et al. 2010; Michelson et al. 1998; Muha and Muller 2013; Vincent et al. 1998). In both cases, the activated FGFR dimer phosphorylates conserved tyrosines in the docking proteins and generates secondary binding sites for the intracellular adapters Grb2 (Kouhara et al. 1997), Crk and Crkl (Birge et al. 2009) as well as the tyrosine phosphatase Shp2/Csw (syn. Corkscrew, Csw, in *Drosophila*) (Gotoh 2008; Hadari et al. 1998; Lax et al. 2002) and the dual specificity guanine nucleotide exchange factor (GEF) Sos, that regulates both Ras and Rac family GTPases (Innocenti et al. 2002). In the nematode *C. elegans*, Grb2 is the only known FGFR docking protein: Frs2 has no FGFR docking function and the genome does not encode a Dof homologue (Lo et al. 2010).

Grb2 is an interesting protein, because it may act as an adapter as well as a docking protein downstream of vertebrate and invertebrate FGFRs. It has an intrinsic FGFR binding activity in both the phosphorylated and unphosphorylated forms and exerts multiple functions on FGFR. In vertebrates, unphosphorylated Grb2 is associated constitutively to the C-terminal domain of inactive FGFR2 dimers, preventing unwanted activation (Belov and Mohammadi 2012; Lin et al. 2012). Upon receptor activation, Grb2 dissociates from such FGFR pairs and only then serves as adaptor between Frs2 and Sos or Shp2.

The FGFR docking proteins Frs2 or Dof, the adapters Grb2, Crk, and Crkl, the GEF Sos and Shp2 thus constitute, in various combinations, an essential toolkit in vertebrate, fly, and worm to control FGF-induced signal transduction in, e.g., cell migration or neuronal differentiation (Bottcher and Niehrs 2005; Muha and Muller 2013; Zhou et al. 2015).

Since Dof and Frs2 dock FGFR in a mutually exclusive manner in fly and vertebrate respectively, and neither are required for FGFR signaling in the nematode, the phylogenetic distributions of docking and downstream signaling components were surveyed, focusing particularly on FGFR docking proteins. Included in this survey were representatives of early diverging animal phyla. Among these, the Cnidaria are of most interest, because FGF signaling is thought to have its origins in the eumetazoan common ancestor (Bertrand et al. 2014), and thus prior to the Cnidaria/Bilateria divergence, which occurred at or near the Ediacaran/Cambrian boundary (Schwaiger et al. 2014).

FGFR signaling has been shown to be essential for development in two evolutionarily distant cnidarians. In *Nematostella vectensis* (Anthozoa) larvae, FGFR/RAS/MAPK signaling is required for the development of the apical organ, a sensory ciliated tuft (Matus et al. 2007; Rentzsch et al. 2008). In the freshwater polyp *Hydra*, FGFR signaling is indispensable for at least two steps of the vegetative budding process. While the FGFR/MEK/dpERK pathway modulates timing of *Hydra* bud detachment (Hasse et al. 2014; Sudhop et al. 2004), an FGFR/Rho/Rock/myosin II pathway controls cell shape changes required for constriction and separation of the tissue bridge connecting parent and bud (Holz et al. 2017).

In the present study, the available sequence databases were scanned for non-bilaterian homologues of Dof/stumps/heartbroken, Frs2, and other key downstream components of the FGFR pathway. Whereas likely Dof orthologues were detected in several cnidarians, canonical Frs2 sequences could not be identified in any non-bilaterians, suggesting that the ancestral (invertebrate) FGFR was Dof-coupled. To test this hypothesis, in situ hybridization was used to investigate the expression pattern of Dof in *Hydra* in relation to those of the FGFRs. Surprisingly, Dof transcripts were not detected in zones of strong FGFR gene expression. In contrast to *Dof*, the transcripts encoding downstream components *Grb2*, *Crkl*, *Sos*, and *Shp2* were strongly and specifically upregulated at the bud base together with both of the *Hydra FGFRs.* Presence of a highly conserved toolkit for FGFR downstream signaling is thus indicated, but whether Dof functions in *Hydra* FGFR signaling needs future investigation.

Materials and methods

Gene prediction

To reveal Frs2 and Dof sequences in *Hydra*, we explored the NCBI (http://www.ncbi.nlm.nih.gov), JGI (http://jgi.doe.

gov/), hydrazome/metazome (http://hydrazome.metazome.net/cgi-bin/gbrowse/hydra), Compagen (http://www.compagen.org) T-CDS: transcript models (contigs) derived from assembled ESTs (Hemmrich and Bosch 2008) and RNASeq project (Wenger and Galliot 2013). Predicted protein sequences were further analyzed for conserved domains using NCBI's conserved domain search tool including CDART (http://www.ncbi.nlm.nih.gov/Structure/cdd/wrpsb.cgi) (Geer et al. 2002; Marchler-Bauer et al. 2015), ExpasyProsite (http://prosite.expasy.org/), Pfam (http://pfam.sanger.ac.uk/), or PhosphoMotif finder (Amanchy et al. 2007). Motif Scan (Pagni et al. 2007) was used to predict domains and identify SH2, SH3-binding site consensus sequences in Dof sequences (http://scansite.mit.edu/cgi-bin/motifscan_seq, 28 July 2016). GPS 5.0 (http://gps.biocuckoo.cn/) was used to identify predicted phosphorylation sites for Crkl. BLAST search revealed homologous or related proteins by sequence similarity (BLAST search parameter: All non-redundant GenBank CDS translations + PDB + SwissProt + PIR + PRF excluding environmental samples from WGS projects). Figures depicting protein domains were established using the IBS illustrator (Liu et al. 2015).

Phylogeny

Predicted *Hydra* protein sequences were aligned with the available protein sequences of the choanoflagellate *Salpingoeca*, the parazoan *Trichoplax*, the ctenophore *Mnemiopsis*, the Cnidaria *Acropora*, and *Nematostella* as well as protein sequences of several bilaterian animals covering protostome and deuterostome phyla as indicated in the figures. Alignments were calculated using ProbCons version 1.12 (Do et al. 2005), clustalX, T-coffee version 8.99 (Notredame et al. 2000), MAFFT L-INS-i version 7.037b (Katoh and Standley 2013), and the COBALT program (Papadopoulos and Agarwala 2007) with default settings. Jalview version 2.8 (Waterhouse et al. 2009) and InterProScan5 was used to visualize and analyze the alignments whereas Genedoc was used to manually edit them. Phylogenetic trees were calculated as indicated in the text using either conserved domains or the whole protein sequences and rooted as specified in the text. Gaps between sequences were deleted. The WAG + G + I model was selected as the best fitting amino acid substitution model according to the Bayesian information criterion in ProtTest version 3.3 (Darriba et al. 2011). Phylogenetic trees were calculated using Mr. Bayes 3.1.2 (Huelsenbeck and Ronquist 2001). Two runs were initiated of four Markov chain Monte Carlo (MCMC) chains of 2×10^7 generations, each from a random starting tree. Sampling made every 1000 generations [additional settings: rates = invgamma, ngammacat = 4, aamodelpr = WAG]. A 25% burn-in was selected and convergence was assessed by standard deviation of split frequencies falling below 0.005. The resultant trees were visualized with Figtree version 1.4.0 (http://tree.bio.ed.ac.uk/software/figtree/).

Hydra culture

Hydra vulgaris AEP strain was cultured in a medium containing (0.29 mM $CaCl_2$, 0.59 mM $MgSO_4$, 0.5 mM $NaHCO_3$, and 0.08 mM K_2CO_3, pH 7.4) at 18 °C. The animals were fed 5 times a week with freshly hatched *Artemia nauplii* to synchronize their growth (Sudhop et al. 2004).

Cloning of sequences

The Quickprep Micro Kit (Amersham) was used to harvest poly(A)$^+$ RNA from the *Hydra vulgaris AEP* strain (*Dof, Frs2-related, Grb2*) or the *Hydra vulgaris Zürich* strain (Sos, Csw). Further poly(A)$^+$ RNA was reverse transcribed using Revert Aid TM Premium First-strand cDNA Synthesis Kit (Fermentas) and diluted 1:100 prior to PCR amplification of the genes of interest. *Dof, Frs2*, *Sos*, *Shp2/Csw*, *Crkl*, *and Grb2* gene sequences were PCR amplified using following the primer pairs:

Dof forward GTTGCAGTTTTTAATTCAAATATACC (111–137)
Dof reverse TTGCAGCTGCTATGTCCATTGG (682–660)
Frs2-related forward ATGGAGGTAATTTTGGAAGG C (1–21 bp)
Frs2-related reverse: GACCTACTACATTCAAATCGA (566–545)
Sos forward GGTTGATCTCCAAATGCACGA (-13–5)
Sos reverse CGACGCTTAGCTAGTGGCTG (560–540)
Shp2/Csw forward CGGCGTTTTTATTGAGCTGC (572–592)
Shp2/Csw reverse CGAACACAGAGAGCTGGCAT (1463–1443)
Grb2 forward CGCAGATCTGAGGCTGAACA (201–221)
Grb2 reverse CGGTATTTTAGGAAGGGGGAGT (1090–1068)
Crkl forward TCGGGTTACTGAGCCAACAC (294–1040)
Crkl reverse CCAGGCGCTACATTAAAGGC (1021–1040)

The full length *Fgfr-b* cDNA was reconstituted by using two sequence fragments encoding the first two Ig-like loops (*fgfr-b*$_{ex}$, 835 bp, and a fragment encoding the tyrosine kinase domain (*fgfr-b*$_{in}$, 516 bp), which had been identified previously in the *Hydra AEP* database (Hemmrich and Bosch 2008; Rudolf et al. 2013). The missing sequence between these two

fragments was isolated from cDNA by PCR using proofreading polymerase (Pfu) and the following primers:

FGFRb forward CGTTTACAGCATGACAAATCC, *FGFRb* reverse CAAATGACCATATATCACTTCGAG. Accession numbers of the two previously existing fragments are HAEP_T-CDS_v02_12177 (Compagen database, encoding Ig-like loops I and II, named here: *FGFRb_ex*) and HAEP_T-CDS_v02_12974 (Compagen database, encodes the tyrosine kinase domain, named here: *FGFRb_in*). Amplified cDNA fragments were AT-cloned (*Dof*, *Frs2-related*, *Sos, Shp2/Csw*, *Grb2*, *Crkl*) into the pGEM T-Easy vector (Promega) or blunt end (*FGFRb*) into the CloneJET vector (ThermoFisher). Clone identity was confirmed by sequencing (SeqLab).

Whole mount in situ hybridization

Full length (*FGFRa*, *Dof, Frs2-related, Sos, Shp2/Csw, Grb2, Crkl*) or partial sequences (*FGFRb*) were used for the synthesis of Dig-labeled RNA sense and antisense probes (ROCHE). *HAEP_Dof* RNA probe (571 bp: nucleotides 1496 to 2067); *HAEP_Frs2-related* RNA probe (561 bp: nucleotides 166 to 727); *Hvz_Sos* RNA probe (889 bp); *Hvz_Shp2/Csw* RNA probe (1,191 bp: nucleotides 471 to 1,662); *Hvz_Grb2* RNA probe (889 bp: nucleotides 674 to 1,563); $FGFRb_{in}$, 516 bp and $FGFRb_{ex}$, 835 bp (two probes were necessary to detect and exclude a cross reaction of the two probes with parts of the *FGFRa* mRNA encoding the highly conserved tyrosine kinase domain). Whole mount in situ hybridization was performed as described previously (Sudhop et al. 2004) with the exception that proteinase K digestion was prolonged for *Hydra vulgaris AEP* from 10 to 15 min. Bud stages were selected according to (Otto and Campbell 1977). The quality of RNA probes was verified by Northern blotting and between 3 and 300 ng of the respective RNA probe were used for WMISH to obtain an optimal signal-to-noise ratio. For each in situ hybridization, at least 5 polyps of a given bud stage were used and the expression pattern is described only if at least 4 of those (80%) show the same pattern in independent experiments. Nonspecific binding patterns of probe and/or antibody which is are unrelated to specific probes are given as examples in Fig. ESM8.

Results

Frs2 and Frs2-related proteins as FGFR adaptors

The FGFR docking proteins of vertebrates, Frs2 homologues, typically, carry an N-terminal myristoylation site (Fig. 1), which ensures their modification by a lipid anchor and constitutive localization to the plasma membrane. A phosphotyrosine-binding (PTB) domain (pfam08416) links Frs2 constitutively to activated vertebrate FGF receptors, and multiple tyrosine phosphorylation sites are essential to dock downstream adaptor proteins like Grb2 or the phosphatase Shp2/Csw via SH2 and SH3 domain binding consensus sequences (Brummer et al. 2010; Gotoh 2009).

Querying the sequence databases with the known Frs2 proteins yielded convincing matches only for deuterostomes, ecdysozoans, and flat worms (Fig. 1). Only in proteins from these groups could the presence of an N-terminal myristoylation sequence (as well as of a PTB domain) be confirmed. In representatives of the Mollusca, Annelida, and Cnidaria, "Frs2-related" proteins were identified (Fig. ESM1A, Fig. ESM1B). Although in these cases a conserved PTB domain sequence was present, a PH (pleckstrin homology) domain replaced the diagnostic N-terminal myristoylation site at the N-terminus. This domain (PH/PTB) combination is characteristic of Dok and IRS proteins, which together with Frs2 form the membrane-linked protein (MLP) superfamily (ESM2A-C). PH domains bind phospholipids and anchor proteins to membranes in an analogous manner to the myristoyl tail (Delahaye et al. 2000; Uhlik et al. 2005). The "Frs2-related" proteins identified here in annelids, mollusk, and cnidarians are clearly members of the MLP superfamily (ESM2), but not of the Frs2 sensu *strictu* clade.

A major challenge in uncovering relationships between the invertebrate/non-metazoan Frs2-related sequences recovered and the true Frs2 proteins of vertebrates and insects was the low sequence similarity, and for many of the former it is difficult to make firm assignments. The choanoflagellate matches, including the *Salpingoeca* sequence XP_004995975, are unconvincing—this latter sequence has a cyclophilin type peptidylproply *cis*-trans isomerase domain as well as PH-like domain. The sponge sequence recovered as XP_003383468.1 is a homologue of proline-rich receptor-like protein kinase, PERK7. It lacks a PH domain, but does have a PTB domain. Although the *Nematostella* sequences XP_001635403.1 and XP_001641972.1 were the best hits in Frs2 BLAST searches, domain searches give stronger hits to the IRS type domain (pfam02174, IRS, PTB domain (IRS-1 type)), and the same is true for the *Acropora* database match. As for *Hydra*, there is, additional to the Frs2-related proteins, an IRS1-like protein annotated (Acc. No. XP_012558666.1), which lacks, however, the IR-binding domain (ESM2A, B). The presence of an N-terminal PH domain in the Frs2-related sequences from Placozoa, cnidarians, annelids, and mollusks rendered them similar to IRS or Dok proteins rather than Frs2. A phylogenetic analysis of Frs2 and Frs2-related protein sequences revealed no convincing relationships (not shown).

In summary, our data imply that true Frs2 proteins are likely to have evolved in Urbilateria and were lost again during the evolution of the lophotrochozoan phyla Annelida and Mollusca.

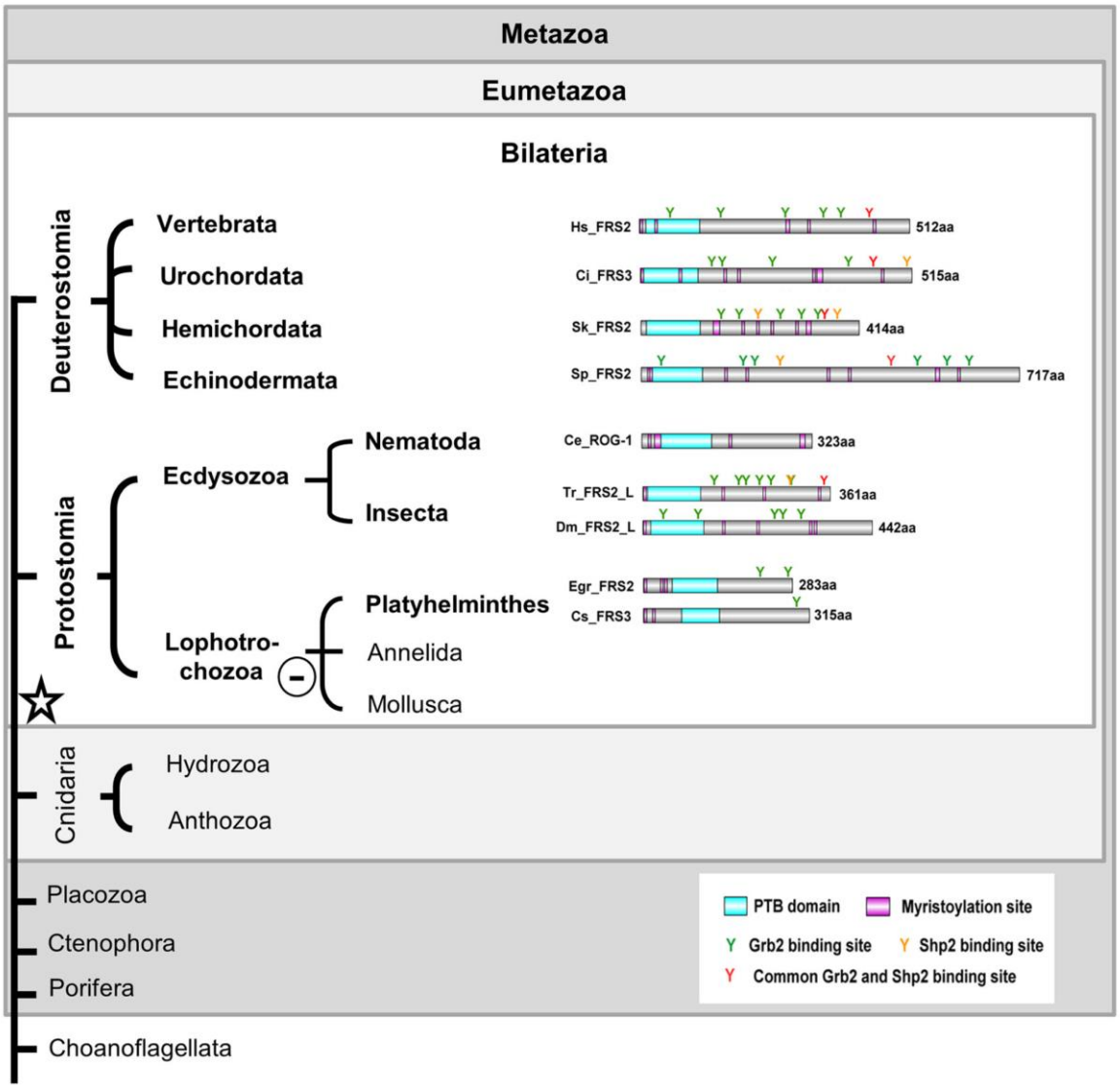

Fig. 1 Schematic summary of structural features of metazoan Frs2 homologues. FRS2 homologues were identified in Bilateria only. Ce_ ROG1, *Caenorhabditis elegans*; Ci_ FRS3, *Ciona intestinalis*; Cs_ FRS3, *Clonorchis sinensis*; Dm_FRS2, *Drosophila melanogaster;* Egr_ FRS2, *Echinococcus granulosus*; Hs_FRS2, *Homo sapiens*; Sk_ FRS2, *Saccoglossus kowalevskii*; Sp_ FRS2, *Strongylocentrotus purpuratus;* Tr_ FRS2, *Tribolium castaneum*

Dof is a candidate FGFR docking protein in Cnidaria

All Dof proteins are characterized by the presence of the DBB (Dof, BCAP, and BANK) domain (pfam14545), which is required for binding to an activated receptor (Fig. 2A). They typically also contain a number of ankyrin repeats (Gotoh 2009; Muha and Muller 2013) which mediate protein–protein interactions in *Drosophila* (Battersby et al. 2003; Vincent et al. 1998; Wilson et al. 2004). Ankyrin repeats have also been maintained in the Dof paralogues BANK and BCAP. More recently annotated proteins were named PI3 kinase adapter proteins (PI3KAP), instead of Dof, due to their similarity to human BCAP, which interacts with PI3 kinase (Lauenstein et al. 2019).

Screening of the available genomic and EST databases with the sequences encoding the DBB domain and ankyrin repeats of fly Dof revealed ESTs encoding full length Dof homologues from *Hydra magnipapillata* and *Hydra vulgaris AEP* (Fig. 2A, Fig. ESM1A, ESM3). Although these differed significantly in size (*H. magnipapillata* Dof is predicted to be 464 amino acid (aa) residues, whereas that from *H. vulgaris AEP* is 598 aa), in terms of domain structure these are both typical Dof proteins. Similar search strategies applied to the data available for anthozoan cnidarians, led to the identification of *Dof* sequences in the corals *Acropora millepora, A. digitifera, Exaiptasia pallida*, and the sea anemone *Nematostella vectensis*. Alignment of these assembled Dof domain sequences with predicted or annotated Dofs from a range of bilaterians (ESM3) implies that these are likely to be

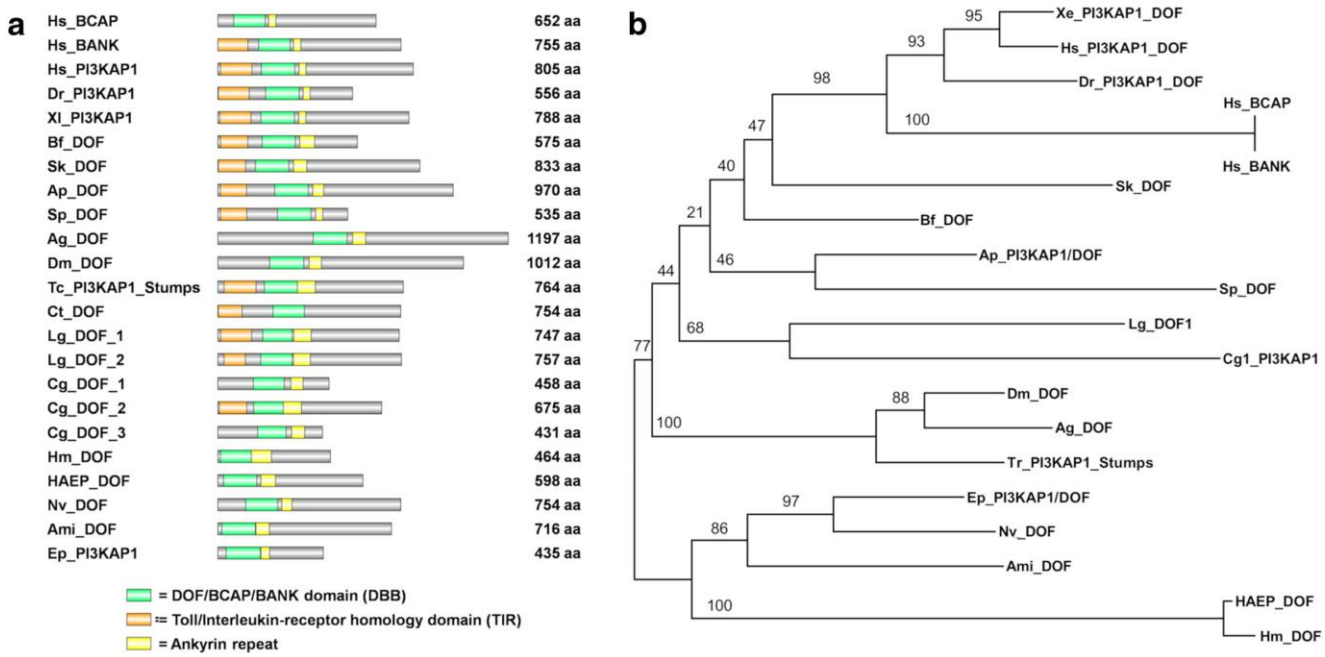

Fig. 2 Structural features and phylogenetic relationship of eumetazoan Dof/PI3KAP proteins. (A) Protein structure of Dof/PI3KAP proteins. (B) Phylogenetic tree of Dof/PI3KAP proteins. Numbers at nodes indicate posterior probability support values. Ami, *Acropora millepora*; *Ag, Anopheles gambiae*; Ap, *Asterina*; Bf, *Branchiostoma floridae*; Cg, *Crassostrea gigas;* Ct, *Capitella teleta;* Dm, *Drosophila melanogaster;* Dr., *Danio rerio*; Ep, *Exaiptasia pallida*; HAEP, *Hydra vulgaris AEP*; Hm, *Hydra magnipapillata*; Hs, *Homo sapiens*; Lg, *Lottia gigantea*; Sk, *Saccoglossus kowalevskii; Sp, Strongylocentrotus purpuratus;* Tc, *Tribolium castaneum*; Xl, *Xenopus laevis*

orthologues. In each case, structure prediction programs (conserved domain search tool, NCBI) identified a DBB domain associated with an ankyrin repeat domain and multiple tyrosine phosphorylation consensus sequences for SH2- and SH3-binding domains of intracellular proteins such as Grb2, Crk, Shp2, PI3K, Src, or RasGAP, respectively (ESM4). Conspicuous was the presence of a structurally defined N-terminal Toll/Interleukin-receptor homology (TIR) domain in most of the bilaterian sequences and its lack in Cnidaria (Fig. 2A).

Although the presence of *Dof* genes in anthozoan and hydrozoan cnidarians as well as in a wide range of bilaterians implies that Dof may have mediated FGFR signaling in Ureumetazoa, homologues of this protein could not be identified in the parasitic flat worms (Platyhelminthes) *Clonorchis sinensis* and *Echinococcus granulosus*, in the nematode *C. elegans* or in the urochordate *Ciona intestinalis*. In some cases, failure to identify Dof homologues may reflect the quality of genome assembly/gene predictions, but in others (e.g., *C. elegans*) gene loss or high levels of sequence divergence are more likely explanations. Despite identification of likely Dof orthologues in several cnidarians, neither Dof nor its vertebrate paralogues BANK or BCAP could be identified in the ctenophore *Mnemiopsis*, the sponge *Amphimedon*, or in the placozoan *Trichoplax*. A phylogenetic analysis confirmed the homology of Dof proteins across the Eumetazoa (Fig. 2B).

Candidate downstream elements of *Hydra FGFR: Grb2, Crkl, Sos*, and *Shp2/Csw*

As outlined above, the FGFR signal is transduced by coupling to several different intracellular signaling pathways in the fly and vertebrates, one of which—the RAS/MAPK pathway leading to Erk1/2 activation—is known to act downstream of FGFRs in both *Nematostella* and *Hydra* (Hasse et al. 2014; Matus et al. 2007; Rentzsch et al. 2008).

To enable further investigation of the signaling system downstream of *Hydra* FGFR, the cDNA sequences of *Grb2, Crkl, Sos*, and *Shp2/Csw* were retrieved from the databases (ESM5). These four proteins clearly all have early origins; the *Hydra* homologues of each closely resemble their bilaterian counterparts in terms of domain structures (ESM6, ESM7). Despite apparent anomalies with respect to some of the *Nematostella* data in GenBank (e.g., the *Nematostella* Grb2 protein entry features an N-terminally truncated SH2 domain (ESM6C)), all four components were also identified in the sponge *Amphimedon* (ESM5). Homologues of Shp2 and Grb2 were also identified in the choanoflagellate *Salpingoeca* and *Monosiga*, so at least these two components pre-date metazoan origins.

In the case of *Drosophila*, database entry NP_651908.1 appears to have been misannotated as a homologue of Crk rather than of Crkl; Crk is a paralogue of Crkl that is only otherwise known in vertebrates (where both proteins are present). To clarify both the identity of NP_651908.1 and

the evolutionary history of these proteins, phylogenetic analyzes of the Crk and Crkl proteins were undertaken. The resulting phylogenetic tree (ESM7B) indicates (i) that *Drosophila* NP_651908.1 falls in a well-supported clade with the nematode and mollusk Crkl homologues, and is well-resolved from true Crk homologues (implying that the database accession information may require modification) and (ii) that Crk likely resulted from a vertebrate-specific duplication of Crkl (ESM7 A, B).

In summary, a suite of proteins that are known to function downstream of FGFR across the Bilateria are also present in non-bilaterian animals and, although FGFR signaling evolved in the ureumetazoan common ancestor, several of the downstream components have earlier origins.

Transcripts of FGFR downstream adaptors and effectors, but not Dof or Frs2-related, are upregulated together with the FGFRs at the bud detachment site

In order to function in FGFR signal transmission, pathway components must co-localize, and may therefore be spatio-temporally co-expressed. *Hydra* FGFRa (Kringelchen) transcripts have previously been shown to be upregulated at the bud base, but the gene is also expressed weakly throughout the body column of *Hydra vulgaris Zurich* and *Hydra vulgaris Ind-Pune* (Sudhop et al. 2004; Turwankar and Ghaskadbi 2019). FGFR signaling is indispensable for bud detachment (Hasse et al. 2014; Holz et al. 2017), and therefore, the expression domains of the *Hydra Dof*, *Frs2-related, Grb2, Crkl, Sos*, and *Shp2/Csw* homologues were compared to those of the *Hydra vulgaris* FGFRs (*FGFRa* and *FGFRb)* in the budding process. Since the *Hydra* FGFRs diverge only in their N-terminal regions, their expression was detected using probes corresponding to either the full length FGFRa or to the divergent N-terminal extracellular domain of FGFRb. Both *FGFR* transcripts as well as those of *Dof, Frs2-related*, and *Sos* were found weakly (and constitutively) expressed along the non-budding body column (Fig. 3(A)–(D) and (F); sense controls in ESM8). *Grb2, Shp2*, and *Crkl*, in contrast, were expressed strongly and their specific expression patterns detectable only by using highly diluted probes (Fig. 3E, G, H; sense controls in ESM8). As reported previously (Sudhop et al. 2004), *kringelchen* (FGFRa) expression is upregulated from stage 2 to stage 4 at the bud tip and from stage 4 onwards at the bud base. The *FGFRb(ex)* probe failed to detect early expression in the bud tip, but colocalized with *FGFRa* at the bud base from stage 4 (Fig. 3(B4)–(B8)). Of the docking protein transcripts, only *Dof* was found co-expressed with *FGFRa* in bud evagination stages 3 and 4 (Fig. 3(C2)–(C3)). Neither *Dof* nor *Frs2-related* transcripts colocalized in the strong *FGFRa* and *FGFRb* expression domains at the bud base. *Dof* mRNA was localized in the upper body region of developing buds as well as later, constitutively in the tentacle zone (Fig. 3(C5)–(C9)), while expression of *Frs2*-related was only detected at low levels at the tentacle bases (Fig. 3(D6)–(D9)).

In the bud detachment phase, both FGFR transcripts are strongly co-expressed with *Grb2, Sos, Shp2/Csw*, and *Crkl* at the bud base from stages 6 to 7 onwards (Fig. 3e, f, g, h), low levels of Crkl expression being already observed in stage 5 (Fig. 3(H4)) and strongly from stage 8 onwards (Fig. 3(H7)–(H8)). Of the downstream components tested, *Crkl* was the first to be upregulated at the bud base.

In addition to expression in the bud detachment zone, and by implication therefore not related to signaling via FGFRs, *Grb2* and *Shp2/Csw* displayed complex expression patterns in the *Hydra* endoderm, and both ecto- and endoderm, respectively. *Shp2/Csw* transcription was upregulated at the bud tip in both epithelia from stages 1 to 2 onwards and persisted until shortly before the bud detached in stage 10 (Fig. 3(G1)–(G7)). No transcripts were detectable in the adult head.

Grb2 transcription was dynamic in budding polyps (Fig. 3(E1)–(E9); ESM8 I, J). Superimposed on ubiquitous background expression, *Grb2* was upregulated endodermally in a circumferential belt of parental tissue immediately above the newly forming bud and persisted in a wedged expression zone until stage 3/4 (Fig. 3(E1); ESM8 I). In tissue transferred to the bud (Fig. 3(E3)–(E5)), expression intensity increased in bud stages 4–5. From stage 4 onwards, *Grb2* was also highly expressed in the bud tip, where the mouth opening developed (Fig. 3(E3)–(E8)). Expression in this region persisted in the adult in a ring of cells surrounding the mouth (Fig. 3(E9)). The intensity of this apical staining was variable as documented in Fig. ESM8 J, compare bud to parent). From stage 7 onwards, expression in the body column of the bud ceased and a strong signal developed in cells surrounding the bud base, trailing behind Crkl (Fig. 3(E6)–(E8)). The dynamic pattern of *Grb2* expression suggests that the corresponding protein fulfills multiple roles during bud development in *Hydra*.

Taken together, the *FGFRs, Grb2, Crkl, Sos,* and *Shp2/Csw* are all expressed at the late bud base and might thus form a toolkit for FGFR signaling required for bud detachment.

Discussion

The evolutionary history of FGFR, Dof and Frs2

The receptor tyrosine kinase superfamily, to which the FGFRs belong, clearly predates multicellularity, as extensive families of RTKs are present in the unicellular holozoans *Capsaspora* and *Ministeria* (Suga et al. 2013) as well as in choanoflagellates such as *Monosiga* (Fairclough et al. 2013; King et al. 2008; Pincus et al. 2008). However, the RTKs of both *Capsaspora* and *Monosiga* have diverged independently from those of metazoans. The animal RTK types that respond

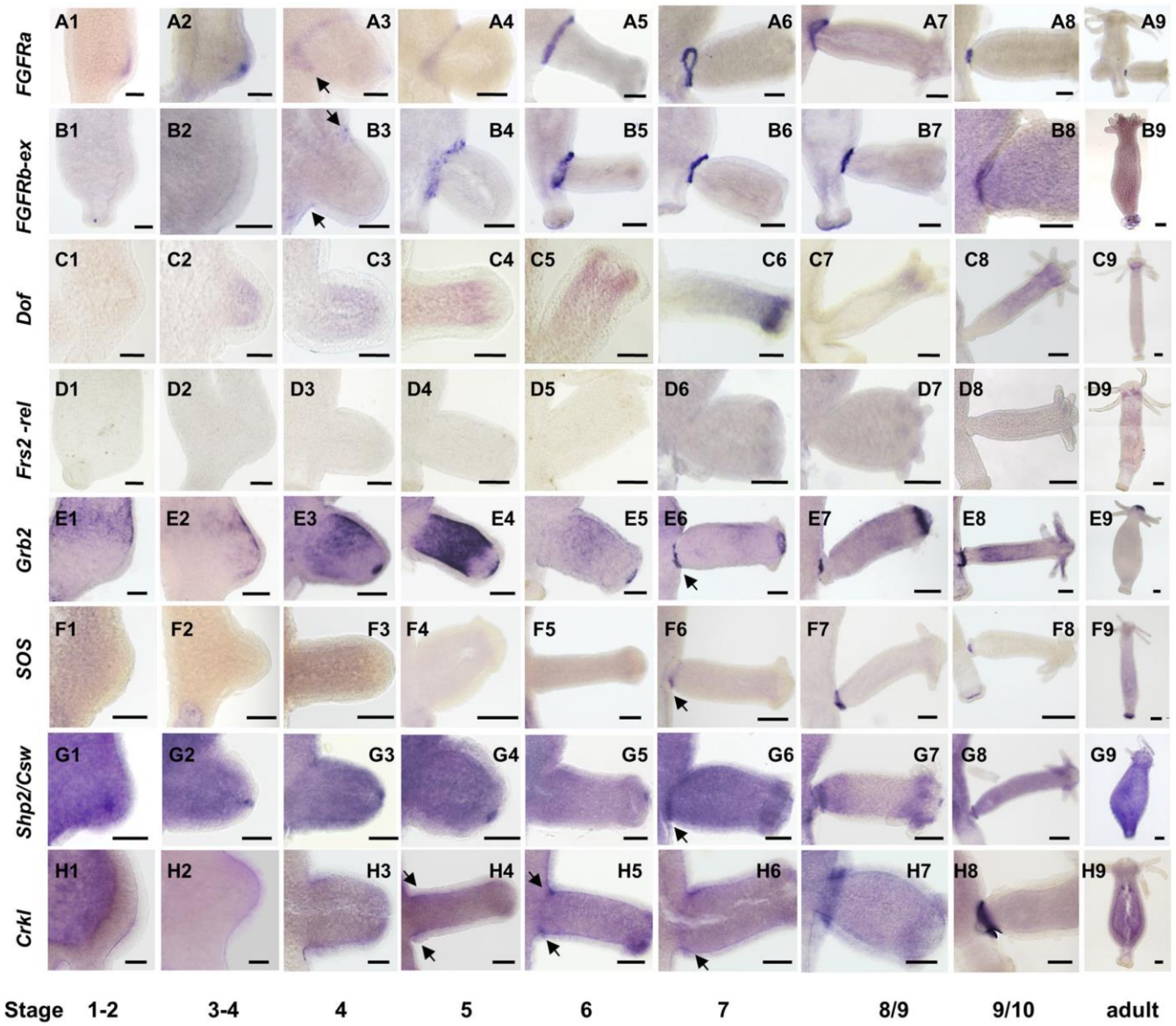

Fig. 3 Expression patterns of *Hydra* FGFRs and their potential downstream signaling elements in the ten bud stages (according to Otto and Campbell 1977)

to growth factors, including the fibroblast growth factor receptors, likely emerged in the eumetazoan ancestor (Bertrand et al. 2014; Rebscher et al. 2009).

Animal RTKs generally require docking or adapter proteins to link an activated receptor dimer to intracellular pathways. This dependency is well established in *Drosophila* and vertebrates, where the FGFR docking proteins Dof or Frs2 are essential respectively, despite being unrelated in sequence. The apparent absence of both Dof and Frs2 from single-celled holozoans and choanoflagellates, as well as representatives of the Porifera, Ctenophora, and Placozoa, is consistent with the hypothesis of a eumetazoan origin of FGFRs (Bertrand et al. 2014). Clear homologues of Dof were identified in Cnidaria (*Hydra* and *Acropora*) and Bilateria, while Frs2 proteins sensu *strictu* were restricted to members of the Bilateria. Although Dof is not upregulated in the strong expression domains of the FGFRs in *Hydra*, *Crkl* expression is upregulated at the bud base near simultaneously with both of the FGFRs (Fig. 3; Fig. 4A), while upregulation of the adapter Grb2 as well as Sos and Shp2 occurs slightly later. This raises the possibility that two (Dof-independent) pathways operate at the bud base–the early phase involving Crkl and a later pathway in which Grb2 and Sos participate.

Scenarios for FGFR adapter evolution

The data presented here suggest at least two possible scenarios for FGF adaptor evolution. In the first of these, the FGFR was originally coupled to downstream signaling pathways via an ancestral Dof protein. The evolutionary origin of Dof

coincides with that of FGFs and FGFR sensu *strictu* in anthozoan and hydrozoan Cnidaria (Hasse et al. 2014; Matus et al. 2007; Rentzsch et al. 2008; Sudhop et al. 2004). As well as their overall similarity to known Dofs from Bilateria, the cnidarian Dof proteins contain all of the domains required for both docking to the activated FGFR and connecting with the downstream elements Grb2 and Shp2/Csw, all of which are consistent with the "Dof first" hypothesis. Mutant rescue experiments also provide some support for this idea. The *Hydra* FGFRa, partially rescued a fly *heartless* mutant (Rudolf et al. 2013), suggesting that the *Hydra* FGF receptor was capable of interacting with the *Drosophila* Dof adapter. However, the *Hydra* FGFR only rescued the very early phase of FGFR activity in fly embryos, prior to its involvement in MAPK signaling, which is absolutely dependent on Dof (Wilson et al. 2004). The fact that Dof shares a zone of expression with FGFRa (Kringelchen) only early in *Hydra* bud development raises the question of its function.

While it is possible that sufficient Dof protein is present to fulfill the FGFR docking function during bud detachment, a

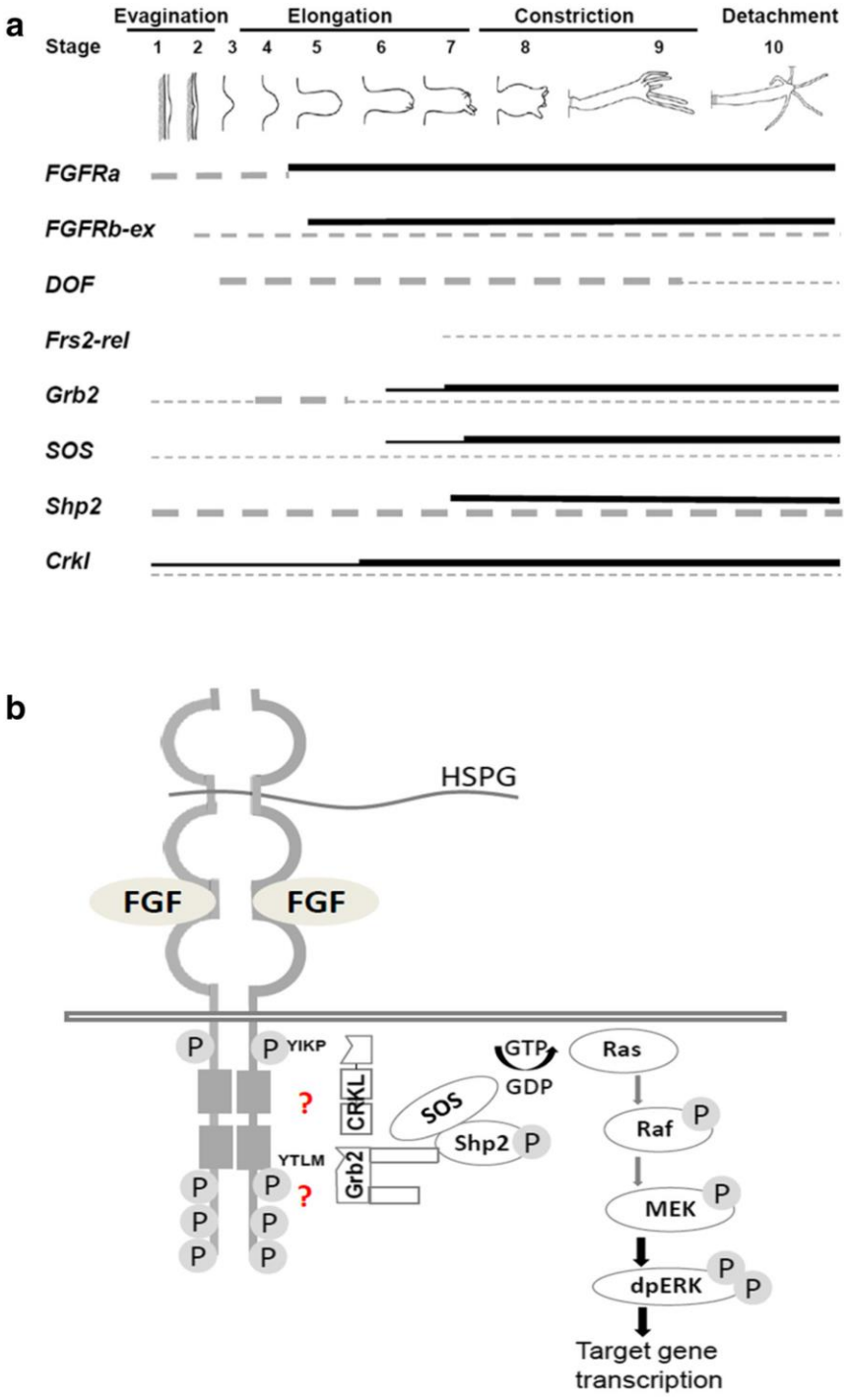

Fig. 4 Schematic summary of the expression profile and of signaling pathways reached via potential *Hydra* FGFR downstream elements. (A) Time course of gene expression at the bud base ectoderm (continuous line) or elsewhere in the animal (dotted line). Expression intensity is indicated by line thickness. (B) Hypothetical alternative FGFR pathways in *Hydra* converging on the Ras/MAPK pathway. The SH2 domain-binding consensus sequences (YIKP, YTLM) in *Hydra* FGFR for direct binding of Grb2 or Crkl, respectively, are indicated

second scenario, in which *Hydra* FGFR requires neither Dof nor Frs2 for signal transduction, would account for the lack of Dof upregulation (Fig. 4B). This interesting alternative is supported by the fact that Grb2 acts as a direct interaction partner for several receptor tyrosine kinases including vertebrate FGFR2.

Grb2 is, for example, recruited directly to receptor tyrosine kinases like EGFR (Rozakis-Adcock et al. 1993). Moreover, the nematode *C. elegans* provides a precedent for FGFR signaling without Dof or Frs2. Neither is required for FGFR activity (and Dof not even encoded in the genome). Instead, the *C. elegans* FGFR Egl15 interacts directly with Grb2/SEM5 (Lo et al. 2010). Whether this mode of action reflects a secondary modification of the FGFR pathway is unclear. Interesting in this context is that Platyhelminthes also lack Dof and possess only atypical short Frs2-related proteins. How their FGFRs transduce signals into the cell would be interesting to know.

Last but not least, the unphosphorylated Grb2 tethers inactive FGFR2 dimers C-terminally and keeps them in a preactivation state (Belov and Mohammadi 2012; Lin et al. 2012). As soon as FGF ligands are available, the tyrosine phosphorylation of Grb2 induces its dissociation from the receptor and binding to Frs2 and only now, Grb2 acts as an adaptor for FGFR downstream signaling.

Both *Grb2* and *Crkl* have early origins, as clearly related proteins are encoded by sponge genomes. A protein similar to Grb2 is encoded by the *Salpingoeca* genome; thus, Grb2 might have functioned as an adapter for RTKs prior to the emergence of FGFRs. The *Hydra* FGFRs, Grb2 and Crkl, are all strongly transcribed in a ring of epithelial cells surrounding the late bud base that had been defined by Notch signaling (Münder et al. 2010), but Dof is not upregulated here. It will be interesting to test whether the second scenario, a direct interaction of FGFR with Grb2 (or Crkl) applies to FGFR signaling in Cnidaria and represents an ancestral mechanism.

Conclusion

Efficient coupling of transmembrane receptors to intracellular signaling pathways often requires docking proteins, and many receptors are capable of interacting with a number of different downstream adaptors. The ability to interact with multiple downstream proteins enables receptors to regulate a range of different functions; in the case of FGFRs, these include roles in cell proliferation, differentiation, migration, boundary formation, and branching morphogenesis. Although the evolutionary origins of the Dof protein coincided with those of FGF signaling, and the cnidarian Dof has all of the structural features required to function as an FGFR docking protein, it missing upregulation at the bud base raises the possibility that it does not fulfill that role in *Hydra*. Protein–protein interaction assays are now required to identify and functionally characterize the interaction partners of *Hydra* FGFR required for signal transduction.

Acknowledgments We thank Nicole Rebscher, LKA Wiesbaden, and Kristian Ullrich, MPI Plön for help with the first sequence analyses in 2014.

Funding information Open Access funding provided by Projekt DEAL. This study was funded by the Deutsche Forschungsgemeinschaft grants HA1732/12 and HA1732/13. D.A. was supported by the DFG Research Training Group "Membrane Plasticity in Tissue Development and Remodeling" (GRK 2213).

Compliance with ethical standards

Conflict of interest The authors declare that they have no conflict of interest.

References

Amanchy R, Periaswamy B, Mathivanan S, Reddy R, Tattikota SG, Pandey A (2007) A curated compendium of phosphorylation motifs. Nat Biotechnol 25:285–286

Babonis LS, Martindale MQ (2017) Phylogenetic evidence for the modular evolution of metazoan signaling pathways. Philos Trans R Soc Lond Ser B Biol Sci 372

Battersby A, Csiszar A, Leptin M, Wilson R (2003) Isolation of proteins that interact with the signal transduction molecule Dof and identification of a functional domain conserved between Dof and vertebrate BCAP. J Mol Biol 329:479–493

Belov AA, Mohammadi M (2012) Grb2, a double-edged sword of receptor tyrosine kinase signaling. Sci Signal 5:pe49

Bertrand S, Iwema T, Escriva H (2014) FGF signaling emerged concomitantly with the origin of Eumetazoans. Mol Biol Evol 31:310–318

Birge RB, Kalodimos C, Inagaki F, Tanaka S (2009) Crk and CrkL adaptor proteins: networks for physiological and pathological signaling. Cell Commun Signal 7:13

Bottcher RT, Niehrs C (2005) Fibroblast growth factor signaling during early vertebrate development. Endocr Rev 26:63–77

Brummer T, Schmitz-Peiffer C, Daly RJ (2010) Docking proteins. FEBS J 277:4356–4369

Csiszar A, Vogelsang E, Beug H, Leptin M (2010) A novel conserved phosphotyrosine motif in the Drosophila fibroblast growth factor signaling adaptor Dof with a redundant role in signal transmission. Mol Cell Biol 30:2017–2027

Darriba D, Taboada GL, Doallo R, Posada D (2011) ProtTest 3: fast selection of best-fit models of protein evolution. Bioinformatics 27:1164–1165

Delahaye L, Rocchi S, Van Obberghen E (2000) Potential involvement of FRS2 in insulin signaling. Endocrinology 141:621–628

Do CB, Mahabhashyam MS, Brudno M, Batzoglou S (2005) ProbCons: probabilistic consistency-based multiple sequence alignment. Genome Res 15:330–340

Fairclough SR, Chen Z, Kramer E, Zeng Q, Young S, Robertson HM, Begovic E, Richter DJ, Russ C, Westbrook MJ, Manning G, Lang BF, Haas B, Nusbaum C, King N (2013) Premetazoan genome evolution and the regulation of cell differentiation in the choanoflagellate *Salpingoeca rosetta*. Genome Biol 14:R15

Feller SM, Knudsen B, Hanafusa H (1994) c-Abl kinase regulates the protein binding activity of c-Crk. EMBO J 13:2341–2351

Geer LY, Domrachev M, Lipman DJ, Bryant SH (2002) CDART: protein homology by domain architecture. Genome Res 12:1619–1623

Gotoh N (2008) Regulation of growth factor signaling by FRS2 family docking/scaffold adaptor proteins. Cancer Sci 99:1319–1325

Gotoh N (2009) Control of stemness by fibroblast growth factor signaling in stem cells and cancer stem cells. Curr Stem Cell Res Ther 4:9–15

Hadari YR, Kouhara H, Lax I, Schlessinger J (1998) Binding of Shp2 tyrosine phosphatase to FRS2 is essential for fibroblast growth factor-induced PC12 cell differentiation. Mol Cell Biol 18:3966–3973

Hasse C, Holz O, Lange E, Pisowodzki L, Rebscher N, Christin Eder M, Hobmayer B, Hassel M (2014) FGFR-ERK signaling is an essential component of tissue separation. Dev Biol 395:154

Hemmrich G, Bosch TC (2008) Compagen, a comparative genomics platform for early branching metazoan animals, reveals early origins of genes regulating stem-cell differentiation. Bioessays 30: 1010–1018

Holz O, Apel D, Steinmetz P, Lange E, Hopfenmuller S, Ohler K, Sudhop S, Hassel M (2017) Bud detachment in hydra requires activation of fibroblast growth factor receptor and a Rho-ROCK-myosin II signaling pathway to ensure formation of a basal constriction. Dev Dyn 246:502–516

Huelsenbeck JP, Ronquist F (2001) MRBAYES: Bayesian inference of phylogenetic trees. Bioinformatics 17:754–755

Innocenti M, Tenca P, Frittoli E, Faretta M, Tocchetti A, Di Fiore PP, Scita G (2002) Mechanisms through which Sos-1 coordinates the activation of Ras and Rac. J Cell Biol 156:125–136

Katoh K, Standley DM (2013) MAFFT multiple sequence alignment software version 7: improvements in performance and usability. Mol Biol Evol 30:772–780

King N, Westbrook MJ, Young SL, Kuo A, Abedin M, Chapman J, Fairclough S, Hellsten U, Isogai Y, Letunic I, Marr M, Pincus D, Putnam N, Rokas A, Wright KJ, Zuzow R, Dirks W, Good M, Goodstein D, Lemons D, Li W, Lyons JB, Morris A, Nichols S, Richter DJ, Salamov A, Sequencing JG, Bork P, Lim WA, Manning G, Miller WT, McGinnis W, Shapiro H, Tjian R, Grigoriev IV, Rokhsar D (2008) The genome of the choanoflagellate *Monosiga brevicollis* and the origin of metazoans. Nature 451:783–788

Kouhara H, Hadari YR, Spivak-Kroizman T, Schilling J, Bar-Sagi D, Lax I, Schlessinger J (1997) A lipid-anchored Grb2-binding protein that links FGF-receptor activation to the Ras/MAPK signaling pathway. Cell 89:693–702

Lange E, Bertrand S, Holz O, Rebscher N, Hassel M (2014) Dynamic expression of a Hydra FGF at boundaries and termini. Dev Genes Evol 224:235

Lauenstein JU, Udgata A, Bartram A, De Sutter D, Fisher DI, Halabi S, Eyckerman S, Gay NJ (2019) Phosphorylation of the multi functional signal transducer B-cell adaptor protein (BCAP) promotes recruitment of multiple SH2/SH3 proteins including GRB2. J Biol Chem 294:19852

Lax I, Wong A, Lamothe B, Lee A, Frost A, Hawes J, Schlessinger J (2002) The docking protein FRS2alpha controls a MAP kinase-mediated negative feedback mechanism for signaling by FGF receptors. Mol Cell 10:709–719

Lemmon MA, Schlessinger J (2010) Cell signaling by receptor tyrosine kinases. Cell 141:1117–1134

Lin CC, Melo FA, Ghosh R, Suen KM, Stagg LJ, Kirkpatrick J, Arold ST, Ahmed Z, Ladbury JE (2012) Inhibition of basal FGF receptor signaling by dimeric Grb2. Cell 149:1514–1524

Liu W, Xie Y, Ma J, Luo X, Nie P, Zuo Z, Lahrmann U, Zhao Q, Zheng Y, Zhao Y, Xue Y, Ren J (2015) IBS: an illustrator for the presentation and visualization of biological sequences. Bioinformatics 31:3359–3361

Lo TW, Bennett DC, Goodman SJ, Stern MJ (2010) Caenorhabditis elegans fibroblast growth factor receptor signaling can occur independently of the multi-substrate adaptor FRS2. Genetics 185:537–547

Marchler-Bauer A, Derbyshire MK, Gonzales NR, Lu S, Chitsaz F, Geer LY, Geer RC, He J, Gwadz M, Hurwitz DI, Lanczycki CJ, Lu F, Marchler GH, Song JS, Thanki N, Wang Z, Yamashita RA, Zhang D, Zheng C, Bryant SH (2015) CDD: NCBI's conserved domain database. Nucleic Acids Res 43:D222–D226

Matus DQ, Thomsen GH, Martindale MQ (2007) FGF signaling in gastrulation and neural devel Dev Genes Evol opment in Nematostella vectensis, an anthozoan cnidarian. 217:137–148

Michelson AM, Gisselbrecht S, Buff E, Skeath JB (1998) Heartbroken is a specific downstream mediator of FGF receptor signaling in Drosophila. Development 125:4379–4389

Muha V, Muller HA (2013) Functions and mechanisms of fibroblast growth factor (FGF) signaling in *Drosophila melanogaster*. Int J Mol Sci 14:5920–5937

Münder S, Käsbauer T, Prexl A, Aufschnaiter R, Zhang X, Towb P, Böttger A (2010) Notch signaling defines critical boundary during budding in Hydra. Dev Biol 344:331–345

Notredame C, Higgins DG, Heringa J (2000) T-Coffee: a novel method for fast and accurate multiple sequence alignment. J Mol Biol 302: 205–217

Otto J, Campbell R (1977) Budding in Hydra attenuata: bud stages and fate map. J Exp Zool 200:417–428

Oulion S, Bertrand S, Escriva H (2012) Evolution of the FGF gene family. Int J Evol Biol 2012:298147

Pagni M, Ioannidis V, Cerutti L, Zahn-Zabal M, Jongeneel CV, Hau J, Martin O, Kuznetsov D, Falquet L (2007) MyHits: improvements to an interactive resource for analyzing protein sequences. Nucleic Acids Res 35:W433–W437

Papadopoulos JS, Agarwala R (2007) COBALT: constraint-based alignment tool for multiple protein sequences. Bioinformatics 23: 1073–1079

Pincus D, Letunic I, Bork P, Lim WA (2008) Evolution of the phosphotyrosine signaling machinery in premetazoan lineages. Proc Natl Acad Sci U S A 105:9680–9684

Rebscher N, Deichmann C, Sudhop S, Fritzenwanker J, Green S, Hassel M (2009) Conserved intron positions in FGFR genes reflect the modular structure of FGFR and reveal stepwise addition of domains to an already complex ancestral FGFR. Dev Genes Evol 219:455–468

Rentzsch F, Fritzenwanker J, Scholz C, Technau U (2008) FGF signaling controls formation of the apical sensory organ in the cnidarian *Nematostella vectensis*. Development 135:1761–1769

Rozakis-Adcock M, Fernley R, Wade J, Pawson T, Bowtell D (1993) The SH2 and SH3 domains of mammalian Grb2 couple the EGF receptor to the Ras activator mSos1. Nature 363:83–85

Rudolf A, Hubinger C, Husken K, Vogt A, Rebscher N, Onel SF, Renkawitz-Pohl R, Hassel M (2013) The Hydra FGFR, Kringelchen, partially replaces the Drosophila heartless FGFR. Dev Genes Evol 223:159–169

Schwaiger M, Schönauer A, Rendeiro AF, Pribitzer C, Schauer A, Gilles AF, Schinko JB, Renfer E, Fredman D, Technau U (2014) Evolutionary conservation of the eumetazoan gene regulatory landscape. Genome Res 24:639–650

Sudhop S, Coulier F, Bieller A, Vogt A, Hotz T, Hassel M (2004) Signaling by the FGFR-like tyrosine kinase, Kringelchen, is essential for bud detachment in Hydra vulgaris. Development 131: 4001–4011

Suga H, Chen Z, de Mendoza A, Sebé-Pedrós A, Brown MW, Kramer E, Carr M, Kerner P, Vervoort M, Sánchez-Pons N, Torruella G, Derelle R, Manning G, Lang BF, Russ C, Haas BJ, Roger AJ, Nusbaum C, Ruiz-Trillo I (2013) The Capsaspora genome reveals a complex unicellular prehistory of animals. Nat Commun 4:2325. https://doi.org/10.1038/ncomms3325

Turwankar A, Ghaskadbi S (2019) VEGF and FGF signaling during head regeneration in hydra. Gene 717:144047

Uhlik MT, Temple B, Bencharit S, Kimple AJ, Siderovski DP, Johnson GL (2005) Structural and evolutionary division of phosphotyrosine binding (PTB) domains. J Mol Biol 345:1–20

Vincent S, Wilson R, Coelho C, Affolter M, Leptin M (1998) The Drosophila protein Dof is specifically required for FGF signaling. Mol Cell 2:515–525

Waterhouse AM, Procter JB, Martin DM, Clamp M, Barton GJ (2009) Jalview Version 2–a multiple sequence alignment editor and analysis workbench. Bioinformatics 25:1189–1191

Wenger Y, Galliot B (2013) RNAseq versus genome-predicted transcriptomes: a large population of novel transcripts identified in an Illumina-454 Hydra transcriptome. BMC Genomics 14:204

Wilson R, Battersby A, Csiszar A, Vogelsang E, Leptin M (2004) A functional domain of Dof that is required for fibroblast growth factor signaling. Mol Cell Biol 24:2263–2276

Yum S, Takahashi T, Hatta M, Fujisawa T. (1998) The structure and expression of a preprohormone of a neuropeptide, Hym-176 in *Hydra magnipapillata*. FEBS Lett 439(1–2):31–4

Zhou L, Talebian A, Meakin SO (2015) The signaling adapter, FRS2, facilitates neuronal branching in primary cortical neurons via both Grb2- and Shp2-dependent mechanisms. J Mol Neurosci 55:663–677

8.2 General Supplementary Information

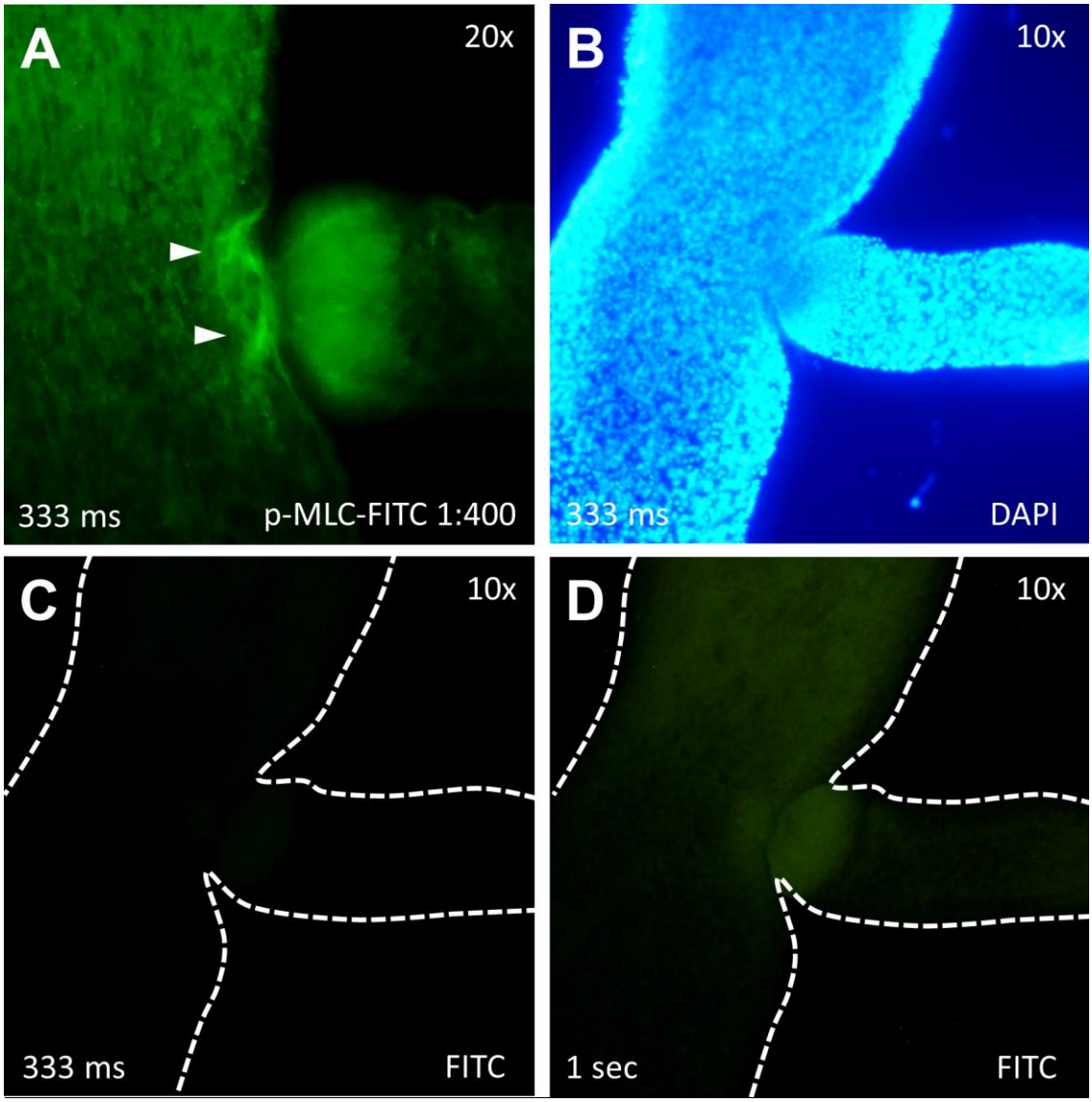

Figure S 1: Control staining of the pMLC20 antibody to verify signal specificity. (A) Polyp was incubated with anti pMLC20 (1:400, abcam) and anti-rabbit FITC (1:750, Sigma-Aldrich). Normal localization of pMLC20-FITC in *Hydra* showing a clear signal at the bud base (arrows) and in the body column. (B – D) Control polyps were incubated with secondary antibody (anti rabbit FITC, 1:750) and DAPI (1:5000). (B) DAPI, 333 ms exposure (C) FITC, 333 ms exposure (D) FITC, 1 second exposure.

Figure S 2: Comparison of the IQ-motif within the neck region of nm myosin II in *homo sapiens* and both class II myosins in *Hydra* for MRLC binding. Accession numbers MYH10 (*homo sapiens*): AAI44669.1, MYH9 (*homo sapiens*): CAG30412.1, nm-MyHC (*Hydra vulgaris*): XP_012560866, st_MyHC (*Hydra vulgaris*): XP_002157926.3. The color code indicates the physicochemical properties of the amino acids illustrated by ClustalW. The asterisks indicate the proposed IQ-motif for RLC interaction.
(IQ-Motif: Bähler and Rhoads, 2002)

8.3 Abbreviations

ATP: adenosine triphosphate

cLSM: confocal laser scanning microscope

cDNA: complementary DNA

DAG: diacylglycerine

DAPI: 4′,6-Diamidin-2-phenylindol

Dig: digoxigenin

DMSO: dimethyl sulfoxide

DNA: deoxyribonucleic acid

ERK: extracellular signal-regulated kinase

dpERK: double phosphorylated ERK

ELC: essential light chain

ECM: extracellular matrix

EM: epitheliomuscle cell

FGFR: fibroblast growth factor receptor

FGF: fibroblast growth factor

F-actin: filamentous actin

FITC: fluorescein isothiocyanate

G-actin: globular actin

ISH: *in situ* hybridization

I-cells: interstitial cells

IP3: inositoltriphosphat

Rho: Ras homologue

LiCl: lithium chloride

MAPK: mitogen-activated protein kinase

MHC: myosin heavy chain

MLCK: myosin light chain kinase

MLCP: myosin light chain phosphatase

MLC: myosin light chain

MRLC: myosin regulatory light chain

MYL9: myosin light chain 9

MCMC: Markov-Chain-Monte-Carlo method

MMPA-3: matrix metalloprotease A-3

mRNA: messenger RNA

nm-myosin II: non-muscle myosin II

nm_MyHC: non-muscle_Myosin heavy chain

pMLC20: phospho myosin light chain serine 20

PI(4,5): phosphatidylinositol-4,5-bisphosphat

PBS: phosphat buffered saline

PBT: phosphat buffered saline containing detergents

PCR: polymerase chain reaction

PLCy: phospholipase C gamma

PFA: paraformaldehyde

p-Tyr: phospho tyrosine

RLC: regulatory light chain

RNA: ribonucleic acid

ROCK: Rho associated kinase

ROI: region of interest

RTK: receptor tyrosine kinase

st_MyHC: striated_Myosin heavy chain

TRITC: tetramethylrhodamine

WMISH: whole mount *in situ* hybridization

ZO-1: Zonula-1

8.4 List of Figures

General Introduction

Chapter 1 ,,Holz et al., 2017”

Chapter 2 ,,Holz et al., 2020”

Chapter 3

General Discussion

8.5 List of Tables

9 *Curriculum Vitae* und Wissenschaftlicher Werdegang

❖ Veröffentlichungen:

Holz O, Apel D and Hassel M **(2020)** Alternative pathways control actomyosin contractility in epitheliomuscle cells during morphogenesis and body contraction. *Dev Biol*, doi.org/10.1016/j.ydbio.2020.04.001

Suryawanshi, A., Schaefer, K., **Holz, O**., Apel, D., Lange, E., Hayward, D. C., Miller, D. J., & Hassel, M**. (2020)** What lies beneath: *Hydra* provides cnidarian perspectives into the evolution of FGFR docking proteins. *Development Genes and Evolution*, 230(3), 227–238. https://doi.org/10.1007/s00427-020-00659-4

Holz O, Apel D**,** Steinmetz P, Lange L, Hopfenmüller S, Ohler K, Sudhop S, Hassel M **(2017)** Bud detachment in *Hydra* requires activation of FGFR and a Rho - ROCK - myosin II signaling pathway to ensure formation of a basal constriction. *Dev Dyn*. 2017 Jul; 246(7):502-516. doi: 10.1002/dvdy.24508. Epub 2017 May 22.

Lange E, Bertrand S, **Holz O,** Rebscher N, Hassel M **(2014)** Dynamic expression of a *Hydra* FGF at boundaries and termini. *Dev Genes Evol* 224(4):235-244. doi:10.1007/s00427-014-0480-1

Hasse C, **Holz O**, Lange E, Pisowodzki L, Rebscher N, Eder MC, Hobmayer B, Hassel M **(2014)** FGFR-ERK signaling is an essential component of tissue separation. *Dev Biol* 395(1):154-66. doi.org/10.1016/j.ydbio.2014.08.010

❖ Beiträge auf wissenschaftlichen Konferenzen:

Poster Präsentation:

März 2015 **Joint Meeting of the German and French Societies of Developmental Biologists** (Nürnberg, Germany)

FGFR-mediated bud detachment in *Hydra* requires targeting of the actin cytoskeleton

September 2015 **Animals Evolution: New perspectives from early emerging metazoans** (Tutzing, Germany)

FGFR-mediated bud detachment in *Hydra* requires targeting of the actin cytoskeleton via RhoA

März 2017 **Joint-meeting of the German and Japanese Societies of Developmental Biologists** (Kiel, Germany)

FGFR-induced actomyosin contractility is essential for tissue separation in *Hydra*

Februar 2019 **Joint Meeting of the German and Israeli Societies of Developmental Biologists** (Vienna, Austria)

Separate signaling pathways control cortical and basal actomyosin function of epitheliomuscle cells in *Hydra*

Orale Präsentation:

Oktober 2016 **11th GfE School | Cell Dynamics in Development and Evolution** (Günzburg, Germany)

Tissue separation in *Hydra:* Involvement of the Actin-cytoskeleton during final bud detachment

September 2017 **The diversification of early emerging metazoans: a window into animal evolution?** (Tutzing, Germany)

Tissue separation in *Hydra:* Involvement of actomyosin complexes during final bud detachment

10 Eidesstattliche Erklärung

Ich versichere, dass ich meine Dissertation mit dem Titel

„Tissue separation in *Hydra*:

Involvement of a Rho dependent pathway and the organization of actomyosin complexes during final bud detachment"

unter der Leitung von Frau Prof. Dr. Monika Hassel (Fachbereich Biologie, Philipps-Universität Marburg) selbstständig, ohne unerlaubte Hilfe angefertigt und mich dabei keiner anderen als der von mir ausdrücklich bezeichneten Quellen und Hilfsmittel bedient habe.

Die Dissertation wurde in der jetzigen oder einer ähnlichen Form an keiner anderen Hochschule eingereicht und hat keinen sonstigen Prüfungszwecken gedient.

_____ _____

Ort, Datum Unterschrift